

Bangor University

DOCTOR OF PHILOSOPHY

Rational design and delivery of peptide drugs

Gupta-Arya, Sona

Award date:
2000

Awarding institution:
Bangor University

[Link to publication](#)

General rights

Copyright and moral rights for the publications made accessible in the public portal are retained by the authors and/or other copyright owners and it is a condition of accessing publications that users recognise and abide by the legal requirements associated with these rights.

- Users may download and print one copy of any publication from the public portal for the purpose of private study or research.
- You may not further distribute the material or use it for any profit-making activity or commercial gain
- You may freely distribute the URL identifying the publication in the public portal ?

Take down policy

If you believe that this document breaches copyright please contact us providing details, and we will remove access to the work immediately and investigate your claim.

RATIONAL DESIGN AND DELIVERY OF PEPTIDE DRUGS

by

Sona Gupta, B.Sc., M.Sc.

*School of Biological Sciences
University of Wales, Bangor*

**A thesis submitted in candidature for the degree of
Doctor of Philosophy of the University of Wales**

July, 2000

**I'W DDEFNYDDIO YN Y
LLYFRGELL YN UNIG**

**TO BE CONSULTED IN THE
LIBRARY ONLY**



For Mum and Dad

ACKNOWLEDGEMENTS

This thesis was undertaken whilst in receipt of a postgraduate research studentship from BBSRC; this is gratefully acknowledged.

Numerous people have been instrumental throughout this project and in making my stay in Bangor enjoyable.

Foremost, I would like to thank my supervisor Prof. John Payne who has been a perfect role model. Without his active encouragement, unfailing support and excellent supervision, this thesis would not have been possible.

I would also like to take this opportunity to express my appreciation to members of the Protein & Peptide Research group. Barry Grail for his creative ideas, technical expertise and calming presence. Gill Payne for her painstaking efforts in guiding the experimental aspects of this work. Neil Marshall for his computer expertise, sound advice and cheerful disposition.

My thanks also go to Dr. John Gorham's group, especially Julian for providing the unlimited supply of coffee and encouragement.

Amongst friends, I must acknowledge Katherine, Antoinette, Elaine, Shell and Wendy, all of whom have been a source of inspiration and strength. In particular, I thank Yusuf for his constant support and his occasional gentle criticism.

Finally, I am grateful to my parents for always being there whenever I have needed them.

SUMMARY

Peptide transporters occur ubiquitously in Nature. The *Escherichia coli* dipeptide permease (Dpp) shares some common substrate specificities with the intestinal PepT1 transporter involved in oral absorption of peptide-based drugs. Structural features determining the uptake of natural peptide substrates and peptide-based drugs, e.g. angiotensin-converting enzyme (ACE) inhibitors, by Dpp were investigated using isoelectric focusing (IEF), agar plate competition assays and radioligand competition filter binding assays. Computer-based conformational analysis was used to determine the conformer distribution profiles of natural peptides, peptidomimetics, ACE inhibitors and antimicrobial smugglins.

Correlation of activity data with the conformer distribution profiles of natural peptides identified molecular recognition templates (MRTs) for substrates for effective uptake by peptide transporters. The established MRTs were applied to evaluate the putative ability of dipeptide mimetics to be transported by Dpp. The majority of peptidomimetics had conformer distribution profiles outside the MRTs. Systematic modifications in mimetic structure produced compounds with conformers within Dpp's MRT. The structural modifications described can be applied to the rational design of peptidomimetics for improved oral bioavailability.

ACE inhibitors are used for the treatment of hypertension and predictions of their oral bioavailability were determined by assessing whether their conformer distribution profiles matched the MRTs. ACE inhibitors had a low percentage of conformers distributed in the MRT sectors. Correlation of molecular modelling data with results from competition filter binding assay, using purified dipeptide-binding protein (DppA), revealed additional features involved in molecular recognition. Knowledge gained from molecular modelling of peptidomimetics and peptides was applied to the rational design of ACE inhibitors. This produced a set of theoretical compounds that matched the MRTs required for effective oral delivery by intestinal peptide transporters.

Natural antimicrobial smugglins had the majority of their conformers distributed in the MRT sectors. This confirmed the established MRTs for peptide transporters, and revealed how these compounds had optimised structural and conformational features for efficient delivery by the peptide permeases.

This study has shown how the established MRTs for peptide transporters may be used to determine the oral bioavailability of peptidomimetics and peptide-based therapeutics, and this requires verification by experimentation. The application of the MRTs for the *rational* design of peptide drugs *in silico* for improved oral delivery has also been illustrated. Results obtained in this study also indicate comparable recognition processes for transporters and peptidases, and provide evidence that the MRTs for peptide transporters may be applied for the design of substrates of peptidases for therapeutic use.

CONTENTS

CHAPTER 1 : INTRODUCTION AND LITERATURE REVIEW

| | |
|--|-----------|
| 1.1. Introduction | 1 |
| 1.2. Transport Systems in Bacteria | 2 |
| 1.3. Bacterial ATP-Binding Cassette (ABC) Transporters | 2 |
| 1.4. Bacterial Peptide Transporters | 4 |
| 1.4.1. The Oligopeptide Permease (Opp) | 4 |
| 1.4.1.1. Substrate Specificity of the Oligopeptide Permease | 4 |
| 1.4.1.2. The Oligopeptide Binding Protein (OppA) | 5 |
| 1.4.1.3. Mechanism of Peptide Transport by Opp | 6 |
| 1.4.2. The Dipeptide Permease (Dpp) | 6 |
| 1.4.2.1 Substrate Specificity of the Dipeptide Permease | 7 |
| 1.4.2.2. The Dipeptide Binding Protein (DppA) | 8 |
| 1.4.3. The Tripeptide Permease (Tpp) | 9 |
| 1.5. Exploitation of Peptide Permeases for Prodrug Delivery | 9 |
| 1.5.1. Natural Smugglins | 11 |
| 1.5.2. Synthetic Smugglins | 14 |
| 1.6. Mammalian Peptide Transporters PepT1 and PepT2 | 16 |
| 1.6.1. Substrate Specificity of PepT1 and PepT2 | 17 |
| 1.6.2. Oral Delivery of Peptide Drugs | 20 |
| 1.7. Modification of Peptides into Peptidomimetics | 21 |
| 1.7.1. The Rational Design of Peptidomimetics | 21 |
| 1.7.2. The Range of Peptidomimetics | 24 |
| 1.7.2.1. Modification of Peptide Backbone | 24 |
| 1.7.2.2. Lactam-Constrained Mimetics | 25 |
| 1.7.2.3. Torsionally-Constrained Mimetics | 25 |
| 1.8. Prodrug Approaches for Improved Peptide Drug Delivery | 26 |
| 1.8.1. Angiotensin-Converting Enzyme (ACE) Inhibitors | 26 |
| 1.8.1.1 The Renin-Angiotensin System (RAS) | 26 |
| 1.8.1.2. Prodrug Modification of ACE Inhibitors | 27 |
| 1.8.1.3. Intestinal Absorption of ACE Inhibitors | 28 |
| 1.9. Aims of Study | 29 |

CHAPTER 2 : MATERIALS AND METHODS

| | |
|---|-----------|
| 2.1. Preparation of Growth Media | 30 |
| 2.1.1. Minimal Medium 'A' | 30 |
| 2.1.2. ML Broth | 30 |
| 2.1.3. Agar Plates | 30 |
| 2.2. Bacterial Strains | 30 |
| 2.2.1. Growth of Bacterial Strains | 31 |
| 2.3. Purification of DppA from JM101 | 32 |
| 2.3.1. Cold Osmotic Shock | 32 |
| 2.3.2. Cation-Exchange Chromatography (Mono S) | 33 |
| 2.3.3. Reverse-Phase Chromatography (RPC) | 33 |
| 2.3.4. SDS-PAGE | 34 |
| 2.3.5. Determination of Protein Concentration | 35 |
| 2.4. Ligand Binding Studies using Isoelectric Focusing (IEF) | 36 |
| 2.4.1. Dipeptides Binding to DppA | 36 |
| 2.4.2. IEF Competition Assay with ACE Inhibitors | 36 |
| 2.5. Radioligand Competition Filter Binding Assays | 37 |
| 2.6. Agar-Plate Competition Assay | 39 |

| | |
|---|-----------|
| 2.7. Computer-Based Molecular Modelling..... | 40 |
| 2.7.1. Sketching of Molecules | 41 |
| 2.7.2. Conformational Analysis using Random Search | 41 |
| 2.7.2.1. Dipeptides | 43 |
| 2.7.2.2. Peptide Mimetics..... | 43 |
| 2.7.2.3. ACE Inhibitors and their Modified Analogues..... | 44 |
| 2.7.2.4. Antimicrobial Smugglins and their Modified Analogues | 44 |
| 2.7.3. Analysis of Results from Random Search | 45 |
| 2.7.3.1. Dipeptides | 45 |
| 2.7.3.1.1. Data Presentation using 3DPR Plots | 46 |
| 2.7.3.2. Dipeptide Mimetics | 47 |
| 2.7.3.3. ACE Inhibitors and their Modified Analogues..... | 49 |
| 2.7.3.4. Antimicrobial Smugglins and their Modified Analogues | 50 |
| 2.7.4. Defining MRT Regions in 3DPR Plots | 51 |

CHAPTER 3 : DPP SUBSTRATE SPECIFICITY AND THE ESTABLISHMENT OF MRTS FOR PEPTIDE TRANSPORTERS

| | |
|--|-----------|
| 3.1. Introduction | 52 |
| 3.2. Results..... | 53 |
| 3.2.1. IEF Assays of DppA Binding to Dipeptides | 53 |
| 3.2.2. Determination of Substrate Binding by Competition Plate Assay | 58 |
| 3.2.2.1. Competition Plate Assay with Inhibitory Val-Dipeptides | 58 |
| 3.2.3. Comparison of Competition Data with IEF Results..... | 61 |
| 3.2.4. Molecular Modelling of Peptides | 62 |
| 3.2.4.1. Correlation of Activity Data with MRT for Dpp and Tpp..... | 63 |
| 3.2.4.2. MRTs for Tripeptides | 64 |
| 3.3. Discussion..... | 65 |
| 3.3.1. Conformational Analysis of Peptides | 65 |
| 3.3.2. Correlation of Activity Data with Molecular Modelling Data..... | 66 |
| 3.3.3. MRTs of Substrates for Peptide transporters | 66 |

CHAPTER 4 : CONFORMATIONAL ANALYSIS OF PEPTIDOMIMETICS

| | |
|--|-----------|
| 4.1. Introduction | 68 |
| 4.2. Results..... | 70 |
| 4.2.1. Conformational Analysis of Dipeptide Isosteres | 70 |
| 4.2.2. Conformational Analysis of Peptide Bond Mimetics | 74 |
| 4.2.3. Conformational Analysis of Lactam-Constrained Mimetics | 77 |
| 4.2.3.1. 4-,5- and 6-Membered Lactam-Ring Mimetics | 78 |
| 4.2.3.1.1. Sulphur Containing 6-Membered Lactam-Ring Mimetics..... | 79 |
| 4.2.3.2. 7-and 8-Membered Lactam-Ring Mimetics | 80 |
| 4.2.3.2.1. Sulphur Containing 7-Membered Lactam-Ring Mimetics | 83 |
| 4.2.4. Conformational Analysis of Torsionally-Constrained Mimetics | 85 |
| 4.2.4.1. 6- Membered Lactams fused with 5-Membered Ring Mimetics | 85 |
| 4.2.4.2. 7-Membered Lactams fused with 5-Membered Ring Mimetics | 87 |
| 4.2.4.3. 7-Membered Lactams fused with 6-Membered Ring Mimetics | 89 |
| 4.2.5. Summary of Results | 93 |
| 4.3. Discussion | |
| 4.3.1. Conformational Analysis of Dipeptide Isosteres | 97 |
| 4.3.2. Conformational Analysis of Peptide Bond Mimetics | 97 |
| 4.3.3. Conformational Analysis of Lactam-Constrained Mimetics | 98 |
| 4.3.4. Conformational Analysis of Torsionally-Constrained Mimetics | 99 |
| 4.3.5. Design of Peptidomimetics with Oral Bioavailability | 100 |

CHAPTER 5 : MOLECULAR MODELLING OF ANGIOTENSIN-CONVERTING ENZYME (ACE) INHIBITORS

| | |
|--|------------|
| 5.1. Introduction | 101 |
| 5.2. Results | 102 |
| 5.2.1. Conformational Analysis of ACE Inhibitors | 102 |
| 5.2.1.1. Ala-Pro | 105 |
| 5.2.1.2. Captopril | 105 |
| 5.2.1.3. Zofenopril | 105 |
| 5.2.1.4. Spirapril | 105 |
| 5.2.1.5. Enalaprilat | 106 |
| 5.2.1.6. Enalapril | 106 |
| 5.2.1.7. Lisinopril | 106 |
| 5.2.1.8. Ramipril | 106 |
| 5.2.1.9. Quinapril | 107 |
| 5.2.1.10. Delapril | 107 |
| 5.2.1.11. Perindopril | 107 |
| 5.2.1.12. Cilazapril | 107 |
| 5.2.1.13. Benazepril (S) | 108 |
| 5.2.1.14. Benazepril (R) | 108 |
| 5.2.1.15. MDLa (S) | 108 |
| 5.2.1.16. MDLa (R) | 109 |
| 5.2.1.17. MDLb (S) | 109 |
| 5.2.1.18. MDLb (R) | 109 |
| 5.2.2. Correlation of Molecular Modelling Data with Activity Data | 111 |
| 5.2.2.1. IEF Competition Assay of DppA Binding to ACE Inhibitors | 111 |
| 5.2.2.2. Competition Filter-Binding Assays of DppA Binding to ACE Inhibitors | 113 |
| 5.2.3. Superimposition of Ala-Ala Cilazapril and Quinapril | 115 |
| 5.3. Discussion | 117 |
| 5.3.1. Molecular Modelling of ACE Inhibitors | 117 |
| 5.3.2. Correlation of Molecular Modelling Data with Activity Data | 118 |
| 5.3.3. Prospects for Improving the Design of ACE Inhibitors | 121 |

CHAPTER 6 : THE RATIONAL DESIGN OF ANGIOTENSIN-CONVERTING ENZYME (ACE) INHIBITORS

| | |
|---|------------|
| 6.1. Introduction | 123 |
| 6.1.1. Aims of Study | 125 |
| 6.2. Results | 126 |
| 6.2.1. Changes in the C-Terminus Amino Acid Residue | 126 |
| 6.2.1.1. Captopril Modifications | 126 |
| 6.2.1.2. Enalapril Modifications | 126 |
| 6.2.1.3. Perindopril Modifications | 126 |
| 6.2.2. Changes in Mimetic Structure | 128 |
| 6.2.2.1. Benazepril Modifications | 130 |
| 6.2.2.2. Quinapril Modifications | 130 |
| 6.2.2.3. Cilazapril Modifications | 130 |
| 6.2.2.4. MDLa (R) Modifications | 131 |
| 6.2.2.5. MDLa (S) Modifications | 130 |
| 6.2.2.6. MDLb (R) Modifications | 132 |
| 6.2.2.7. MDLb (S) Modifications | 132 |
| 6.3. Discussion | 133 |
| 6.3.1. The Rational Design of ACE Inhibitors | 133 |
| 6.3.2. Future Prospects | 136 |

CHAPTER 7 : CONFORMATIONAL ANALYSIS OF NATURAL ANTIMICROBIAL SMUGGLINS

| | |
|--|------------|
| 7.1. Introduction | 138 |
| 7.2. Results | 139 |
| 7.2.1. Bacilysin (Ala-X) | 139 |
| 7.2.1.1. Modified Bacilysin (X-Ala) | 139 |
| 7.2.1.2. Modified Bacilysin (Val-X) | 140 |
| 7.2.2. Tabtoxin (X-Thr) | 140 |
| 7.2.2.1. Tabtoxin (X-Ser) | 140 |
| 7.2.2.2. Modified Tabtoxin (Thr-X) | 141 |
| 7.2.2.3. Modified Tabtoxin (X-Ala) | 141 |
| 7.2.3. Amiclenomycin-Peptides | 141 |
| 7.2.3.1. Stravidin (MeIle-X) | 141 |
| 7.2.3.2. Acm-Dipeptide (Ile-X) | 142 |
| 7.2.3.3. Acm-Dipeptide (MeVal-X) | 142 |
| 7.2.3.4. Modified Acm-Dipeptide (Val-X)..... | 142 |
| 7.2.3.5. Modified Acm-Dipeptide (MeAla-X) | 143 |
| 7.2.3.6. Modified Stravidin (MeX-Ile) | 143 |
| 7.2.4. Lindenbein (FCDP-Ala) (X-Ala) | 144 |
| 7.2.4.1. Modified Lindenbein (Ala-FCDP) (Ala-X)..... | 144 |
| 7.3. Discussion | 145 |
| 7.3.1. Molecular Modelling of Natural Smugglins | 145 |
| 7.3.2. Choice of Amino Acid as the Transport Moiety..... | 146 |


CHAPTER 8 : FINAL DISCUSSION

| | |
|---|------------|
| 8.1. Introduction | 148 |
| 8.2. Molecular Recognition of Peptides by Peptide Permeases | 148 |
| 8.3. Rational Design of Peptidomimetics | 150 |
| 8.3.1. Synthesis of 'Ideal' Dpp and Tpp Substrates..... | 150 |
| 8.4. Molecular Modelling of ACE Inhibitors | 151 |
| 8.5. Rational Design of ACE Inhibitors | 152 |
| 8.6. Rational Design of Antimicrobial Smugglins | 152 |
| 8.7. Rational Design of Peptide Drugs for Improved Oral Delivery | 153 |
| 8.7.1. Virtual Combinatorial Chemistry | 154 |
| 8.7.1.1. Application of Structural Modification Rules..... | 155 |
| 8.8. Conclusions and Future Prospects | 156 |

CHAPTER 9 : REFERENCES

| | |
|----------------------------|------------|
| 9. References | 157 |
|----------------------------|------------|

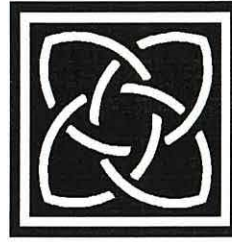
ABBREVIATIONS



| | |
|-----------------|---|
| Å | Angstrom |
| A-I | Angiotensin I |
| A-II | Angiotensin II |
| A _x | Absorbency at stated wavelength of x nm |
| AA | Amino acid |
| ABC | ATP-binding cassette |
| ACE | Angiotensin-converting enzyme |
| Ala(P) | L-1-Aminoethyl phosphonic acid |
| ATP | Adenosine 5'-triphosphate |
| ATPase | Adenosine triphosphatase |
| BCA | Bicinchonic acid |
| BSA | Bovine serum albumin |
| BPD | Binding protein dependent |
| C _{ar} | Carbon aromatic |
| CADD | Computer-aided drug design |
| CFTR | Cystic fibrosis transmembrane conductance regulator |
| χ | Chi, used to denote side chain torsion angles |
| Cpm | Counts per minute |
| ° | Degree |
| Da | Daltons |
| Dpm | Disintegrations per minute |
| Dpp | Dipeptide permease |
| DppA | Dipeptide permease binding protein |
| 3DPR | Three-dimensional pseudo-Ramachandran |
| EDTA | Ethylenediaminetetraacetic acid |
| FCDP | <i>N</i> ³ -(4-fumarylcarboxyamido-L-2,3,-diaminopropionyl) |
| FMDP | <i>N</i> ³ -(4-methoxyfumaroyl)-L-2,3,-diaminopropanioc acid |
| FPLC | Fast protein liquid chromatography |
| GI | Gastrointestinal tract |
| HEPES | <i>N</i> -2-hydroxyethyl piperazine- <i>N</i> '-2-ethane sulphonic acid |
| IEF | Isoelectric focusing |
| M | Mimetic |
| M _l | Modified mimetic |
| MDR | Multidrug resistance protein |
| M _r | Relative molecular mass |

| | |
|----------|---|
| MRT | Molecular recognition template |
| MSS | Molecular spreadsheet in SYBYL |
| NMR | Nuclear magnetic resonance |
| N.4 | Nitrogen sp ³ positively charged |
| ω | Omega (backbone torsion angle about C'-N) |
| O.co2 | Oxygen in carboxylate groups |
| Opp | Oligopeptide permease |
| OppA | Oligopeptide permease binding protein |
| PAGE | Polyacrylamide gel electrophoresis |
| PBM | Peptide bond mimetic |
| ϕ | Phi (backbone torsion angles about N-C ^{α}) |
| pI | Isoelectric point |
| ψ | Psi (backbone torsion angles about C ^{α} -C) |
| QSAR | Quantitative structure-activity relationship |
| RAS | Renin-angiotensin system |
| RPC | Reverse-phase chromatography |
| RMS | Root mean square difference between 2 conformations |
| rpm | Revolutions per minute |
| SAR | Structure-activity relationship |
| SDS | Sodium dodecyl sulphate |
| TCA | Trichloroacetic acid |
| TEMED | N,N,N', N'-tetramethyl-ethylenediamine |
| TFA | Trifluoroacetic acid |
| Tpp | Tripeptide permease |
| Tris | Tris(hydroxymethyl)(aminomethane) |

Amino acids are described by their standard three letter codes.



CHAPTER 1
INTRODUCTION AND LITERATURE
REVIEW

1. INTRODUCTION AND LITERATURE REVIEW



1.1. Introduction

In both prokaryotic and eukaryotic organisms, peptides play an important nutritional role, and the presence of peptide transport systems facilitates the absorption of these polar nutrients. The structural specificities of peptide transporters towards their substrates are similar in all organisms, including bacteria, fungi, plants and mammalian tissues e.g., intestine, kidney, lung, placenta and brain (Matthews & Payne, 1980; Matthews, 1991; Payne & Smith, 1994; Steiner *et al.*, 1995; Fei *et al.*, 1998; Yang *et al.*, 1999). Peptides are also important molecules for drug discovery, as they function as hormones and neurotransmitters involved in the regulation of biological processes. In addition to their natural peptide substrates, the mammalian peptide transporters play a key role in the delivery of peptide drugs such as β -lactam antibiotics, the antitumour agent bestatin, angiotensin-converting enzyme (ACE) inhibitors, and renin inhibitors to their intracellular target sites (Ganapathy & Leibach, 1996; Leibach & Ganapathy, 1996; Fei *et al.*, 1998; Daniel, 1996; Yang *et al.*, 1999). The potential for nutritional, clinical, and therapeutic applications of peptide transporters necessitates further investigations of the molecular aspects of substrate recognition by these systems.

The bacterial peptide transporters will be used for the study of structure-activity relationship (SAR) of peptide transporters. Features that govern the recognition of natural peptide substrates by the bacterial peptide transporters, may be applied for the rational design of peptide-based drugs for effective transport and recognition by intestinal peptide transporters. This review will initially discuss peptide transport systems in Gram-negative bacteria, and the exploitation of these systems for the delivery of antimicrobial peptide prodrugs. The role of mammalian peptide transporters in drug delivery will then be discussed, followed by descriptions of the conversion of peptides into peptidomimetics and prodrugs, as strategies for improving the transport and oral bioavailability of peptide drugs.

1.2. Transport Systems in Bacteria

The cytoplasmic membrane of bacteria is impermeable to most solutes therefore, specialised transport systems are present to mediate the active uptake of solutes across the cell membrane. In *Escherichia coli* these active transport systems fall into three main classes: i) Phosphoenolpyruvate sugar phosphotransferase that phosphorylate specific mono-and disaccharides during transport; ii) transport systems that require membrane-bound components that are energised by the proton-motive force, and iii) the periplasmic binding protein-dependent (BPD) ABC transporters, that utilise the energy of ATP hydrolysis for transport (vanVeen & Konings, 1997, 1998).

1.3. Bacterial ATP-Binding Cassette (ABC) Transporters

The ABC superfamily, also known as trafficATPases, consists of both prokaryotic and eukaryotic transporters, including the medically important P-glycoprotein, and the cystic fibrosis transmembrane conductance regulator (CFTR), known to be a Cl⁻ channel (Ames & Lecar, 1992). The archetypal ABC transporter consists of four domains. Two of these domains are highly hydrophobic, membrane-spanning domains, that form the channel through which substrates cross the membrane. The other two domains are peripherally located at the cytoplasmic face of the membrane, that bind ATP and couple ATP hydrolysis to the transport process. In bacteria, each of these four domains are generally encoded as a separate polypeptides, while in eukaryotes they are expressed as single, large multifunctional polypeptides (Linton & Higgins, 1998).

Bacterial ABC transporters contain a ligand-specific binding protein that is located in the periplasm of Gram-negative bacteria, while in Gram-positive bacteria it is a lipoprotein associated with the external face of the cytoplasmic membrane (Sutcliffe and Russell, 1995). Outer membrane proteins (OMPs) facilitate solute entry into the periplasm where the periplasmic receptor provides the primary substrate binding site for solute uptake and delivers substrates to the membrane-associated domains (Linton & Higgins, 1998). Early X-ray crystal structures of binding proteins from several ABC transporters have revealed some common features (Quioco, 1990, 1992; Quioco & Ledvina, 1996).

These common features include: i) an ellipsoidal shape consisting of two distinct globular domains separated by a deep cleft or groove; ii) a ligand-binding site located in the deep cleft between the two domains; iii) a hinge-bending motion between the two domains to allow access to and from the binding site; iv) irrespective of the nature of the ligand, the specificity and affinities of the binding sites are achieved through salt-bridges and hydrophobic interactions; v) binding of ligands induces a large protein conformational change; vi) three different structures have been observed among binding proteins; unliganded “open cleft”, liganded “open cleft” and liganded “closed cleft” (Quioco, 1990, 1992; Quioco & Ledvina, 1996).

The periplasmic-BPD transporters form the largest family of ABC transport systems for the uptake of sugars, amino acids, peptides and other nutrients, and their mechanism of substrate translocation and ATP hydrolysis has been investigated by several researchers. An intensively studied ABC transport system is the histidine permease of *Salmonella typhimurium* (Liu *et al.*, 1997; Liu & Ames, 1998; Nikaido & Ames, 1999; Liu *et al.*, 1999a,b). The membrane-bound complex of the histidine permease is composed of two hydrophobic, integral membrane proteins, HisQ and HisM, and two copies of the ATP-binding subunit, HisP. ATP hydrolysis occurs upon induction of transport activity by the liganded soluble receptor, the periplasmic histidine-binding protein, HisJ (Liu & Ames, 1998). The 3-D structure of HisP has been solved and shown to have an “L” shape, with one of its arms (arm I) being involved in ATP binding and the other one (arm II) being proposed to interact with the hydrophobic subunits HisQM (Hung *et al.*, 1998; Liu *et al.*, 1999a,b). Liu and Ames (1998) have shown that HisP is an absolute requirement for ATP hydrolysis, and that HisQM alone cannot hydrolyse ATP. In addition, HisP depends on HisQM to relay the inducing signal from the soluble receptor HisJ, and HisQM regulates the ATPase activity of HisP. Liu and Ames have also shown that HisP undergoes conformational changes upon exposure to phospholipids (Liu & Ames, 1998). In a recent study, Nikaido & Ames have shown that one intact ATP-binding subunit is sufficient to support ATP hydrolysis and translocation in the histidine permease of *S. typhimurium* (Nikaido & Ames, 1999).

1.4. Bacterial Peptide Transporters

E. coli and *S. typhimurium* possess three genetically distinct peptide permeases with overlapping substrate specificities: the oligopeptide, dipeptide and tripeptide permeases (Payne & Smith, 1994). Several other putative peptide transporters in *E. coli* have recently been revealed by database homology searching and have been reviewed (Saier, 1998, 1999a,b; Paulsen *et al.*, 1998; Smith *et al.*, 1999).

1.4.1. The Oligopeptide Permease (Opp)

The existence of the oligopeptide permease (Opp) in *E. coli* was first demonstrated by the isolation of mutants resistant to the toxic peptide triornithine (Payne, 1968). Opp is the main peptide-transport system and is encoded by five genes, *oppABCDF* (Hiles *et al.*, 1987a,b). The oligopeptide-binding protein (OppA) is the product of the first gene (*oppA*) with a molecular weight of 58.8 kDa (Higgins & Hardie, 1983). The *oppB* and *oppC* genes encode membrane-bound proteins OppB and OppC, respectively, that are analogous to HisQ and HisM of the histidine permease. The *oppD* and *oppF* genes encode proteins OppD and OppF, respectively, of similar amino acid sequences, and contain ATP-binding sites, like HisP, and are involved in the energization of transport (vanVeen & Konings, 1997, 1998; Linton & Higgins, 1998).

1.4.1.1. Substrate Specificity of The Oligopeptide Permease

A variety of transport assays and fluorescence-labelling techniques have been used to characterise the substrate specificities for Opp (Payne & Smith, 1994). Oligopeptides up to and including hexapeptides may be transported by Opp, but in the whole cell, this size restriction is controlled by the OMPs (Alves & Payne, 1980; Andrews & Short, 1985). Peptides with a positively-charged *N*-terminal α -amino group are required for effective transport. Modifications such as α -*N*-acyl or α -*N*-dialkyl substitutions, effectively inhibit transport (Payne, 1980). In contrast, the *C*-terminal carboxyl group only plays a minor role in substrate recognition, and may be absent or derivatized (Atherton *et al.*, 1983; Morley *et al.*, 1983a,b). Peptides containing all L-residues are transported most effectively, with D-residues decreasing transport activity (Payne, 1980). All natural amino acid side chains and various derivatized ones are accepted by OppA (Alves & Payne, 1980; Perry & Gilvarg, 1984).

The normal *trans* ω peptide bonds are preferred for efficient substrate transport, methylation of the peptide-bond nitrogen decreases transport rate (Payne, 1980).

1.4.1.2. *The Oligopeptide Binding Protein (OppA)*

The crystal structure of OppA has revealed high tertiary structure similarity with other periplasmic binding proteins, however, the most striking feature was its three-domain organisation, unlike other periplasmic binding proteins (Tame *et al.*, 1994). Crystal structures of a series of OppA-peptide complexes have revealed an enclosed but versatile peptide binding pocket, and have shown how tri- and tetrapeptide ligands are accommodated. The majority of the ligand backbone interactions are provided by domain III (Tame *et al.*, 1994, 1995, 1996). The residues involved in ligand binding have been investigated by studying the crystal structure of OppA in complex with Lys-Lys. These studies have revealed that the α -amino group of the ligand forms an ion pair interaction with Asp⁴¹⁹, however, the α -carboxylate group was found to form water-mediated interactions with the guanidinium groups of Arg⁴⁰⁴ and Arg⁴¹³ (Sleigh *et al.*, 1997), rather than the direct salt-bridges to Arg⁴¹³ and His³⁷¹, observed in the tripeptide and tetrapeptide complexes, respectively (Tame *et al.*, 1994, 1995). Isothermal titration calorimetric measurements of the binding of lysine-containing peptides to OppA, showed that the dipeptide Lys-Lys is bound with a similar to 60-fold lower affinity than related tri- and tetrapeptides (Sleigh *et al.*, 1997). In a recent study, Davies *et al.* (1999) investigated the binding of a variety of tripeptides of the form Lys-X-Lys, where X is a primary amine, a straight chain alkane or a ring system. These ligands were designed to examine the effects of small changes to the central side chain and results showed a definite preference for the binding of hydrophobic residues over the positively charged side chains (Davies *et al.*, 1999). Sleigh *et al.* (1999) determined the binding of Lys-X-Lys peptides, where X is any of the 20 commonly occurring amino acids. They found that various side-chains at position 2 on the ligand fit into a hydrated pocket, with the majority of side-chains restrained to particular conformations within the pocket. Water molecules were thought to act as flexible adapters, but predicting the thermodynamics of binding from the structure of the complexes was highly complicated by the influence of water on the system (Sleigh *et al.*, 1999).

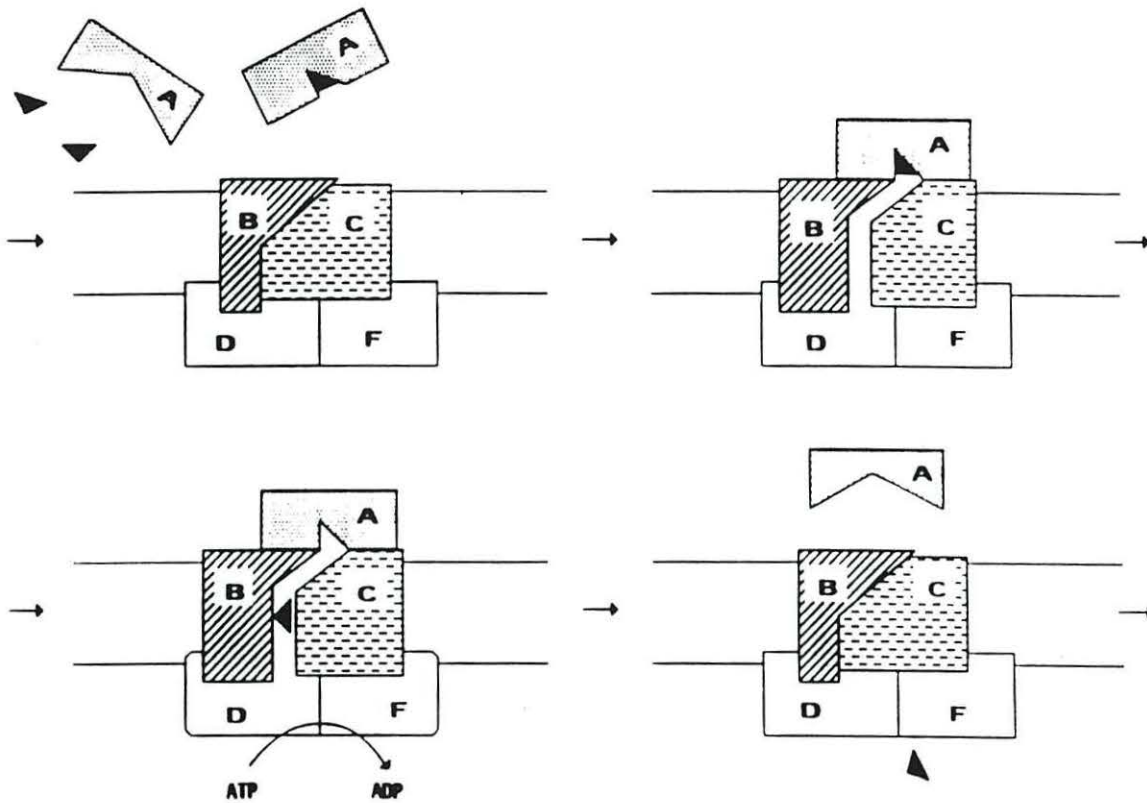


Figure 1-1: A Model for Peptide Transport by the Oligopeptide Permease.

The speculative sequence of events is initiated (top Left) by a peptide substrate (\blacktriangle) interacting with the periplasmic oligopeptide-binding protein OppA (A); binding of the peptide ligand leads to a conformational change in OppA. This change facilitates ligand-complex binding to one or more of the membrane-bound proteins OppB and OppC (B,C) (top right); this binding in turn causes a conformational change that creates a transmembrane pore. Peptide translocation through the pore is triggered by this conformational re-arrangement and may be linked to ATP hydrolysis by one or more of the peripheral proteins OppD, OppF (D,F) (bottom left). Some specific interactions of the substrate with residues in the membrane pore may occur. Ligand release into the cytoplasm is followed by a return to the initial state of the permease (bottom right), either spontaneously or by energy-dependent conformational re-arrangement.

1.4.1.3. Mechanism of Peptide Transport by Opp

The proposed mechanism of peptide transport by Opp is shown in Fig.1-1, and is based on the hypothetical model based on substrate translocation and ATP hydrolysis by histidine permease (Liu *et al.*, 1999a,b) (section 1.3.). For peptide transport by Opp, the initial specificity-determining step involves the interaction of the peptide with the binding protein OppA. This results in substrate-induced conformational changes in OppA that cause it to have increased affinity for the membrane-bound complex, most probably for OppB and/or OppC. Evidence for substrate-induced changes in OppA have been confirmed by isoelectric focusing (Tyreman, 1990; Tyreman *et al.*, 1992). Three species with different pI values have been observed. An unliganded form with a pI value of 6.20 and two liganded forms produced by addition of AlaAlaAla, or LysAlaAla with pI values of 6.26 and 6.55, respectively. Attachment of liganded-OppA promotes further conformational changes in the membrane proteins which result in translocation. These conformational changes will lead to the binding and hydrolysis of ATP by OppD and OppF (Payne & Smith, 1994; Liu & Ames, 1998). A translocation pore region is created within the transmembrane domains of the integral membrane proteins, which may be co-ordinated with the dissociation of the substrate via an “open-liganded” form of OppA. The presence of low affinity, substrate-recognition features aligned within the transmembrane pore may facilitate the unidirectional translocation of the substrate. Release of ADP would contribute to a reverse sequence of conformational changes, with dissociation of the binding protein restoring the initial permease state. This model of transport is hypothetical and many elements require further investigation (Payne & Smith, 1994; Payne, 1995; Liu *et al.*, 1999a,b).

1.4.2. The Dipeptide Permease (Dpp)

The dipeptide permease (Dpp) in *E. coli* was identified as a result of work on mutants that were defective in the Opp system (Payne, 1968). Evidence that Dpp is a traffic ATPase came from identification of a periplasmic dipeptide-binding protein (DppA) with a molecular weight of 56 kDa (Tyreman, 1990; Abouhamad *et al.*, 1991; Olson *et al.*, 1991), and from sequencing the *dpp* locus which comprises an operon of five genes *dppABCDF* (Abouhamad & Manson, 1994).

Its organisation is the same as the Opp operon of *S. typhimurium*. The first gene in the operon, *dppA*, encodes the periplasmic dipeptide-binding protein (DppA). In *E. coli*, DppA has also been shown to be the primary receptor for peptide chemotaxis (Manson *et al.*, 1986). The membrane-associated components of Dpp are similar to other periplasmic-BPD transport systems (vanVeen & Konings, 1997, 1998). The DppB and DppC proteins are highly hydrophobic and have a strong similarity to OppB and OppC membrane proteins of Opp. DppD and DppF possess the consensus ATP-binding sites (Linton & Higgins, 1998).

1.4.2.1. Substrate Specificity of The Dipeptide Permease

Dpp has a preference for dipeptide substrates but can also transport tripeptides to a lesser extent (Alves & Payne, 1980; Tyreman *et al.*, 1992). Studies similar to those used to characterise Opp have shown that Dpp has similar structural specificities, but are somewhat more restrictive. The specificity towards the *N*-terminal α -amino group is the same, but loss or derivatization (amidation, esterification) of the *C*-terminal α -carboxyl on a dipeptide greatly reduces its uptake (Payne, 1980). In addition, peptide analogues that lack peptide bonds but retain features of charge and spatial separation, such as 5-aminolevulinic acid, also show binding to DppA (Marshall, 1994) and transport in *E. coli* and *S. typhimurium* (Elliott, 1993; Verkamp *et al.*, 1993). The nature of residue side-chains affects Dpp transport more compared with Opp, but a range of modified dipeptides are transported (Alves and Payne, 1980; Perry and Gilvarg, 1984). More detailed information on the substrate specificity of purified DppA from *E. coli* has been recently determined, using filter-binding assays (Smith *et al.*, 1999). A substrate:DppA stoichiometry of 1:1 was found with both [¹⁴C]AlaAla and Ala[¹⁴C]Phe. Isoelectric focusing (IEF) analysis showed that DppA had different pI forms in its native and liganded form. The native form has a pI value of 6.1, but can be converted to at least two other forms, with pI values of 5.9 and 6.0, upon binding with dipeptide substrates. The changes in the pI value of DppA upon binding different peptide substrates, are considered to arise from conformational changes in the protein, as described for OppA (Smith *et al.*, 1999).

Using [$^{125}\text{I}_2$]Tyr-peptides as substrates in competition assays, the relative binding affinities for a range of dipeptides were found to parallel their overall transport rates in *E.coli* through Dpp, showing that DppA alone controls the specificity of Dpp (Tyreman *et al.*, 1992, 1998; Smith *et al.*, 1999). With a series of *N*-terminal α -amino group substituted glycyl peptides, binding affinity was progressively enhanced by alkylation from methyl to butyl. These results contribute to the fundamental information required for evaluating the structural basis of molecular recognition by DppA, and for the rational design of peptide carrier prodrugs able to be transported by Dpp (Smith *et al.*, 1999).

1.4.2.2. The Dipeptide Binding Protein (DppA)

DppA has been crystallised in both an unliganded form, and with bound Gly-Leu (Nickitenko *et al.*, 1995; Dunten & Mowbray, 1995). The overall structure of DppA is similar to that of *S. typhimurium* OppA and also contains three domains. These domains are connected by two hinge segments which form part of the base of the wide groove between the domains. The relative orientation of these domains gives the protein a “pear-like” shape. Domain I, which is composed of two integral subdomains (Ia and Ib), is folded from two separated polypeptide segments from the amino and carboxyl terminus end. The three domains I, II and III, in *S. typhimurium* OppA are equivalent to subdomain Ia, Ib and domain II in DppA, respectively (Dunten & Mowbray, 1995). The binding site is located between domain I and II, and is designed to recognise the ligand’s backbone while providing space to accommodate a variety of side chains. Some repositioning of protein side chains lining the binding site is thought to occur when the dipeptide’s second residue is larger than Leu. Asp⁴⁰⁸ in the binding pocket forms an ion pair with the amino terminus of the ligand, and Arg³⁵⁵ forms an ion pair with the carboxyl terminus of the ligand. The spacing of the Asp⁴⁰⁸ and Arg³⁵⁵ residues favours dipeptide binding over that of amino acids, and the limited movement of the Arg³⁵⁵ side chain enables DppA to accept some tripeptides (Dunten & Mowbray, 1995). Fig. 1-2 shows the X-ray crystal structure of DppA and the residues involved in ligand binding.

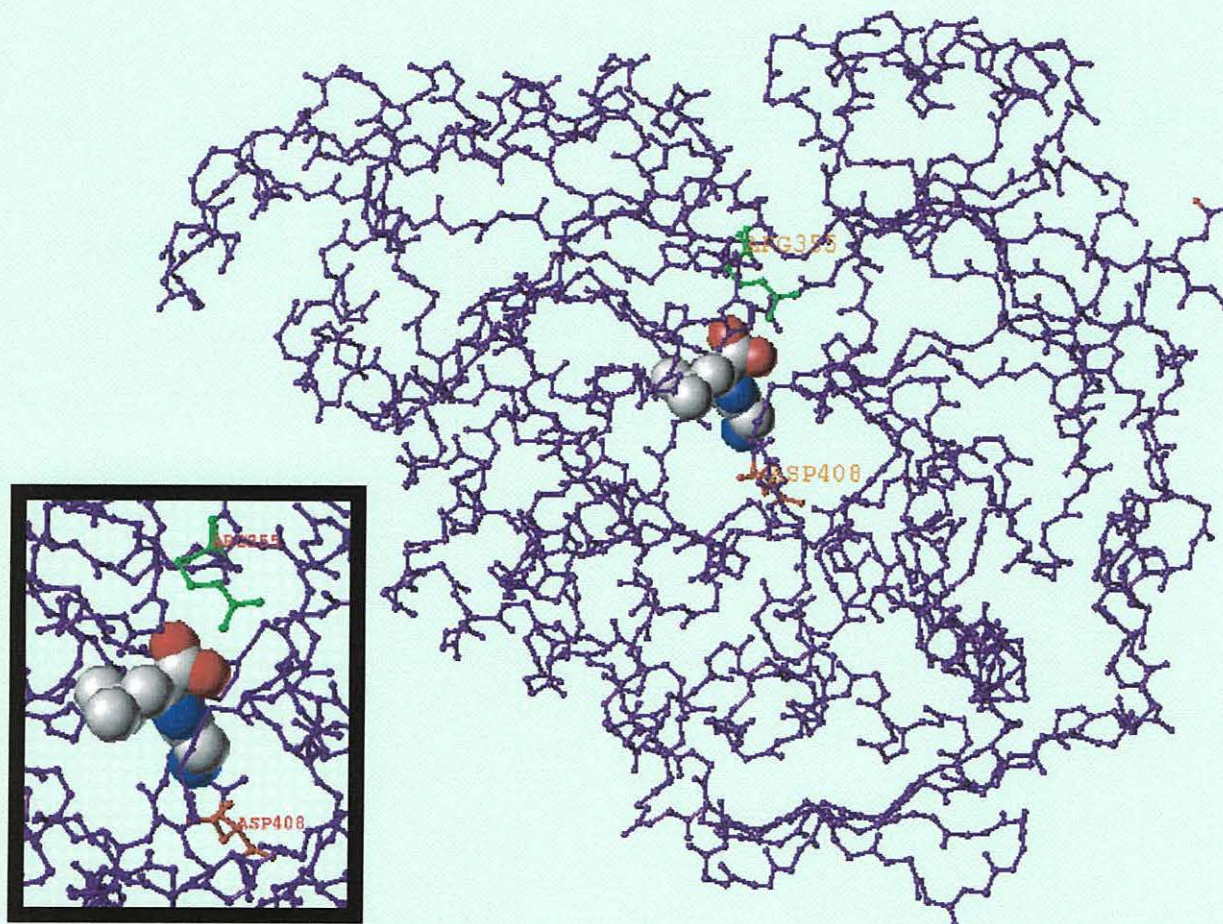


Figure 1-2: Crystal Structure of DppA and the Residues Involved in Ligand Binding.

1.4.3. The Tripeptide Permease (Tpp)

The tripeptide permease (Tpp) is the least well characterised of the three main peptide permeases. Its presence in *E.coli* was first confirmed when *opp* mutants were shown to grow on a restricted range of tripeptides (Barak & Gilvarg, 1975; Naider & Becker, 1975). Early studies on peptide uptake indicated that Tpp possessed similar specificities as Opp with regards to the *N*- and *C*-termini (Barak & Gilvarg, 1975; Naider & Becker 1975). Additional studies using *opp dpp* mutants demonstrated that Tpp can transport a variety of tripeptides and also dipeptides. However, it was unable to transport tetra-or higher peptides (Alves & Payne, 1980; Payne, 1983). Its specificity towards side-chain residues is somewhat more restrictive compared with Dpp and Opp. Tpp favours peptides composed of hydrophobic residues, especially with *N*-terminal Met or Val residues (Payne, 1983; Gibson *et al.*, 1984). Tpp has a relatively minor role in peptide transport compared with Opp and Dpp, and is not a traffic ATPase but belongs to the class of transporters that have only a single membrane protein in which transport is energised by proton-motive force (Smith, 1992; Smith *et al.*, 1999). The transport of di-and tripeptides into *Lactococcus lactis* by the DtpT transport protein is also mediated by a proton motive force, and shares similarity with eukaryotic peptide transporters (Hagting *et al.*, 1997).

1.5. Exploitation of Peptide Permeases For Prodrug Delivery

The concept of attaching or incorporating toxic impermeant moieties into peptide structures, to form peptide carrier prodrugs, soon followed the characterisation of microbial peptide permeases. This process was first experimentally validated by using peptides containing the impermeant residues histidinol phosphate and homoserine phosphate (Ames *et al.*, 1973; Fickel & Gilvarg, 1973) and, since then, a variety of terms have been proposed to describe peptide prodrug transport, these include: “illicit transport” coined by Ames and co-workers (Ames *et al.*, 1973), and “warhead delivery” proposed by Ringrose (Ringrose, 1980). The peptide-carrier complexes themselves have been termed “smugglins” by Payne (Payne, 1976). The overall process of illicit transport is illustrated in Fig. 1-3.

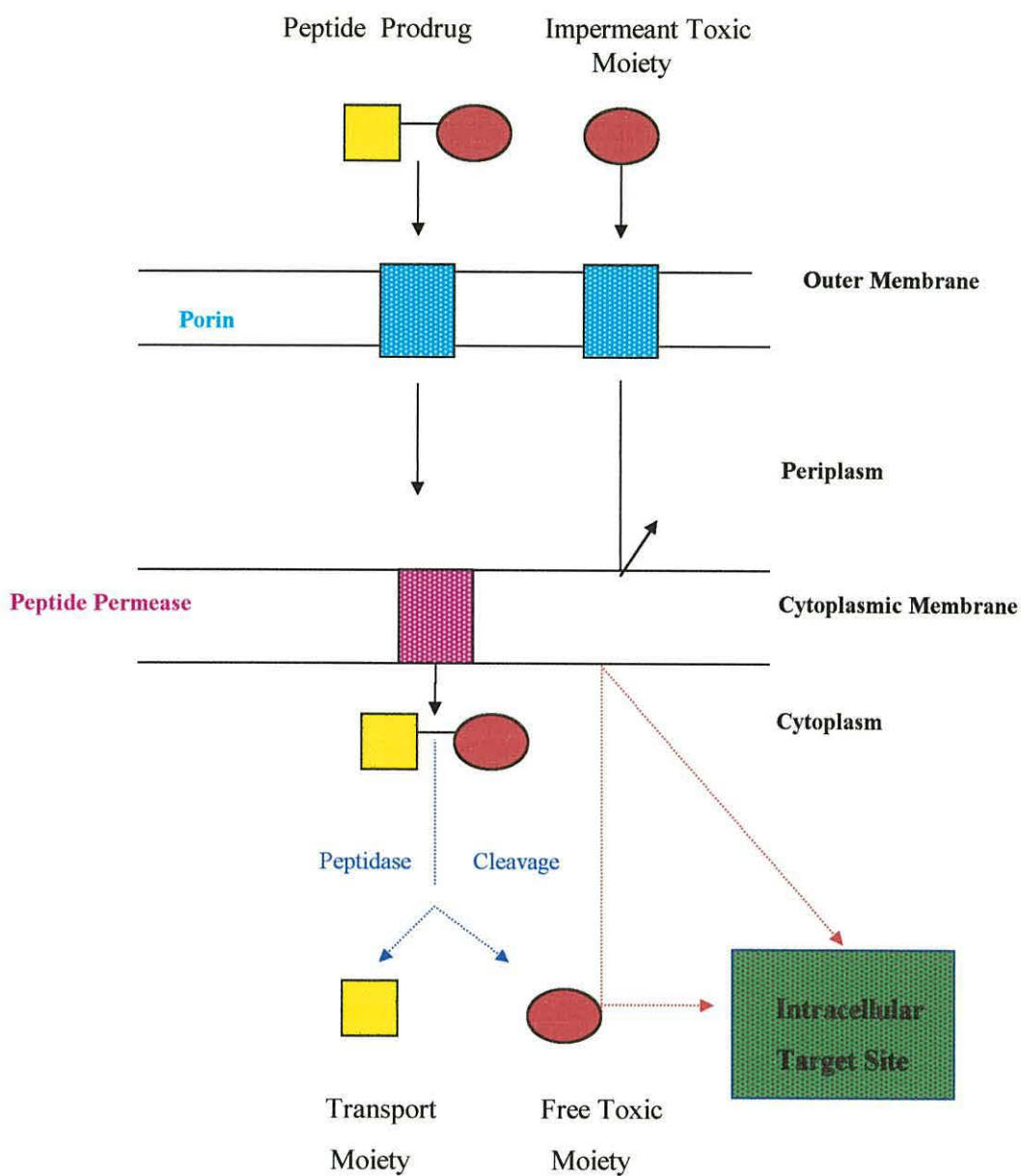




Figure 1-3: Exploitation of Peptide Permeases by Peptide-Carrier Prodrugs.

The toxic moiety  is impermeant in its free form, but can be actively accumulated through a peptide permease when linked to a transport moiety . Following intracellular peptidase cleavage, the free toxic moiety can reach a high concentration in the cytoplasm and inhibit its intracellular target site.

Antimicrobial smugglins are generally composed of a transport moiety, which may be one or more amino acids at either the *N*- or *C*-terminus, and a warhead moiety, linked by a peptidase-labile bond. To function as a prodrug, the smugglin must be cleaved intracellularly (most commonly by peptidase action), to release its toxic amino acid mimetics or “warhead”. Once released, the inhibitory compound is unable to cross the membrane except as a smugglin component, and, therefore, cannot undergo exodus. This results in accumulation of the toxic moiety to a high concentration intracellularly (Ames *et al.*, 1973). Exploitation of peptide permeases by antimicrobial smugglins has been extensively reviewed (Ringrose, 1980; Naider & Becker, 1988; Payne & Smith, 1994; Becker & Naider, 1995; Payne, 1995; Tyreman *et al.*, 1998), and this review will discuss some selected examples of natural and synthetic peptide smugglins.

1.5.1. Natural Smugglins

The dipeptide bacilysin (tetaine, bacillin), produced by *Bacillus subtilis* (Kenig & Abraham, 1976) is one of the earliest examples of a naturally occurring smugglin to be identified. It comprises an *N*-terminal Ala residue and the *C*-terminal amino acid mimetic, L- β -(2,3-epoxycyclohexanono-4)-alanine, known as anticapsin. Anticapsin itself is not antibacterial, but as the dipeptide derivative it has both antibacterial and antifungal activity (Kenig *et al.*, 1976). Bacilysin has been shown to be transported predominantly through Dpp and is hydrolysed to yield anticapsin, which acts as a glutamine analogue and inhibits peptidoglycan synthesis in bacteria, and mannoprotein and chitin synthesis in fungi (Chmara & Zahner, 1984; Chmara, 1985; Milewski *et al.*, 1986).

Lindenbein [N^3 -fumarylcarboxyamido-L-2,3-diaminopropionyl-L-alanine] (FCDP-Ala), isolated from *Streptomyces collinus*, is another natural antibiotic related to bacilysin (Molloy *et al.*, 1972). FCDP-Ala is cleaved by intracellular peptidases to release the *N*-terminal amino acid mimetic FCDP which acts as a glutamine analogue, like bacilysin, and inhibits glucosamine synthetase (Chmara *et al.*, 1984). A common property of naturally occurring antibacterial peptides is that although they are structurally diverse, their warheads interfere with either the synthesis or subsequent utilisation of glutamine, and L-alanine is often the transport moiety (Ringrose, 1980).

A novel class of natural smugglins includes those that contain β -lactam rings, such as the phytotoxin tabtoxin (Ringrose, 1980). Tabtoxin or wildfire toxin or is a dipeptide exotoxin produced by a plant-pathogenic strain of *Pseudomonas tabaci*. Its structure was found to contain an *N*-terminal amino acid mimetic with a β -lactam side-chain (Stewart, 1971). The *C*-terminal moiety is usually threonine but can also be the closely related amino acid serine. Hydrolysis of tabtoxin *in vivo* by peptidases releases tabtoxine- β -lactam, which inhibits glutamine synthetase causing chlorosis and death of the tobacco plant (Stewart, 1971).

The clavams differ from conventional β -lactams in possessing an oxygen atom in place of the sulphur atom at position 1 and are active against bacteria and fungi (Rohl *et al.*, 1987). Valclavam is one such antibiotic that incorporates the β -lactam residue hydroxy-ethyl clavam, the toxicity of which is enhanced when it is incorporated into the peptide carrier form to allow its transport (Baldwin *et al.*, 1993). Valclavam is transported by both Dpp and Tpp, and mutants defective in one or the other system retain sensitivity, a feature that is important for efficacious, synthetic smugglin design (Payne, 1995; Tyreman *et al.*, 1998).

Several peptide antibiotics containing ampicillin (Acm) have been isolated from *Streptomyces venezuelae* including: L-MeIle-L-Acm [Stravidin (MSD 235 S₃)], L-Ile-L-Acm, L-MeVal-L-Acm, L-MeIle-L-Acm-L-Gln, L-Ile-L-Acm-L-Gln, L-Val-L-Acm-L-Gln (Poetsch *et al.*, 1985). Some of these peptides are unusual in that their terminal amino group is *N*-methylated such that the transport moiety is *N*-methylisoleucine or *N*-methylvaline. These di- and tripeptides are active against Gram-negative bacteria and are transported by peptide permeases (Poetsch *et al.*, 1985).

Many natural smugglins use phosphorous-containing amino acid mimetics as their toxic warhead. The tripeptide bialaphos (phosphinothricyl-Ala-Ala), has L-2-amino-4-methylphosphinobutyric acid as its toxic moiety, which is a δ -phosphinate analogue of glutamic acid. This inhibits glutamine synthetase *in vitro*, whereas only the smugglin bialaphos shows antibacterial activity. (Diddens *et al.*, 1976, 1979). Examples of some natural smugglins are shown in Fig. 1-4.

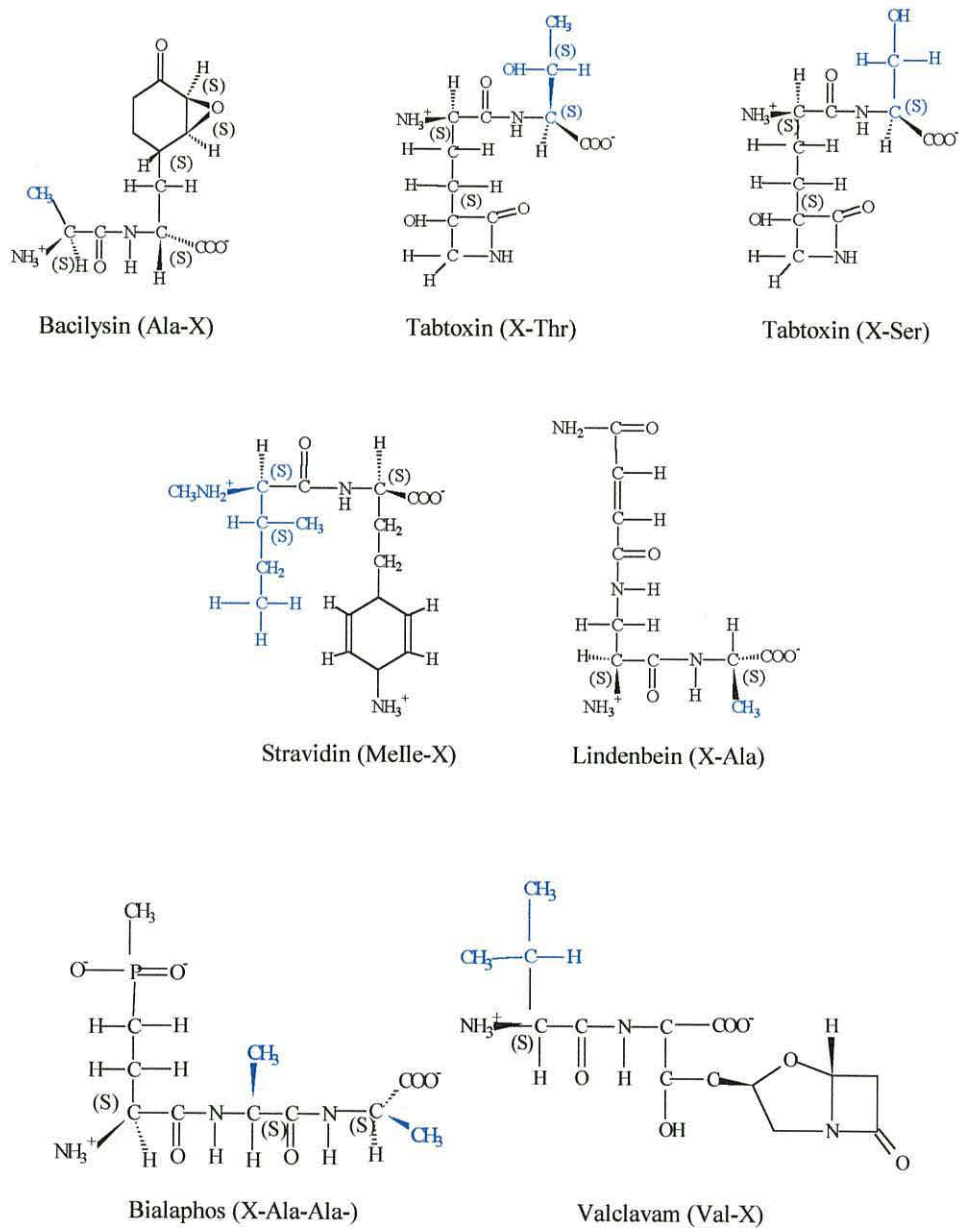


Figure 1-4: Examples of Some Natural Antimicrobial Smugglins.

Antimicrobial smugglins generally consist of an amino acid transport moiety (side chains shown in blue) attached to a toxic warhead (X).

1.5.2. Synthetic Smugglins

Pioneering work by Ames *et al.* (1973) initiated the synthesis of peptide smugglins able to use microbial peptide permeases. The best studied example is the dipeptide alafosfalin (alaphosphin, Ro-03-7008), in which the *N*-terminal alanyl residue serves to transport the toxic alanine mimetic, L-1-aminoethylphosphonic acid [Ala(P)]. Alafosfalin showed broad-spectrum antibacterial activity against Gram-negative and Gram-positive bacteria, which primarily involved inhibition of alanine racemases and, thus, peptidoglycan synthesis (Allen *et al.*, 1979a,b). The rationale for the design of alafosfalin was based on known specificities of Opp from *E. coli*, but alafosfalin was later shown to be taken up predominantly by Tpp, and can be used to select for Tpp mutants (Payne, 1983). Phosphono-dipeptides based on 4-amino-4-phosphonobutyric acid (phosphonic acid analogue of glutamic acid, Glu(P)) have also been synthesised and evaluated for their antibacterial activity. Dipeptides containing *N*-terminal Ala, Leu, Ile, Phe or Lys showed marked activity against *E. coli*. The structure-activity relationship, i.e., the dependence of activity on the nature of the *N*-terminal component, indicated that transport of the peptide through the bacterial cytoplasmic membrane constitutes a crucial step in its antibacterial activity (Zboinska *et al.*, 1993).

Peptides containing different derivatives of N³-(4-methoxyfumaroyl)-L-2,3-diaminopropanoic acid (FMDP) (including the N³-fumaroyl substituent found in lindenbein), have also been synthesised and shown to have both antibacterial and antifungal activity (Andruszkiewicz *et al.*, 1987; Milewski *et al.*, 1991). These mimetics were rationally designed as glutamine analogues that are active against glucosamine-6-phosphate synthase. FMDP inactivates the enzyme by forming a covalent bond with the Cys-1 residue localised in the glutamine-binding domain. FMDP itself is poorly transported into microbial cells but incorporation of this compound into a peptide structure, according to the 'warhead delivery' concept, resulted in a series of FMDP-peptides that could be transported by Opp and Dpp (Chmara *et al.*, 1998).

In the examples above, amino acid mimetics have been attached to a peptide carrier at either the *N*- or *C*-terminus; other studies have explored the effects of modifications to the peptide backbone. Thus, a series of di- and trialanine analogues, in which the usual peptide linkage (-CO-NH-) was reversed (-NH-CO-) (retro), extended as in -CO-NH-NH (hydrazino) or -CO-NH-O (aminoxy), or an α -carbon was replaced by a nitrogen (α -aza) have been studied. The aminoxy and hydrazino compounds were found to be inhibitory towards Gram-negative and Gram-positive bacteria (Morley *et al.*, 1983a,b; Payne *et al.*, 1984). Surprisingly, synthetic analogues with a D-OAla residue proved more antibacterial than the corresponding L-OAla homologues. The ability to transport peptides containing D-residues contrasted sharply to the normal situation, in which the D-stereochemical configurations severely restricted uptake (Payne *et al.*, 1984). Although results from these studies contributed towards defining structural features that are acceptable to bacterial peptide permeases, the intrinsic toxicity of these particular mimetics precluded their therapeutic applications. Fig. 1-5 shows some examples of synthetic smugglin design.

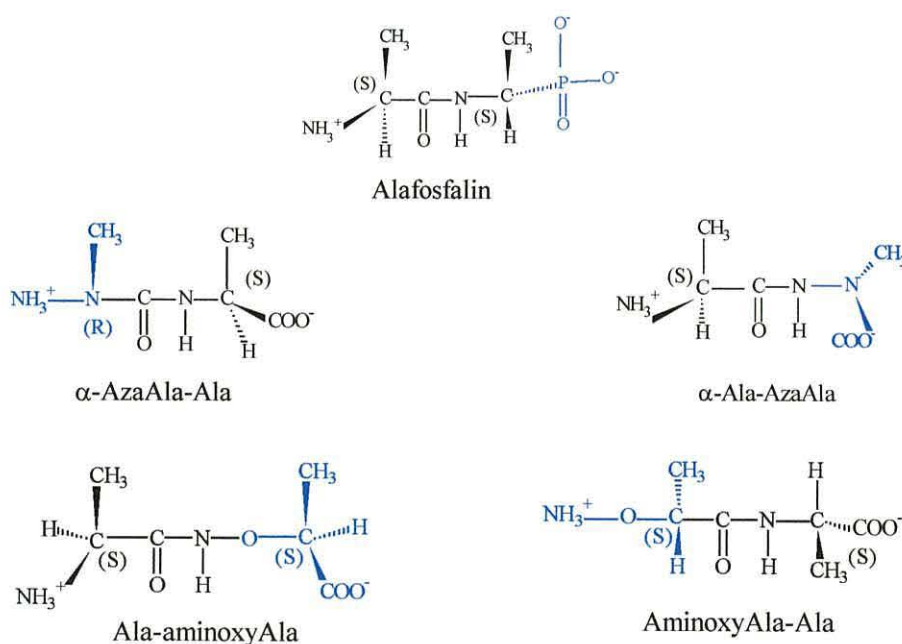


Figure 1-5: Examples of Some Synthetic Peptide Smugglins.

Synthetic smugglins containing peptide backbone-modifications (shown in blue), with alanine as the transport moiety.

1.6. Mammalian Peptide Transporters PepT1 and PepT2

Although the existence of a transport system for intact peptides in the brush border membranes of intestinal and renal absorptive epithelial cells was known, a comprehensive knowledge concerning their structure and function has only recently been obtained through biochemical and molecular biological studies (Daniel & Herget, 1997; Fei *et al.*, 1998). These studies have led to the identification of two distinct peptide transporters, PepT1 and PepT2, that not only have nutritional roles but also pharmacological relevance (Leibach & Ganapathy, 1996; Balimane *et al.*, 1998; Yang *et al.*, 1999).

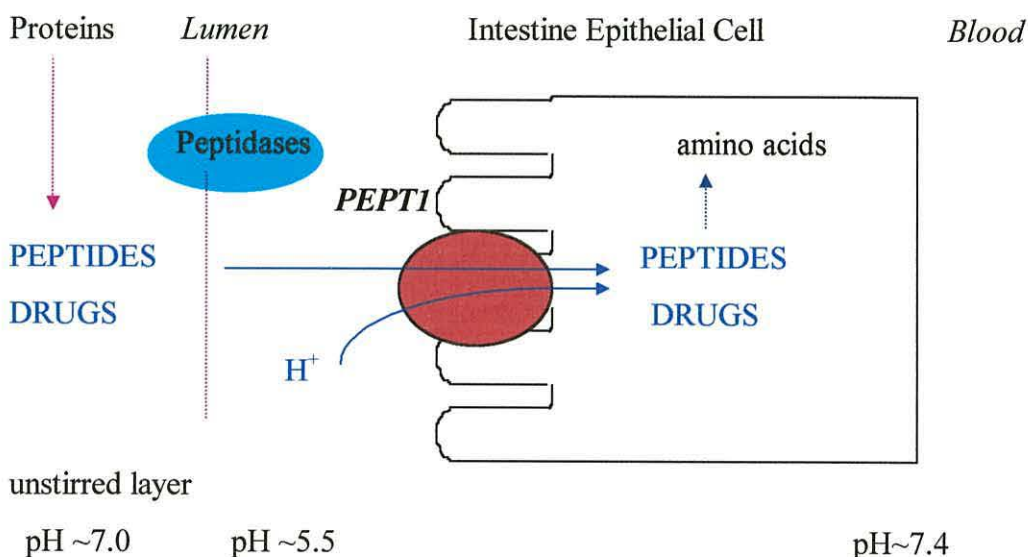


Figure 1-6 : Active Transport of Oligopeptides and Peptide-Based Drugs into Intestinal and Renal Epithelia.

Small peptides and peptide-based drugs, such as β -lactam antibiotics and ACE inhibitors, are actively transported across intestinal or renal brush border membrane via the H⁺-coupled oligopeptide transporters PepT1, in a process driven by the proton-motive force. Inside the cells some peptides are degraded into single amino acids and exit the basolateral membrane via specific amino acid transporters, or are further metabolised. Similar mechanisms for the absorption of oligopeptides and peptide-based antibiotics exist in renal epithelia, which strongly expresses the H⁺-coupled oligopeptide transporter PepT2.

PepT1 provides the major route for the absorption of the end-products of protein digestion in the intestine (Matthews, 1991). In renal proximal tubules, PepT2 reabsorbs filtered di- and tripeptides and protein degradation products, as well as peptide-like drugs (Fig. 1-6) (Daniel & Herget, 1997). PepT1- and PepT2-mediated peptide transport is driven by the proton-motive force, which is provided by the acidic environment of the unstirred aqueous layer lining the surface of the intestinal and renal brush border membranes (Ganapathy *et al.*, 1994; Nussberger *et al.*, 1997). Studies on the H⁺-coupling stoichiometry for neutral, acidic and basic peptides have shown that the proton to peptide coupling ratios are 1:1, 2:1 and 1:1, respectively (Nussberger *et al.*, 1997). The residues involved in catalytic activity have shown to be His⁵⁷ in PepT1 and His⁸⁷ in PepT2 (Fei *et al.*, 1997). The peptide transporters have a broad substrate specificity, but differ in their *affinity* for substrates, PepT1 being a low-affinity transporter and PepT2 being a high-affinity transporter. Both PepT1 and PepT2 proteins consist of 12 transmembrane domains (TMD) and exhibit significant similarity to each other at the level of their respective amino acid sequences. The differences in their substrate affinity is thought to be a result of variations in the structure of the putative substrate binding site in TMDs 7,8, and 9 of the transporters (Fei *et al.*, 1998). In addition, the functional regions which are associated with the extracellular pH changes and are responsible for substrate recognition by PepT1 and PepT2 are thought to be located in the *N*-terminal halves of the proteins. The domain that affects substrate affinity is postulated to exist in the *C*-terminal as well as in the *N*-terminal half of PepT2 (Terada *et al.*, 2000).

1.6.1. Substrate Specificity of PepT1 and PepT2

There have been several recent studies regarding the characterisation of the structural requirements for substrates that can be recognised by the intestinal and renal peptide transporters. PepT1 has been shown to actively transport di- and tripeptides and a variety of peptidomimetics (Leibach & Ganapathy, 1996; Daniel, 1996; Adibi, 1997; Walter *et al.*, 1996). Temple and co-workers reported that 4-aminophenylacetic acid, a peptide mimetic lacking a peptide bond, could act as a substrate for the intestinal peptide transporter (Temple *et al.*, 1998).

Replacing the peptide bond in Ala-Pro by a thioxo peptide bond has been shown to be tolerated by PepT1 when in a *trans* conformation (Brandsch *et al.*, 1998), and amino acid aryl amides can also be transported with high affinity (Börner *et al.*, 1998). Döring *et al.* (1998) discovered that δ -aminolevulinic acid, used for tumour treatment, is a substrate for PepT1 and PepT2 (Döring *et al.*, 1998). The substrate specificities of PepT1 and PepT2 are similar to that of the bacterial peptide transporters, in that peptide analogues which lack peptide bonds but retain features of charge and spatial separation, may also show binding and transport (Elliott, 1993; Verkamp *et al.*, 1993; Marshall, 1994).

Chemotherapeutic agents such as acyclovir and valacyclovir are transported across the gastrointestinal (GI) tract by a number of transporters, including the H⁺-coupled peptide transporters. Thus, it is desirable to understand the precise nature of the absorption mechanism of these drugs to improve their bioavailability and reduce the variability that is commonly observed *in vivo* in human patients (Balimane & Sinko, 1999). Like the delivery of antimicrobial peptide prodrugs in bacteria (section 1.5; Fig. 1-3), several groups have reported the higher oral bioavailability of the prodrug valacyclovir, compared to acyclovir, via its transport by PepT1 (Ganapathy *et al.*, 1998; Han *et al.*, 1998; Guo *et al.*, 1999).

Structural features believed to be crucial for substrate-carrier interaction are molecular size, stereo-isomerism, spatial arrangement, hydrophobicity, polarity and charge. In order to determine the minimal structural requirements of substrates for recognition by PepT1, Döring and co-workers have shown that the electrogenic transport of substrates is related to the distance between the carboxylic carbon and the amino nitrogen (Döring *et al.*, 1998). Results from Li and co-workers study on structure-affinity relationships of ValVal and ValValVal, also indicated that the distance between the *N*-terminal amino group and the *C*-terminal carboxyl group is important for interaction of substrates with the oligopeptide transporter (Li *et al.*, 1998). The transport of dipeptides containing proline residues by the peptide transporters has been the subject of a number investigations (Miyamoto *et al.*, 1987; Tiruppathi *et al.*, 1990; Daniel *et al.*, 1992; Thwaites *et al.*, 1994). These studies have shown that some X-Pro dipeptides are good substrates for both renal and intestinal peptide transporters.

However, Miyamoto *et al.* (1987) and Daniel *et al.* (1992) found very low or undetectable uptake of Pro-Gly and Pro-Leu by the renal peptide transporter (Miyamoto *et al.*, 1987; Daniel *et al.*, 1992). Similarly, in Caco-2 cells, an excess of Pro-Gly (> 20 mM) inhibited the uptake of Gly-Sar by only 59% (Thwaites *et al.*, 1994) and that of cephalexin by only 67% (Gochoco *et al.*, 1994). Such results have led to the prevailing view that, in contrast to X-Pro dipeptides, Pro-X dipeptides are generally not good substrates for peptide carriers. In a similar study, Brandsch *et al.* (1999) investigated the decisive structural determinants for the interaction of proline derivatives with the intestinal H⁺-coupled peptide transporter. They measured the affinity of X-Pro and Pro-X dipeptides for the peptide carrier by the ability of these dipeptides to inhibit Gly-Sar transport in Caco-2 cells. Gly-Sar is commonly used as a reference substrate for peptide transport because of its relatively high resistance to peptidase activity (Brandsch *et al.*, 1997). Results from Brandsch and co-workers study showed that X-Pro dipeptides display a striking correlation between their *cis/trans* ratios and their affinity constants, with *trans* conformations having a higher affinity. These results revealed the critical role of the peptide bond conformation for recognition by PepT1, even for a transport protein that has a broad substrate specificity (Brandsch *et al.*, 1999).

Swann and co-workers examined the relationship between chemical structure and affinity for PepT1 using comparative molecular field analysis (CoMFA), as a 3-D approach towards building quantitative structure-activity relationships (QSAR). Various biological activity parameters and molecular descriptors were examined and their resulting field map provides information on the geometry of the binding site cavity (Swaan *et al.*, 1998). Recently, Bailey and colleagues have determined a template for PepT1 substrate specificity. This model was obtained by relating the substrate specificities of a range of compounds including: i) dipeptides; ii) dipeptide mimetics; iii) tripeptides; iv) β -lactams and v) other drugs, with their *in vitro* binding and transport studies. By considering different combinations of potential binding features, they identified a template for these PepT1 substrates (Bailey *et al.*, 2000).

Their model identifies key binding sites in PepT1, whilst the 3-D layout of the template is defined by other stereochemical and conformational features, including: i) a strong binding site for an *N*-terminal NH_3^+ group; ii) preference for L-stereochemistry to accommodate the $\text{C}\alpha$ near the *N*-terminus; iii) an extended planar backbone from the *N*-terminal $\text{C}\alpha$ to the second $\text{C}\alpha$; iv) a hydrogen bond to the carbonyl group of the first peptide bond and v) alkylation of the amide nitrogen allows recognition. This template provides a model for the orientation of the key binding features of substrates for PepT1, and allows prediction of high, medium or low substrate affinity for PepT1. Some classes of compounds do not “fit” this model (Bailey *et al.*, 2000).

1.6.2. Oral Delivery of Peptide Drugs

In addition to their physiological function of absorbing di- and tripeptides resulting from digestion of dietary proteins, the intestinal transporters also absorb some orally administered peptidomimetic drugs and, therefore, play an important factor in the bioavailability of these compounds (Yang *et al.*, 1999). Administration of drugs by the oral route is the desired method for drug delivery as it has improved patient compliance compared with intramuscular (IM) or intravenous (IV) routes. Although peptide-based drugs benefit from the unique absorption capability of the intestine, they also suffer from its digestive ability. Amino acids, peptides and peptide-type drugs are absorbed through the brush border membrane by specific transport systems for amino acids and small peptides (Matthews, 1991; Bai & Amidon, 1992). Various exo- and endopeptidases which are anchored to the brush border membrane cleave polypeptides and protein fragments, resulting from the actions of gastric and pancreatic enzymes, to amino acids and di/tripeptides (Fig. 1-6). Factors determining oral bioavailability of peptides are intestinal membrane permeability, size limitation, intestinal and hepatic metabolism and, in some cases, solubility limitations. For this reason, peptides are modified to peptidomimetics and prodrugs in order to improve their oral delivery by the intestinal transporters (Taylor & Amidon, 1995; Borchardt *et al.*, 1997; Wang *et al.*, 1999).

1.7. Modification of Peptides into Peptidomimetics

A key area in peptide drug design is the synthesis of peptidomimetic molecules that are expected to have the same therapeutic effects as natural peptides, but with the added advantage of metabolic stability (Hruby *et al.*, 1997; Kieber-Emmons *et al.*, 1997; al-Obeidi *et al.*, 1998). The term “peptidomimetic” has been defined in a number of ways including: “ a molecule that mimics the biological activity of a peptide but is no longer peptidic in nature, such as pseudo-peptides, semi-peptides and peptoids” (Moore, 1994). Giannis and Kolter (1993) discuss peptidomimetics in terms of ligands for receptors and define a mimetic as “a compound that, as a ligand of a receptor, can imitate or block the biological effect of a peptide at the receptor level” (Giannis and Kolter, 1993). Modified peptides are also used for investigations into molecular recognition and protein folding, and Kemp (1990) defines peptidomimetics as “elements which mimic the structure of natural peptide components” (Kemp, 1990).

1.7.1. The Rational Design of Peptidomimetics

Pioneering work by a number of academic and industrial research groups has led to a fundamental approach using molecular design and synthetic chemistry strategies for the modification of peptides into peptidomimetics (Fig. 1-7) (Taylor & Amidon, 1995; Hruby *et al.*, 1997; Muller & Giera, 1998). The rational design of peptide mimetics starts with the identification of the primary structure of the biologically-active peptide. Shorter analogues are synthesised to identify the minimal sequence required for biological activity. The role of each individual amino acid and its contribution to biological activity is determined by the replacement of the side chain moieties by e.g. methyl groups, pseudoisosteric groups, or by groups with different physicochemical properties. Identification of the bioactive conformation of a peptide, i.e., those regions of the peptide that are essential for its recognition by and interaction with the complementary domains of the receptor or enzyme, is a key aspect of peptidomimetic design and is achieved by combining X-ray crystallography, NMR and computational chemistry data with synthetic chemistry (Zhang *et al.*, 1998; Abel *et al.*, 1998; Pellegrini & Mierke, 1999; Hornak *et al.*, 1999; Oakley & Wilce, 2000; Ooms, 2000).

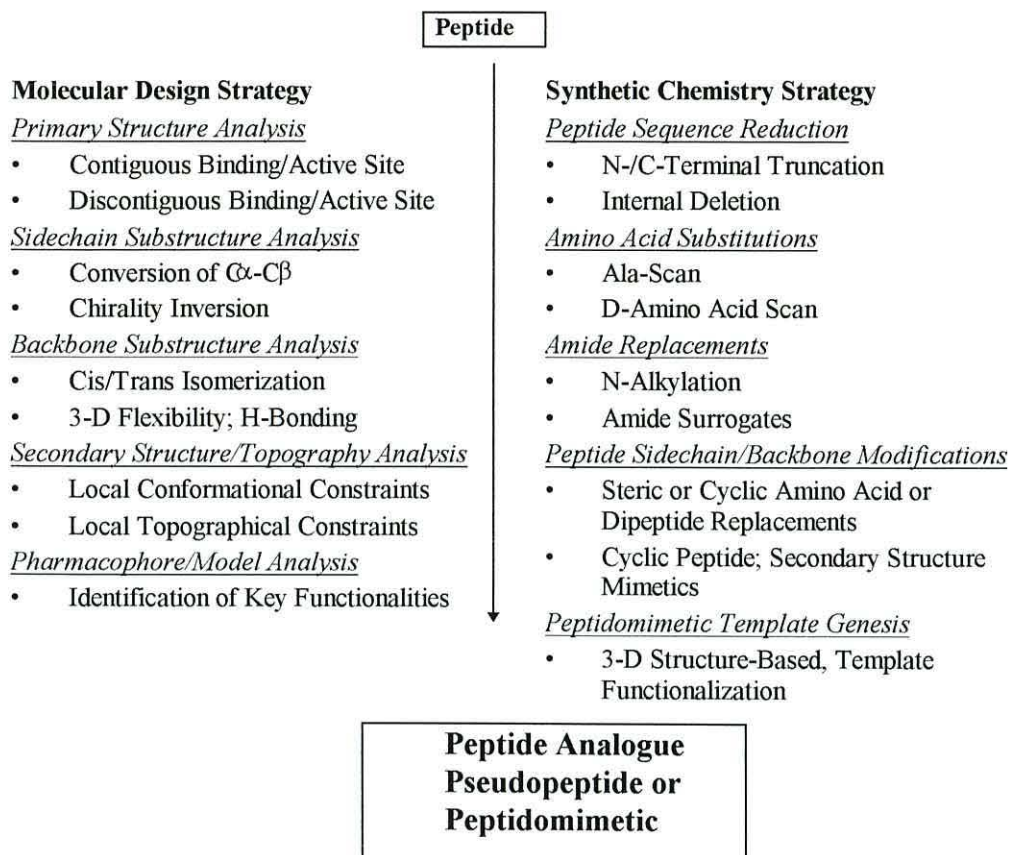


Figure 1-7: The Modification of Peptides into Peptidomimetics.

Molecular design and synthetic chemistry approaches are integrated for the rational design of peptidomimetics.

X-ray crystallography is the optimal method of getting a complete 3-D structure; but since it is the structure in the solid state, it may not truly reflect the biologically active conformation of the peptide being studied. Determination of receptor geometry to a high resolution using X-ray crystallography is difficult for several reasons, including availability of sufficient quantities of receptor and growing good quality crystals suitable for X-ray diffraction (Oakley & Wilce, 2000; Smyth & Martin, 2000).

NMR has the advantage of elucidating the structure of oligopeptides in both solid state and in solution. This technique can provide information of the free molecule in solution, and when complexed with another macromolecule, i.e., a receptor. However, the major drawback of this technique is that the information for a rather complex molecule may not be very accurate, and refinement of the structural data becomes complicated for larger complexes (Pellegrini & Mierke, 1999).

X-ray crystallography and NMR methods can be complemented by theoretical computational techniques to lead to Computer-Aided Drug Design (CADD). A variety of computational chemistry techniques such as steric fitting, molecular mechanics, molecular dynamics, Monte Carlo simulations, free energy perturbation and quantum chemical calculations in combination with computer graphics have been used for structural analysis of compounds (Bohm, 1996; Hornak *et al.*, 1999; Koehler & Villar, 2000; Ooms, 2000).

Once the 3-D structure of a target peptide is known, further establishment of its conformation can be done by constrained analogue design using a database of constrained or metabolically stable peptide moieties. Conformational constraint is an attractive strategy for peptidomimetic design as it can improve the affinity, selectivity and efficacy of peptide ligands, as well as increase stability against enzymatic hydrolysis. The effect of conformational constraints on receptor affinity can be discussed simply in terms of Fischer's "lock-and-key" model. It can be considered that certain conformers present in conformer equilibrium of a flexible peptide in solution would interact with the receptor without undergoing a significant conformational change. "Freezing" of this "bioactive" conformation through introduction of conformational constraints would lead to an increased affinity since most/all of the molecules, rather than a small fraction, would be able to bind to the receptor (Giannis & Kolter, 1993).

Synthetic peptides can be conformationally fixed by introducing local or global conformational constraints. Local constraints include the replacement of the amide moiety by isosteres and the introduction of amino acid residues with conformational-restricting ability. The latter approach is based on the assumption that the insertion of these residues with reduced conformational space available for ϕ and ψ torsional angles will have an impact on the overall conformation of a small peptide. The disadvantage of local constraints is that the resulting overall conformation is not always predictable. Therefore, defining the conformational template for the biologically active conformation requires the development of global constraints (Moore, 1994; Hruby *et al.*, 1997).

Global constraints in peptides include cyclic side-chain-to-side-chain structures, cyclic side-chain-to-backbone structures (lactams), cyclic backbone-to-backbone structures and mimics of secondary structures, e.g., α -helices, β -sheets, β -turns and γ -turns. The influence of constraints on the conformation of the peptide is investigated using biophysical techniques, in order to obtain conformer-activity relationships (Giannis & Kolter, 1993).

The final phase of rational design is the synthesis of compounds with topological constraints. At this stage the previously obtained insights are used to position the amino acid side chains correctly into a molecular template, a so-called scaffold, in a particular spatial order that is in agreement with the previously defined bioactive topology. The optimal molecular scaffold is a polyfunctional, small (5-7-membered) ring of defined stereochemistry, that can adopt only one significant conformation and have strong stability against enzymic degradation (Hruby *et al.*, 1997).

1.7.2. The Range of Peptidomimetics

The application of molecular design and synthetic chemistry has produced an extensive range of peptidomimetics which have been reviewed (Rizo & Gierasch, 1992; Giannis & Kolter, 1993; Taylor & Amidon, 1995; Hanessian *et al.*, 1997; Gillespie *et al.*, 1997; Fletcher & Campbell, 1998). This review will discuss examples of peptide backbone modifications, lactam-constrained mimetics and torsionally-constrained mimetics.

1.7.2.1. Modification of Peptide Backbone

Modification of the peptide backbone can be achieved by insertion of unusual amino acids which can lead to an increase in the biological half life of a compound and does not generally involve restrictions in conformations. Partial synthetic modifications of peptides to yield pseudopeptides with amide bond replacements have been reported and include aminomethylene, ketomethylene, ethylene, retroamide, thioamide, ester, hydroxymethylene and hydroxyethylene structures (Taylor & Amidon, 1995; Gillespie *et al.*, 1997). These amide bond replacements provide insight into conformational and H-bonding characteristics at the particular site of the chemical modification, and impart stability towards enzymic cleavage.

These compounds may also be used in the design of peptidase inhibitors as a result of their transition-state mimicry, and be used for antagonist discovery (Gillespie *et al.*, 1997). The partial double bond character of the amide bond leads to *cis* and *trans* isomerism. In peptides, the *trans* configuration is generally more energetically favourable. Amide bonds with *cis* configuration have been found in cyclic peptides and β -turns and dipeptide analogues that mimic “*cis*-amide bonds” that occur in peptides have been synthesised (Giannis & Kolter, 1993).

1.7.2.2. Lactam-Constrained Mimetics

Lactam rings are commonly used as conformational constraint in peptides in order to obtain the bioactive conformation, or to increase the biological potency of a peptide. Syntheses that also allow the incorporation of side chains have been described, and these structural variations can be extended further by decreasing or increasing the size of the lactam ring, by incorporation of heteroatoms, or by attachment to aromatic rings. “Freidinger lactams” have commonly been used to enforce a *trans* amide conformation and have been incorporated into many metalloprotease inhibitors as conformationally constrained analogues of Phe-Pro or Ala-Pro (Gillespie *et al.*, 1997; Hanessian *et al.*, 1997). The β -turn is a structural motif common to many biologically active, cyclic peptides and has been postulated in many cases as the biologically-active form of linear peptides. For this reason, it is the most frequently imitated secondary structure and there are a number of compounds designed and synthesised as β -turn mimetics (Gillespie *et al.*, 1997; Hruby *et al.*, 1997).

1.7.2.3. Torsionally-Constrained Mimetics

These motifs are characterised by specific angular and torsional parameters, in addition to an important 10-membered intramolecular H-bond that orients two peptide units from each end. Such a highly constrained dipeptide mimetic has been categorised under the general name of a bicycloalkane skeleton by Hanessian *et al.* (1997). The attachment of one or more rings to this basic bicyclic amino acid structure is possible, and it can also encompass heteroatom analogues in which the carbon is replaced by sulphur, oxygen or nitrogen at different sites. These compounds are categorised as carbo-, thio, oxa -and diaza-bicycloalkane amino acids (Hanessian *et al.*, 1997).

These templates in which the peptide backbone geometry and sidechain functionality are restrained in bicycloalkane ring systems, have found important use as antibacterials and as constituents of metalloprotease inhibitors.

An overview of peptide modifications used for the development of therapeutic peptides has been provided in a number of reviews including Giannis & Kolter, 1993; Adang *et al.*, 1994; Taylor & Amidon, 1995; Hanessian *et al.*, 1997; Kieber-Emmons *et al.*, 1997 and Ooms, 2000.

1.8. Prodrug Approaches for Improved Peptide Drug Delivery

Prodrug design comprises another area concerned with the optimisation of peptide drug delivery (Taylor & Amidon, 1995; Oh *et al.*, 1999; Wang *et al.*, 1999). A prodrug is a pharmacologically inactive derivative of a parent drug molecule that requires spontaneous or enzymatic transformation within the body to release the active drug. Several drugs are efficiently absorbed from the GI tract but show limited bioavailability due to presystemic metabolism in the intestinal lumen, at the brush border of the intestinal cells, or in the mucosal cells lining the GI tract, or in the liver. To solve these delivery problems, derivatives of the bioactive peptides are used to produce prodrugs. Such derivatization may protect small peptides against degradation by enzymes present at the mucosal barrier as well as render hydrophilic peptides more lipophilic and facilitate their passive absorption. Several bioreversible derivatives for the functional groups or chemical entities, such as carboxyl, hydroxyl, thiol, amino and amido groups, occurring in the amino acids and peptides have been explored and discussed (Taylor & Amidon, 1995; Naider & Becker, 1997; Wang *et al.*, 1999; Borchardt, 1999). This review will focus on the prodrug modification of angiotensin-converting enzyme (ACE) inhibitors for their improved oral absorption.

1.8.1. Angiotensin-Converting Enzyme (ACE) Inhibitors

1.8.1.1. The Renin-Angiotensin System (RAS)

The RAS cascade is involved in the physiological control of blood pressure and starts with the secretion of the enzyme renin in response to low blood pressure. Renin acts on angiotensinogen to produce angiotensin I (A-I), a biologically inactive prohormone. Angiotensin I is then cleaved to form the active hormone angiotensin II (A-II), by angiotensin-converting enzyme (ACE) (Fig. 1-8).

The treatment of hypertension by modulation of the RAS has focused mainly on the regulation of the concentration of angiotensin-II (A-II), which is a potent vasoconstrictor (Adang *et al.*, 1994).

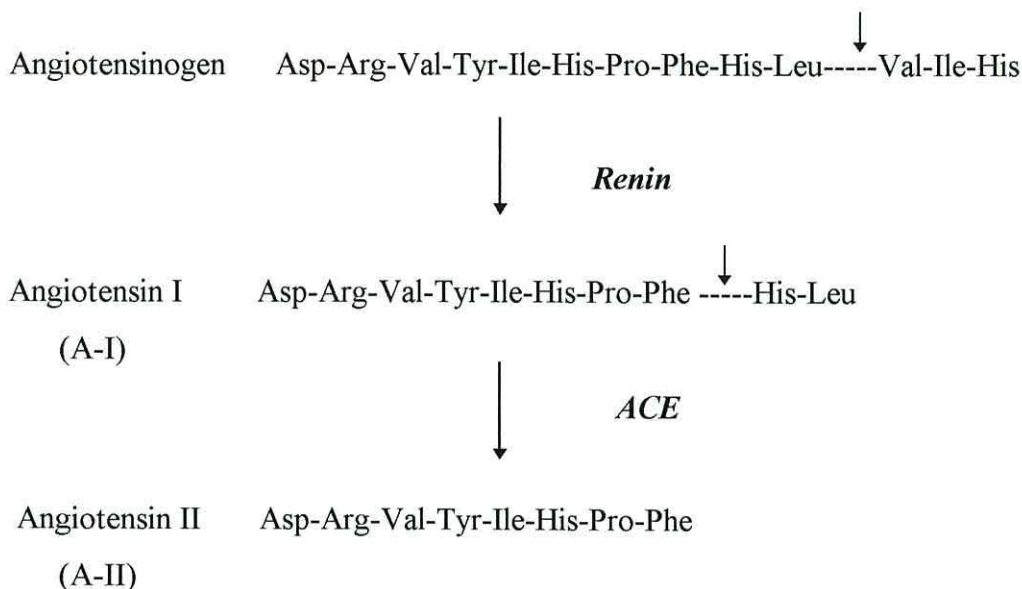


Figure 1-8: The Renin-Angiotensin System (RAS)

Inhibition of either ACE or renin will decrease the formation of A-II and thus lead to lowering of the blood pressure by reducing vasoconstriction ↓ (denotes cleavage site).

1.8.1.2. Prodrug Modification of ACE Inhibitors

As antihypertensives usually have to be taken over extended periods of time, both oral availability and long duration of action are important parameters in the clinical efficacy of these compounds. A prodrug strategy has been widely used to improve the oral delivery of ACE inhibitors to their intracellular target sites. The majority of ACE inhibitors are *ester prodrugs* that are converted by hepatic esterolysis to an active diacid metabolite (Cleland, 1993). The ACE inhibitor enalapril is an ester prodrug of the pharmacologically active enalaprilat. The prodrug approach of esterification of the diacid enalaprilat to form enalapril was required in order to enhance its oral bioavailability (Kubo & Cody, 1985). Although enalapril has low activity as an ACE inhibitor, it is fairly well absorbed from the GI tract and subsequently hydrolysed to the active diacid form by esterases in the gut, liver, blood and other tissues (Fig. 1-9). Enalapril became the prototype for the development of other structurally-related prodrug ACE inhibitors, and these are discussed later.

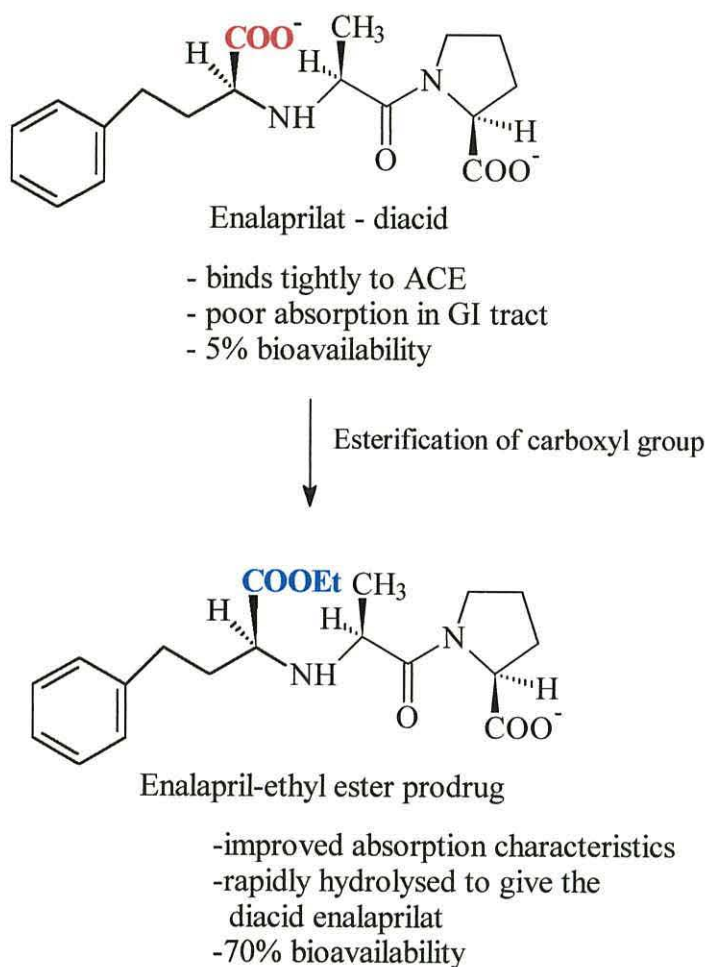


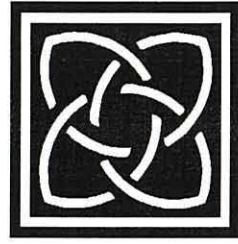
Figure 1-9: Prodrug Modification of the ACE Inhibitor Enalaprilat to Enalapril.

1.8.1.3. Intestinal Absorption of ACE Inhibitors

The transport of ACE inhibitors by intestinal peptide transporters has been studied by several groups, and their uptake has been shown to be significantly inhibited by small peptides and β -lactams (Hu & Amidon, 1988; Friedman & Amidon, 1989a,b; Thwaites *et al.*, 1995; Swaan *et al.*, 1995). In a recent study of structure-transport relationship of the intestinal peptide carrier, Schoenmakers and colleagues used enalapril and a modified analogue, enamipril, with a reduced peptide bond. From their study, Schoenmakers and colleagues conclude that the carbonyl group is an essential structural requirement for transport by the small-peptide carrier (Schoenmakers *et al.*, 1999).

1.9. Aims of Study

- Recent advances in structural characterisation of biomolecules, computer science and molecular biology have provided an aid to rational drug design.
- However, a better understanding of the *molecular recognition processes* involved in protein-ligand interactions is required for the successful design of peptide drugs with good oral bioavailability, as well as biological potency.
- The bioavailability of peptide drugs is dependent on peptide transport systems that are widely distributed in Nature. The main aim of this study is to establish the molecular recognition templates (MRTs) that govern the effective uptake of natural peptides by peptide transporters, and to apply this to the *rational* design of peptide drugs.
- Bacterial peptide permeases have some common substrate specificities with mammalian PepT1 and PepT2 transporters and will be used for the study of SAR of peptide transport.
- The substrate specificity of the dipeptide permease binding protein (DppA) of *E.coli* will be investigated using a number of microbiological and biochemical techniques, and molecular modelling will be used to determine the bioactive *conformations* of natural peptides.
- Results from these study will establish the molecular recognition templates (MRTs) that define the structural and conformational features involved in uptake of substrates by peptide transporters.
- The established MRTs will then be applied as preliminary screens to assess the oral bioavailability of peptidomimetics, peptide drugs, e.g. ACE inhibitors, and antimicrobial smugglins by the intestinal PepT1 transporter, using computer-based conformational analysis.
- Computer-aided drug design will be used for the *rational* design of peptidomimetics and peptide-based drugs to produce theoretical compounds with structural and conformational features that match the MRTs.
- Application of the MRTs to the *rational* design of peptidomimetics and peptide drugs will lead to effective oral delivery by PepT1 and PepT2 transporters, and an improvement in oral bioavailability of these compounds.



CHAPTER 2
MATERIALS AND METHODS

2. MATERIALS AND METHODS

2.1. Preparation of Growth Media

All reagents were purchased from either Sigma Chemical Co. Ltd., Dorset, U.K. or from Merck-BDH Ltd., Dorset, U.K., unless stated otherwise.

2.1.1. Minimal Medium 'A'

Minimal medium 'A' (Davis and Mingioli, 1950), was made as a 10x concentrate. One litre of this medium, in distilled water, contained: 70g K₂HPO₄, 30g KH₂PO₄, 1g MgSO₄.7H₂O, 5g tri-sodium citrate.3H₂O and 15g (NH₄)₂SO₄. The pH of a 10-fold dilution of this was checked to be pH 7.2. The solution was autoclaved (15 psi for 15 min at 121 °C), in 200 ml aliquots and stored at room temperature. For use, this medium was diluted to a 1x concentrate with sterile distilled water, 0.5 % (w/v) D-glucose and any supplements required by the strain to be grown. All supplements were sterilised separately by autoclaving as above, except tryptophan, which was filter sterilised using pre-sterilised Oxoid cellulose acetate 0.45 µm pore filters (Oxoid Ltd., Hants., U.K.).

2.1.2. ML Broth

ML broth (Miller, 1972) was made as a 1x concentrate. One litre of this medium, in distilled water, contained: 10g Bacto tryptone (Difco Laboratories Ltd., Surrey, U.K.), 5g yeast extract (Oxoid Ltd., Hants., U.K.) and 5g NaCl. This was autoclaved and stored in 5 ml aliquots at room temperature.

2.1.3. Agar Plates

Agar plates were composed of either ML broth or Medium 'A' containing 1.5 % (w/v) agar (Difco Bacto-agar, Difco Laboratories Ltd., Surrey, U.K.), 0.5 % (w/v) D-glucose and any supplements required by the strain to be grown. Agar-containing media was poured into petri dishes and plates were dried under sterile conditions.

2.2. Bacterial Strains

Table 2.1. shows the *E.coli* K-12 strains used in this study. JM101 was used as the source of DppA, as this strain has the ability to overexpress DppA, when grown in minimal media (Olson *et al.*, 1991).

Table 2.1. *E. coli* K-12 Strains Used in this Study

| Strain | Genotype/ Phenotype | Source | Reference/ Comment | Supplements Required |
|--------|---|--|--|--|
| JM101 | <i>supE, thi,</i> $\Delta(lac-proAB)$ [F' <i>traD36 proA</i> ⁺ <i>proB</i> ⁺ <i>lacFZ</i> $\Delta M15$] | Dr.E.Olson Parke-Davis Pharmaceutical Division, Michigan U.S.A. | Overproduces DppA in minimal media | 2 μ g ml ⁻¹ Thiamine |
| M2034 | <i>trpE9851 leu 277F IN</i> (<i>rrnD-rrnE</i>) | C.G.S.C. U.S.A. | (Morse & Guertin, 1972) | Leu, Trp, Glucose |
| PA0183 | $\Delta(tdk-tonB)opp$ | This laboratory | Derivative of M2034 | Leu, Trp, Fe ³⁺ |
| PA0410 | $\Delta(tdk-tonB)opp, tpp$ | This laboratory | Derivative of PA0183 | Leu, Trp, Fe ³⁺ |

E. coli M2034 (Morse & Guertin, 1972) was used as a parental strain from which peptide-transport mutants were derived. Dpp mutants (*dpp*) were isolated from strain PA0183, which carries a deletion, $\Delta(tdk-tonB)$, that includes *opp* (Smith *et al.*, 1999). Mutants defective in Tpp were selected from PA0183 by resistance to ValValVal coupled with cross-resistance to alafosfalin (Smith & Payne, 1990). One such mutant, strain PA0410, was used for measurements of transport by Dpp.

2.2.1. Growth of Bacterial Strains

Routinely, bacterial strains were removed from a frozen glycerol stock culture (40 % (v/v) glycerol, stored at -70 °C), using a sterile, wooden cocktail stick, and used to inoculate 5 ml ML broth in a McCartney bottle. This culture was grown overnight, with shaking at 37 °C, and then streaked onto an appropriate agar plate using a flame-sterilised platinum wire loop. These were grown up overnight at 37 °C and then stored at 4 °C. When required, bacteria were removed from agar plates, using a flame-sterilised platinum wire loop, and used to inoculate either 5 ml ML broth or appropriately supplemented 'A' medium and cells were grown overnight as before.

2.3. Purification of DppA from JM101

For purification of DppA from JM101, 100 μ l of cells in ML broth was used to inoculate 5 flasks containing 800 ml of minimal media, supplemented with 1 μ g/ml thiamine and 0.5% glucose. The cells were grown overnight with shaking at 37°C.

2.3.1. Cold Osmotic Shock

This was done by modification of the procedure of Neu & Heppel (1965), and was developed in this laboratory (Smith *et al.*, 1999). The cold osmotic shock procedure involves the plasmolysis of bacterial cells in the presence of EDTA and sucrose. The plasmolyzed cells are harvested and then resuspended in ice-cold deionized water, followed by the addition of 50 mM MgCl₂ solution. This method selectively releases proteins located within the periplasmic space (Furlong, 1987). Cells from JM101 were grown to late-exponential phase, A₆₆₀ = 0.6, and transferred to four 250 ml centrifuge tubes (200 ml cells per bottle). Cells were harvested by centrifugation at 10,000 rpm for 10 min in a Beckman JA 20-21 centrifuge using a JA-14 rotor. The supernatant solution was discarded and cells were resuspended in 20 ml of 10 mM Tris/HCl pH 7.3/30 mM NaCl solution at room temperature. Cells were transferred to JA-20 (50 ml) centrifuge tubes and further centrifuged at 10,000 rpm for 5 min. The supernatant was removed and cells were resuspended in 27 ml of 10mM Tris/HCl pH 7.3/30 mM NaCl solution. Cells were centrifuged at 10,000 rpm for 5 min, the supernatant solution was discarded, and cells were resuspended in 13 ml Tris/HCl pH 7.3 solution. 13ml of a solution containing 40 % (w/v) sucrose, 33 mM Tris/HCl pH 7.3 and 2 mM EDTA was added to each tube. Cells were mixed at room temperature for 5 min and then centrifuged at 12,000 rpm for 10 min. The cell pellets were rapidly resuspended in 27 ml of ice-cold distilled water and kept on ice for 3 min. 530 μ l of 50 mM cold MgCl₂ solution was added and cells were left on ice for a further 10 min. Cells were centrifuged at 10, 000 rpm for 10 min, and the supernatant solution was collected and filtered using Oxoid cellulose acetate 0.45 μ m pore filters. The filtrate was transferred to a dialysis bag and dialysed overnight against 4 l of 2 mM *N*-ethylmorpholine/HCl pH 7.2 at 4 °C. After dialysis, the shockate fluid was divided into 5 ml aliquots and freeze-dried overnight.

2.3.2. Cation-Exchange Chromatography (Mono S)

Each freeze-dried sample, was redissolved in 50 mM malonic acid/NaOH pH 4.8, and placed as 1 ml aliquots in 1.5 ml eppendorf tubes and centrifuged at 12,000 rpm for 5 min. 1 ml samples were injected onto a Pharmacia Mono S HR 5/5 cation-exchange column (Pharmacia LKB Biotechnology, Bucks., U.K.), connected to a Pharmacia FPLC system and pre-equilibrated with 50 mM malonic acid-NaOH pH 4.8. Proteins were eluted using 50 mM malonic acid containing 1 M NaCl with an increasing linear gradient of NaCl (0-1 M), with the flow rate maintained at 1.5 ml min⁻¹. The absorbance of the eluate was continuously monitored at 280 nm. Fig. 2-1A shows a typical chromatogram for this column for *E.coli* JM101 osmotic shock fluid. Two peaks were observed and fractions corresponding to both peaks were collected (fraction volume ca. 1 ml). The larger, second peak corresponds to DppA, as judged by SDS-PAGE analysis (Fig. 2-2). and fractions corresponding to this peak were combined, transferred to dialysis bags and dialysed overnight against 2 mM *N*-ethylmorpholine/HCl pH 7.2. The contents of all dialysis bags were combined and divided into 5 ml aliquots, lyophilised and stored at -20 °C. Fractions from the other peaks were also combined together and stored at -20 °C and 1 ml aliquots were used for SDS PAGE analysis when required.

2.3.3. Reverse-phase Chromatography (RPC)

RPC was used on some Mono-S samples to free DppA from endogenous ligands. Trifluoroacetic acid (TFA) was obtained from Pierce Warriner Ltd., Cheshire, U.K. and acetonitrile (HPLC grade) from Rathburn, Borders, Scotland. The solvent system used for RPC consisted of 0.1 % (v/v) TFA in distilled water and 0.1 % (v/v) TFA in acetonitrile. Lyophilised Mono S DppA samples were redissolved in aqueous 0.1 % (v/v) TFA and applied to the column, pre-equilibrated with the same buffer. Desorption of bound components was effected by using a linear gradient of acetonitrile containing 0.1 % (v/v) TFA. The Pharmacia Pep-RPC HR5/5 column was run at a flow rate of 0.3 ml min⁻¹ at 214 nm with a gradient of 55 % acetonitrile. A single peak was obtained (Fig. 2-1B) and the corresponding fractions were collected and lyophilised directly without further treatment.

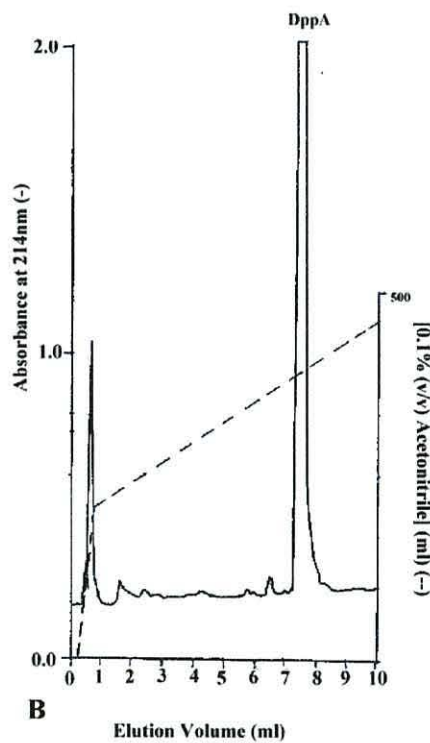
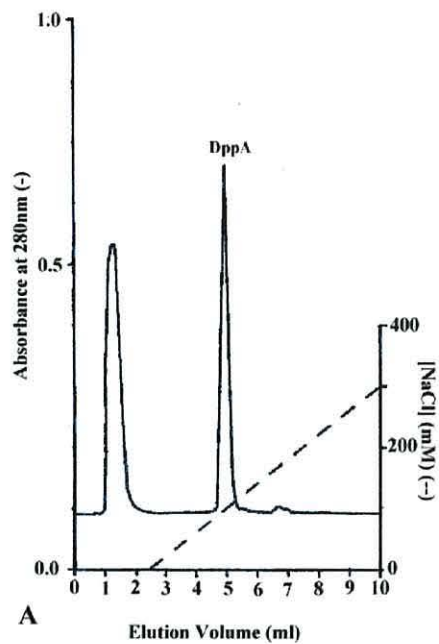


Figure 2-1 : A; Mono-S and B; RPC Purification of DppA from *E. coli* JM101.

1ml of shockate was applied to a Mono S HR 5/5 column in 50 mM Malonic Acid/NaOH pH 4.8. Proteins were eluted from this column with a linear increase of NaCl from 0-1M. Purified DppA from Mono S in 0.1% (v/v) TFA was applied to Pep-RPC HR5/5 column. Desorption of bound components was effected by a linear increase of 0.1% (v/v) TFA in acetonitrile. The peaks corresponding to DppA are indicated.

2.3.4. SDS-PAGE

SDS-PAGE was performed on 10% gels, as described by Laemmli (1970). Resolving gel was composed of deionised water, 30% Acrylamide/bisacrylamide (37:1), 10% ammonium persulphate, 10% SDS, Temed and 1 M Tris/HCl pH 8.8. The stacking gel was also made of the same components as for the resolving gel, but 1 M Tris/HCl pH 6.8 buffer was used. 250 μ l of 5 % (v/v) β -mercaptoethanol was added to 5x concentrate Laemmli sample buffer (Laemmli, 1970), which consisted of 1M Tris/HCl, pH 6.8, 10 % (w/v) SDS, 10 % (w/v) sucrose, 2.5 % (w/v) bromophenol blue. Samples were prepared for mini gel-electrophoresis using Bio-Rad System.

Shockate fluid pre-dialysis, shockate fluid post-dialysis and the fractions from the first peak of Mono-S were mixed with 5x concentrated Laemmli sample buffer. Lyophilised Mono S samples corresponding to the DppA peak (pre-and post-dialysis) were redissolved in distilled water to a concentration of 2 μ g/ μ l of protein. These samples were diluted to obtain 10 μ g, 6 μ g and 4 μ g of DppA and mixed with 2x concentrated Laemmli sample buffer. Sigma 6H molecular mass calibration markers were also used which had proteins with Mr ranging from 10,000 to 70,000 k.

All samples were boiled for 2 min prior to running on 10 % slab gels (18cm x 12cm x 1mm thick) at 100 V through the stacker and 200 V through the resolving gel for 1 h. After electrophoresis, gels were stained with 0.5 % (w/v) Kenacid R in 7 % (v/v) acetic acid, 50 % (v/v) methanol, and destained with 7 % (v/v) acetic acid, 50 % (v/v) methanol, with gentle shaking at room temperature. Gels were rinsed with distilled water, placed between 2 layers of cellophane and attached to a drying frame and dried in an Easy Breeze Gel Dryer for 3-4 h.

Two peaks were seen from the 280 nm elution profile of the osmotic shock proteins from Mono S. The presence of DppA binding protein in the second absorbance peak was shown by the results of SDS-PAGE in Fig. 2-2. The presence of a single band from the fractions containing DppA indicates a high degree of purification. The first elution peak also contained proteins, but importantly, not DppA. Purified protein samples from RPC were also examined by SDS-PAGE and isoelectric focusing (IEF).

The results from IEF showed a shift in the pI value of unliganded DppA from 6.1, to 6.0 of DppA bound with a ligand. This was in agreement with the results of Smith *et al.* (1999).

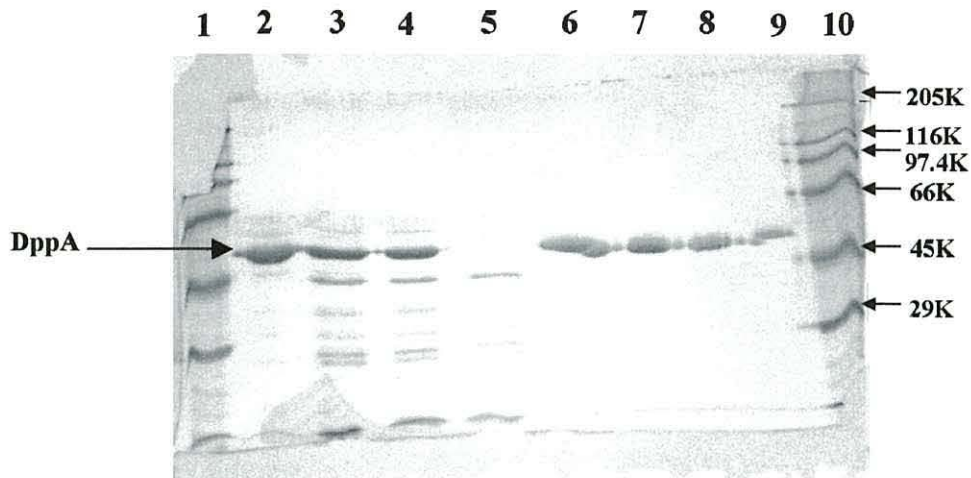


Figure 2-2: SDS PAGE of Samples from Cold Osmotic Shock and Mono S.

Lane 1; Mr Markers; Lane 2; 8µg DppA (control); Lane 3; 10µg Shockate (Pre-Dialysis); Lane 4; 10µg Shockate (Post-Dialysis); Lane 5; Fractions 1,2,3 (first Mono-S peak); Lane 6; Fractions 8,9,10,11 (second Mono-S peak) \equiv 10µg Mono-S DppA (Pre-Dialysis); Lane 7; 10µg Mono-S DppA (Post-Dialysis); Lane 8; 6µg Mono-S DppA (Post-Dialysis); Lane 9; 4µg Mono-S DppA (Post-Dialysis); Lane 10; Mr Markers.

2.4.5. Determination of Protein Concentration

The concentration of purified DppA was determined using the Pierce BCA assay, according to the manufacturer's instructions (Pierce Warriner Ltd., Cheshire, U.K.). Standards of 0-10µg bovine serum albumin (BSA) were used to produce a linear calibration curve. The results showed that typically 10 mg of DppA was obtained from a 4 l culture of *E.coli* JM101.

2.4. Ligand Binding Studies Using Isoelectric Focusing (IEF)

2.4.1. Dipeptides Binding to DppA

These studies were based upon the methods described in Smith *et al.* (1999). Lyophilised RPC-purified DppA was redissolved in 10 mM HEPES/NaOH pH 7.3 to give a final concentration of 2 µg/µl, and incubated at 37 °C for 60 min. Different amounts of 20 mM stock solutions of a variety of dipeptides were diluted in 10 mM HEPES/NaOH pH 7.3 to obtain a molar range of protein:peptide ratios. 2 µl of each protein:peptide concentration solution was added to 2 µl of DppA. 2 µl of unliganded RPC DppA was mixed with 2 µl of 10 mM HEPES/NaOH pH 7.3 to act as a control. All samples were mixed by spinning at high speed in the microcentrifuge for 10 seconds, and incubated at 37 °C for 30 min before application to Pharmacia IEF Phast Gels, with a pH range of 5-8. 2.5 µl of Pharmacia pI calibration markers were used and electrophoresis was carried out on a Pharmacia Phast System, according to manufacturer's instructions, at 2000 V, ca. 30 min at 15 °C. After electrophoresis, gels were fixed with 20 % (w/v) trichloroacetic acid for 1 h, rinsed in distilled water and placed in 10 % (v/v) acetic acid for 1 h. Gels were stained with 0.5 % (w/v) Kenacid R in 7 % (v/v) acetic acid, 50 % (v/v) methanol, and destained with 7 % (v/v) acetic acid, 50 % (v/v) methanol, at room temperature with gentle shaking. Gels were dried in an Easy Breeze Gel Dryer.

2.4.2. IEF Competition Assay with ACE Inhibitors

For some ligands, the results from IEF did not show shifts in the band positions of unliganded to liganded DppA. The IEF assay was modified by competing DppA with a substrate, and a dipeptide known to give a measurable pI shift. Thus, unliganded DppA has a band position corresponding to a particular pI value; addition of a dipeptide such as dialanine causes a conformational change in the protein resulting in a shift in the band position. However, if a competitor is mixed with dialanine, two bands may be seen, one band corresponding to the pI of DppA liganded with dialanine and the second band that of the competitor binding to the protein, but having the same pI as unliganded DppA. This effect can be explored usefully by varying the ratio of competitor:ligand (e.g., dialanine) and observing the consequent ratio of the two pI-forms.

A lyophilised, unliganded DppA sample was redissolved in 10 mM HEPES/NaOH pH 7.3 to give a final concentration of 2 µg/µl and was incubated at 37 °C for 60 min. Dialanine solution at a 1:1 molar ratio of protein:peptide, final concentration of 35 µM, was used as the competing peptide. As controls, 4 µl of DppA was added to 4 µl of distilled water, this indicated the position of unliganded DppA, and additionally, 4 µl of DppA was added to 2 µl of dialanine solution and 2 µl of distilled water, which allowed the pI of the liganded protein to be measured. In typical studies, 4 µl of DppA was added to 2 µl of 1:500, 1:1000 and 1:2000 molar ratio of protein:substrate solutions of δ-aminolevulinic acid (a known poor DppA substrate), and 1:100, 1:500 and 1:2000 molar ratios of protein:ACE inhibitor solutions. All samples were mixed by spinning at high speed in a microcentrifuge for 10 seconds. After 10 min incubation at 37 °C, 2 µl of 1:1 molar ratio of dialanine was added to all the substrate and drug samples. Samples were incubated for a further 20 min at 37 °C before application to the gel as described in section 2.4.1. After electrophoresis, all gels were treated as in method section 2.4.1.

2.5. Radioligand Competition Filter Binding Assays

Filter binding assays were originally developed in this laboratory for the study of OppA substrate specificity (Tyreman, 1990; Tyreman *et al.*, 1992). In this assay, binding of a radioactively-labelled peptide substrate is measured as a protein-ligand complex after its precipitation by ammonium sulphate on a membrane filter; the relative affinities of other peptides are determined from their competitive abilities to prevent binding of the radioactively-labelled substrate. Similar studies using Gly[¹²⁵I₂]Tyr as a substrate, and a representative collection of peptide competitors, have been done in order to determine the substrate specificity of DppA (Marshall, 1994; Smith *et al.*, 1999). These studies have shown that the relative binding affinities for a range of dipeptides and tripeptides for DppA and OppA parallel their overall transport rates in *E.coli* through the dipeptide and the oligopeptide permease, respectively. Thus, DppA and OppA alone control the specificity of Dpp and Opp, respectively (Smith *et al.*, 1999). In this study, filter binding competition assays were used to measure the binding of peptide-based substrates, such as ACE inhibitors to DppA.

The results from these assays were used to relate to the predicted activity of these substrates for Dpp, based on molecular modelling studies. The binding affinities for a collection of ACE inhibitors were determined by measuring their relative abilities to compete for binding to DppA with radioactively labelled [¹⁴C]Gly-Sar (Cambridge Research Biochemicals, U.K.) and [¹⁴C]Gly-Leu (Amersham Int. U.K.) dipeptides. ACE inhibitors were obtained by Technologie Servier, France, Gödecke, Roche, U.K., Zeneca, U.K. and Bristol-Myers Squibb, U.K.

A lyophilised, unliganded DppA sample (0.6 mg) was redissolved in 10 mM HEPES/NaOH pH 7.3, to give a stock concentration of 25 µM and incubated at 37 °C for 60 min. 10 µl of DppA (10 µM final concentration) was mixed with 10 µl of a range of increasing molar ratios from 1:1 to 1:1000 protein:inhibitor concentration of ACE inhibitors in 1.5 ml eppendorf tubes. Non-specific binding was measured by the addition of radiolabelled peptide to 20 µl of 10 mM HEPES/NaOH pH 7.3, with no binding protein or ACE inhibitor present. Total binding of radiolabelled peptide to DppA was measured by mixing 10 µl of 10 mM HEPES/NaOH pH 7.3 with 10 µl DppA, with no ACE inhibitors present. A positive control sample was prepared by mixing 5 µl of 250 µM dialanine and 5 µl of 250 µM ACE inhibitor, with DppA. This allowed the natural dipeptide to compete with the drug at 1:1 molar ratios for the single DppA binding site. Samples were mixed by brief centrifugation (< 10 sec) in a microcentrifuge and incubated for 5 min at 37 °C. 5 µl of 200 µM radiolabelled peptide in 10 mM HEPES buffer/NaOH pH 7.3 (40 µM final concentration) was added to each mixture and allowed to compete with the drug for the DppA binding site.

All samples were prepared as duplicates with a total assay volume of 25 µl. After the addition of the radiolabelled peptide, samples were briefly centrifuged and incubated for 30 min at 37 °C. Protein-substrate complexes were precipitated by the addition of 900 µl of saturated ammonium sulphate at 4 °C. Each sample was transferred to a Millipore 12 well filtration manifold (model 1225) and filtered under vacuum (500-600 mm Hg), using an ABM Vacuubrand ME2 electric diaphragm pump (ABM Vacuubrand, West Germany) through (0.2 µm pore) polycarbonate filters (Nucleopore), pre-wetted with distilled water.

Each filter was washed with 3 x 2 ml of the same cold saturated ammonium sulphate and transferred to plastic scintillation vials (5.5 cm x 1.5 cm diameter). 5 ml of Econofluor scintillation fluid was added and samples were allowed to stand for 1 h. Scintillation vials were placed into glass outer vials and transferred into racks for 5 min counting using a Beckman LS7500 liquid scintillation counter (Beckman Ltd., Cheshire, U.K.). Counts were measured for beta-emissions (^{14}C radioactivity).

2.6. Agar-Plate Competition Assay

An assay that allowed a quick and convenient assessment of the relative abilities of a range of putative substrates to be recognised and transported by Dpp was required. In order to achieve this, a modification of an agar-plate inhibition assay was developed in this laboratory. In a standard agar-plate inhibition assay, a range of concentrations of an antibacterial agent is pipetted onto antibiotic susceptibility discs, and the inhibition zones caused in the bacterial lawn on the agar surface are measured. This agar-plate assay was modified here in order to determine the competitive activity of non-inhibitory peptides, and was based on the ability of di- and tripeptides to compete with toxic peptides for uptake by Dpp. The principles and applications of this assay have been described (Payne *et al.*, 2000).

The uptake of peptides by Dpp can be determined by using the mutant PA0410 (dpp^+ , opp^- , tpp^-), enabling the transport and competitive ability of a range of peptides to be characterised specifically for Dpp. 3 ml of top agar (0.7 % (w/v)), containing appropriately supplemented growth medium was inoculated with 100 μl of a culture of PA0410 \equiv O.D. 0.2 giving a final density of approximately 7×10^6 bacteria ml^{-1} . The solution was vortexed and poured onto an agar plate, containing the same growth medium and allowed to set for 20 min. Valine, and hence peptides containing valine are inhibitory to strains of *E.coli* K-12 (Payne & Smith, 1994). An antibiotic susceptibility disc with 15 μl of 20 mM Val-Gly solution that acts as an inhibitor, was placed at the centre of the plate, and 4 discs containing the same amount of competitor peptides, were placed around the plate at different distances from the centre. This effectively allowed the competitor peptides to compete with Val-Gly to varied extents for Dpp.

The agar plates were inverted and incubated overnight at 37 °C. After overnight incubation, the maximum diameter of the circular inhibition zone caused by Val-Gly was measured to the nearest mm. When competition occurred, the normally circular inhibition zone had its shape changed to various degrees in the vicinity of the surrounding discs. For a good competitor, the inhibition zone radius would decrease as the disc separation distance of the competing peptide decreased. For a poor competitor, the inhibition zone radius would be the same, regardless of the disc separation distance of the competitor. For each competitor peptide, the radius of the inhibition zone caused by Val-Gly was measured, and plotted against the competitor disc separation distance. A linear regression of the inhibition radius data was done, and peptides were ranked according to their competitive abilities based upon their competition gradients.

2.7. Computer-Based Molecular Modelling

Peptide transport systems have evolved to transport a wide range of peptide substrates in a largely sequence independent manner and one of the main aims of studies conducted in this laboratory has been to identify the individual molecular recognition templates (MRTs) of substrates for these systems. Molecular modelling was carried out on a range of simple dipeptides and “peptide-like” compounds such as peptide mimetics, ACE inhibitors and antimicrobial agents, in order to determine their main conformations in solution, and to relate these to their recognition by peptide transporters. These investigations provided an insight into the MRTs of substrates that are likely to be recognised by peptide transporters. The design of new peptide therapeutics has largely been based upon a combinatorial chemistry and screening approach with reference to crystal structure data obtained from X-ray crystallography and NMR. In this study, molecular modelling was used for the *rational* design of peptidomimetics and ACE inhibitors, to produce theoretical compounds with structural and conformational features required for recognition by bacterial Dpp and/or Tpp, and possibly for improved oral delivery by mammalian peptide transporters.

Computer modelling was carried out using SYBYL molecular modelling package (Tripos Inc., St. Louis.) installed on a Silicon Graphics Indigo II or Octane workstation. The Indigo II used Irix 5.2 with a R5K platform 200 MHz processor, whereas the Octane used Irix 6.4 with a R10K platform 175 MHz processor.

2.7.1. Sketching of Molecules

Compounds were constructed using the SKETCH facility of SYBYL 6.2/4 and were freely sketched on the screen using a mouse. Upon entering the SKETCH command, the cursor is automatically defined as a carbon atom and to draw the next atom, another point is picked on the screen, and a line (bond) between the two atoms is automatically drawn. This process is repeated until the desired chain length of the molecule is obtained. Drawing a ring is accomplished by a similar method. The backbone of the ring is sketched by picking points at appropriate positions on the screen. The ring is closed by selecting the first atom of the ring again, thereby causing a bond to be drawn between this atom and the last atom drawn. Aromatic bonds are designated by alternating single and double bonds with in the ring, with C.ar atoms and C.ar bond types.

Compounds were modelled with a positively-charged amino terminus and a negatively-charged carboxyl terminus when appropriate, with L or D stereochemistry for amino acids or, more generally for analogues, S or R chirality. Default SYBYL atom types were generally applied, except for protonated amino groups and carboxylate oxygen's, which were assigned N.4 and O.co2, respectively. Charges on the molecule were calculated using the Pullman method and the completed structures were minimised using MAXIMIN2 in SKETCH. Minimised completed sketched structure, with the correct atom types, chirality and charges were saved as mol2 files in a molecular database in SYBYL.

2.7.2. Conformational Analysis Using Random Search

The atoms in a molecule can generally assume many different relative positions without undergoing a rearrangement of their chemical bonds. Each of these relative arrangements of atoms is termed a conformation. Random search implemented in SYBYL can be used to explore the different conformations of molecules and has the advantage over Systematic search, in that it can be used for complex molecules and is less time consuming.

Conformational analysis using Random search consists of two steps. The first is that up to 3 of the bonds selected for searching are set to random torsion angles, and then minimised to the closest energy minimum. The minimisation is performed in 2 stages so that molecules with energy higher than the cut-off can be eliminated at an early stage. The second stage of the minimisation uses a gradient termination to ensure that the minimisation is completed. This stops the minimisation algorithm when gradient convergence has been rendered i.e. no more reduction in energy will be found.

After minimisation, the new structure is then compared with all the structures previously found. This comparison is based on the RMS match between atoms in the previously found conformers and the current conformer. If chirality checking is not desired, the molecule is reflected and checked again against all previously found conformations, to see if the opposite chirality molecule has been found. Energy cut-offs can be used to remove high-energy conformers before the second stage of minimisation.

If the conformation generated is found to be unique after all these tests, it is added to a database, if not, it is counted as another occurrence of a previously found conformers and a count is kept of how many times that conformation has been found. The cycle of random changes and minimisation is repeated many times (1000-5000), and the search will end if either of the following two criteria are met: exhaustion of the number of search cycles or finding all unique conformers a minimum number of times. This is measured by counting the number of times each unique conformation has been found.

If each unique conformation has been found 'many' times, there is a chance that all the conformations have been found. Random search was used in this study to identify low energy conformers of a variety of compounds; random torsion angle changes were applied to selected bonds of a molecule followed by minimisation using the Powell method with gradient termination. The energy of each conformer was calculated using the Tripos force field and Pullman charges and electrostatics were included in this calculation.

2.7.2.1. Dipeptides

The conformational flexibility of peptides has largely limited the use of computational methods to the study of systems where constrained analogues have been available. The modelling of small peptides has generally considered them as portions of protein structure, using *N*- and *C*-terminally blocked peptides. In this laboratory, conformational analysis of a range of dipeptides with charged *N*- and *C*-termini, was done using Random search in SYBYL and has been described (Payne *et al.*, 2000; Grail & Payne, 2000). In this study, the basic methodology used for random search of dipeptides was applied for conformational analysis of peptide mimetics, ACE inhibitors and peptide smugglins, with slight modifications in the search criteria where required.

2.7.2.2. Peptide Mimetics

A range of peptidomimetics was chosen from literature reviews that contained illustrated examples of compounds classified as dipeptide isosteres, lactam-constrained mimetics and torsionally-constrained mimetics (Giannis and Kolter, 1993; Taylor & Amidon, 1995; Gillespie *et al.*, 1997; Hanessian *et al.*, 1997). The peptidomimetics assessed were confined to those structures that harbour a 6-atom subunit forming a dipeptide backbone, with an amino “end”, a central amide group and one carboxyl “end”. These mimetics were termed “dipeptide mimetics” in the literature, but their *C*- and *N*-termini are typically blocked with amide or ester groups respectively, resulting in a more tripeptide-like unit. In this study, dipeptide mimetics were modelled as having charged *N*- and *C*-termini, as found in a normal dipeptide at physiological pH, which would allow a direct comparison of their structure-conformer distribution in relation to a natural dipeptide. When sketching these compounds, particular attention was paid to atom types, and stereochemistry of these structures. Systematic structural variations to the generic compound were done, which included modifying the amide bond, changing the stereochemistry, adding different atoms, substituents to ring structures, or by attaching methyl or phenyl groups to their backbone. Minimised starting structures of dipeptide mimetics and their modified structures were submitted for conformational analysis using Random search.

For each compound, all potentially rotatable backbone bonds, including ring structures and side chains were marked for the search. The energy cut-off option defines the maximum allowable energy for a conformation and an absolute energy cut-off of 70 kcal/mol (SYBYL 6.2) or a relative cut-off of 7.0 kcal/mol (SYBYL 6.4) was used to eliminate high energy conformers. To determine if two conformers were identical, an RMS threshold of 0.2 Å was used with chirality checking to ensure only unique conformers with the correct chirality, as compared with the initial structure were collected. Aqueous solvation was simulated by using a distance-based dielectric function with a constant of 80, and the maximum number of minimisation cycles was generally set for 1000 iterations.

2.7.2.3. ACE Inhibitors and their Modified Analogues

ACE inhibitors have a dipeptide-like backbone, therefore features that govern the transport of natural peptide substrates by peptide transporters, can be applied to assess the bioavailability of these peptide-based therapeutics. A number of ACE inhibitors was chosen from the literature for conformational analysis (Cleland, 1993; Adang *et al.*, 1994; Taylor & Amidon, 1995). These molecules were sketched as described (section 2.7.1.), with a positively-charged *N*-terminus and a negatively-charged *C*-terminus. Particular attention was paid to the atom types and stereochemistry of these structures. These compounds were submitted for Random search as described for dipeptide mimetics (section 2.7.2.2.). The generic structure of a variety of ACE inhibitors was modified by the knowledge gained from conformational analysis of peptides and dipeptide mimetics. These modifications included changes in *C*-terminal amino acid residue and amide bond chemistry, changes in stereochemistry and addition of different atoms to ring structures. These *rationally* designed ACE inhibitors were also sketched (section 2.7.1.) and submitted for Random search (section 2.7.2.2).

2.7.2.4. Animicrobial Smugglins and their Modified Analogues

A range of natural dipeptide smugglins was selected from the literature (Ringrose, 1980; Payne, 1995) to determine whether their conformer distribution profile matched that of dipeptides as described by Grail & Payne (2000). The generic structure of these compounds was modified by changing the amino acid transport moiety side chains.

The position of the transport and the toxic warhead components on the *N*- and *C*-termini were also altered, e.g., from Ala-X to X-Ala. This was done in order to determine whether the structures of these peptide prodrugs were optimised for transport by the peptide permeases. Minimised starting structures of natural smugglins and their modified analogues were submitted for conformational analysis using Random search as described (section 2.7.2.2.). An absolute energy cut-off of 40 kcal/mol (SYBYL 6.2) was used to eliminate high energy conformers. As these compounds are highly flexible, each antimicrobial peptide prodrug and its modified analogue were subjected to several independent searches, with a different starting conformation that was obtained from the spreadsheet of the initial search. Results from several Random searches, generally 3 x 1000 iterations and a 5000 iteration, were combined for each compound.

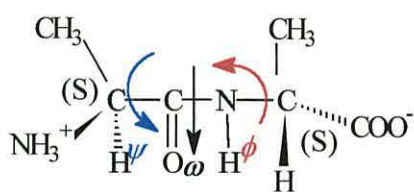
2.7.3. Analysis of Results from Random Search

For each compound, the conformational search produced a database of conformers listed in a SYBYL Molecular Spreadsheet (MSS), where the ENERGY and the COUNT for each conformer were displayed. Calculations on the conformer set were carried out within the MSS, using either the AUTOFILL functions, or user-defined scripts written in SYBYL programming language (Spl). Conformers were initially sorted and ranked according to their increasing energy, and the Boltzmann distribution was applied, using the minimum-energy value. The Boltzmann distribution ($N_i/N_0 = e^{-\Delta E/RT}$) relates the abundance of each conformer to the minimum-energy form, dependent upon the differences in energy between the two. ΔE = Difference in energy between the lowest energy conformer (N_0) and the energy of the i^{th} conformer (N_i), R = The Gas Constant ($1.98 \text{ cal K}^{-1} \text{ mol}^{-1}$), T = Temperature in Kelvins (310K). Summation of the Boltzmann distribution values, using a specially written Spl, allowed the contribution of each conformer to be expressed as a percentage of the total.

2.7.3.1. Dipeptides

This has been described in Grail & Payne (2000) and Payne *et al.* (2000). Peptide conformers were displayed in SYBYL MSS where calculations of Boltzmann distribution, percentage contribution and measurements of: *N-C* distance and backbone torsion angles ψ (Tor2), ω (Tor3) and ϕ (Tor4) were carried out.

Fig. 2-3 shows the ψ , ω and ϕ torsion angles for a dipeptide. More than 50 dipeptides were subjected to conformational analysis and each individual peptide's, ψ and ϕ angles were divided into thirty six 10° sectors, and ω torsions were categorised as *cis* (0°) or *trans* ($\pm 180^\circ$). The percentage contributions of conformers within each ψ , ω , ϕ combination were summed. Data accumulated from all related peptides, e.g., dipeptides were combined and the overall percentage contribution in all ψ , ω , ϕ combinations calculated.



Dipeptide Ala-Ala

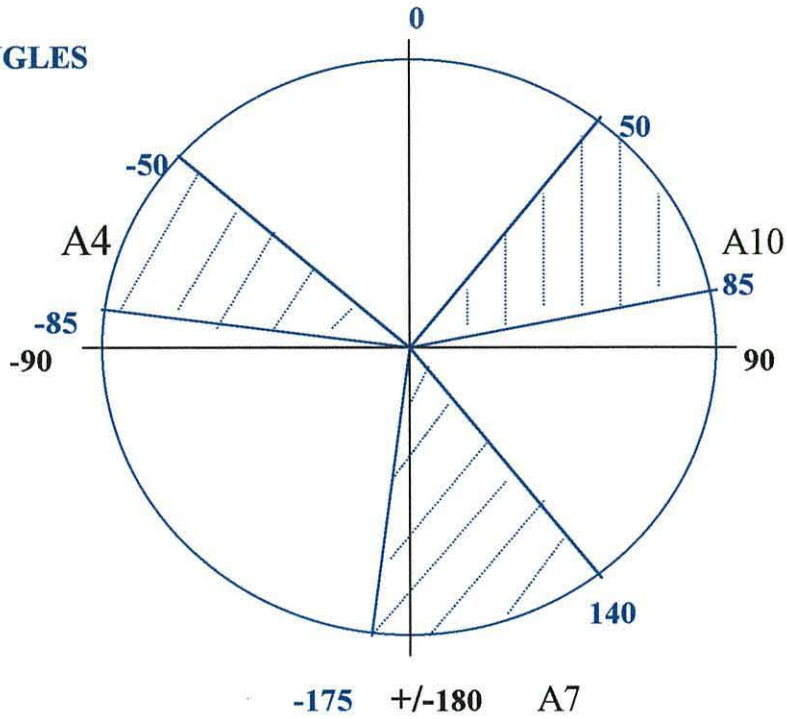
Figure 2-3: Backbone Torsion Angles of Psi (ψ), Omega (ω) and Phi (ϕ) for the Dipeptide Ala-Ala.

The torsion angle nomenclature is as ψ , $N^\alpha-C^\alpha-C'-N^\alpha$, ω , $C^\alpha-C'-N^\alpha-C^\alpha$, ϕ , $C'-N^\alpha-C^\alpha-C'$; where ω is the amide bond torsion angle. With respect to ω , the *trans* geometry is more energetically favoured for most typical dipeptide structures. When the C-terminal residue is Pro or other *N*-alkylated or cyclic amino acids, the *cis* geometry is more likely.

2.7.3.1.1. Data Presentation using 3-D pseudo-Ramachandran (3DPR) Plots

In order to display complex data sets from conformational analysis of several dipeptides, it proved necessary to find a novel method to display the results. To this end it was found that the conformer distribution was best visualised using a 3DPR plot. The conventional Ramachandran plot is used to represent graphically protein secondary structure, where adjacent ψ and ϕ torsion angles are plotted in 2-D to produce a scatter graph of torsion values. This conventional plot was modified into a 3-D format by plotting ψ and ϕ torsion angles of each conformer, and its percentage contribution. Using this graphical representation, the weighted distribution of dipeptide conformers, between ψ and ϕ space, was found to be more restricted than expected.

TOR2 (ψ) ANGLES



TOR4 (ϕ) ANGLES

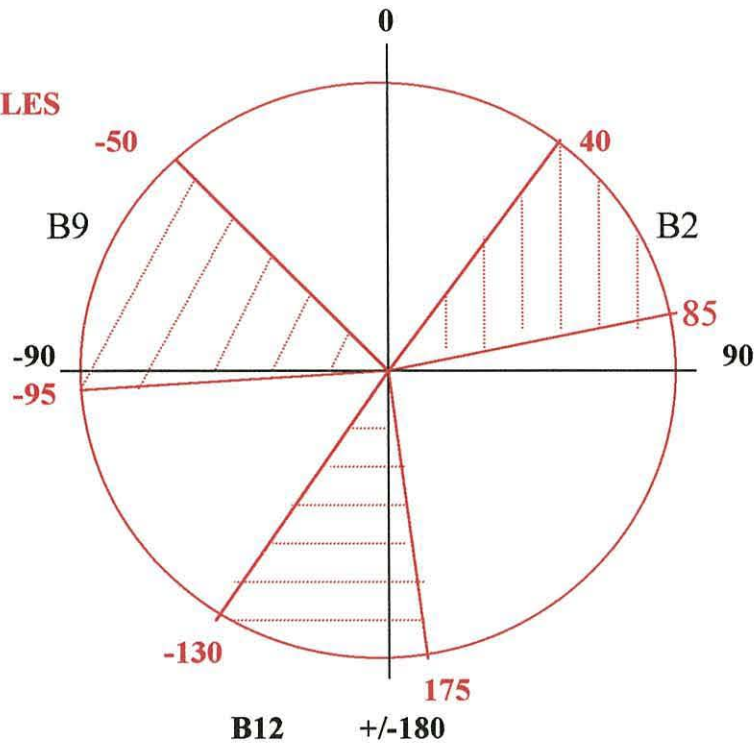


Figure 2-4: MRT Backbone Torsion Angles of ψ (Tor2) and ϕ (Tor4) for Recognition by Peptide Transporters.

The dipeptide permease recognises conformers with ψ (Tor2) angles in A7 and ϕ (Tor4) angles in B9 and B12. The tripeptide permease recognises conformers with ψ (Tor2) angles in A4 and A10, and ϕ (Tor4) angles in B9 and B12. Conformers in B2 regions are not recognised by peptide transporters.

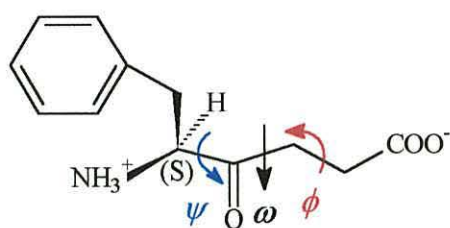
There were nine preferred backbone torsion angle combinations and to classify these sets of conformer structures, the ψ , ϕ conformational space was divided into twelve 30° sectors designated A1 to A12 and B1 to B12, respectively. Each class was described by reference to its principle location within the 3DPR grid, e.g. A7B9. The preferred ψ values were identified as -50 to -85°, +140 to -175°, and +50° to +85°, designated A4, A7 and A10, respectively; and for ϕ , +40 to +85°, -95 to -50°; and -130° to +175°, designated B2, B9 and B12, respectively (Payne *et al.*, 2000).

The use of 3DPR plots provided a tremendous insight into the predominant conformational features of individual and groups of dipeptides and allowed the identification of the molecular recognition templates (MRTs) available for the recognition of substrates by the peptide transporters (Payne *et al.*, 2000; Grail & Payne, 2000). The *backbone torsion angles* ψ (Tor2) and ϕ (Tor4) of the MRTs of substrates for recognition by the peptide transporters are illustrated in Fig. 2-4. One of the main aims of this study was to determine the *backbone torsion angles* of dipeptide mimetics, ACE inhibitors and antimicrobial prodrugs, as an *initial* screen for the prediction of their activity as substrates for the peptide transporters.

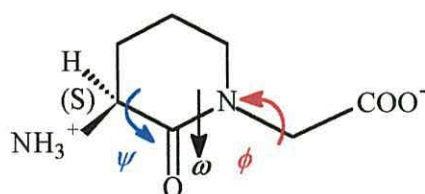
2.7.3.2. Dipeptide Mimetics

Random search of these compounds produced conformers that were displayed in a SYBYL MSS where calculations of Boltzmann distribution, percentage contribution and measurements the backbone torsion angles and *N-C* distance were made. The torsion angles used for ψ , ω and ϕ measurements for various dipeptide mimetics are shown in Fig. 2-5. The majority of peptidomimetics did not have their backbone torsion angles in the MRTs for peptides, therefore data were initially assessed by visual examination of the percentage distribution of conformers with torsion angles outside the MRTs. For flexible structures, this was only done for conformers contributing down to 1% of the total percentage distribution. Most of the mimetics had constrained structures, so only a few conformers were produced after Random search and this facilitated the summation of the percentage distribution range of conformers.

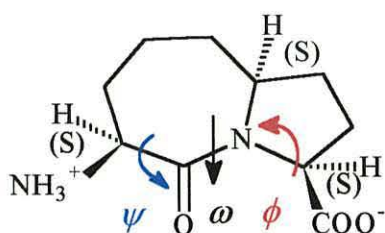
However, to take account of *all* the conformations produced by random search of dipeptide mimetics and their modified analogues, the conformer distribution range was optimally displayed using a 3DPR plot. Using specially written in-house Spl programmes, conformers were put into 10 ° bins according to their psi and phi angle combinations, with usually only *trans* ω bonds, and their % conformer distribution. These data were then used to plot a 3DPR plot for each compound modelled.



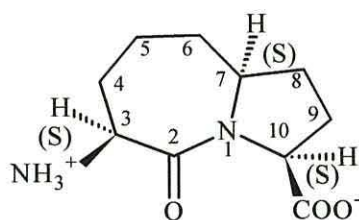
Dipeptide Isostere



Lactam-Constrained Mimetic



Torsionally-Constrained Mimetic



Labelling of Atoms (Clockwise Direction)

(Hanessian *et al.*, 1997)

Figure 2-5: The Backbone Torsion Angles Used for Psi (ψ), Omega (ω) and Phi (ϕ) Measurements for Various Dipeptide Mimetics and the Numbering of Atoms in Ring Structures.

2.7.3.3. ACE Inhibitors and their Modified Analogues

Random search of these compounds produced conformers that were displayed in a SYBYL MSS, where calculations of Boltzmann distribution, percentage contribution and measurements of the backbone torsion angles and *N-C* distance were made. The backbone torsion angles used for ψ , ω and ϕ measurements are illustrated in Fig. 2-6. The majority of ACE inhibitors modelled did have some conformers in or near the MRT regions, and as with the dipeptide mimetics, the percentage distribution of the conformer range was initially summed manually. Later, Spl command files were written in-house that allowed selection of conformers with backbone torsion angles in MRT regions, as shown in Fig. 2-4. Conformers with ψ angles in A7 (+140° to +180° and -180° to -175°), A4 (-50° to -85°) and A10 (+50° to +85°), and ϕ angles in B9 (-50° to -95°), B2 (+40° to +85°) and B12 (-130° to -180° and +180° to +175°), with their calculated percentage contribution in solution were selected. A *cis* omega was defined as having a value of (0.0° to +5.0°) or (0.0° to -5.0°) range, and a *trans* omega was defined as having a value of (+180° to +175°) or (-180° to -175°) range. For each compound modelled, these Spls gave the percentage of conformers with *backbone torsion* angles present in the MRT for recognition by the peptide transporters.

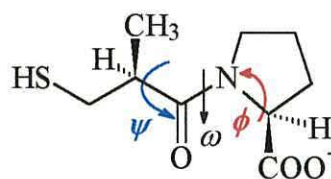
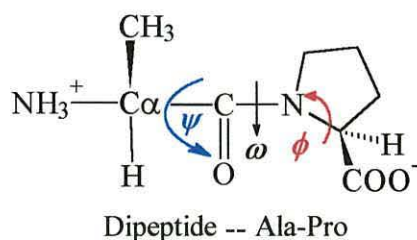
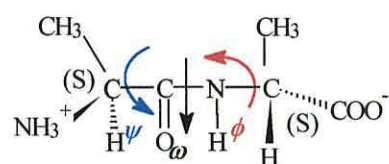


Figure 2-6: Backbone Torsion Angles of Psi (ψ), Omega (ω) and Phi (ϕ) for the Dipeptide Ala-Pro and the Corresponding Torsion Angles for ACE Inhibitors that have Structurally Analogous Peptide Backbones.

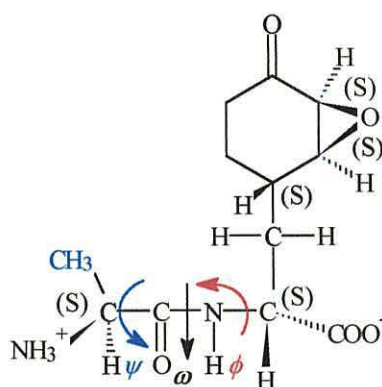
In order to identify the distribution ranges of *all* the conformations produced by a random search of ACE inhibitors and their modified analogues, the conformer distribution range was best visualised using a 3DPR plot. As with the dipeptide mimetics, conformers produced from Random search were put into 10 ° bins according to their psi and phi angle combinations, with only *trans* ω bonds, and their % conformer distribution. These data were then used to plot a 3DPR plot for each ACE inhibitor and its rationally designed analogue.

2.7.3.4. Antimicrobial Smugglins and their Modified Analogues

The results from individual random searches for each compound produced a database of conformers that were combined in a SYBYL MSS. Backbone torsion angles ψ , ω and ϕ were evaluated, and *N-C* distances were measured. The backbone torsion angles used for psi (ψ), omega (ω) and phi (ϕ) measurements are illustrated in Fig. 2-7. For each compound, any duplicate conformers produced from independent searches, i.e., those having the same energy value and torsion angles, were removed. The Boltzmann distribution and percentage contribution were then re-calculated for only unique conformers.



Dipeptide Ala-Ala



Bacilysin (Ala-X)

Figure 2-7: Backbone Torsion Angles of Psi (ψ), Omega (ω) and Phi (ϕ) for the Dipeptide Ala-Ala and the Corresponding Torsion Angles for Dipeptide Smugglins such as Bacilysin (Ala-X), that have Structurally Analogous Peptide Backbones.

Most of the natural peptide smugglins had a conformer distribution range similar to natural dipeptides, therefore, data analysis was done using the Spl command files that allowed selection of conformers with backbone torsion angles in MRT regions, as described (section 2.7.3.3.). For each compound, conformers were then put into 10 ° bins according to their psi and phi angle combinations, with only *trans* omega bonds, and their % conformer distribution. These data were then used to plot a 3DPR plot for each smugglin and its modified analogue.

2.7.4. Defining MRT Regions in 3DPR Plots

To distinguish the main conformational types of all the compounds and their modified analogues, data from conformational analysis were used to plot 3DPR plots of psi (ψ) v phi (ϕ) v % conformers. The main conformational types of dipeptides, based on their psi and phi angles, were also established by analysing data using a 3DPR plot. The psi sectors on these plots were labelled A1 through to A12, with A1 to A6 covering the range (-180° to 0.0°), and A7 to A12 from (+180° to 0.0°). The phi sectors were labelled B1 through to B12, with B1 to B6 covering the range (0.0° to +180°), and B7 to B12 from (0.0° to -180°) (Payne *et al.*, 2000; Grail & Payne, 2000). As further studies on molecular modelling was progressing, the labelling of axes on 3DPR plots was modified from that adopted in recent publications from this laboratory. For clarification, all the 3DPR plots in this study have their axes labelled with the three psi MRT sectors A7, A10 & A4 and the phi MRT sectors B9, B12 plus B2, to facilitate visualisation of Random search data for modelled structures and to identify whether these compounds contain conformers in the MRT sectors. The colours of the peaks are for visual clarity only. Compounds with conformers in A7(B9,B12) sectors can be recognised by Dpp and conformers in A4(B9,B12) and A10(B9,B12) are recognised by Tpp; hence, the conformers for any molecule can be assessed for transport by these archetypal peptide transporters based on their conformer distribution range.



CHAPTER 3

**DPP SUBSTRATE SPECIFICITY AND THE
ESTABLISHMENT OF MRTS FOR
PEPTIDE TRANSPORTERS**

3.1. INTRODUCTION

Small peptides comprising 2-5 amino acid residues are substrates for the peptide transporters that occur ubiquitously in Nature. Many peptide-based therapeutics are also delivered to their intracellular target site at a suitable concentration by exploitation of peptide transporters (Taylor & Amidon, 1995; Yang *et al.*, 1999). The substrate specificities of peptide transporters have been extensively studied by a number of researchers who have identified the general features of substrate recognition. These include: a free, protonated *N*-terminal α -amino group; a free, *C*-terminal carboxylate; all α -chiral centres of L-stereochemistry and a *trans* ω peptide bond; in short, features shared by all peptides (Matthews & Payne, 1980; Matthews, 1991; Payne & Smith, 1994; Fei *et al.*, 1998; Smith *et al.*, 1999). Bacterial transporters provide model systems for the study of structure-activity relationships of peptide transport. *E.coli* and *S.typhimurium* have the ABC peptide transporters Dpp and Opp, and Tpp, which is energised by a proton motive force (Smith *et al.*, 1999). X-ray crystal structures of the periplasmic peptide-binding proteins DppA and OppA with bound peptide ligands have revealed how their charged *N* and *C*-termini are stabilised, and side chains accommodated in cavities containing variable water molecules (Tame *et al.*, 1994, 1995; Dunten & Mowbray, 1995; Sleight *et al.*, 1997; Sleight *et al.*, 1999). However, the features that govern the *affinity* of peptide ligands for initial uptake and transport are still unclear. As part of a group project, the affinity of di- and tripeptides for *E.coli* Dpp and Tpp transporters were investigated using isoelectric focusing analysis and agar plate competition assays. Molecular modelling was used for conformational analysis of a range of peptides in order to determine their bioactive conformations. The results from this study have led to a better understanding of molecular recognition by peptide transporters, and have established *molecular recognition templates* (MRTs) for substrates for these systems. These MRTs can be applied for the *rational* design of antimicrobial smugglers and of peptide-based drugs for effective oral delivery by intestinal peptide transporters (Payne *et al.*, 2000).

3.2. RESULTS

3.2.1. IEF Assays of DppA Binding to Dipeptides

DppA from *E.coli* JM101 was purified (section 2.3.) and IEF assays were done as described (section 2.4.1.). Routinely, to maximise use of tracks in IEF gels, pI markers were not always included. Gels were generally run in batches allowing ease of measurement of pI values between gels. A typical run with pI markers is shown in Fig. 3-6. Unliganded DppA has a certain pI value, the binding of substrates may change the overall pI of the substrate-DppA complex leading to an observed shift in the gel, without a significant conformational change in DppA. Different ratios of peptide to DppA were used for various peptides depending on their binding affinity. The molar ratio of peptide:protein at which a change in the pI value occurred as a result of ligand binding, was compared for a range of dipeptide substrates. Most of the dipeptides with Ala at the *N*-terminus (Ala-X) had good affinity for DppA, with Ala-Ala, Ala-Gln and Ala-Phe producing a complete shift of protein into a band with a different pI value at 1:1 protein:peptide ratios. Fig. 3-1 shows an IEF gel of Ala-Ala binding to DppA, in which a progressive shift from unliganded DppA to a single sharp band of liganded DppA was obtained at 1:1 protein:peptide ratio. Ala-Gly had a much lower affinity for DppA as it did not produce a complete shift in the band position even at the highest molar protein:peptide ratio of 1:100 (data not shown). Ala-Asp had the poorest affinity for DppA of all the Ala-X peptides tested, as even at the highest molar ratio of 1:500 two bands were still seen, indicating DppA was only about 50% liganded. Fig. 3-2 is an IEF gel of DppA binding to Ala-Asp showing the band positions of unliganded DppA and of DppA bound to Ala-Asp. Asp-X peptides, such as Asp-Ala, Asp-Gln, Asp-Glu, Asp-Lys and Asp-Phe did not cause a shift in the pI value even at high protein:peptide ratios, indicating they were poor substrates for DppA. These peptides were potentially more sensitive substrates to assay, because the charge on the peptide might be expected to produce a pI shift. Fig. 3-3 shows an IEF gel of DppA incubated with Asp-Ala showing no shift in the band position of DppA, even at the highest molar ratio of 1:150.

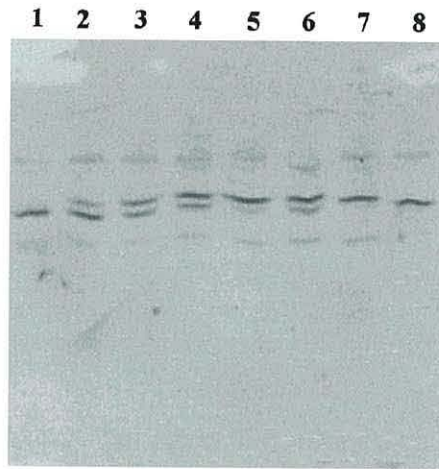


Figure 3-1: IEF gel of DppA Binding To Increasing Molar Ratios of Ala-Ala.

Lane 1; RPC-purified DppA pI 6.0; Lanes 2-8; DppA bound to increasing molar ratios of protein:peptide of 1:0.2, 1:0.3, 1:0.4 , 1:0.5, 1:0.6, 1:0.8 and 1:1 of Ala-Ala, respectively. At a molar ratio of 1:1 DppA was completely bound to Ala-Ala and had a pI value 5.98. A complete band shift at 1:1 protein:peptide ratio indicated that Ala-Ala had a high affinity for binding to DppA.

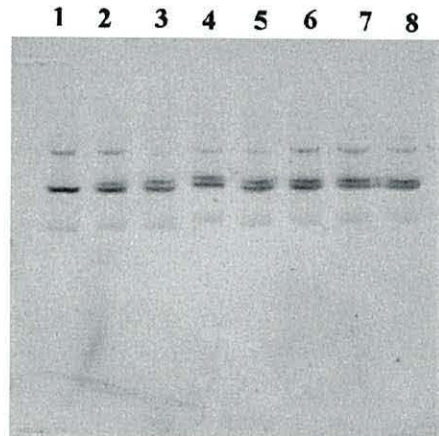


Figure 3-2: IEF gel of DppA Binding To Increasing Molar Ratios of Ala-Asp.

Lane 1; RPC-purified DppA pI 6.0; Lanes 2-8; DppA and increasing protein:peptide molar ratios of 1:200, 1:250, 1:300 , 1:350, 1:400, 1:450 and 1:500 of Ala-Asp. At a molar ratio of 1:500 2 bands are seen at approximately equal intensities, indicating poor substrate affinity.

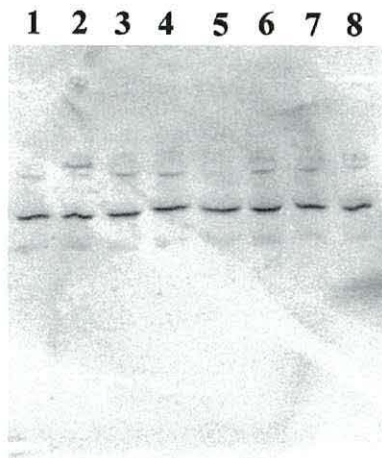


Figure 3-3: IEF gel of DppA Binding To Increasing Molar Ratios of Asp-Ala.

Lane 1; RPC-purified DppA; Lanes 2-8; DppA and increasing protein:peptide molar ratios of 1:1, 1:5, 1:10, 1:50, 1:20, 1:100 and 1:150 of Asp-Ala, respectively. At the highest molar ratio of 1:150 no shift what so ever was detectable in the band position of DppA, indicating the very poor substrate affinity of Asp-Ala for DppA.

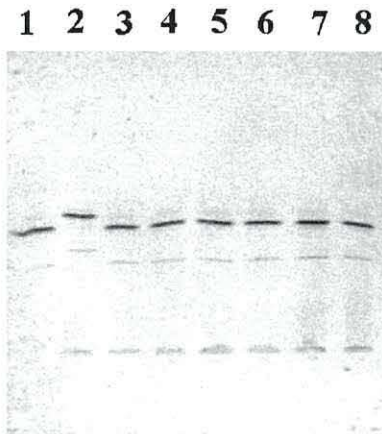


Figure 3-4 : IEF gel of DppA Binding To Increasing Molar Ratios of Gly-Sar.

Lane 1; RPC-purified DppA at pI 6.01; Lane 2; DppA and Ala-Ala at 1:1 molar ratio at pI 5.98; Lanes 3-8; 1:1, 1:10, 1:50, 1:100, 1:250 and 1:500 of Gly-Sar, respectively. At 1:500 molar ratio Gly-Sar no shift in the pI value was detectable, indicating extremely poor affinity of Gly-Sar for DppA.

The *N*-terminal Gly-peptides Gly-Phe and Gly-Tyr had low binding affinities for DppA and a shift in the pI value was not observed until a 1:150 and 1:400 protein:peptide molar ratio was used, respectively. However, no shift in band position was seen with Gly-Sar even at the highest protein:peptide ratio of 1:500 (Fig. 3-4), compared with the control substrate Ala-Ala. In this instance, this assay could be modified by using radioactively-labelled Gly-Sar and detecting the increase in radioactive counts of [¹⁴C]Gly-Sar binding to DppA using autoradiography; this might allow a more sensitive assay of low levels of ligand binding. Additionally, it might be used in a competition assay (see below).

Most of the Val-X peptides produced a good shift in the pI value of DppA. Fig. 3-5 shows an IEF gel of DppA binding to Ala-Phe and Val-Phe, with Ala-Phe having a different pI value and a slightly higher affinity for DppA, compared with Val-Phe. Val-Ala, Val-Pro, Val-Ser and Val-Val still produced 2 bands at 1:1, although the predominant forms were liganded in each case, with pI value of 6.01 for unliganded DppA and 5.98 for liganded DppA. Fig. 3-6 shows an IEF gel of DppA binding to Ala-Phe, Val-Pro and Val-Ser. Val-Gly did not induce a change in the pI value of unliganded DppA, even at the highest protein:peptide ratio of 1:500, indicating again the detrimental effect of Gly residues on peptide recognition and binding.

Some of peptides did not show a significant shift in the band position from unliganded DppA. Therefore, it was hard to distinguish whether the substrates were actually binding to the protein but not producing a shift from the original pI, or that there was indeed no binding of what were truly very poor substrates and, therefore, no shift in the pI was obtainable. It seemed possible to distinguish these situations using a competition-IEF assay. In principle, if DppA is mixed with a substrate e.g. Ala-Ala that binds well and produces a good pI shift, then by adding increasing amounts of a second putative substrate, either no change in band distribution will be seen or if competitive binding occurs, the liganded (Ala-Ala) band will be decreased, and the band with pI equivalent to unliganded band will increase proportionally. Although this approach was not used here for peptides, it proved effective with ACE inhibitors (section 5.2.1.).



Figure 3-5: IEF gel of DppA Binding To Increasing Molar Ratios of Ala-Phe and Val-Phe.

Lane 1; RPC-purified DppA at pI 6.1; Lanes 2-4; DppA and increasing protein:peptide molar ratios of 1:1, 1:20, and 1:50 of Ala-Phe, respectively. At 1:1 molar ratio Ala-Phe produces an almost complete shift in the pI value to 5.9, indicating high affinity for DppA. Lanes 6-8; 1:1, 1:20, and 1:50 molar ratios of Val-Phe respectively, with pI values of 6.1 and 6.0, indicating relatively good binding by DppA.

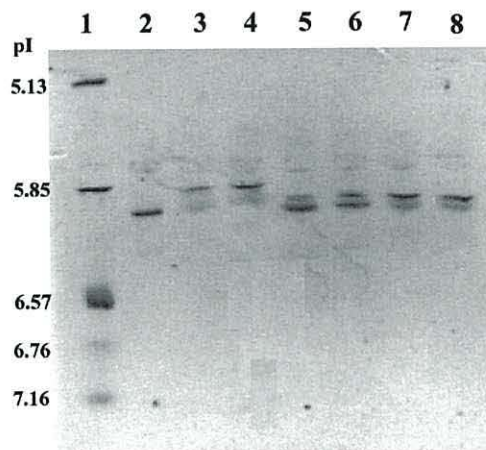


Figure 3-6: IEF gel of DppA Binding To Increasing Molar Ratios of Ala-Phe, Val-Pro and Val-Ser.

Lane 1; pI markers; Lane 2; RPC-purified DppA at pI 6.01; Lanes 3-4; DppA and increasing protein:peptide ratios of 1:1 and 1:20 of Ala-Phe, respectively. At 1:1 molar ratio Ala-Phe produces an almost complete shift, indicating high affinity for DppA. Lanes 5-6; 1:1, 1:20 ratios of Val-Pro, respectively, with pI values of 6.01 and 5.98, showing relatively good binding affinity for DppA. Lanes 7-8; 1:1, 1:20 molar ratios of Val-Ser, respectively, with pI values of 6.01 and 5.98, showing relatively better binding affinity.

3.2.2. Determination of Substrate Binding by Competition Plate Assay

Competition plate assays were also done (section 2.6.), that were quick and simple to perform, and were used to assess the binding of 50 or more peptide substrates for Dpp. Dipeptides were selected as being representative of the wide range of side chain chemistries, and also because they were available for experimentation. Val is inhibitory to *E.coli* K-12 strains (Smith & Payne, 1994) and hence peptides containing Val residues are also toxic. This assay was based on the ability of di- and tripeptides to compete with Val-Gly for Dpp and therefore stop its inhibitory activity. A normal, symmetric inhibition zone was seen for competitor peptides that were poor substrates for Dpp compared with Val-Gly (Fig. 3-7). Peptides that competed well with Val-Gly for uptake by Dpp produced a decrease in the inhibition zone radius around the competitor discs (Fig. 3-8). The radius of the inhibition zone around the competitor and, the disc separation distance from the centre disc were measured and plotted for each peptide (section 2.6.). The linear regression of the slope was calculated to obtain intercept and gradient values, and peptides were ranked for their competitive ability for Dpp based on their competition gradient, see Fig. 3-9 and Table 3.1. In general, neutral aliphatic amino acids such as alanine, leucine; and the hydroxyamino acids serine and threonine showed good affinity at the *N*- or *C*-terminus of dipeptides. The sulphur-containing amino acid methionine also showed good competitive ability for DppA, as well as the aromatic amino acids phenylalanine, tyrosine and tryptophan at the *N*- or *C*-terminus. The basic amino acids lysine and histidine had high affinity for Dpp, whereas aspartic and glutamic amino acids at the *N*-terminus of dipeptides had poorer activity than at the *C*-terminus, i.e. Ala-Asp was a better competitor than Asp-Ala for Dpp. Peptides with D-amino acid residues had poor activity. The tripeptides had a much lower affinity for Dpp than the dipeptides, with Met-Gly-Met being the best tripeptide substrate.

3.2.2.1. Competition Plate Assay with Inhibitory Val-Dipeptides

Valine containing dipeptides were also ranked for their ability to be transported by Dpp by doing a plate assay with Ile-Asn as a competitor as described (section 2.6). Table 3.2. shows their ranking according to their gradient for their ability to compete with Ile-Asn for Dpp.

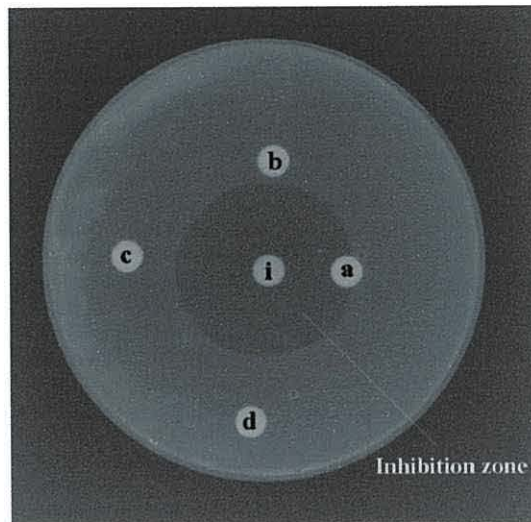


Figure 3-7: A Peptide Substrate showing Poor Competitive Ability for Dpp.

In zero to poor competition, the peptide does not compete well for the binding of DppA with the inhibitor, therefore the inhibitor is taken up by the Dpp system and a large inhibition zone is seen around the disc. Disc i: Val-Gly inhibitor; Discs a,b,c,d: Competitor discs at different distances from the centre of the plate with amount added equivalent to Val-Gly.

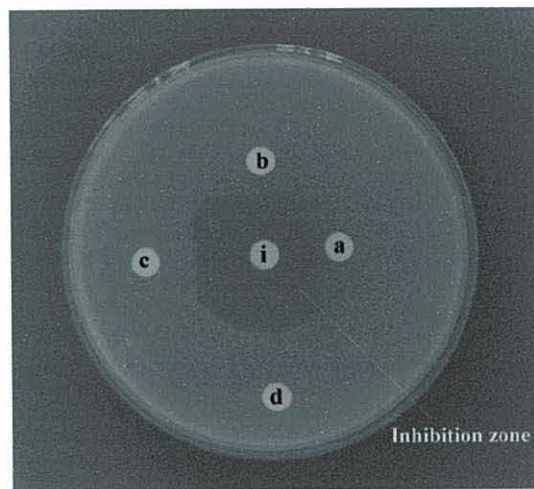


Figure 3-8: A Peptide Substrate showing Good Competitive Ability for Dpp.

In good competition, the peptide will be transported via the Dpp resulting in increased growth around the competitor discs and a decrease in the inhibition radius. Disc i: Val-Gly; Discs a,b,c,d: Competitor discs at different distances from the centre of the plate with amount added equivalent to Val-Gly.

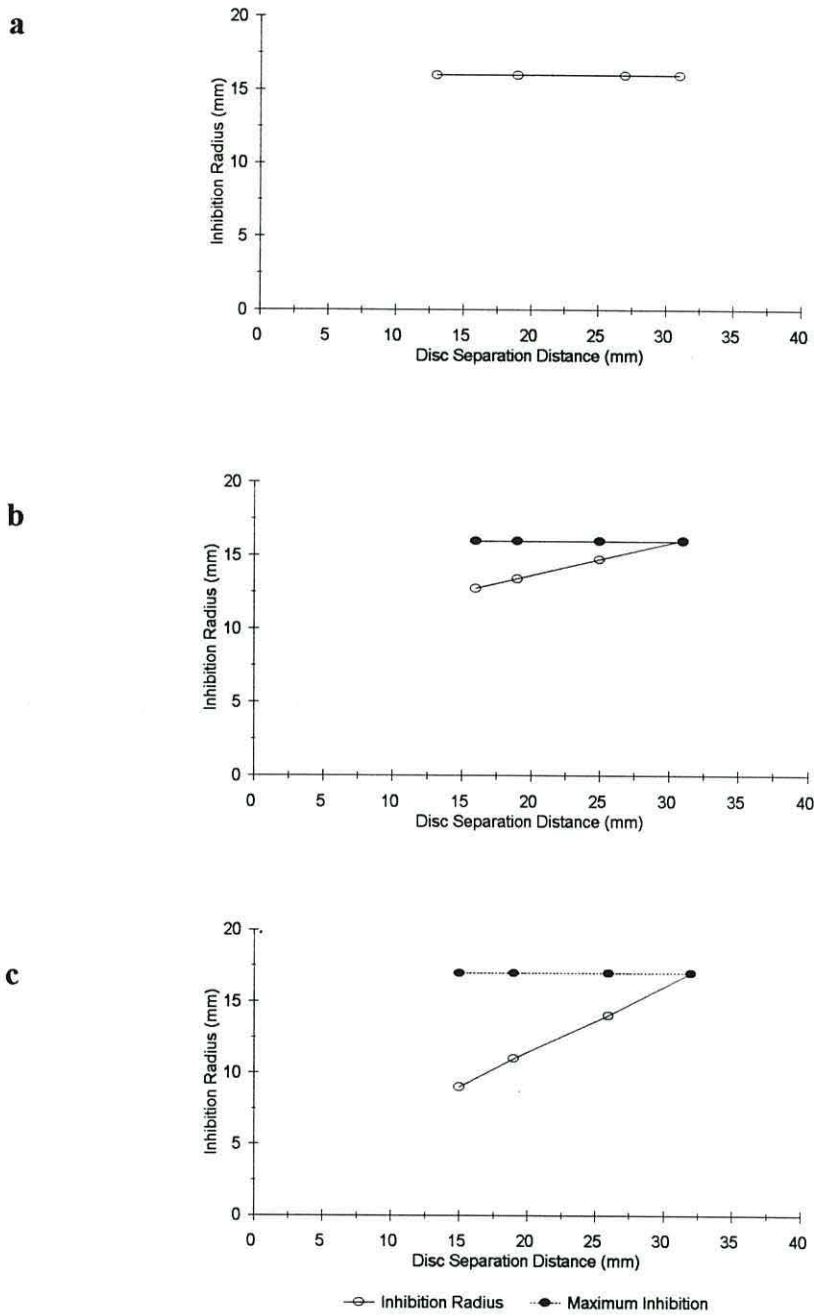


Figure 3-9: Competition Gradients of a) Zero to Very Poor; b) Poor to Medium; and c) Medium to Good Peptide Substrates.

Table 3.1. Ranking of Peptides Based on their Competitive Ability against Val-Gly.

| Peptide | Gradient | Peptide | Gradient | Peptide | Gradient |
|---------|----------|-------------|----------|------------------|----------|
| Leu-Ala | 0.60 | Gly-Ser | 0.37 | Ala-Ala-Ala | 0.15 |
| Lys-Lys | 0.58 | Lys-Ala | 0.36 | Gly-Sar | 0.14 |
| Leu-Met | 0.55 | Gly-Tyr | 0.35 | Pro-Gly | 0.13 |
| Met-Leu | 0.50 | Phe-Ala | 0.34 | Lys-Ala-Ala | 0.10 |
| Leu-Tyr | 0.49 | Ala-Trp | 0.33 | Orn-Orn-Orn | 0.09 |
| Thr-Ser | 0.49 | Ala-Leu | 0.33 | Glu-Glu | 0.09 |
| Ala-Thr | 0.47 | Ala-Pro | 0.32 | Gly-Leu-Gly | 0.07 |
| Tyr-Ala | 0.46 | Phe-Leu | 0.32 | Gly-Gly-Leu | 0.05 |
| His-Leu | 0.46 | Ala-Glu | 0.31 | Met-Ala-Ser | 0.05 |
| Ala-Ala | 0.46 | Leu-Phe | 0.30 | L-Ala-L-Ala-DAla | 0.01 |
| Trp-Ala | 0.46 | Leu-Gly | 0.30 | D-Leu-D-Leu | 0.01 |
| Ala-Gln | 0.45 | Gly-Leu | 0.30 | Gly-Gly-Gly | 0.00 |
| Met-Ala | 0.44 | Ala-Ser | 0.30 | Asp-Phe | 0.00 |
| Ala-Lys | 0.44 | Ala-Met | 0.28 | L-Ala-D-Ala | 0.00 |
| Trp-Tyr | 0.42 | Gly-Pro | 0.28 | L-Leu-D-Leu | 0.00 |
| Gln-Gln | 0.41 | Met-Gly-Met | 0.27 | Leu-Gly-Gly | 0.00 |
| Ala-Phe | 0.41 | Asp-Ala | 0.27 | Leu-Leu-Leu | 0.00 |
| Pro-Ala | 0.41 | D-Ala-L-Ala | 0.22 | Ser-Ser-Ser | 0.00 |
| Leu-Trp | 0.40 | His-Ala | 0.22 | Asp-Gln | 0.00 |
| Ser-Ala | 0.40 | Lys-Asp | 0.22 | Lys-Lys-Lys | 0.00 |
| Ala-Asp | 0.39 | Gly-Gly | 0.19 | D-Ala-D-Ala | 0.00 |
| Gly-Ala | 0.38 | Asp-Glu | 0.19 | Asp-Lys | 0.00 |
| Glu-Ala | 0.37 | Glu-Lys | 0.19 | Gly-Asp | 0.00 |
| Ala-Gly | 0.37 | Gly-Phe | 0.18 | Lys-Trp-Lys | 0.00 |

Table 3.2. Ranking of Valine Dipeptides Based on their Competitive Ability against Ile-Asn

| Peptide | Gradient |
|-------------|----------|
| Val-Gly | 0.72 |
| Val-Lys | 0.67 |
| Val-Pro | 0.66 |
| Val-Ala | 0.51 |
| Val-Ser | 0.40 |
| Val-Phe | 0.40 |
| D-Val-D-Val | 0.01 |

3.2.3. Comparison of Competition Data with IEF Results

Similar rankings were generally found between the competition gradient of a peptide and its effectiveness at forming liganded DppA, as measured by a shift in pI in the IEF assay. The majority of peptides that had a high competition gradient, also showed a complete pI shift to liganded DppA at 1:1 protein:peptide ratios e.g. Ala-Ala, Ala-Gln, Ala-Phe, Val-Phe and Val-Ser. The poorer substrates such as Gly-Phe had a low competition gradient, and required a higher protein:peptide ratio of 1:150 to produce a marked shift to the liganded pI value of DppA. Gly-Sar and Asp-Gln had low or negative competition gradients and gave no detectable shift in the IEF assay, even at the highest protein:peptide ratio, indicating they have very poor Dpp activity.

Results from these studies correlated well with radioactively-labelled competition filter binding studies and cell-uptake experiments on peptide substrates done by other workers in this laboratory (Smith *et al.*, 1999). In addition, the competition data for Dpp also correlated well with the results obtained by isothermal titration calorimetry studies of peptides binding to DppA (unpublished results). Thus, these diverse and complementary transport and ligand binding studies provided information on the structural features required for binding to DppA and uptake by Dpp. To try and relate these SAR and to better understand substrate recognition, molecular modelling was used to see what conformational forms peptides adopt in solution. This would lead to the identification of the *conformational* features that govern their recognition and transport by Dpp.

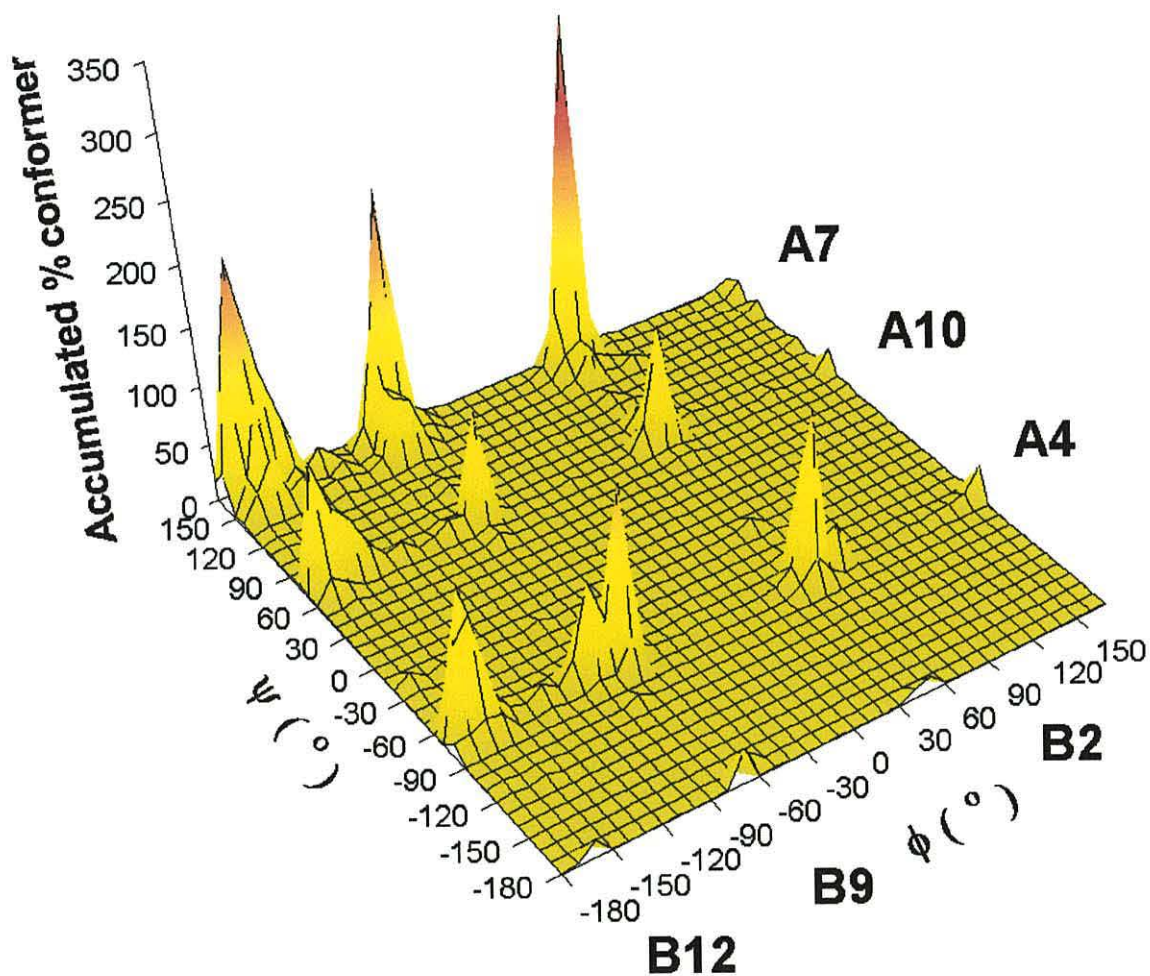


Figure 3-10: 3DPR Plots for 50 Dipeptides.

The accumulated percentage of conformers with particular ψ and ϕ torsion angles were plotted against their ψ and ϕ angles (Grail & Payne, 2000).

3.2.4. Molecular Modelling of Peptides

Conformational analysis of over 50 di- and tripeptides was carried out as described (section 2.7.2.1.). These were selected as being representative of the wide range of side chain chemistries found amongst the 400 possible dipeptides present in the substrate pool derived from protein hydrolysis, and also because they were available for experimentation. For each peptide, a collection of conformers resulted after Random search which were ranked by energy, and the percentage contribution of each calculated using Boltzmann distribution (section 2.7.3.1.). For each conformer the psi (ψ) and phi (ϕ) space was divided into 10° sectors. The distribution of conformers was computed in SYBYL spreadsheet and plotted as a 3DPR plot relating ψ , ϕ and percent accumulated conformers (section 2.7.3.1.1.). General conclusions about predominant torsional types were strengthened by combining outputs for collections of dipeptides. The results from conformational analysis showed that dipeptides adopt a limited set of nine combinations of ψ and ϕ ; for ψ , -50 to -85° ; $+140$ to -175° ; and $+50$ to $+85^\circ$, designated A4, A7, and A10, respectively; and for ϕ , $+40$ to $+85^\circ$; -95 to -50° ; and -130 to $+175^\circ$, designated B2, B9 and B12, respectively (Fig. 3-10). If peptides with G or P are excluded, these angular ranges become considerably tighter. These sets of conformational types were related to substrate specificity determined experimentally for Dpp and Tpp (Payne *et al.*, 2000; Grail & Payne, 2000).

A plot of the *N-C* distance against accumulated percentage contributions for all conformers for 50 dipeptides showed that they distributed into discrete groups with different lengths (Fig. 3-11a). The main groups have conformer lengths between 4.5 and 6.3 Å; the smallest group around 3.5 Å, has conformers with *cis* ω bond, arising from X-Pro peptides. This grouping of *N-C* distances is a consequence of the favoured conformations described above, with particular combinations of backbone torsional angles imposing particular *N-C* geometries on the conformers. This effect was illustrated by plotting *N-C* distances for specific torsional combinations, e.g. A7(B9,B12) (Fig. 3-11b), A4(B9,B12) (Fig. 3-11c) and A10(B9,B12) (Fig. 3-11d).

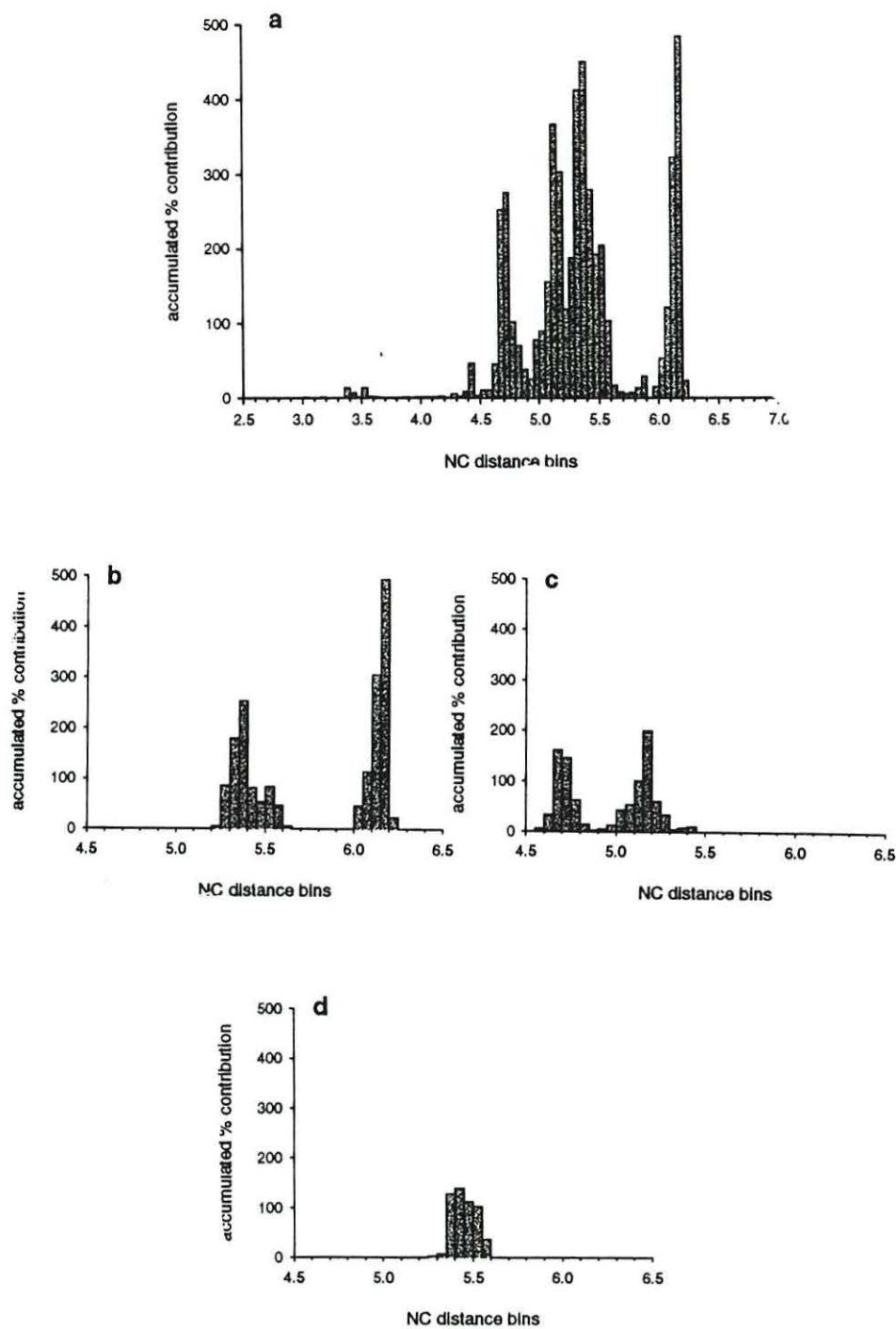


Figure 3-11: Relationship Between $N-C$ Distance and ψ and ϕ Torsion Angles.

$N-C$ distance was divided into 0.05 \AA and the accumulated percentages of conformers within each 0.05 \AA were calculated and then plotted a) all conformers, b) all A7B9 ($\sim 5.4 \text{ \AA}$) and A7B12 ($\sim 6.2 \text{ \AA}$) conformers, c) all A4B9 ($\sim 4.7 \text{ \AA}$) and A4B12 ($\sim 5.2 \text{ \AA}$) conformers, d) all A10 (B9, B12) ($\sim 5.4 \text{ \AA}$) conformers (Grail & Payne, 2000).

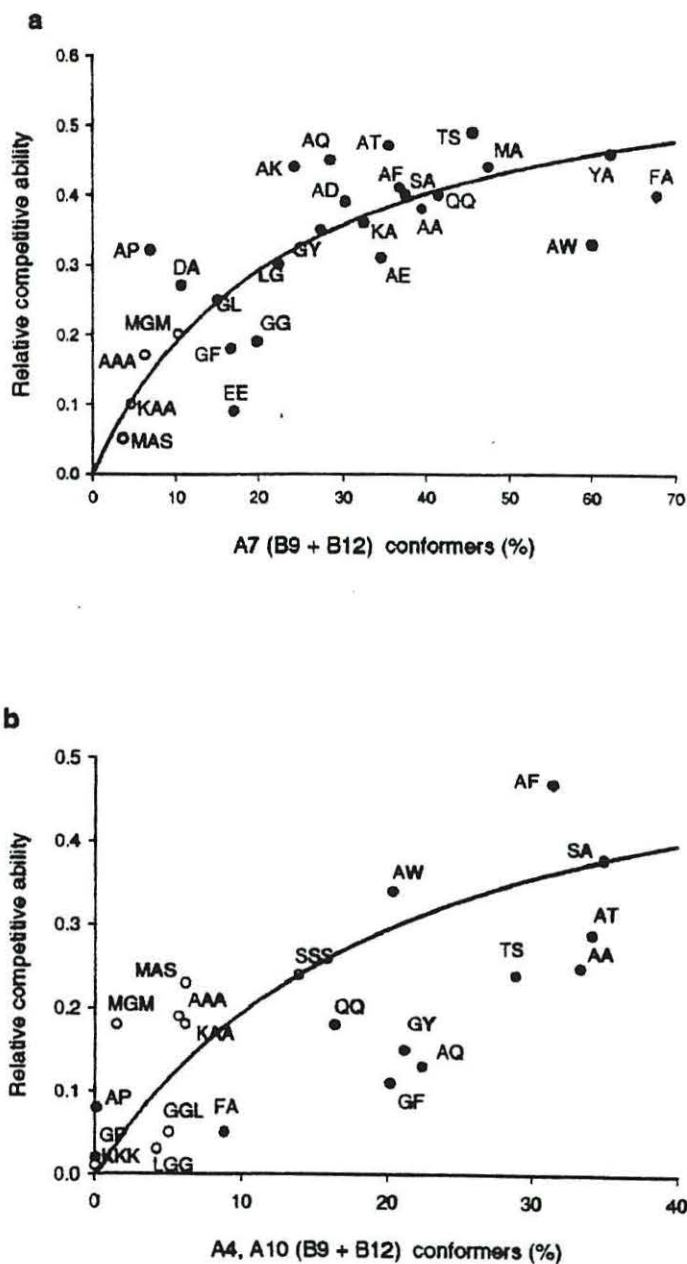


Figure 3-12: a) Relationship between amount of peptide conformers in A7 (B9+B12) conformations and relative competitive abilities of peptides overcoming inhibition arising from uptake of VG by Dpp. The transport mutant PA0410 (*opp*⁻, *tpp*⁻) of *E. coli* K12, which is sensitive to valine was used. For tripeptide conformers, an additional screen of N-C distance of 4.5-6.0 Å was applied to identify folded conformers. b) Relationship between amount of peptide conformers in A4, A10(B9+B12) conformations and relative competitive abilities of peptides overcoming inhibition arising from uptake of VG by Tpp. The transport mutant PA0333 (*dpp*⁻, *opp*⁻) of *E. coli* K12 was used. Amino acid residues are abbreviated using single letter code; tripeptides (○) and dipeptides (●). For tripeptide conformers, an additional screen of N-C distance of 4.5-5.5 Å was applied to identify folded conformers (Payne *et al.*, 2000).

3.2.4.1. Correlation of Activity Data with the MRT for Dpp and Tpp

The ranking of peptides in order of their competitive ability in Table 3.1 was related to the calculated subsets of ψ and ϕ angles of conformers populated by these peptides. The substrate affinity for Dpp was correlated to peptides having their backbone torsion angles ψ and ϕ in A7 (B9+B12) MRT with *trans* omega peptide bonds (Fig. 3-12a). Results from ligand binding studies showed that amino acids such as Ala, Val, Leu, Ser and Thr at the *N*-or *C*-terminus of dipeptides, had a high affinity for binding to DppA. These peptides contained a large percentage of conformers with backbone torsion angles in A7(B9+B12) MRT (Fig. 3-12a). In addition, their side chains are not charged so they do not interfere with the positive-and negative-charge of the *N*-and *C*-terminus required for ligand binding. DppA also has pockets filled with variable amounts of water to accommodate any of the naturally occurring amino acid side chains. The chi-space of these amino acids can be readily accommodated in the binding pockets, contributing to them being good substrates for Dpp.

Peptides containing Gly and or Pro residues had poor substrate affinity as these peptides have their backbone torsion angles at the extreme edge of the MRT regions (Grail & Payne, 2000). Gly-Gly is found to be especially poorly recognised by peptide transporters in all tested species (Matthews & Payne, 1980; Matthews, 1991; Payne & Smith, 1994). The aromatic amino acids Phe, Tyr and Trp at the *N*-or *C*-terminus of dipeptides also showed high affinity for DppA, as they have a high percentage of conformers in A7B9+B12. Dipeptides containing aromatic residues have their minimum energy conformers contributing a large percentage to the total conformer distribution. This can in certain instances be a disadvantage, as examination of their chi space has shown that in some conformers the side chains are not be in the right orientation to fit into the binding pockets. Asp and Glu amino acids at the *N*-terminus of dipeptides had poorer activity than at the *C*-terminus, i.e. Ala-Asp was a better competitor than Asp-Ala for Dpp. This arises because in certain conformers their chi-space causes the negative charge of these amino acid to interfere with the positive charge of the *N*-terminus, precluding binding to Asp⁴⁰⁸ in the binding site (Grail & Payne, 2000).

For Tpp, competitive ability to protect against the inhibition resulting from uptake of VG and direct assays of substrate transport, were determined in an *E.coli* mutant strain PA0333 lacking Dpp and Opp activities (Smith *et al.*, 1999). These relative activities were related to all subsets of conformers and found to correlate only with the sum of A4(B9+B12) plus A10(B9+B12) conformers, a result that indicates the torsional specificities of the MRT for Tpp (Fig. 3-12b) (Payne *et al.*, 2000).

3.2.4.2. MRTs for Tripeptides

Tripeptides are also transported by both Dpp and Tpp although less well than dipeptides. Thus, MRTs of these transporters need to embrace conformational features shared by both peptide groups. Therefore, amongst tripeptide conformers it may be expected that ones exist with appropriate ψ and ϕ angles, and have the critical charged *N-C*-termini with *N-C* distance geometries matching those for dipeptide substrates (Payne *et al.*, 2000).

A collection of tripeptides was subjected to conformational analysis, and conformers were screened for ones with A7(B9+B12) plus an *N-C* distance of 4.5-6.0 Å, and this identified a subset of matching folded structures as putative Dpp substrates, and using the parameters for Tpp (A4,A10 (B9+B12) with an *N-C* distance of 4.0-5.5 Å a further subset was identified. For these unique folded conformers, atom-superimposition procedures showed they effectively matched the dipeptide-derived MRTs at the critical *N*- and *C*-termini, and the first peptide unit (ψ , ϕ , and ω) and side chain; the second peptide bond and *C*-terminal side chain effectively formed a structural unit orientated similarly to the *C*-terminal side chain of dipeptides allowing it to fit into the relevant pocket of transporter proteins. These folded forms generally comprised just a few percent of total conformers (Payne *et al.*, 2000)..

The percentage of relevant folded conformers of tripeptides was related to results for their competitive effects on uptake of inhibitory VG, and good correlations were obtained. Similarly, for Tpp a good correlation was found for the folded tripeptide conformers identified as putative substrates when these were related to transport rates and to competition with VG (Fig. 3-12a,b) (Payne *et al.*, 2000).

3.3. DISCUSSION

3.3.1. Conformational Analysis of Peptides

Although the idea of peptides having specific bioactive conformation(s) is a basic premise in studies of molecular recognition, attempts to identify them have largely been restricted to inspection of crystal structures of free and/or bound forms or considerations of results from NMR studies (Marshall *et al.*, 1993; Nikiforovich, 1994; Wilkinson, 1996; Cornell *et al.*, 1997). Several computation approaches have been used, but very few using computational analysis of simple charged peptides, probably because of reservations concerning the conformational flexibility of these compounds (Knapp-Mohammady *et al.*, 1999).

Studies in this laboratory have shown that conformational analysis using Random search can provide a useful description of the complement of conformers present in solution for any individual or group of peptides (Grail & Payne, 2000). In practice, conformers of an individual peptide may undergo interconversion in solution, but a dynamic equilibrium will exist in which the repertoire of conformers remains essentially constant under fixed conditions, with each particular conformer being present at a relatively fixed concentration related to its energy.

The 3DPR plot allows graphical visualisation of this equilibrium conformer profile for any peptide substrate(s). The predominant backbone features displayed by the peptide pool overall can be present to varied degrees in the conformer population of an individual dipeptide. However, they may not necessarily be present in the minimum energy conformer of any particular peptide. X-ray crystallography, or minimum energy conformations, of a ligand provides limited insight into molecular recognition. This information may only be obtainable from consideration of the complete conformer profile of the substrate(s) (Grail & Payne, 2000).

3.3.2. Correlation of Activity Data with Molecular Modelling Data

Correlation of molecular modelling results with biological specificity of Dpp and Tpp has allowed the MRTs of peptide transporters to be identified and iteratively refined.

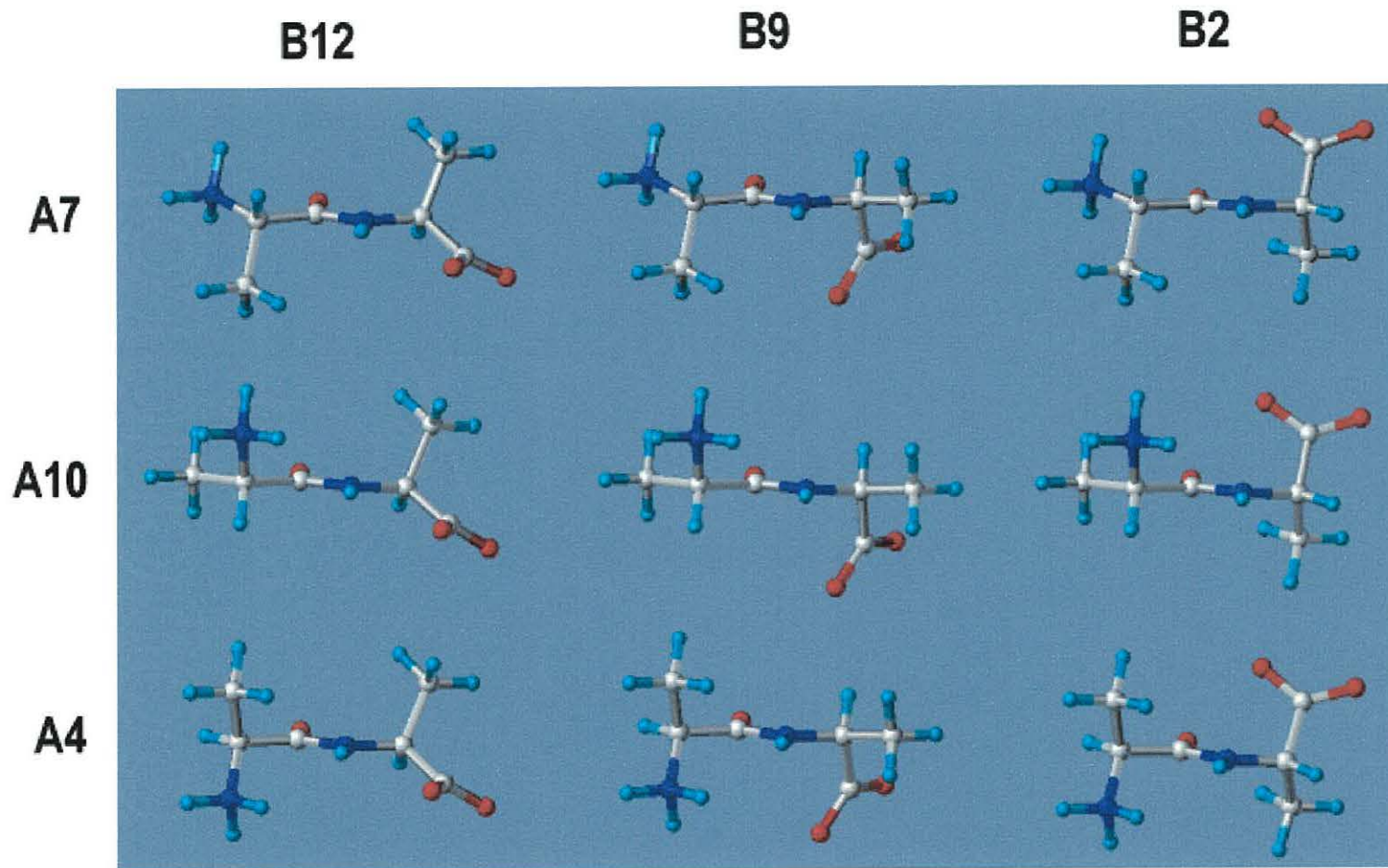


Figure 3-13: Ball & Stick Structures of Ala-Ala Illustrating the Nine Predominant Torsional Forms (Grail & Payne, 2000).

The MRTs for Dpp and Tpp have identified “active” conformers as those with ψ angles in A7, A4 and A10 and with ϕ angles only in B9 and B12 regions. Fig. 3-13 shows the nine predominant torsional forms for the dipeptide Ala-Ala. Most dipeptides possess a majority of their conformers in both MRT recognition types, A7(B9+B12) and A4,A10(B9+B12), making them good substrates for both Dpp and Tpp, whereas some e.g. YA, FA, exist predominantly in one or the other type making them rather specific for only one system, a feature already noted in transport studies (Payne & Smith, 1994). For any particular peptide, its lowest energy conformers may not be substrates for either transporter, a situation that is understandable when such peptides are seen as being only individual components of a larger peptide pool.

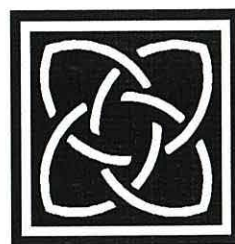
These identified relationships between unique conformers and biological activity of Dpp were confirmed independently by the reported crystal structure of GL bound to DppA (Dunten & Mowbray, 1995), in which GL occurs as an A7B9 conformer with an *N-C* distance of 5.6 Å, see Fig. 1-2. The conformers predicted as the MRT of Dpp have their peptide bond N and O atoms orientated so that H-bonding with protein backbone atoms in DppA is optimised, and the side chains are directed so as to occupy appropriate cavities (Dunten & Mowbray, 1995). Conformers with B2 torsion angles are “inactive” and not recognised by peptide transporters. The B2 conformers have their side chains orientated so as to preclude interaction of the *C*-terminus to Arg³⁵⁵ in the binding pocket when the *N*-terminus is anchored to its cognate negatively-charged group (Payne *et al.*, 2000).

3.3.3. MRTs of Substrates for Peptide Transporters

The parameters important for molecular recognition of substrates by peptide transporters include i) charged *N*-terminal and *C*-terminal groups, allowing electrostatic and H-bond donor and acceptor interactions; ii) combinations of torsion angles (ψ , ϕ and ω) in the backbone; iii) stereochemistry at α -carbon chiral centres; iv) *N-C* distance between terminal amino *N* and carboxylate *C* atoms; v) chi (χ)-space torsion angles of the side chain; vi) H-bond acceptor and donor properties of peptide bond O and N atoms; and vii) charge fields around *N*-terminal α -amino and *C*-terminal α -carboxylate groups.

Some of the features of the MRT established here correlate with the model for the orientation of the key binding features of substrates for PepT1 described by Bailey *et al.* (2000), however their template only provides limited information on substrate affinity (Bailey *et al.*, 2000).

Knowledge of the MRTs for substrates for peptide transporters gained in this study, can now be applied for the *rational* design of bioactive mimetics and peptidomimetic drugs, such as ACE inhibitors, for their effective absorption and delivery by intestinal peptide transporters.



CHAPTER 4
CONFORMATIONAL ANALYSIS OF
PEPTIDOMIMETICS

4.1. INTRODUCTION

The use of peptides as therapeutic agents is limited by a number of factors including conformational flexibility, instability to peptidases and poor bioavailability. In order to address these limitations, peptides are modified into peptidomimetics (section 1.7.). Molecular modelling is generally used to search for the *bioactive* conformation of a peptide and has proved useful in identifying prototypic leads, and to develop peptidomimetics into drug candidates. However, the pharmacological efficacy of peptide therapeutics not only depends on the recognition and binding to intracellular enzymes or receptors, but also their oral delivery via peptide transporters.

The aim of this study is to show how conformational analysis, using molecular modelling, can be applied to assess the *bioavailability* of peptidomimetics at the initial discovery and development stage. Molecular modelling, using Random search in SYBYL, has been used to evaluate the MRTs required for recognition of substrates by peptide transporters (Chapter 3). The MRTs provide a description of structural and conformational features of peptide substrates, and includes a definition of sets of *backbone torsion angles* for psi (ψ), omega (ω) and phi (ϕ) required for recognition by Dpp and Tpp (Payne *et al.*, 2000; Grail & Payne, 2000).

In this study a range of dipeptide mimetics will be investigated for their putative ability to be transported by Dpp and Tpp by assessing whether their conformer distribution range match the MRTs. Predictions of putative Dpp/Tpp transport activities will be related only to preliminary considerations of the *backbone torsion angles*; other potentially important features of the MRT will be later examined. Systematic structural changes to peptidomimetic structures will also be done in order to identify chemical modifications that produce *backbone torsion angles* in the MRT sectors required for recognition by peptide transporters. The information gained from these studies will then be applied to the *rational* design of peptidomimetics that have structural features required for effective transport.

Conformational analysis was carried out upon a range of peptidomimetics and their modified analogues (section 2.7.2.2.) and analysis of results was done as described (section 2.7.3.2.). Results for each compound are presented in tabular forms with the mimetic number, generally adapted from Gillespie *et al.* (1997), and its structure. In some cases, mimetic number followed by * is used to differentiate two different mimetic structures obtained from different literature sources, but having a similar nomenclature to Gillespie *et al.* (1997). The nomenclature used for peptide bond mimetics (PBM) has been developed in this study to clarify these specific set of modifications from the dipeptide isosteres, lactam-constrained mimetics and torsionally-constrained mimetics. The mimetic number followed by an underscore (e.g. M5_1) represents a modified mimetic structure, designed in this study, that is not available in the literature. The results from molecular modelling of all peptidomimetics and their modified analogues are also displayed as 3DPR plots (section 2.7.3.1.1.), in order to illustrate the conformer distribution range and to identify conformers within the MRT sectors required for transport. The colours of the peaks are for visual clarity only and do not uniformly correspond to any percentage values.

4.2. RESULTS

4.2.1. Conformational Analysis of Dipeptide Isosteres

Table 4.1. shows the results from conformational analysis of dipeptide isosteres. Random search of these compounds produced a large number of unique conformers, with the minimum energy conformers generally contributing only a small percentage to the total conformers' distribution range. Natural peptides have *trans* (and some *cis*) ω peptide bonds, these dipeptide isosteres had 'pseudo' peptide bonds that were either *cis* and/or *trans*, or had variable ω torsion angles that were neither *cis* nor *trans*.

Table 4.1. Minimum Energy Conformers of Dipeptide Isosteres Showing their ψ (Tor2), ω (Omega), ϕ (Tor4) Torsion Angles, NC Distance and their Total Percentage Distribution of Conformer Range.

| M | Structure | Energy kcal/mol | % | ψ ° (Tor2) | ω ° Omega | ϕ ° (Tor4) | NC Å | % Total Range |
|----|-----------|--------------------|-------|--------------------|---------------------|--------------------|---------|---------------------|
| 4 | | 35.82 | 39.9 | 155.1 | 177.8 | -115.1 | 5.92 | 61% A7 <i>t</i> - |
| | | 36.67 | 9.96 | -67.4 | -178.2 | 110.4 | 5.51 | 24% A4 <i>t</i> - |
| | | 36.83 | 7.74 | -50 | -178.6 | 117.5 | 5.38 | 4% A10 <i>t</i> -- |
| 11 | | 0.65 | 12.98 | 102.5 | 77.4 | 61.5 | 5.34 | 19% -- * B9 |
| | | 0.82 | 9.89 | 131.4 | 169.3 | -65.3 | 5.50 | 14% -- * B2 |
| | | 0.94 | 8.1 | 86.6 | 109.5 | -58.1 | 4.81 | 8%~A10 * B9 |
| 6 | | 1.99 | 16.11 | 158.8 | 174.5 | 57.9 | 5.24 | 29% A7 <i>t</i> B2 |
| | | 2.67 | 5.27 | 51.7 | 174.9 | 161 | 5.26 | 16% A10 * B2 |
| | | 2.68 | 5.19 | 55.6 | 160.7 | 151.2 | 5.30 | 14% A10 <i>t</i> -- |
| 7 | | 3.23 | 11.16 | -167.7 | 176.8 | 60 | 5.38 | 18% A4 <i>t</i> B2 |
| | | 3.51 | 7.10 | -62.9 | -175.9 | 61.2 | 5.41 | 15% -- <i>t</i> B2 |
| | | 3.53 | 6.93 | -56.9 | -173.9 | 61.7 | 5.37 | 11% A7 * B2 |
| 8 | | 0.79 | 25.84 | 141.2 | 179.8 | 128.3 | 5.68 | 39% A7 <i>t</i> -- |
| | | 1.25 | 12.1 | 117.8 | -0.7 | 73.2 | 4.70 | 21% -- <i>t</i> -- |
| | | 1.57 | 7.19 | 129.9 | 179.5 | -41.5 | 5.28 | 12% -- <i>c</i> B2 |

Table 4.1. Continued.

| M | Structure | Energy kcal/mol | % | ψ° (Tor2) | ω° Omega | ϕ° (Tor4) | NC Å | % Total Range |
|----|-----------|--------------------|-------|------------------------|-------------------------|------------------------|---------|---------------|
| 5 | | 23.97 | 30.9 | -112.7 | -69.9 | 157.6 | 5.51 | 47% -- * -- |
| | | 24.71 | 9.13 | 107.4 | 68 | -90.7 | 4.53 | 23% -- * B9 |
| | | 24.72 | 9.03 | -110.9 | 71.6 | -72.5 | 3.37 | 16% -- * B2 |
| 32 | | 14.2 | 22.01 | -174.3 | -0.5 | -135.7 | 5.72 | 22%~A7c B12 |
| | | 14.35 | 17.21 | 84.8 | -0.2 | -134.9 | 4.45 | 17%A10c B12 |
| | | 14.55 | 12.57 | -75.9 | -0.3 | -123.8 | 4.87 | 13% A4 c -- |
| 43 | | 6.74 | 38.79 | 46.4 | -162.4 | 92.5 | 4.22 | 39%~A10*-- |
| | | 6.84 | 32.79 | 153.7 | -163.7 | 93.5 | 4.89 | 33% A7 * -- |
| | | 7.49 | 11.26 | 160.7 | 165.5 | 142.1 | 5.86 | 11% A7 * -- |
| 46 | | 22.97 | 18.79 | -43.8 | -177.6 | -179.9 | 5.17 | 63% -- t B12 |
| | | 22.99 | 18.1 | -36.1 | -176.5 | 177.5 | 5.19 | 35% A7 t B12 |
| | | 23.17 | 13.54 | -41.4 | -176.4 | 176.9 | 5.17 | |
| 47 | | 31.14 | 26.58 | 146.1 | 177.6 | -177.8 | 6.02 | 63% -- t B12 |
| | | 31.34 | 19.35 | -30.8 | -177.6 | 177.8 | 5.40 | 35% A7 t B12 |
| | | 31.36 | 18.64 | 134.9 | 178 | 179 | 5.96 | |
| 48 | | 39.84 | 34.2 | -31.4 | -178.4 | 178.2 | 5.32 | 80% -- t B12 |
| | | 40.12 | 21.57 | -27.7 | -178.5 | -179.1 | 5.31 | 17% A7 t B12 |
| | | 40.43 | 13.06 | 142.5 | 178.5 | -178.3 | 6.01 | |

-- denotes outside the MRT regions of A7, A4, A10 and B9, B2 and B12 *t* denotes trans omega *c* denotes cis omega
 * denotes not cis or trans omega **Dpp substrate**

M4 has a similar structure to the dipeptide Phe-Gly, and has the amide peptide bond substituted by carbon atoms linked by a double bond. M4 had ψ (Tor2) angles in A7, A4 and A10, with *trans* ω , and ϕ (Tor4) angles outside B2, B9 and B12. Even though M4 had conformers in A7, A4 and A10 with *trans* ω , it would be predicted to have poor transport activity as it does not have its ϕ (Tor4) angles in B9 and B12 MRT.

M11 is also similar to Phe-Gly, but has the amide nitrogen substituted by a carbon atom. M11 had most of its conformers outside A7 and A4 and a few conformers near A10. The ω bond had variable torsion angles that were neither *cis* nor *trans*, with ϕ (Tor4) angles in B9 and B2. M11 would be predicted to have poor transport activity as it does not have *trans* ω conformations. **M6** has the amide peptide bond substituted by carbon atoms with a hydroxyl group, the second C α has an additional phenyl group. M6 had ψ (Tor2) angles in A7, A4, A10, with either *trans* or variable ω torsion angles, and ϕ (Tor4) angles mainly in B2 or outside B12. M6 would be predicted to have poor Dpp and Tpp activity because of its variable omegas, and almost half of its conformers are in A7B2 and A10B2 which are recognised for transport. **M7** is similar to the dipeptide Phe-Ala, but has its amide peptide bond substituted by carbon atoms. M7 had ψ (Tor2) angles in A4, outside A7, and a few conformers in A10. The majority of its conformers had ϕ (Tor4) angles in B2, with some conformers in B9 and B12. The ω bond was mainly *trans*, with fewer conformers having omegas that were neither *cis* nor *trans*. M7 would be predicted to have poor bioavailability due to variable ω and its high proportion of B2 conformers. **M8** is an unsaturated analogue of M7, where the carbon atoms are joined by a double bond. M8 had ψ (Tor2) angles in or near A7, with some conformers in or outside the A4. In contrast to M7, all the conformers had either *cis* or *trans* ω as seen with M4. Very few conformers had ϕ (Tor4) angles within the recognised regions, the main conformer being near B12 with some conformers outside B9 and B2. This is in contrast to M4 which had the majority of its ϕ (Tor4) angles near B12. M8 may be predicted to have poor Dpp activity as most of its conformers with *trans* ω are in A7 but outside B9 and B12. **M5** does not have a linear peptide backbone and the peptide bond is substituted by carbon atoms that form part of a benzene ring. M5 had ψ (Tor2) outside A4, A10 and A7 as well as ω bond conformations that were neither *cis* nor *trans*. ϕ (Tor4) angles were outside B12, with some conformers in B9 and B2. M5 would be expected to have poor Tpp and Dpp activity as it does not have A7, A4 and A10 conformers. **M32** has a Gly-Ala dipeptide backbone, but the carbonyl group of the peptide bond is cyclized with a 5 membered ring.

M32 had ψ (Tor2) angles in A7, A10 and A4, with a majority of ϕ (Tor4) angles in or near B12, and some in B9 and B2. Unlike the conformations obtained with other isosteres in this group, all the conformers had *cis* ω conformations. This showed that cyclization of the carbonyl group produced only *cis* ω s, with no *trans* ω . M32 would have very poor transport activity due to the absence of *trans* ω s. **M43** is similar to M32, but is cyclized from the carbonyl carbon to the second C α near the C-terminus. It contains the amide group of a peptide bond and an additional nitrogen atom in its 5 membered ring. M43 had ψ (Tor2) angles in or near A7, with some conformers in or near A10, and ϕ (Tor4) angles outside B2, B12 and B9. The peptide bond had torsion angles outside a *trans* ω , but lacked *cis* ω conformations. Conformers of M43 would also be predicted to have poor transport activity as the ω torsion value fall outside the recognised range of $180^\circ \pm 5^\circ$. **M46** is cyclized from the carbonyl carbon to the second C α near the C-terminus, with a 5-membered ring containing a sulphur atom. M46 had ψ (Tor2) angles constrained only in A7 or outside A4, with *trans* ω conformation, and ϕ (Tor4) angles constrained only in B12. As M46 has A7 *trans* B12 conformers, it would be expected to have better Dpp activity than M43. **M47** is the same as M46, but the sulphur atom in the 5-membered ring is changed to an oxygen atom. This also had conformers with *trans* ω bonds, with ψ (Tor2) angles constrained in A7 and near A4 and ϕ (Tor4) angles constrained in B12 as seen with M46. As M47 also has the same amount of A7 *trans* B12 conformers as M46, it would also be expected to have similar Dpp activity. **M48** is similar to both M46 and M47, but has an amide group instead of a sulphur or an oxygen atom in its 5 membered ring. M48 had a higher percentage of conformers with ψ (Tor2) angles near A4, with less conformers in A7 compared with M46 and M47. Like M46 and M47, all the conformers had *trans* ω conformations and ϕ (Tor4) angles constrained in B12. M48 would be predicted to be a Dpp substrate but may show lower activity than either M46 or M47 as it has less A7B12 conformers than these two analogues. Fig. 4-1 shows 3DPR plots for M46, M47, M48 and M43 showing their percentage conformer distribution range.

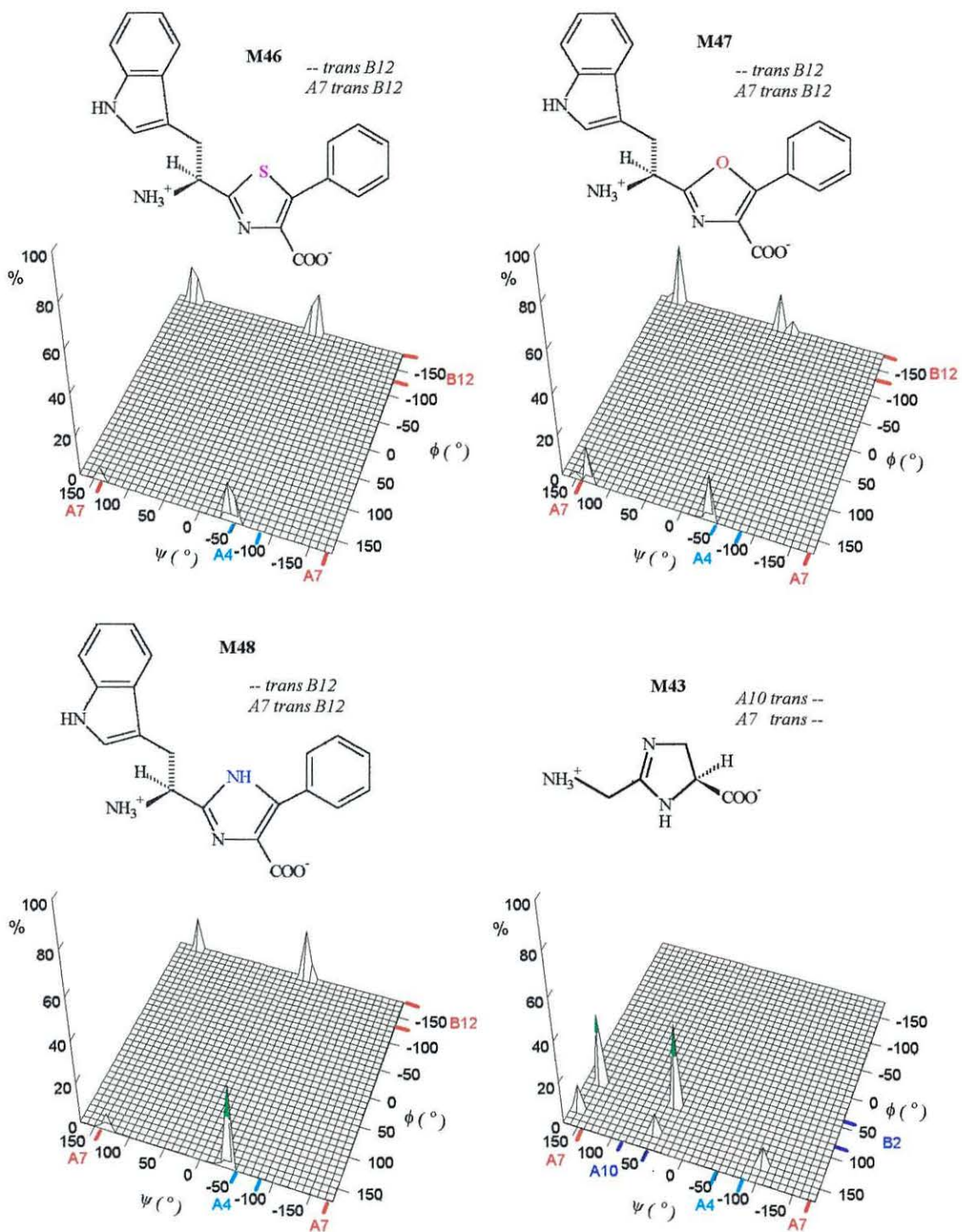


Figure 4-1: 3DPR Plots of ψ vs ϕ vs % Conformers for M46, M47, M48 and M43.

4.2.2. Conformational Analysis of Peptide Bond Mimetics

The aim of this study was to investigate the preferred ω torsion conformations when the chemical structure of the peptide bond is changed. The dipeptide Ala-Ala is a Dpp and Tpp substrate and its predominant conformers have ψ (Tor2) angles in A7, A4 and A10, with *trans* ω , and ϕ (Tor4) angles in B2, B9 and B12. A number of Ala-Ala peptides were modelled containing a modified peptide bond and the results are shown in Table 4.2.

Table 4.2. Minimum Energy Conformers of Ala-Ala and its Peptide Bond Mimetics Showing their ψ (Tor2), ω (Omega), ϕ (Tor4) Torsion Angles, NC Distance and their Total Percentage Distribution of Conformer Range.

| PBM | Structure | Energy kcal/mol | % | ψ ° (Tor2) | ω ° Omega | ϕ ° (Tor4) | NC Å | %Total Range |
|-----|-----------|--------------------|-------|--------------------|---------------------|--------------------|---------|---------------|
| AA | | 2.40 | 23.19 | 164.9 | 178.4 | -65.2 | 5.30 | 23% A7 t B9 |
| | | 2.57 | 17.64 | 165.3 | -179.1 | -159.1 | 6.12 | 18% A7 t B12 |
| | | 2.67 | 15.01 | 164.3 | 178.6 | 51.3 | 5.06 | 15% A7 t B2 |
| 1 | | 5.74 | 33.83 | 145.7 | -179.7 | 49.3 | 4.83 | 34% A7 t B2 |
| | | 6.02 | 21.41 | 148.8 | 178.8 | -135.2 | 6.03 | 27% A7 t B12 |
| | | 6.41 | 11.38 | 92.8 | 179.8 | 50.4 | 4.69 | 11% ~A10 t B2 |
| 2 | | 2.28 | 2.74 | 47.0 | 179.3 | 61.8 | 4.70 | 32% ~A10 t B9 |
| | | 2.31 | 12.29 | 46.6 | 178.7 | -53.9 | 5.18 | 13% ~A10 t B2 |
| | | 2.42 | 10.13 | 46.7 | 178.9 | -54.4 | 5.20 | 7% A4 t B9 |
| 3 | | 5.08 | 37.89 | 0.0 | 179.4 | -65.3 | 4.94 | 40% -- t B9 |
| | | 5.17 | 32.83 | -0.1 | -178.8 | -159.7 | 5.06 | 34% -- t B12 |
| | | 5.34 | 24.89 | 0.0 | 179.3 | 51.5 | 4.98 | 26% -- t B2 |
| 4 | | 2.78 | 23.31 | 156.4 | 178.4 | -66.5 | 5.43 | 23% A7 t B9 |
| | | 3.07 | 14.51 | -62.3 | 178.9 | -66.6 | 4.68 | 15% A4 t B9 |
| | | 3.14 | 12.92 | 99.9 | 179.2 | -65.8 | 5.44 | 13% -- t B9 |
| 5 | | 2.21 | 23.91 | 120.1 | 180.0 | 119.1 | 5.37 | 79% -- t -- |
| | | 2.25 | 22.51 | 120.2 | 180.0 | 119.7 | 5.36 | 7% A4 t -- |
| | | 2.81 | 9.10 | 119.8 | -180.0 | -28.4 | 5.22 | |

Table 4.2. Continued.

| PBM | Structure | Energy kcal/mol | % | ψ (Tor2) ° | ω Omega° | ϕ (Tor4) ° | NC Å | % Range | Total |
|-----|-----------|--------------------|-------|--------------------|--------------------|--------------------|---------|-------------|-------|
| 6 | | 1.64 | 13.67 | 59.9 | 71.9 | -98.2 | 3.59 | 15%A4 * B12 | |
| | | 1.87 | 9.43 | 59.0 | -125.9 | 51.4 | 3.39 | 14%A10*~B9 | |
| | | 2.07 | 6.80 | 179.0 | 109.8 | -146.5 | 5.80 | 11%A10 * B2 | |
| 7 | | 2.60 | 8.15 | 175.0 | -158.8 | 57.6 | 4.97 | 21%A7 * B2 | |
| | | 2.64 | 7.62 | 153.9 | -100.1 | 59.1 | 4.01 | 15%A10 * B2 | |
| | | 2.85 | 5.40 | 72.3 | -123.1 | 57.6 | 3.27 | 13%A7 * B12 | |
| 8 | | 3.28 | 22.31 | 60.0 | 172.4 | 59.0 | 4.95 | 38%A10~t B2 | |
| | | 3.46 | 16.39 | 175.9 | -174.2 | 61.7 | 5.28 | 19%A7~t B2 | |
| | | 3.48 | 15.89 | 56.6 | 57.7 | 53.6 | 4.57 | 10% A4~t B2 | |
| 9 | | 3.52 | 30.79 | 59.3 | 56.3 | 52.9 | 4.55 | 49%A10 * B2 | |
| | | 4.05 | 12.88 | 67.5 | 170.5 | 60.6 | 4.98 | 13%A7 * B12 | |
| | | 4.30 | 8.60 | 179.2 | -54.5 | -179.4 | 5.99 | 10% A7 * B2 | |

-- denotes outside the MRT regions of A7, A4, A10 and B9, B2 and B12 *t* denotes trans omega *c* denotes cis omega
 * denotes not cis or trans omega
 Dpp substrate Tpp substrate

PBM1 has an *N*-methylamide peptide bond that had *trans* ω bond angles similar to Ala-Ala, with ψ (Tor2) angles in A7 and near A10. Unlike Ala-Ala however, no conformers were found in A4. ϕ (Tor4) angles were mainly in B2 and B12, with very few B9 conformers. PBM1 would be predicted to be a substrate for Dpp and Tpp, but to have poorer transport activity than Ala-Ala, as it has a higher percentage of B2 conformers. **PBM2** has a retroamide peptide bond which produced a dramatic shift in the conformer distribution range. ψ (Tor2) angles were mainly near A10, or in A4 or near A7, with ϕ (Tor4) angles mainly in B2, B9 and B12. Like Ala-Ala all the conformers had *trans* ω peptide bonds. PBM2 may be predicted to have Tpp activity based on its *backbone torsion angles*, however the reversal of the carbonyl and amide groups would interfere with the H-bonding functions of the peptide backbone. **PBM3** contains a double bond forming a *trans* C=C isostere, and had ψ (Tor2) angles constrained outside A4, A10 and A7, with ϕ (Tor4) angles in B2, B9 and B12. PBM3 would be expected to have poor bioavailability as it does not have any A7, A4 and A10 conformers.

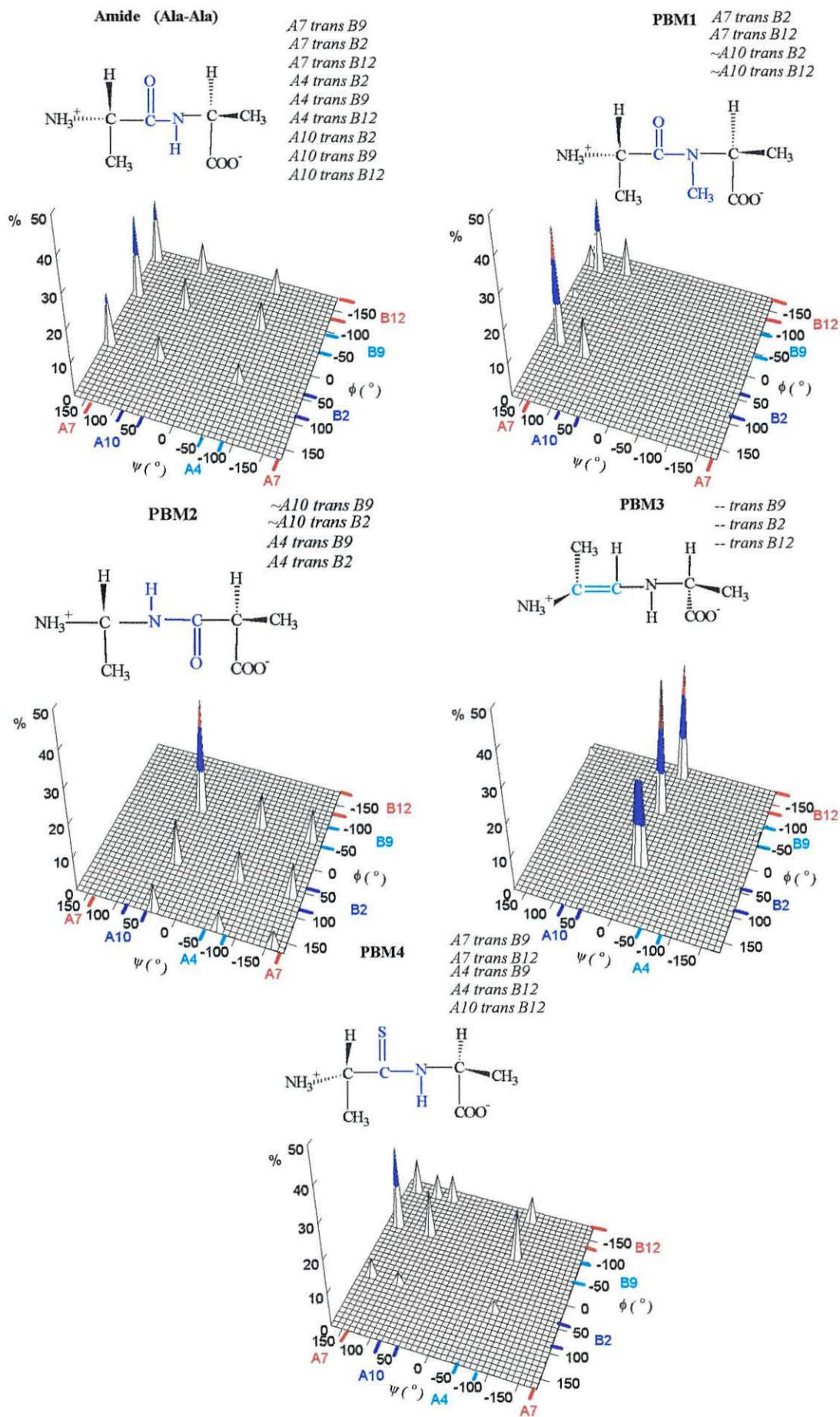
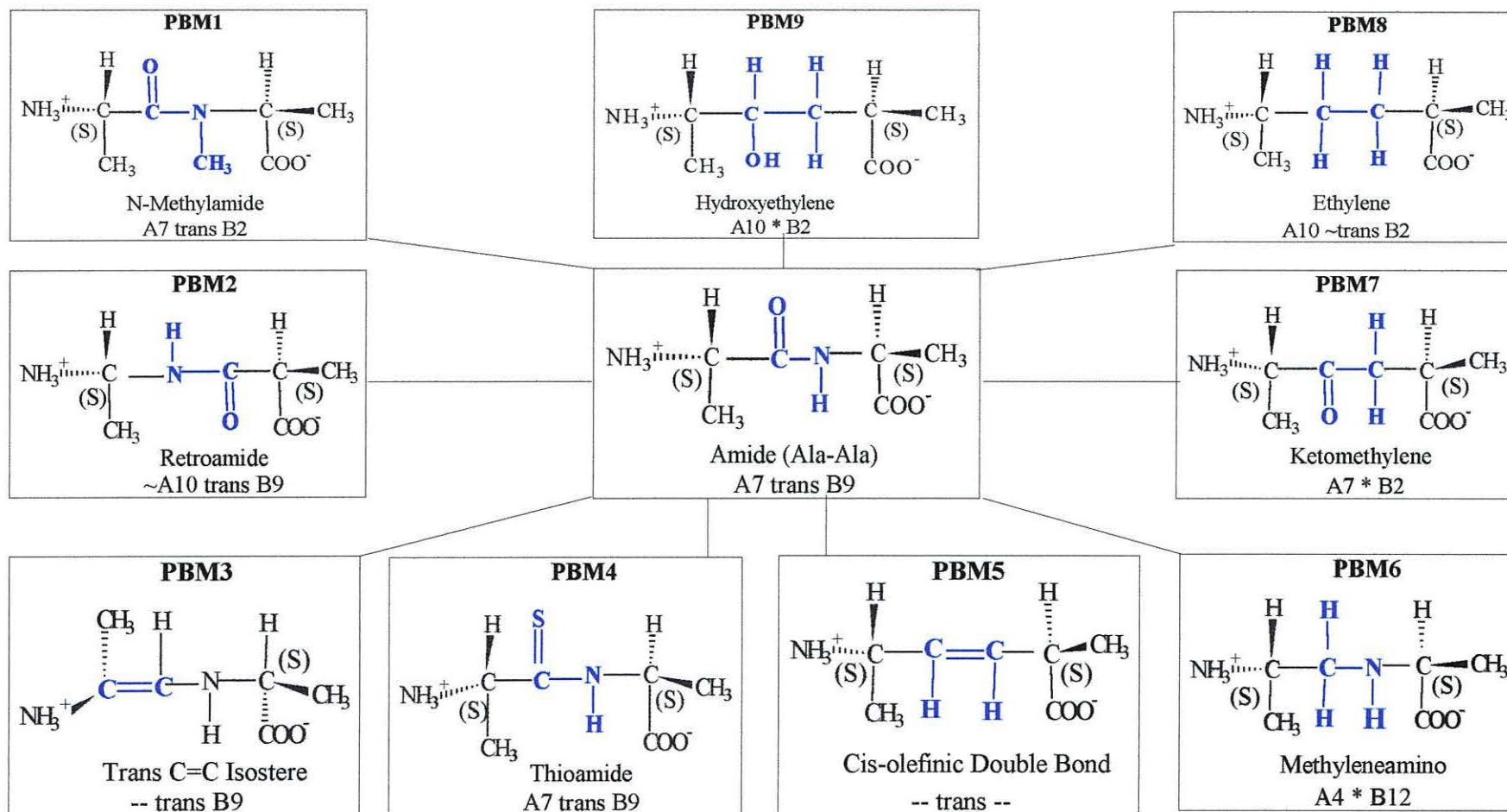


Figure 4-2: 3DPR Plots of ψ vs ϕ vs % Conformers for Ala-Ala and PBM1, PBM2, PBM3 and PBM4.

PBM4 has a thioamide peptide bond in which the carbonyl carbon is attached to a sulphur atom instead of an oxygen atom. PBM4 had most conformers in A7 and A4, and some conformers outside A10, with ϕ (Tor4) angles mainly in B9 and B12, and few B2 conformers. Like Ala-Ala, the low energy conformers had *trans* ω conformations. PBM4 would be expected to show both Dpp and Tpp activity as it has A7 *trans* B9/B12 and A4 *trans* B9/B12 conformers. Fig. 4-2 shows 3DPR plots for AA, PBM1, PBM2, PBM3, PBM4 showing the changes in their percentage conformer distribution range caused by modifications in their peptide bonds. **PBM5** has a cis-olefinic double bond with ψ (Tor2) angles outside A7 and A10 with a few conformers in A4. ϕ (Tor4) angles were outside B2, B9 and B12. PBM5 would be predicted to have poor transport activity as its ψ and ϕ angles are outside the MRT sectors. **PBM6** had the carbonyl group replaced by a carbon atom to form methyleneamino structure, and had ψ (Tor2) angles in A7, A4 and A10, with ϕ (Tor4) angles in B2, B12 and near B9. However, the peptide bond conformations were neither *cis* nor *trans* ω , therefore, PBM6 would be poorly transported by Dpp and Tpp, compared with Ala-Ala. **PBM7** has its amide bond modified to a ketone structure in which the amide nitrogen is replaced by a carbon atom. This had ψ (Tor2) angles in A7 and A10, and ϕ (Tor4) angles in B2, B12 and B9, but the peptide bond conformations were neither *cis* nor *trans* ω . PBM7 would also be predicted to show poor Dpp and Tpp activity due to a variation in omega. **PBM8** is an ethylene-like structure in which the carbonyl and amide groups are substituted by two carbon atoms. This had ψ (Tor2) angles in A10, A7 and A4, and the majority of ϕ (Tor4) angles in B2, with variable ω torsion angles. PBM8 would also be expected to have poor Dpp and Tpp activity as it has a high percentage of B2 conformers, and does not have good *trans* omega conformations. **PBM9** has a hydroxy-ethylene structure and had the majority of its ψ (Tor2) angles in A10 and A7, with (Tor4) angles in B2 and B12, with neither *cis* nor *trans* ω . Therefore, PBM9 would also be predicted to show poor Dpp and Tpp activity. Chart 1 shows the structures and conformations for Ala-Ala and its peptide bond modified analogues.

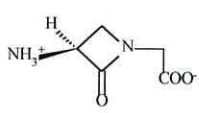
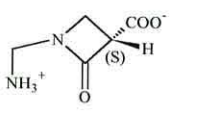
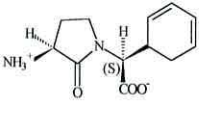
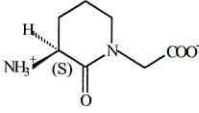
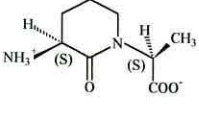
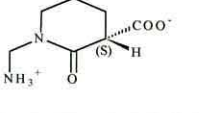
Chart 1: Structures and Conformations for Ala-Ala and its Peptide Bond Mimetics.



4.2.3. Conformational Analysis of Lactam-Constrained Mimetics

These compounds have their backbone cyclized with different size lactam rings from the C α to the amide nitrogen of the peptide bond. Lactam-constrained mimetics usually have peptide bonds constrained in the *trans* ω conformation. Random search of a variety of these structures showed that they had fewer unique conformers in solution than the isosteres and the peptide bond mimetics, due to the conformational constraint of the lactam ring. Table 4.3. shows the results obtained for conformational analysis of 4-,5- and 6-membered lactam ring mimetics.

Table 4.3. Minimum Energy Conformers of 4-,5- and 6-Membered Lactam-Ring Mimetics Showing their ψ (Tor2), ω (Omega), ϕ (Tor4) Torsion Angles, NC Distance and their Total Percentage Distribution of Conformer Range.

| M | Structure | Energy kcal/mol | % | ψ ° (Tor2) | ω ° (Omega) | ϕ ° (Tor4) | NC Å | %Total Range |
|------|---|-----------------|-------|-----------------|--------------------|-----------------|------|----------------------|
| 65 |  | 40.03 | 20.96 | -116 | 176.4 | -75.5 | 4.68 | 39% -- <i>t</i> B9 |
| | | 40.13 | 17.96 | -116.2 | 176.3 | -81 | 4.65 | 33% -- <i>t</i> B2 |
| | | 40.14 | 17.58 | -115 | -177.1 | 75.1 | 5.40 | 14% -- <i>t</i> B12 |
| 65_1 |  | 40.84 | 29.18 | 78.3 | -176.7 | -114.8 | 5.40 | 29% A10 <i>t</i> -- |
| | | 40.84 | 29.03 | -78.1 | 176.9 | -116.0 | 4.69 | 29% A4 <i>t</i> -- |
| | | 40.03 | 21.03 | 155.8 | 176.9 | -116.2 | 5.34 | 21% A7 <i>t</i> -- |
| 55 |  | 5.41 | 4.83 | -142.4 | -179.9 | 54.4 | 5.41 | 52% -- <i>t</i> B2 |
| | | 5.84 | 17.23 | -99.6 | 179.2 | 58 | 5.37 | 13% -- <i>t</i> B12 |
| | | 6.04 | 12.50 | -98.8 | -179.8 | -145.9 | 5.18 | |
| 56 |  | 5.09 | 34.48 | -145.2 | 179.8 | -66.8 | 4.94 | 43% -- <i>t</i> B9 |
| | | 5.15 | 31.37 | -144.1 | -178.5 | 69.1 | 5.38 | 40% -- <i>t</i> B2 |
| | | 6.0 | 7.9 | -143.4 | -179.0 | -165.4 | 6.01 | 13% -- <i>t</i> B12 |
| 56_1 |  | 5.76 | 39.31 | -145.5 | 179.9 | 52.4 | 5.22 | 48% -- <i>t</i> B2 |
| | | 5.94 | 29.27 | -142.5 | -177.6 | -152.6 | 5.91 | 34% -- <i>t</i> B12 |
| | | 6.44 | 12.79 | -146.6 | 178.3 | -67.9 | 4.90 | 15% -- <i>t</i> B9 |
| 56_2 |  | 5.68 | 27.05 | -68.2 | 178.0 | -102.1 | 4.68 | 27% A4 <i>t</i> -- |
| | | 5.76 | 23.63 | -64.9 | 180.0 | -142.6 | 4.94 | 24% A4 <i>t</i> B12 |
| | | 5.79 | 22.39 | 68.5 | -179.2 | -141.3 | 5.41 | 23% A10 <i>t</i> B12 |

-- denotes outside the MRT regions of A7, A4, A10 and B9, B2 and B12 *t* denotes trans omega *c* denotes cis omega

Tip substrate

4.2.3.1. 4-,5- and 6-Membered Lactam-Ring Mimetics

M65 is cyclized with a 4-membered ring, and had ψ (To2) angles outside A4, with *trans* ω , and ϕ (Tor4) angles in B9, B2 and B12. M65 would be expected to have poor transport activity as it does not have A7, A4 or A10 conformers. M65 was modified to **M65_1** by reversing the peptide bond to form a retro amide, similar to PBM2. This caused ψ (Tor2) angles to be in A7, A10 and A4, in contrast to M65, but ϕ (Tor4) angles shifted from B9, B2 and B12 to outside B9 and B12, with all *trans* omegas. M65_1 would be expected to have poor transport activity as it does not have B9 and B12 conformers. **M55** is cyclized with a 5-membered ring and had the majority of its ψ (Tor2) angles outside A7 and A4, with *trans* ω , and ϕ (Tor4) angles in B2 and B12. M55 would be predicted to have poor transport activity as it does not have A7 and A4 conformers. **M56** has a 6-membered lactam ring, and all its conformers had *trans* ω bonds, with ψ (Tor2) angles outside A4 and A7, and ϕ (Tor4) angles mainly in B9, B2 and some in B12. M56 would be predicted to have poor transport activity as it does not have A7, A4 or A10 conformers. **M56_1** was designed as a modification of M56 to see the effect of addition of a methyl group to the second C α near the C-terminus. ψ (Tor2) angles were outside A7, A4 and A10, as seen in M56, with *trans* ω , and ϕ (Tor4) angles were in B2 with an increase in B12 conformers, compared with M56 that had a higher percentage of B9 conformers (Table 4.3.). It seems that the addition of a methyl group to the C α near the C-terminus increases the amount of B12 conformers, and decreases the amount of B9 conformers. **M56_2** is a modification of M56, but has the peptide bond reversed to form a retro amide. This resulted in ψ (Tor2) angles in A4 and A10, with *trans* ω , and ϕ (Tor4) angles constrained outside B9, or in B12. Reversing the peptide bond in M56_2, had a dramatic effect on the range of conformer distribution, as seen with PBM2 and M65_1. ψ (Tor2) and ϕ (Tor4) angles shifted from inactive regions to MRT regions. M56_2 would be predicted to have better Tpp activity than M56 as it has A4B12 and A10B12 conformers, however the amide and the carbonyl groups are not in the right place for optimal H-bonding interactions.

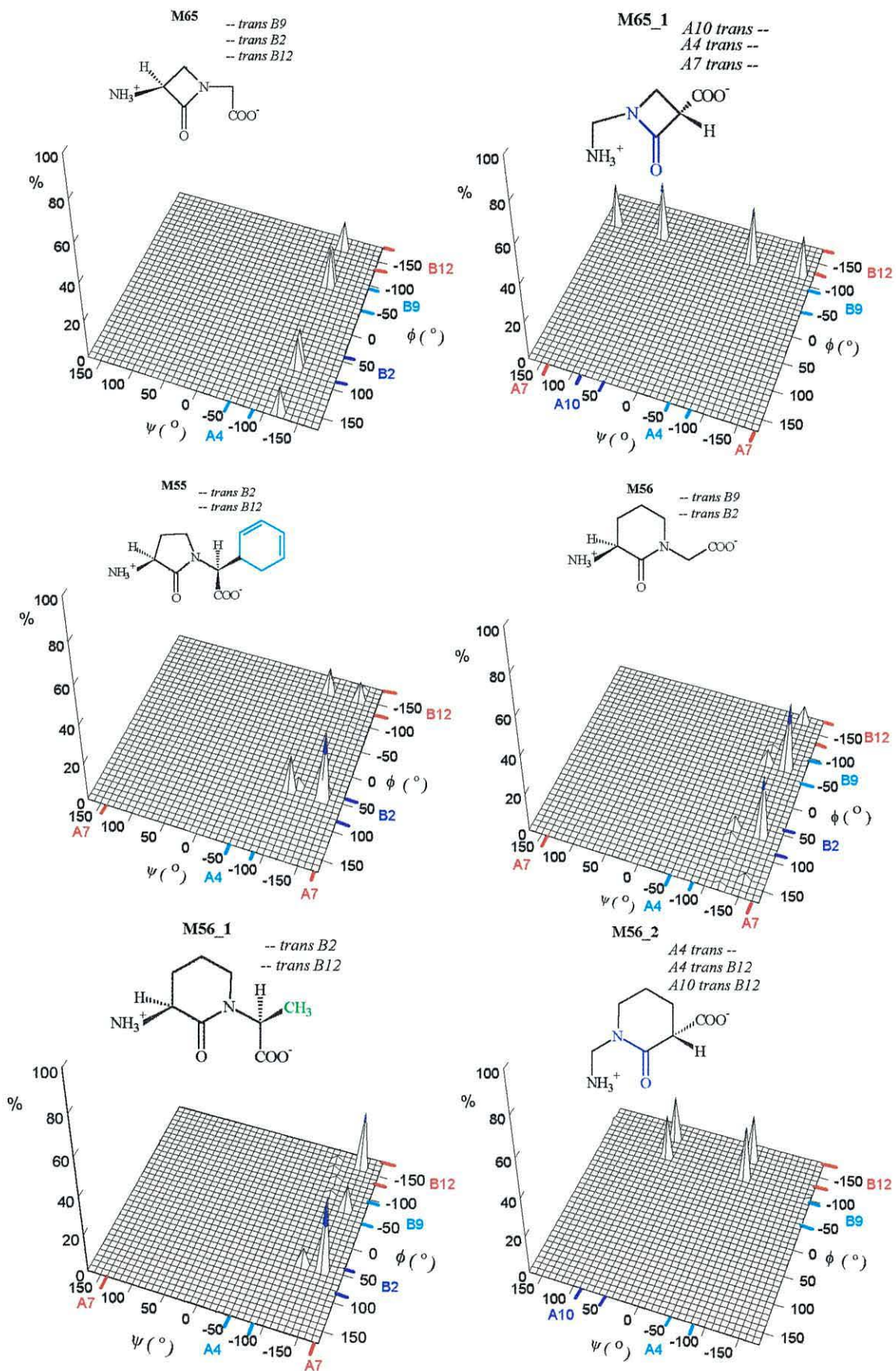


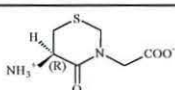
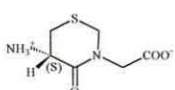
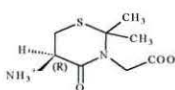
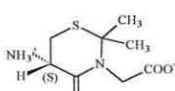
Figure 4-3: 3DPR Plots of ψ vs ϕ vs % Conformers for M65, M65_1, M55, M56, M56_1 and M56_2.

These studies have shown that the addition of a phenyl group to the C α near the C-terminus favours B2 and B12 conformers, unlike a methyl group which also produces some B9 conformers. Fig. 4-3 shows 3DPR plots for M65, M65_1, M55, M56, M56_1 and M56_2 showing the differences in their percentage conformer distribution range.

4.2.3.1.1. Sulphur Containing 6-Membered Lactam Ring Mimetics

Results for conformational analysis of sulphur-containing 6-membered lactam ring mimetics are shown in Table 4.4. **M68** is similar to M56 (Table 4.3.) but contains a sulphur atom in its 6-membered lactam ring. In contrast to M56, M68 had ψ (Tor2) angles in A7, with *trans* ω and ϕ (Tor4) angles in B9 and B2, similar to M56. These results show that the addition of a sulphur atom to a 6-membered lactam ring has a *dramatic* effect on the conformer distribution range. ψ (Tor2) angles are shifted from inactive regions to the A7 MRT required for transport. Based on these modelling results, M68 would be predicted to have better Dpp activity than M56 as it has a high percentage of A7B9 conformers.

Table 4.4. Minimum Energy Conformers of Sulphur-Containing 6-Membered Lactam-Ring Mimetics Showing their ψ (Tor2), ω (Omega), ϕ (Tor4) Torsion Angles, NC Distance and their Total Percentage Distribution of Conformer Range.

| M | Structure | Energy kcal/mol | % | ψ ° (Tor2) | ω ° Omega | ϕ ° (Tor4) | NC Å | %Total Range |
|------|---|--------------------|-------|--------------------|---------------------|--------------------|---------|---------------------|
| 68 |  | 4.01 | 45.71 | 179.5 | 178.3 | -75.3 | 5.30 | 46% A7 <i>t</i> B9 |
| | | 4.22 | 32.78 | -178.8 | -179.2 | 70.8 | 5.25 | 33% A7 <i>t</i> B2 |
| | | 5.26 | 6.02 | -149.6 | 179.3 | -66.5 | 4.93 | 6% -- <i>t</i> B9 |
| 68_1 |  | 4.01 | 45.71 | -179.5 | -178.3 | 75.1 | 5.30 | 52% A7 <i>t</i> B2 |
| | | 4.22 | 32.78 | 178.0 | 179.2 | -70.9 | 5.25 | 33% A7 <i>t</i> B9 |
| | | 5.26 | 6.02 | 149.6 | -179.3 | 66.5 | 4.93 | |
| 68_2 |  | 6.12 | 25.08 | -159.2 | 179.0 | -65.1 | 4.95 | 25% -- <i>t</i> B9 |
| | | 6.18 | 22.59 | -158.1 | -179.2 | 66.2 | 5.23 | 23% -- <i>t</i> B2 |
| | | 6.20 | 21.90 | -173.3 | -179.0 | -92.2 | 5.44 | 22% ~A7 <i>t</i> B9 |
| 68_3 |  | 6.12 | 25.08 | 159.1 | -179.0 | 65.1 | 4.95 | 25% A7 <i>t</i> B2 |
| | | 6.18 | 22.59 | 158.1 | 179.2 | -66.2 | 5.23 | 23% A7 <i>t</i> B9 |
| | | 6.20 | 21.90 | 173.3 | 179.0 | 92.3 | 5.44 | 22% A7 <i>t</i> -- |

-- denotes outside the MRT regions of A7, A4, A10 and B9, B2 and B12 *t* denotes trans omega *c* denotes cis omega

Dpp substrate

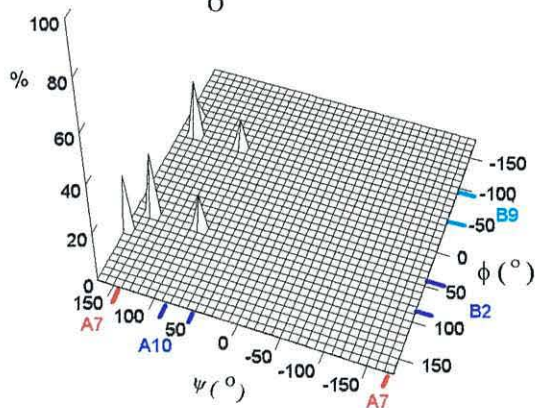
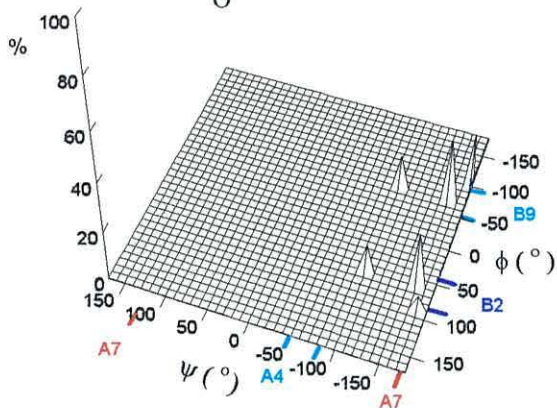
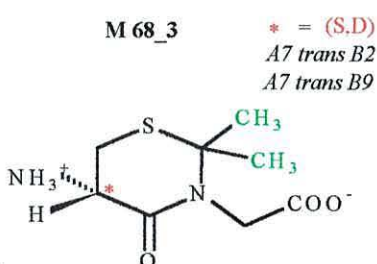
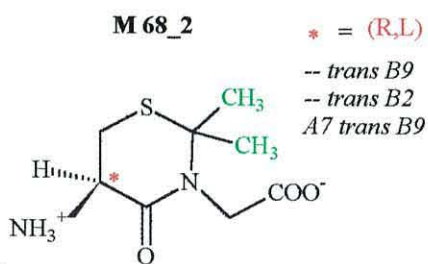
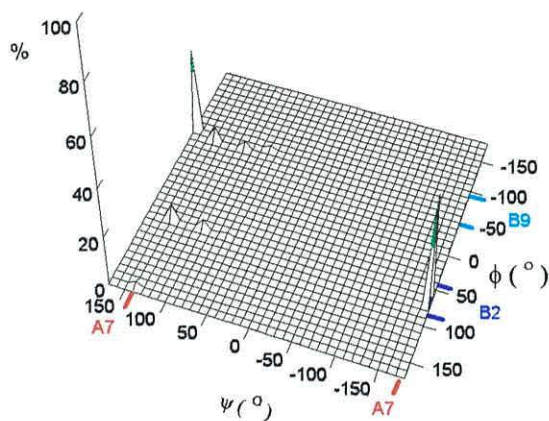
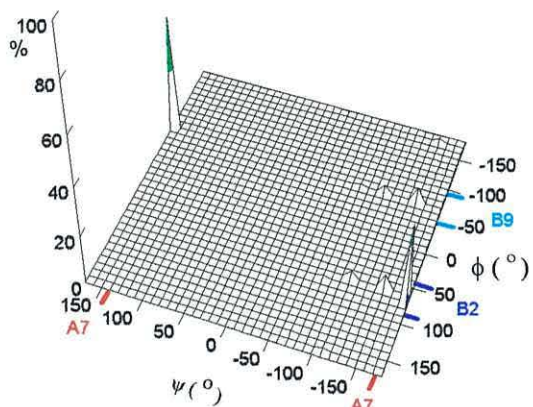
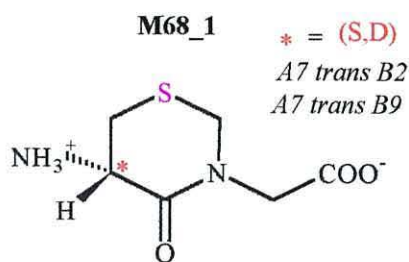
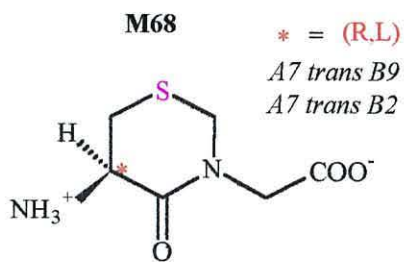


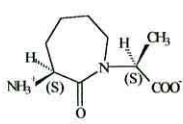
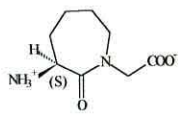
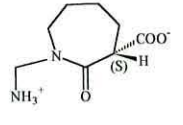
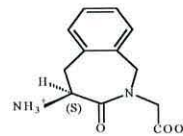
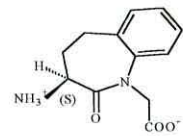
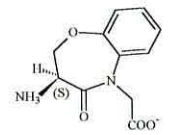
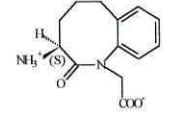
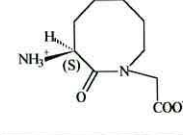
Figure 4-4: 3DPR Plots of ψ vs ϕ vs % Conformers for Sulphur-Containing 6-Membered Lactam Mimetics M68, M68_1, M68_2 and M68_3.

Changing the chirality of the C α near the *N*-terminus from R (L) to S (D) of M68 resulted in **M68_1**, and this changed the minimum energy conformer from A7B9, as seen in M68, to A7B2 (Table 4.4). M68_1 would also be expected to show some Dpp activity, as it has some A7B9, but have poorer activity compared with M68 as it has greater percentage of inactive B2 conformers. **M68_2** was designed as a modification of M68 with 2 methyl groups attached directly to C6. The C α near the *N*-terminus had R (L) chirality, and ψ (Tor2) angles shifted from A7, to being mainly outside A7. ϕ (Tor4) angles were in B9 and B2, as seen with M68, with *trans* omegas. M68 would be predicted to have better Dpp activity as it has more A7B9 conformers than M68_2. Changing the chirality of the C α near the *N*-terminus from R (L) to S (D), in M68_2, gave **M68_3**, that had conformers mainly in A7, and a few near A10, with *trans* ω , and ϕ (Tor4) angles in B2 and B9. As M68_3 has Dpp conformers it would be predicted to have better Dpp activity than M68_2 (Table 4.4). Fig. 4-4 shows 3DPR plots for M68, M68_1, M68_2 and M68_3 illustrating the effect of addition of sulphur atoms, methyl groups and chirality on percentage conformer distribution range for 6-membered lactam ring mimetics.

4.2.3.2. 7- and 8-Membered Lactam-Ring Mimetics

The results for 7- and 8-membered lactam ring mimetics are shown in Table 4.5. **M69** is cyclized with a 7-membered lactam ring and has a methyl sidechain attached to the C α near the *C*-terminus. M69 had all of its conformers constrained in A7 with ϕ (Tor4) angles mainly in B12 and B2, and *trans* ω peptide bonds. As M69 has A7B12 and a few A7B9 conformers, it would be predicted to have better Dpp activity than its analogous 6-membered ring mimetic M56_1 (Table 4.4). **M69_1** is similar to M69 but was modified by removing the methyl group from the C α near the *C*-terminus. This resulted in ψ (Tor2) angles being in A7, same as M69, and ϕ (Tor4) angles in B9 and B2. These results are similar to the conformational differences seen between M56 and M56_1 (Table 4.3, Fig. 4-3), where a methyl group on the C α side chain near the *C*-terminus produces B12 conformers, and removal of a methyl group, as in M69_1, produces mainly B9 conformers.

Table 4.5. Minimum Energy Conformers of 7- and 8-Membered Lactam Ring Mimetics Showing their ψ (Tor2), ω (Omega), ϕ (Tor4) Torsion Angles, NC Distance and Their Total Percentage Distribution of Conformer Range.

| M | Structure | Energy kcal/mol | % | ψ° (Tor2) | ω° Omega | ϕ° (Tor4) | NC Å | %Total Range |
|------|---|--------------------|-------|------------------------|-------------------------|------------------------|---------|----------------------|
| 69 |  | 7.68 | 49.67 | 174.1 | 179.1 | -141.2 | 6.03 | 50% A7 <i>t</i> B12 |
| | | 7.73 | 45.41 | 170.8 | 179.4 | 51.0 | 4.95 | 45% A7 <i>t</i> B2 |
| | | 9.24 | 3.90 | 173.4 | 175.8 | -60.3 | 5.04 | 4% A7 <i>t</i> B9 |
| 69_1 |  | 7.00 | 26.76 | 172.8 | 177.4 | -62.8 | 5.13 | 77% A7 <i>t</i> B9 |
| | | 7.03 | 25.53 | 170.4 | 178.1 | -80.9 | 5.35 | 23% A7 <i>t</i> B2 |
| | | 7.06 | 24.35 | 170.2 | 177.8 | -89.2 | 5.47 | |
| 69_2 |  | 7.99 | 29.36 | -66.5 | 178.4 | 172.0 | 5.21 | 29% A4 <i>t</i> B12 |
| | | 8.02 | 28.28 | 77.0 | 177.8 | 174.6 | 5.26 | 28% A10 <i>t</i> B12 |
| | | 8.18 | 21.58 | -77.9 | -178.5 | -69.8 | 4.79 | 22% A4 <i>t</i> B9 |
| 75 |  | 8.80 | 30.49 | 168.0 | 174.4 | -71.8 | 5.26 | 30% A7 <i>t</i> B9 |
| | | 8.94 | 24.31 | 168.0 | 175.3 | -113.4 | 5.77 | 45% A7 <i>t</i> -- |
| | | 9.03 | 21.14 | 167.3 | 174.9 | -100 | 5.60 | 18% A7 <i>t</i> B2 |
| 58 |  | 7.40 | 40.40 | 162.4 | -176.8 | 73.1 | 5.18 | 40% A7 <i>t</i> B2 |
| | | 7.60 | 29.31 | 163.0 | -177.4 | -151.8 | 6.12 | 29% A7 <i>t</i> B12 |
| | | 7.64 | 27.51 | 162.7 | -178.0 | -56.7 | 5.23 | 28% A7 <i>t</i> B9 |
| 77 |  | 8.61 | 42.53 | 165.9 | -175.6 | 74.3 | 5.22 | 43% A7 <i>t</i> B2 |
| | | 8.89 | 26.65 | 166.1 | -178.6 | -59.7 | 5.25 | 27% A7 <i>t</i> B9 |
| | | 8.94 | 24.89 | 166.4 | -176 | -151.0 | 6.12 | 25% A7 <i>t</i> B12 |
| 80 |  | 10.20 | 36.30 | 141.4 | -176.7 | 66.9 | 4.89 | 36% A7 <i>t</i> B2 |
| | | 10.28 | 31.86 | 142.9 | -177.4 | -159.6 | 6.05 | 32% A7 <i>t</i> B12 |
| | | 10.32 | 30.10 | 141.3 | -178.2 | -70.2 | 5.38 | 30% A7 <i>t</i> B9 |
| 80_1 |  | 12.10 | 31.13 | 157.3 | 179.4 | -66.3 | 5.24 | 43% A7 <i>t</i> B9 |
| | | 12.18 | 27.15 | 157.4 | 179.6 | 68.3 | 4.97 | 53% A7 <i>t</i> B2 |
| | | 12.62 | 13.32 | 157.4 | -178.9 | 82.5 | 5.14 | |

-- denotes outside the MRT regions of A7, A4, A10 and B9, B2 and B12 *t* denotes trans omega *c* denotes cis omega
Dpp substrate Tpp substrate

In contrast to M56 which has a 6-membered ring with ψ (Tor2) angles outside the MRT, M69_1 with a 7-membered ring has *all* its conformer distribution in A7 (Table 4.5.). Based on these results, M69_1 would be predicted to have better Dpp activity than M56, as it has a higher percentage of A7B9 conformers. **M69_2** is a modification of M69_1 containing a retro-amide peptide bond. The second C α near the C-terminus is cyclized, whereas the C α near the N-terminus is not constrained. This modification had a *dramatic* effect on the conformer distribution range, as seen with M56_2. ψ (Tor2) angles were in A4 and A10, unlike other mimetics in this group, that had ψ (Tor2) angles only in A7. ϕ (Tor4) angles were constrained only in B9 and B12, with no B2 conformers (Table 4.5.). Based on these results M69_2 would be predicted to have good Tpp activity as it has all Tpp conformers. Using molecular modelling, this modification illustrates how a Dpp substrate can be changed to a Tpp substrate. **M75** is similar to M69_1, but has a benzene ring fused on top, at C5 and C6, of the 7-membered lactam ring. ψ (Tor2) angles were constrained in A7, as in M69_1, with *trans* ω , and ϕ (Tor4) angles were in or near B9 and some in B2. As M75 has A7B9 conformers it would be predicted to have Dpp activity. **M58** is similar to M75, but has the benzene ring fused at C6 and C7. Its ψ (Tor2) angles were constrained in A7, as with M75, with *trans* ω , and ϕ (Tor4) angles were constrained in B2, B9 and B12. These results indicate that the position of fusion of the benzene ring causes a change in the conformer distribution, the main effect being the production of B12 conformers. M58 would be predicted to have better Dpp activity, as it has both A7B9/B12 conformers, than M75 which only has A7B9 conformers. **M77** is like M58 but has an oxygen atom in its 7-membered lactam ring. Modelling studies showed that its conformer distribution profile was similar to M58 with ψ (Tor2) angles in A7, and ϕ (Tor4) angles in B2, B12 and B9. This indicates that the addition of an oxygen atom *does not* effect the conformer distribution range. M77 would also be predicted to show Dpp activity as it has Dpp conformers. Fig. 4-5 shows 3DPR plots for M69, M69_1, M69_2, M75, M58, M77 showing the effects of fusion of benzene rings, and the addition of oxygen atoms on the percentage conformer distribution range of 7-membered lactam ring mimetics.

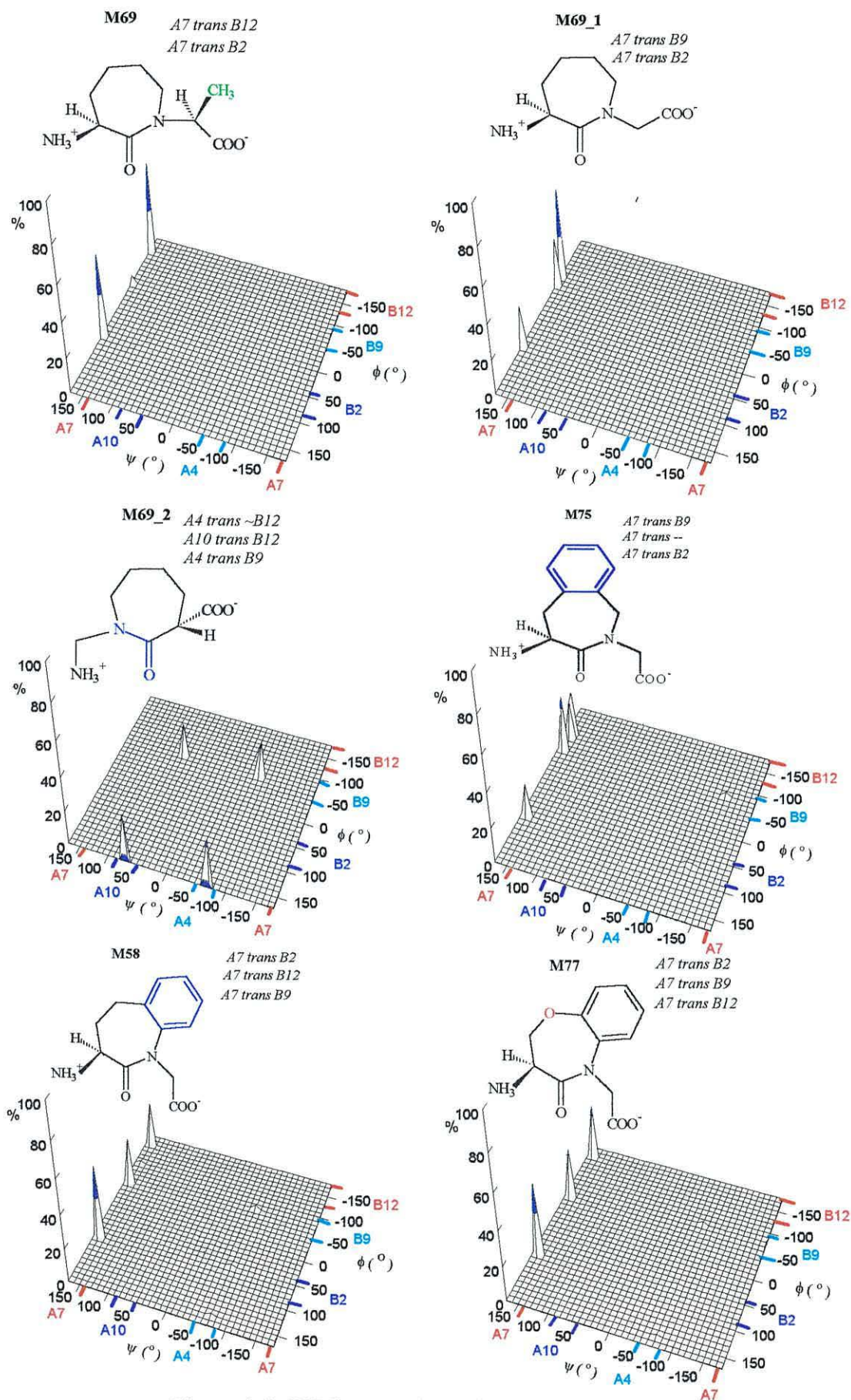


Figure 4-5: 3DPR Plots of ψ vs ϕ vs % Conformers for M69, M69_1, M69_2, M75, M58 and M77.

M80 is similar to M58, but contains an 8-membered lactam ring. M80 had ψ (Tor2) angles constrained at the edge of A7, with *trans* ω , and ϕ (Tor4) angles in B2, B12 and B9, like M58 (Table 4.5.). As M80 contains A7B9/B12 conformers it would be predicted to show, like M58, Dpp activity. Removal of the fused benzene ring at C7 and C8 ring resulted in **M80_1**. Like mimetic M69_1, M80_1 also had conformers with ψ (Tor2) angles constrained in A7, with *trans* ω , and ϕ (Tor4) angles in B9 and B2. M80_1 would be predicted to show some Dpp activity as it has A7B9 conformers, but have poorer activity than M80, which has both A7B9/B12 conformers. Fig. 4-6 shows 3DPR plots for M80 and M80_1 showing the differences in percentage conformer distribution range with and without fusion of an additional benzene ring at C7 and C8.

4.2.3.2.1. Sulphur Containing 7-Membered Lactam-Ring Mimetics

Table 4.6. shows the results for sulphur-containing 7-membered lactam ring mimetics.

Table 4.6. Minimum Energy Conformers of Sulphur-Containing 7-Membered Lactam Ring Mimetics Showing their ψ (Tor2), ω (Omega), ϕ (Tor4) Torsion Angles, NC Distance and Their Total Percentage Distribution of Conformer Range.

| M | Structure | Energy kcal/mol | % | ψ ° (Tor2) | ω ° Omega | ϕ ° (Tor4) | NC Å | % Total Range |
|------|-----------|--------------------|-------|--------------------|---------------------|--------------------|---------|---------------------|
| 78 | | 7.41 | 37.32 | 155.9 | -176.5 | 70.9 | 5.10 | 37% A7 <i>t</i> B2 |
| | | 7.45 | 35.03 | 156.2 | -179.2 | -61.5 | 5.29 | 35% A7 <i>t</i> B9 |
| | | 7.62 | 26.47 | 156.8 | -177.1 | -154.8 | 6.11 | 26% A7 <i>t</i> B12 |
| 78_1 | | 7.41 | 37.32 | -155.9 | 176.5 | -70.8 | 5.10 | 37% -- <i>t</i> B9 |
| | | 7.45 | 35.03 | -156.2 | 179.2 | 61.5 | 5.29 | 35% -- <i>t</i> B2 |
| | | 7.62 | 26.47 | -156.8 | 177.1 | 154.8 | 6.11 | 26% -- <i>t</i> -- |
| 57_1 | | 7.14 | 26.29 | 169.3 | 176.3 | -60.4 | 5.11 | 52% A7 <i>t</i> B9 |
| | | 7.18 | 24.24 | 169.8 | 177.6 | 76.0 | 5.18 | 44% A7 <i>t</i> B2 |
| | | 7.22 | 22.85 | 166.2 | 177.8 | -80.7 | 5.36 | |
| 57_2 | | 7.14 | 26.56 | -169.3 | -176.3 | 60.4 | 5.11 | 50% -- <i>t</i> B2 |
| | | 7.18 | 24.48 | -169.8 | -177.6 | -76.1 | 5.18 | 44% -- <i>t</i> B9 |
| | | 7.22 | 23.09 | -166.2 | -177.8 | 80.3 | 5.36 | |

-- denotes outside the MRT regions of A7, A4, A10 and B9, B2 and B12 *t* denotes trans omega *c* denotes cis omega

Dpp substrate

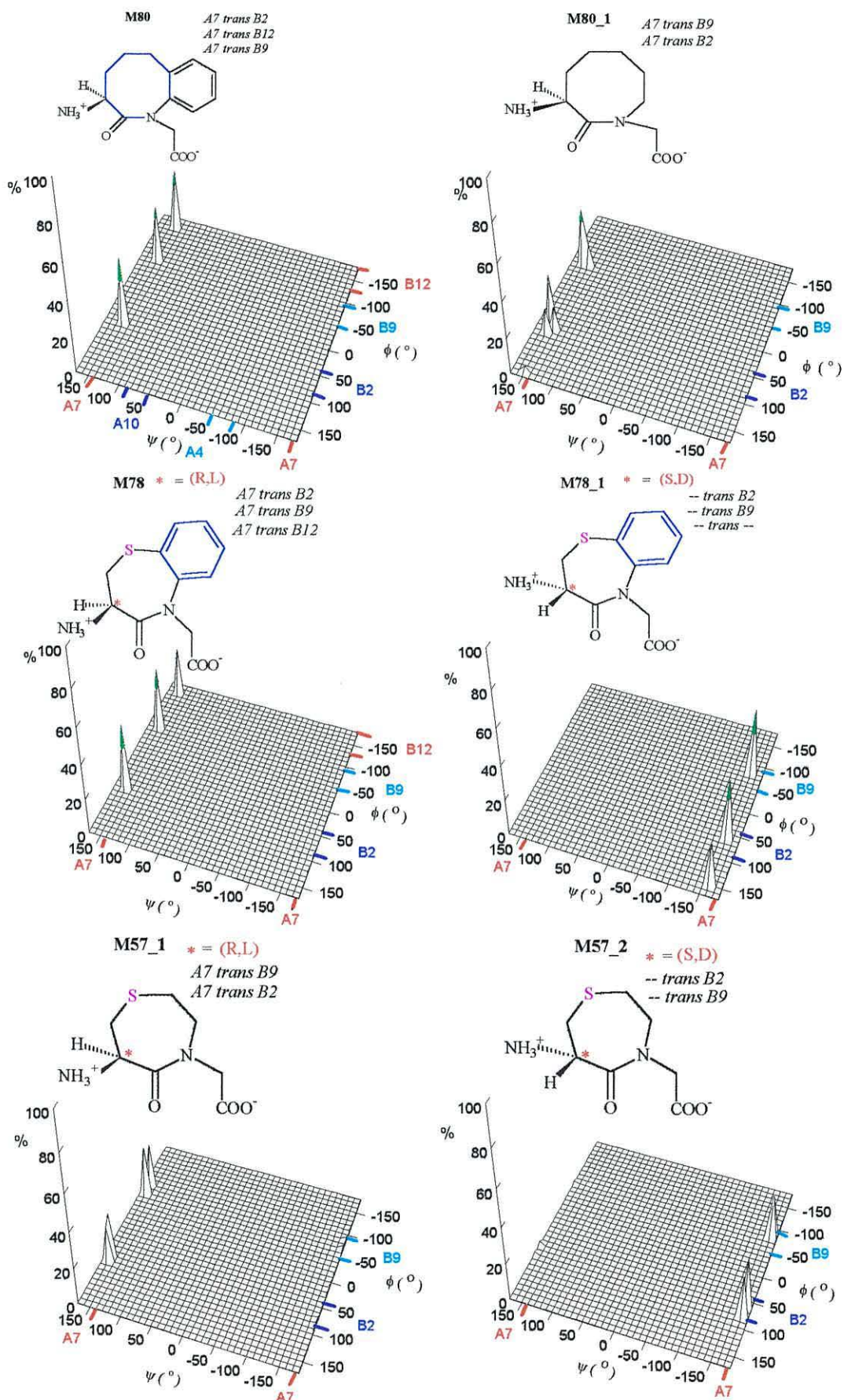
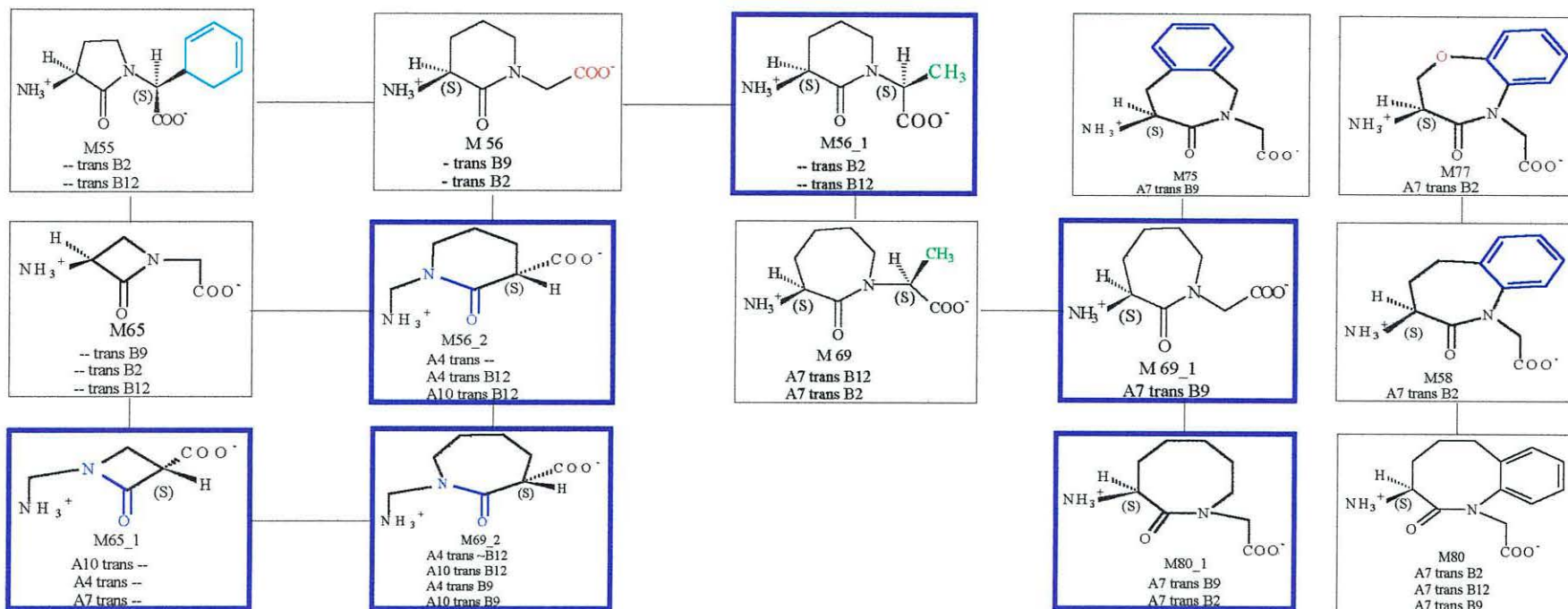


Figure 4-6: 3DPR Plots of ψ vs ϕ vs % Conformers for M80, M80_1, and Sulphur-Containing 7-Membered Lactam Mimetics M78, M78_1, M57_1 and M57_2.

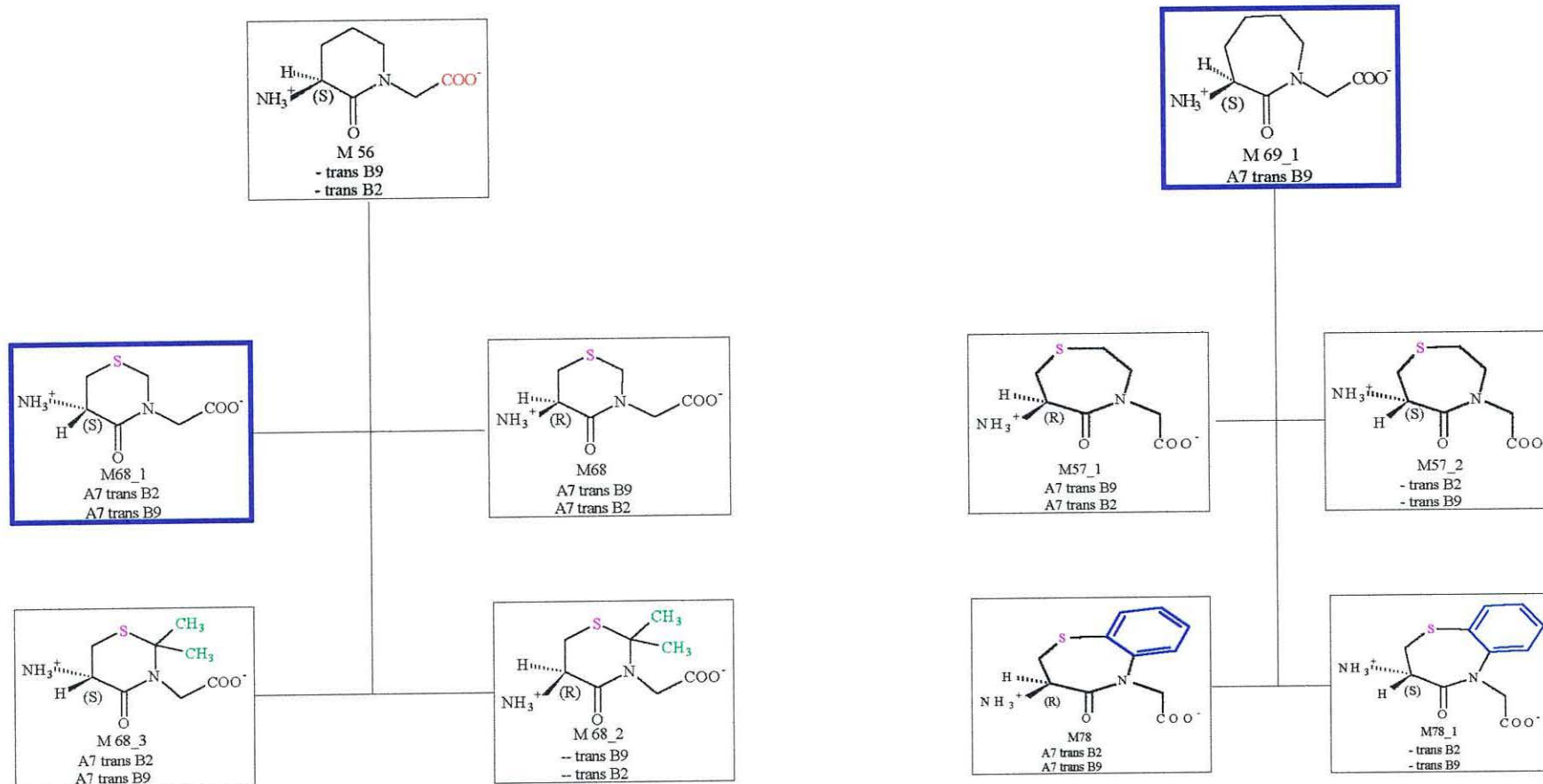
M78 is similar to M77 but has a sulphur atom instead of an oxygen in its lactam ring. The addition of a sulphur atom had an effect on the orientation of the chemical groups around the chiral centre. Modelling structures with C α near the *N*-terminus having R (L) chirality, produced conformers with ψ (Tor2) angles in A7, with *trans* ω , and ϕ (Tor4) angles in B2, B9 and B12. These conformations were similar to those obtained for M77 and M58 (Table 4.5.). Changing the chirality of the C α to S (D), in **M78_1**, caused a change in the conformer distribution range. ψ (Tor2) angles shifted from A7 to outside A7, and ϕ (Tor4) angles were in B2 and B9. This indicates that introduction of a sulphur atom increases the flexibility of a 7-membered ring. As M78 (R) has A7B9/B12 conformers, it would be predicted to have better Dpp activity than M78_1 (S). **M57_1** is the same as M78, but does not have any methyl groups or a benzene ring attached. C α near the *N*-terminus having R (L) chirality, produced conformers with ψ (Tor2) angles constrained in A7, and ϕ (Tor4) angles in B9 and B2, as obtained for M69_1, which does not have a sulphur atom. Like M78_1 and M57_1, changing the chirality to S in **M57_2**, shifted ψ (Tor2) angles outside A7, with ϕ (Tor4) angles in B2 and B9. Based on these results, M57_2 would be predicted to have better Dpp activity, as it has a higher percentage of A7B9 conformers than M57_3. Fig. 4-6 shows 3DPR plots for M78, M78_1, M57_1 and M57_2, illustrating the effects of chirality and the fusion of benzene ring on sulphur-containing 7-membered lactam ring mimetics. Charts 2 and 3 show the structures and conformations of all the lactam-constrained mimetics modelled.

Chart 2 : Structures and Conformations for 4-, 5-, 6-, 7- and 8-Membered Lactam Ring Mimetics.



Blue Frame = Modified Mimetics

Chart 3: Structures and Conformations for Sulphur-Containing 6- and 7-Membered Ring Mimetics



Blue Frame = Modified Mimetics

4.2.4. Conformational Analysis of Torsionally-Constrained Mimetics

Torsionally-constrained mimetics are cyclized by the fusion of two or more rings across the peptide backbone. These highly constrained structures only had a few unique conformers in solution, compared with the isosteres and the lactam-constrained mimetics, and consequently the minimum energy conformers formed a large percentage of the total conformer distribution range.

4.2.4.1. 6-Membered Lactams fused with 5-Membered Ring Mimetics

Table 4.7. shows the results obtained for conformational analysis of 6-membered lactams fused with 5-membered ring mimetics.

Table 4.7. Minimum Energy Conformers of 6-Membered Lactams fused with 5-Membered Rings Showing their ψ (Tor2), ω (Omega), ϕ (Tor4) Torsion Angles, NC Distance and their Total Percentage Distribution of Conformer Range.

| M | Structure | Energy kcal/mol | % | ψ ° (Tor2) | ω ° Omega | ϕ ° (Tor4) | NC Å | %Total Range |
|-------|-----------|--------------------|-------|--------------------|---------------------|--------------------|---------|---|
| 113 | | 11.77 | 68.87 | -115.1 | 171.4 | -63.5 | 4.62 | 69% _t B9 |
| | | 13.20 | 6.75 | -168.5 | 176.1 | -72.4 | 5.24 | |
| | | 13.81 | 2.49 | -170.4 | -177.8 | -74.6 | 5.11 | |
| 113_3 | | 11.34 | 98.31 | -138.3 | -172.3 | -63.8 | 5.10 | 98% _t B9 |
| | | 14.13 | 1.04 | -84.9 | -172.9 | -65.9 | 4.90 | |
| | | 14.43 | 0.64 | -133.7 | -167.8 | -102 | 5.43 | |
| 113_1 | | 9.36 | 72.75 | -179.9 | 179.6 | -51.5 | 5.20 | 97% _{A7} _t B9 |
| | | 10.04 | 23.95 | 178.2 | -173.9 | -89.5 | 5.58 | |
| | | 11.27 | 3.27 | 108.3 | -173 | -62.8 | 5.40 | |
| 113_2 | | 10.78 | 51.65 | 78.1 | 174 | -68.3 | 5.45 | 52% _{A10} _t B9 48% _{A7} _t B9 |
| | | 10.82 | 47.99 | 141.5 | 171.9 | -63.7 | 5.37 | |
| | | 13.98 | 0.28 | 80.4 | 167.8 | -36.2 | 5.41 | |
| 111 | | 11.15 | 96.81 | -102 | 167.5 | -57.7 | 4.44 | 97% _t B9 |
| | | 13.32 | 2.84 | -164.5 | 174.8 | -70.7 | 5.20 | |
| | | 14.72 | 0.29 | -164.5 | 174 | -33.4 | 5.09 | |
| 112 | | 11.15 | 97.04 | -139.3 | -170.6 | -67.0 | 5.16 | 97% _t B9 |
| | | 13.48 | 2.20 | -86.4 | -168.8 | -74.2 | 4.98 | |
| | | 14.39 | 0.49 | -136.2 | -167.3 | -105.1 | 5.49 | |

-- denotes outside the MRT regions of A7, A4, A10 and B9, B2 and B12 *t* denotes trans omega *c* denotes cis omega
Dpp substrate Tpp substrate

M113 has a 6-membered lactam ring fused to a 5-membered ring with the bridging carbon having S chirality (Table 4.7.). M113 had ψ (Tor2) angles outside A4 and A7, with *trans* ω , and all ϕ (Tor4) angles constrained in B9. **M113_3** was a modification of M113 to see the effect of changing the chirality at the bridging carbon from S to R. This still produced conformers with ψ (Tor2) angles outside the A7, with *trans* ω , and ϕ (Tor4) angles constrained in B9. 6-membered lactam rings fused with 5-membered rings do not produce any A7 or A4 conformers. These results are similar to the conformation distributions found for lactam-constrained mimetics. A 6-membered lactam ring mimetic, such as M56 (Table 4.3.), did not have A7 conformers, but a 7-membered lactam ring mimetic such as M69_1 (Table 4.5.) produced conformers with ψ (Tor2) angles within A7. Based on the modelling studies of **M68** (Table 4.4.), M113 was modified to **M113_1** by inserting a sulphur atom in the 6-membered lactam ring (Table 4.7.) in order to produce A7 conformers. As a sulphur atom has an effect on chiral centres, the C α near the N-terminus was modelled as having R (L) chirality. As *predicted*, M113_1 had nearly *all* of its conformers with ψ (Tor2) angles in A7, with *trans* ω , and all ϕ (Tor4) angles in B9. This modification in mimetic structure highlights how *rational* changes can be applied to the design of substrates with conformational features required for transport. Based on these molecular modelling results, the *rationally* designed peptidomimetic M113_1 would be predicted to have better Dpp activity than M113_3. Changing the chirality of the bridging carbon of M113_1 from R to S, resulted in M113_2 (Table 4.7.) M113_2 had 50% of its total percentage conformers as A10 *trans* B9, and 50% of it as A7 *trans* B9, therefore M113_2 would be expected to have both Dpp and Tpp activity. **M111** is like M113 but the 6-membered lactam ring contains an oxygen atom instead of a sulphur. M111 had the majority of its ψ (Tor2) angles outside A4, as seen with M113, with *trans* ω , and ϕ (Tor4) angles constrained in B9 (Table 4.7.). As with lactam-constrained mimetics, the addition of an oxygen atom had no significant effect on ψ (Tor2) angles, unlike a sulphur atom. M112 is the same as M111, but the bridging carbon has R chirality. M112 had ψ (Tor2) angles outside A4 and A7, like M113_3 and ϕ (Tor4) angles in B9.

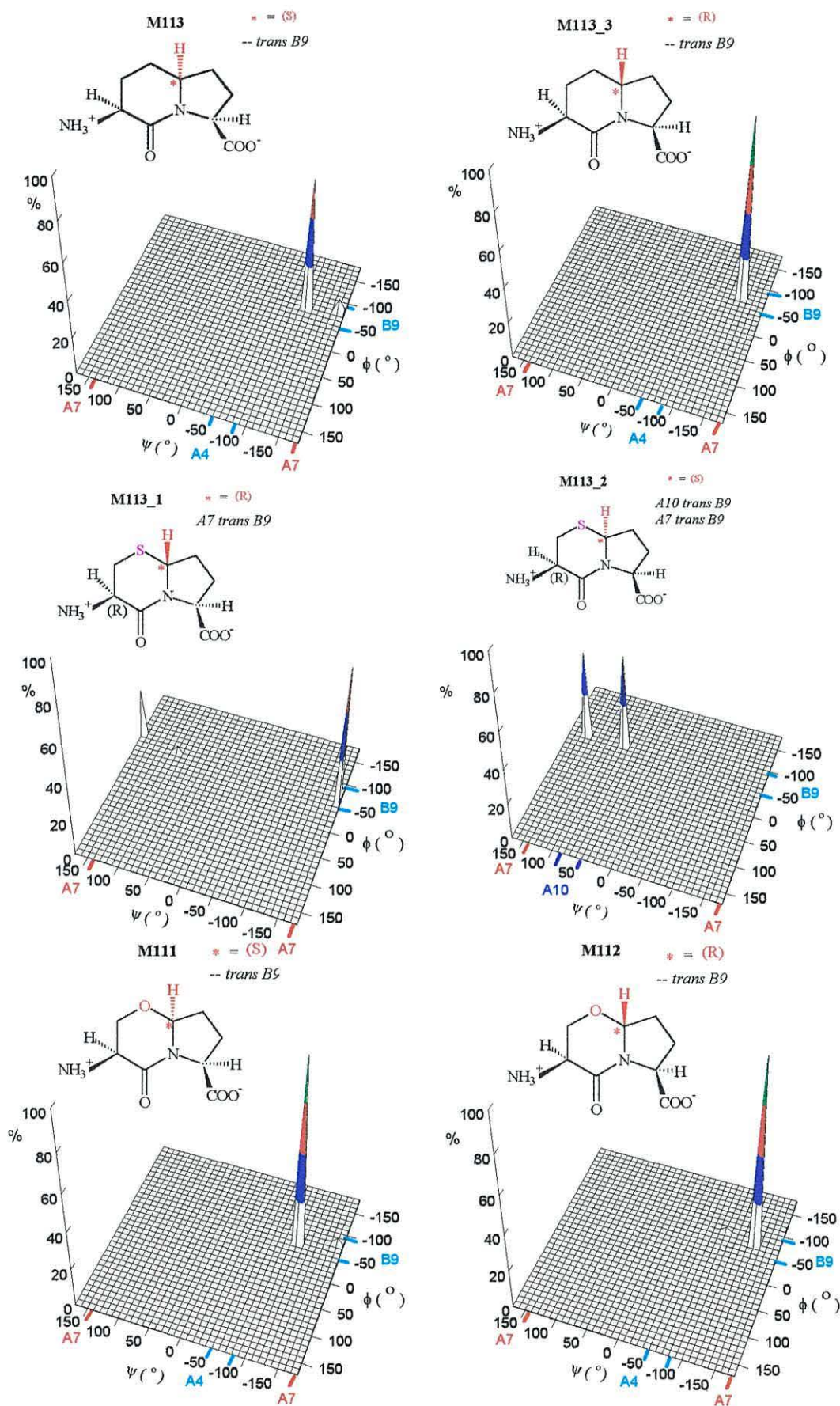
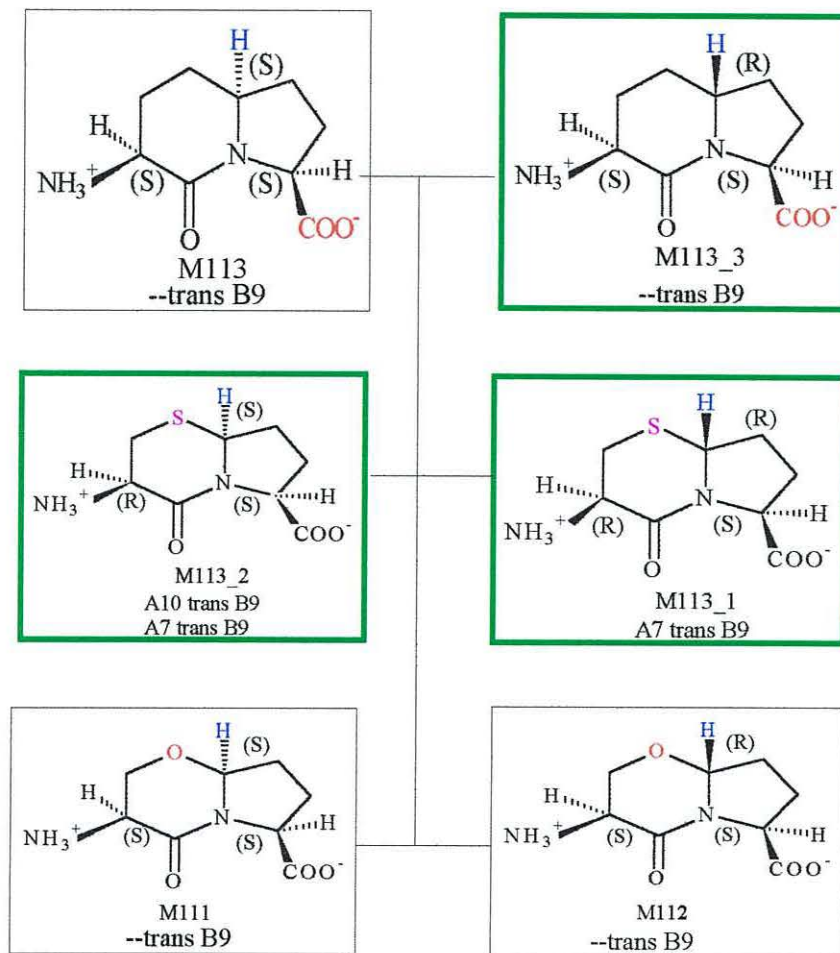


Figure 4-7 : 3DPR Plots of ψ vs ϕ vs % Conformers for M113, M11_3, M113_1, M113_2, M111 and M112.

Chart 4: Structures and Conformations for 6-Membered Lactams fused with 5-Membered Ring Mimetics.



Green Frame = Modified Mimetics

Both M111 and M112 would be expected to have poor transport activity as their ψ (Tor2) angles are outside A7 and A4. Fig. 4-7 shows 3DPR plots for M113, M113_3, M113_1, M113_2, M111 and M112, showing the addition of sulphur and oxygen atoms and the effect of *chirality* of the bridging carbon, on the percentage conformer distribution range of torsionally constrained mimetics. Chart 4 shows the structures and conformations for 6-membered lactams fused with 5-membered ring mimetics.

4.2.4.2. 7-Membered Lactams fused with 5-Membered Ring Mimetics

Table 4.8 shows the results for 7-membered lactams fused with 5-membered ring mimetics (Gillespie *et al.*, 1997; Hanessian *et al.*, 1997). **M127** has a 7-membered lactam ring fused to a 5-membered ring. The bridging carbon has S chirality with a hydrogen atom attached to it. M127 had all ψ (Tor2) angles in A7, with *trans* ω , and ϕ (Tor4) angles in or near B9. Changing the chirality of the bridging carbon from S to R in **M127_1**, had a significant effect on ψ (Tor2) angles (Table 4.8.). The conformer distribution shifted from A7 to A4, with only a few conformers outside A7. ϕ (Tor4) angles were constrained in or near B9 with all *trans* ω conformations. Modelling studies of this mimetic again show the importance of *stereochemistry* on conformer distribution range. M127 (S) would be expected to be a good Dpp substrate, as it has nearly all A7B9 conformers. M127_1 (R) on the other hand, would be a good Tpp substrate as it has A4B9 conformers. **M4*** and **M5*** (Hanessian *et al.*, 1997) are similar to M127 and M127_1, but have a sulphur atom in the second 5-membered ring. As seen with the lactam-constrained mimetics, sulphur atoms affect the stereochemistry and the orientation of the groups around the chiral centres. Both M4* and M5* were modelled with S chirality at the C α near the C-terminus. This resulted in a change in the orientation of the groups from L to D forms. M4* with bridging carbon at S chirality and had ψ (Tor2) angles in A4, with *trans* ω , and ϕ (Tor4) angles in B2. M5*, with bridging carbon at R chirality, produced, in contrast to M4*, ψ (Tor2) angles in A7, and ϕ (Tor4) angles in or near B2, as seen with M4*. The production of B2 conformers by the addition of a sulphur atom, would result in these mimetics having poor activity

Table 4.8. Minimum Energy Conformers of 7-Membered Lactams fused with 5-Membered Rings Showing their ψ (Tor2), ω (Omega), ϕ (Tor4) Torsion Angles, NC Distance and their Total Percentage Distribution of Conformer Range.

| M | Structure | Energy kcal/mol | % | ψ ° (Tor2) | ω ° Omega | ϕ ° (Tor4) | NC Å | %Total Range |
|-------|-----------|--------------------|-------|--------------------|---------------------|--------------------|---------|---------------------|
| 127 | | 11.23 | 51.24 | 174.5 | 175.2 | -49.6 | 5.11 | 51%A7 <i>t</i> -B9 |
| | | 11.27 | 48.55 | 170.9 | -173.8 | -85.6 | 5.49 | 49%A7 <i>t</i> B9 |
| | | 14.79 | 0.16 | 163.5 | -177.9 | -72.4 | 5.41 | |
| 127_1 | | 14.47 | 47.12 | -78.6 | -174.9 | -80.2 | 4.95 | 47% A4 <i>t</i> B9 |
| | | 14.56 | 41.23 | -73.5 | 172.3 | -46.7 | 4.70 | 41% A4 <i>t</i> -B9 |
| | | 15.45 | 9.64 | -156.1 | 179.2 | -59.4 | 4.97 | |
| 4* | | 10.31 | 74.4 | -74.8 | 178.1 | 83.5 | 5.55 | 94% A4 <i>t</i> B2 |
| | | 11.13 | 19.69 | -81.7 | -173.5 | 43.5 | 5.40 | |
| | | 12.17 | 3.60 | -155.5 | -176.8 | 70.7 | 5.29 | |
| 5* | | 7.09 | 64.19 | 173.5 | 179.9 | 81.6 | 5.31 | 93% A7 <i>t</i> B2 |
| | | 7.59 | 28.42 | 172.4 | -178.3 | 83.2 | 5.29 | 7% A7 <i>t</i> -B2 |
| | | 8.43 | 7.25 | 167.5 | -175.2 | 38.4 | 4.94 | |
| 138_1 | | 13.73 | 93.63 | 166.0 | 178.8 | -85.1 | 5.95 | 98% A7 <i>t</i> B9 |
| | | 15.98 | 2.38 | 170.0 | 175.5 | -57.1 | 5.21 | |
| | | 16.03 | 2.20 | 170.1 | 168.5 | -49.8 | 5.12 | |
| 138_2 | | 17.10 | 41.26 | -140.1 | 175.4 | -53.1 | 4.74 | 79% -- <i>t</i> B9 |
| | | 17.17 | 37.30 | -113.2 | -179.0 | -77.3 | 4.85 | 21% A4 <i>t</i> B9 |
| | | 17.53 | 20.58 | -65.5 | -176.9 | -53.9 | 4.95 | |
| 138 | | 21.55 | 59.55 | -178 | -176.5 | -80.3 | 5.35 | 86% A7 <i>t</i> B9 |
| | | 21.99 | 29.03 | 161.7 | -159 | -93.9 | 5.72 | 10% A4 <i>t</i> B9 |
| | | 22.64 | 10.08 | -76.2 | 173.7 | -55.6 | 4.59 | |

-- denotes outside the MRT regions of A7, A4, A10 and B9, B2 and B12 *t* denotes trans omega *c* denotes cis omega

Dpp substrate Tpp substrate

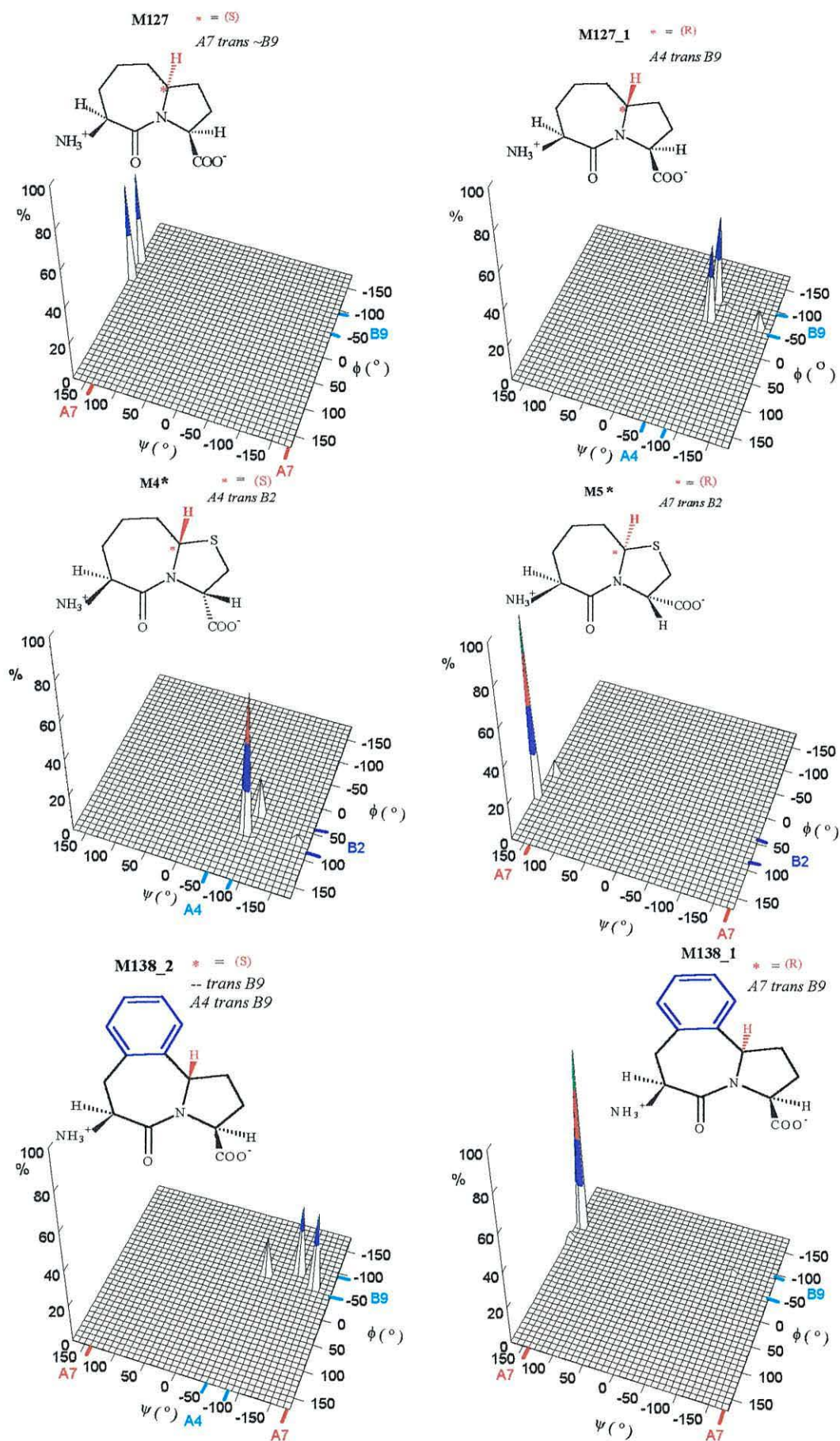
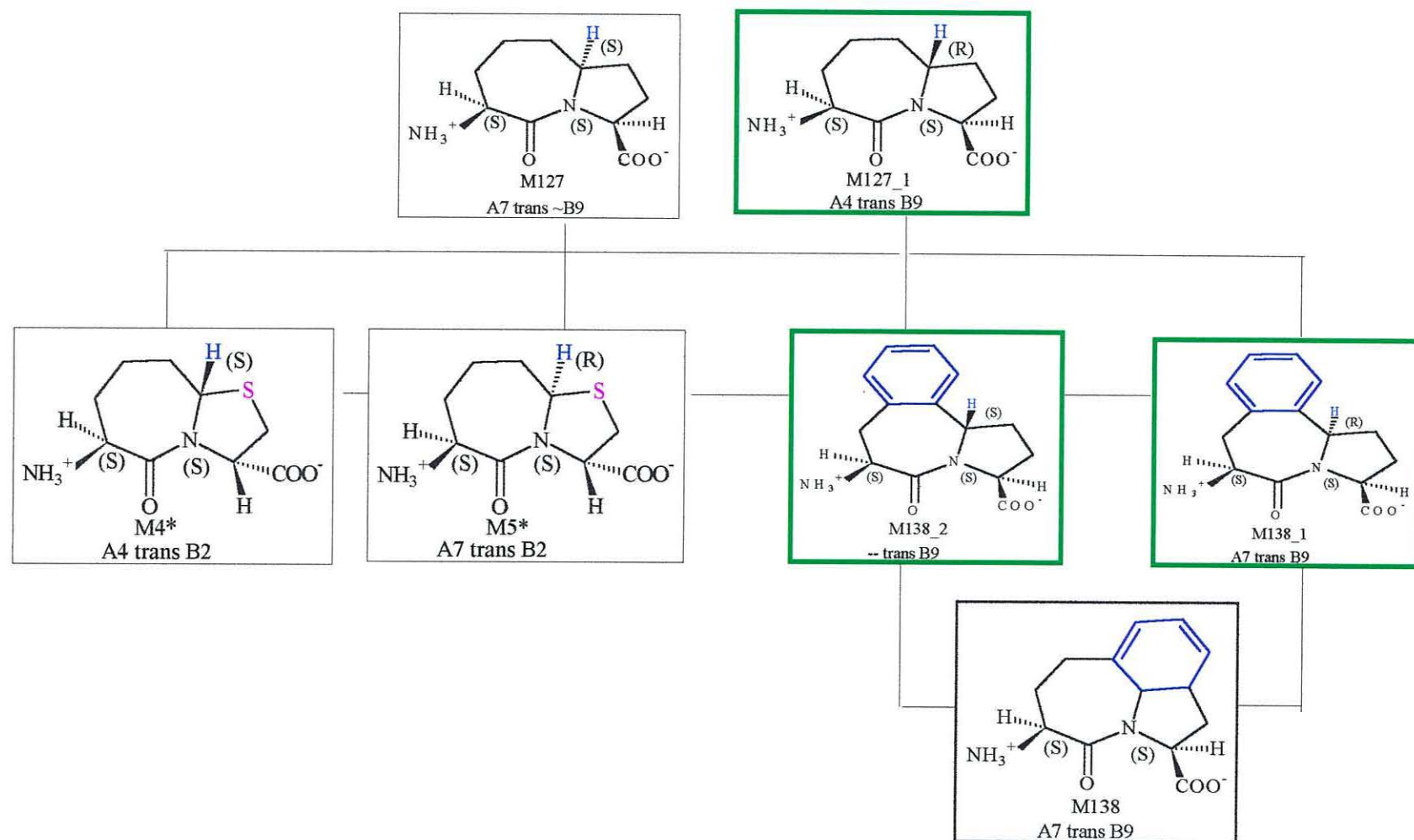


Figure 4-8: 3DPR Plots of ψ vs ϕ vs % Conformers for M127, M127_1, M4*, M5*, M138_1 and M138_2.

Chart 5: Structures and Conformations for 7-Membered Lactams fused with 5-Membered Ring Mimetics.



Green Frame = Modified Mimetics

M138_1 is a modification of M138 from Gillespie *et al* (1997). This mimetic is similar to M127, but has a benzene ring fused on top of the 7-membered lactam ring at C5 and C6, and the bridging carbon has R chirality. M138_1 had nearly all A7 *trans* B9 conformers. This showed that placing the benzene ring on top of the 7-membered lactam ring at C5 and C6, moved all ψ (Tor2) angles into the A7 (Table 4.8.). As M138_1 (R) had more A7B9 conformers than M127(S), it would be predicted to have improved Dpp activity. **M138_2** had the bridging carbon of S chirality, and this produced conformers outside A7, and in or near A4, with *trans* ω bonds. All the conformers had ϕ (Tor4) angles constrained in B9. As seen with other mimetics, changing the chirality of the bridging carbon affected the distribution of ψ (Tor2) angles. M138_2 had less A4 conformers than M127_1. Based on these results, M138_2 would be expected to have poorer Tpp activity than M127_1. **M138** is similar to M127 but has an additional benzene ring fused in between the 7-membered and 5-membered rings, forming a highly constrained structure (Table 4.8.). This mimetic was modelled in order to obtain an A7B9 minimum energy conformation, and the results showed that M138 had mainly A7 *trans* B9 conformers. Fig. 4-8 shows 3DPR plots for M127, M127_1, M4*, M5*, M138_1 and M138_2, showing the effects of chirality of the bridging carbon, the addition of a sulphur atom and fusion of a benzene ring, on torsionally-constrained mimetics. Chart 5 shows structures and conformations for 7-membered lactams fused with 5-membered torsionally-constrained mimetics modelled.

4.2.4.3. 7-Membered Lactams fused with 6-Membered Ring Mimetics

Table 4.9. shows the results for conformational analysis of 7-membered lactams fused with 6-membered ring mimetics. **M79** is a highly constrained structure similar to M138, and has a 7-membered ring fused to a 6-membered ring with an additional benzene ring in the middle (Table 4.9.). M79 had ψ (Tor2) angles in A7, with ϕ (Tor4) angles in B9 or outside B12. This is in contrast to M138 which had all its ϕ (Tor4) angles in B9 range. M79 would be expected to have lower Dpp transport activity than M138 as it has a lower percentage of A7B9 conformers.

Table 4.9. Minimum Energy Conformers of 7-Membered Lactams fused with 6-Membered Rings Showing their ψ (Tor2), ω (Omega), ϕ (Tor4) Torsion Angles, NC Distance and their Total Percentage Distribution of Conformer Range.

| M | Structure | Energy kcal/mol | % | ψ ° (Tor2) | ω ° Omega | ϕ ° (Tor4) | NC Å | %Total Range |
|-------|-----------|--------------------|-------|--------------------|---------------------|--------------------|---------|--|
| 79 | | 8.90 | 59.77 | 161 | -170.3 | -66.3 | 5.33 | 60% A7 <i>t</i> B9 39% A7 <i>t</i> _ |
| | | 9.17 | 38.94 | 160.8 | -169.1 | -124.1 | 5.98 | |
| | | 11.28 | 1.26 | -58.8 | 168.1 | -56.5 | 4.47 | |
| 148 | | 14.79 | 76.7 | 171.1 | 169.7 | -90.2 | 5.45 | 98% A7 <i>t</i> B9 |
| | | 15.64 | 19.33 | 175.7 | 176.6 | -86.7 | 5.41 | |
| | | 17.19 | 1.54 | 176.5 | 164.6 | -35.1 | 4.92 | |
| 148_1 | | 16.38 | 74.67 | -88.1 | -174.2 | -111.5 | 5.14 | 77% ~A4 <i>t</i> _ 18% A7 <i>t</i> B12 |
| | | 17.24 | 18.39 | 173.4 | -170.8 | -139.1 | 6.04 | |
| | | 18.57 | 2.10 | -89.0 | 176.6 | -41.4 | 4.67 | |
| 149 | | 13.16 | 95.28 | 173.8 | 171 | 90.7 | 5.48 | 95% A7 <i>t</i> -- |
| | | 15.62 | 1.73 | -170.1 | 179.5 | 123.3 | 5.90 | |
| | | 15.72 | 1.48 | 175.5 | 170.2 | -27.7 | 4.97 | |
| 149_1 | | 15.1 | 50.72 | -93.5 | -174.3 | 86.1 | 5.56 | 51% _~B2 37% A7 <i>t</i> _ 5% _ <i>t</i> _ |
| | | 15.3 | 36.86 | 175.8 | -176.4 | -39.0 | 5.00 | |
| | | 16.49 | 5.27 | -133.6 | 177.9 | 114.9 | 5.87 | |
| 105 | | 11.6 | 85.95 | 174.8 | 165.6 | -77.7 | 5.21 | 96% A7 <i>t</i> B9 |
| | | 13.28 | 5.51 | 171.0 | -175.3 | -63.4 | 5.12 | |
| | | 13.47 | 4.04 | 179.9 | 173.1 | -79.8 | 5.27 | |
| 105_1 | | 15.37 | 43.96 | 165.6 | -167.4 | -124.9 | 5.96 | 44% A7 <i>t</i> ~B12 32% -- <i>t</i> B9 |
| | | 15.57 | 32.10 | -160.8 | 172 | -82.2 | 5.07 | |
| | | 16.62 | 5.79 | -82.5 | -171.3 | -94.6 | 5.14 | |
| 8* | | 13.98 | 32.74 | 165.1 | -168.6 | -131.5 | 6.02 | 44% A7 <i>t</i> B12 14% A4 <i>t</i> _ |
| | | 14.49 | 14.19 | -82.3 | -172.8 | -103.3 | 5.17 | |
| | | 14.63 | 11.32 | 171.9 | -156 | -143 | 6.07 | |
| 8_1 | | 10.44 | 37.98 | 172.1 | 174.7 | -68.6 | 5.15 | 84% A7 <i>t</i> B9 |
| | | 10.48 | 35.53 | 173.5 | 169.5 | -76.8 | 5.24 | |
| | | 11.23 | 10.44 | 175.0 | 173.2 | -56.4 | 4.99 | |

-- denotes outside the MRT regions of A7, A4, A10 and B9, B2 and B12 *t* denotes trans omega *c* denotes cis omega
Dpp substrate

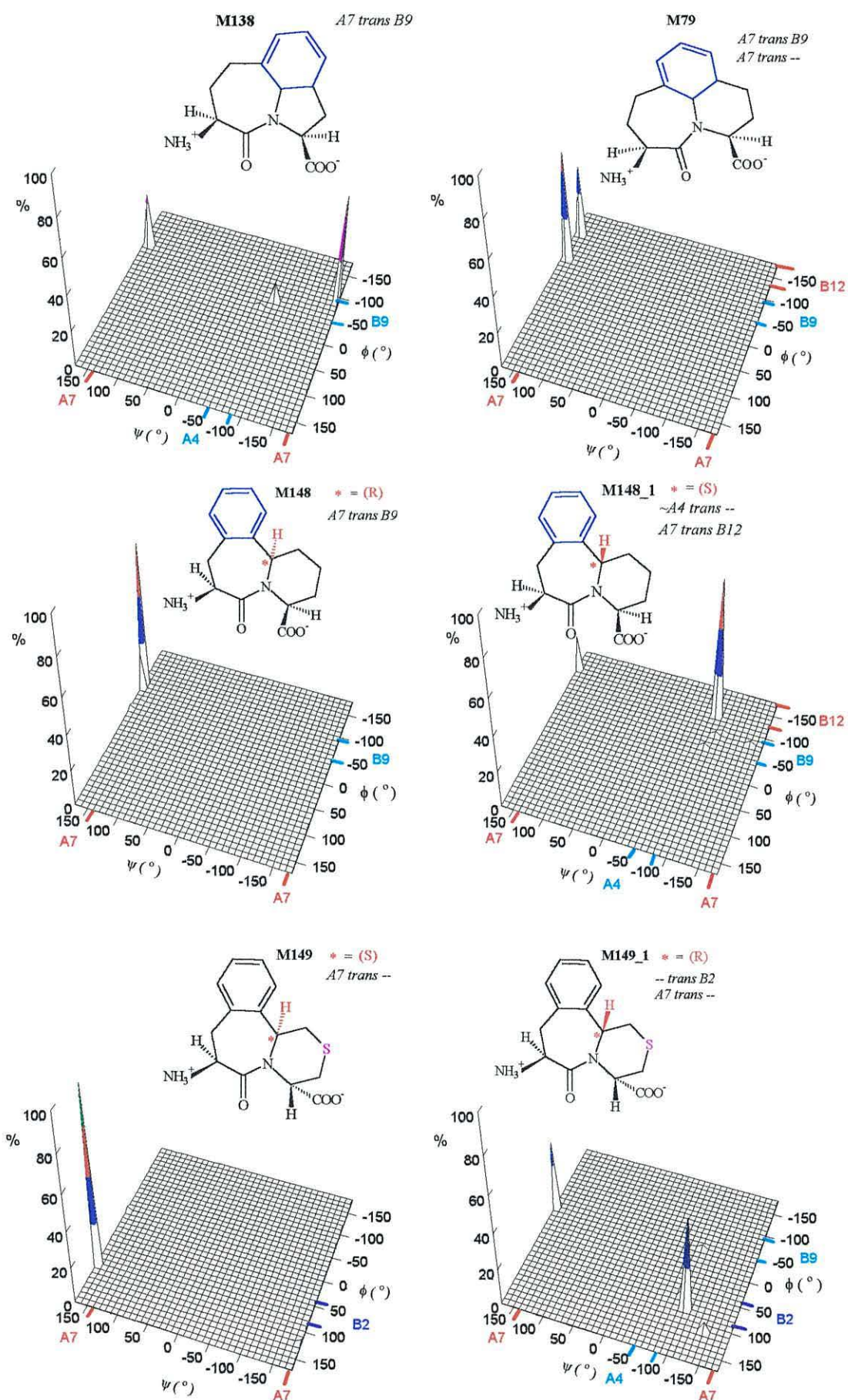


Figure 4-9: 3DPR Plots of ψ vs ϕ vs % Conformers for M138, M79, M148, M148_1, M149 and M149_1.

M148 is a 7-membered lactam fused with a 6-membered ring with an additional benzene ring fused on top, at C5 and C6, of the 7-membered lactam ring. M148 with the bridging carbon of R chirality (Table 4.9.), had all ψ (Tor2) angles constrained in A7, with *trans* ω bonds, and ϕ (Tor4) angles in B9. These results show that placing the benzene ring on top of the 7-membered lactam ring still produced A7B9 conformers, like M138_1 (Table 4.8.). M148 would be predicted to be a good Dpp substrate as it has all A7B9 conformers. M148 was modified to **M148_1** by changing the chirality of the bridging carbon to S. This produced ψ (Tor2) angles near A4, with some conformers in A7, unlike M138_2 (Table 4.8.) that had the majority of its ψ (Tor2) angles outside the MRT sectors, and ϕ (Tor4) angles outside B9 or in B12. M148_1 may show some Dpp activity as it has some A7B12 conformers. **M149** is the same as M148, but the second 6-membered lactam ring contains a sulphur atom. The bridging carbon had S chirality, and as seen with other sulphur containing mimetics, the orientation of the C α near the C-terminus changed from S to R chirality. M149 had A7 conformers, like M148, with *trans* ω s, and conformers outside B2, in contrast to M148 which had B9 conformers. M149 would be predicted to have poor transport activity as it does not have any B9 or B12 conformers. M149 was modified to **M149_1** by changing the bridging carbon's chirality to R. This produced conformers outside A4, and some in A7, with *trans* ω s, and ϕ (Tor4) angles near B2 or outside B9. M149_1 would also be predicted to have poor Dpp and Tpp activity due to the lack of B9 and B12 conformations. Both M148 and M148_1 would be expected to have better Dpp activity than either M149 or M149_1, as they have a higher percentage of Dpp conformers. Fig. 4-9 shows 3DPR plots for M138, M79, M148, M148_1, M1490 and M149_1 showing their percentage conformer distribution range. **M105** is similar to M148, but does not have an additional benzene ring fused in the middle, and has a bridging carbon with S chirality (Table 4.9.). M105 had ψ (Tor2) angles in A7 and ϕ (Tor4) angles constrained in B9, with *trans* ω bonds. Changing the chirality of the bridging carbon to R in **M105_1**, caused a change in conformer distribution range (Table 4.9.).

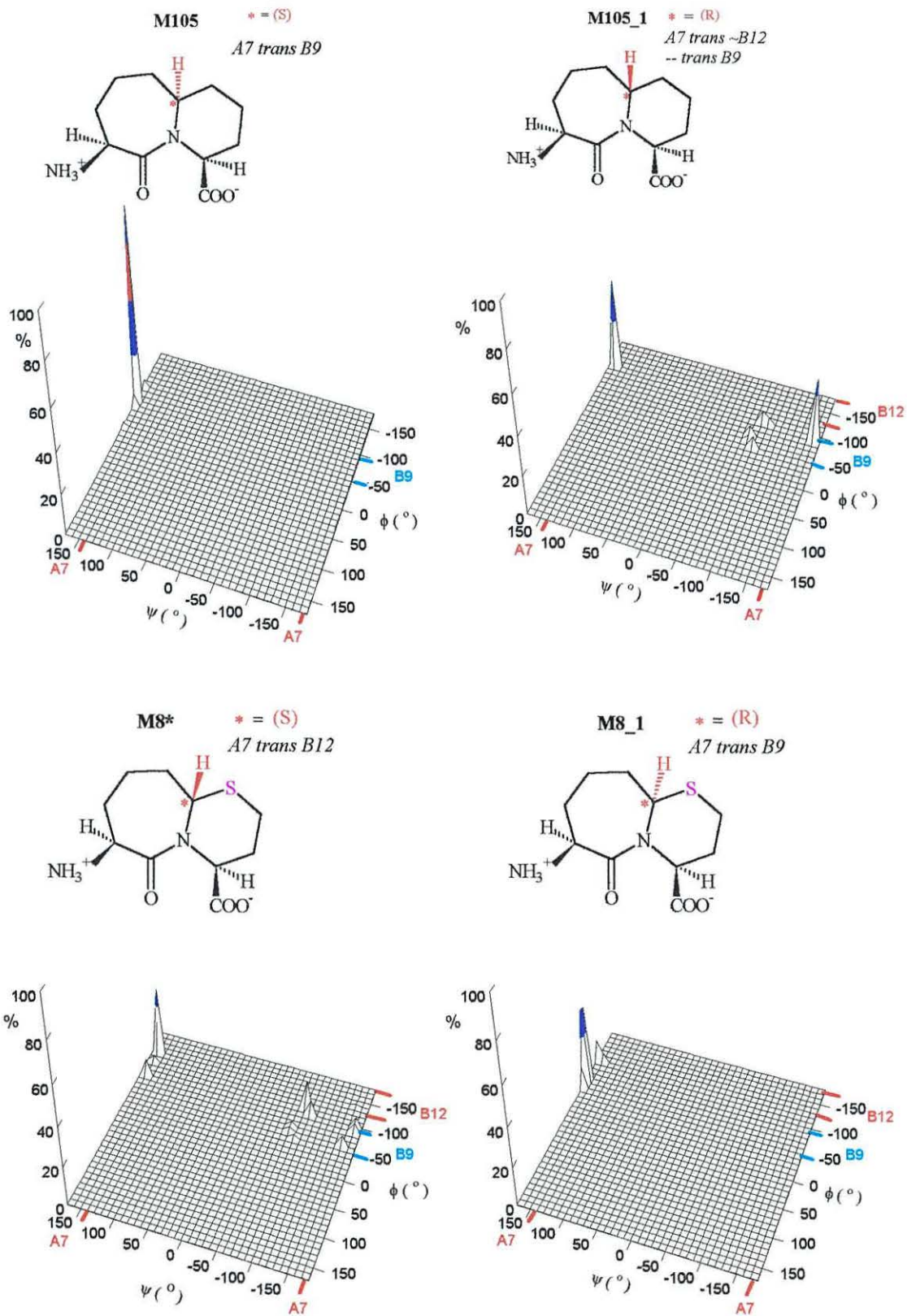
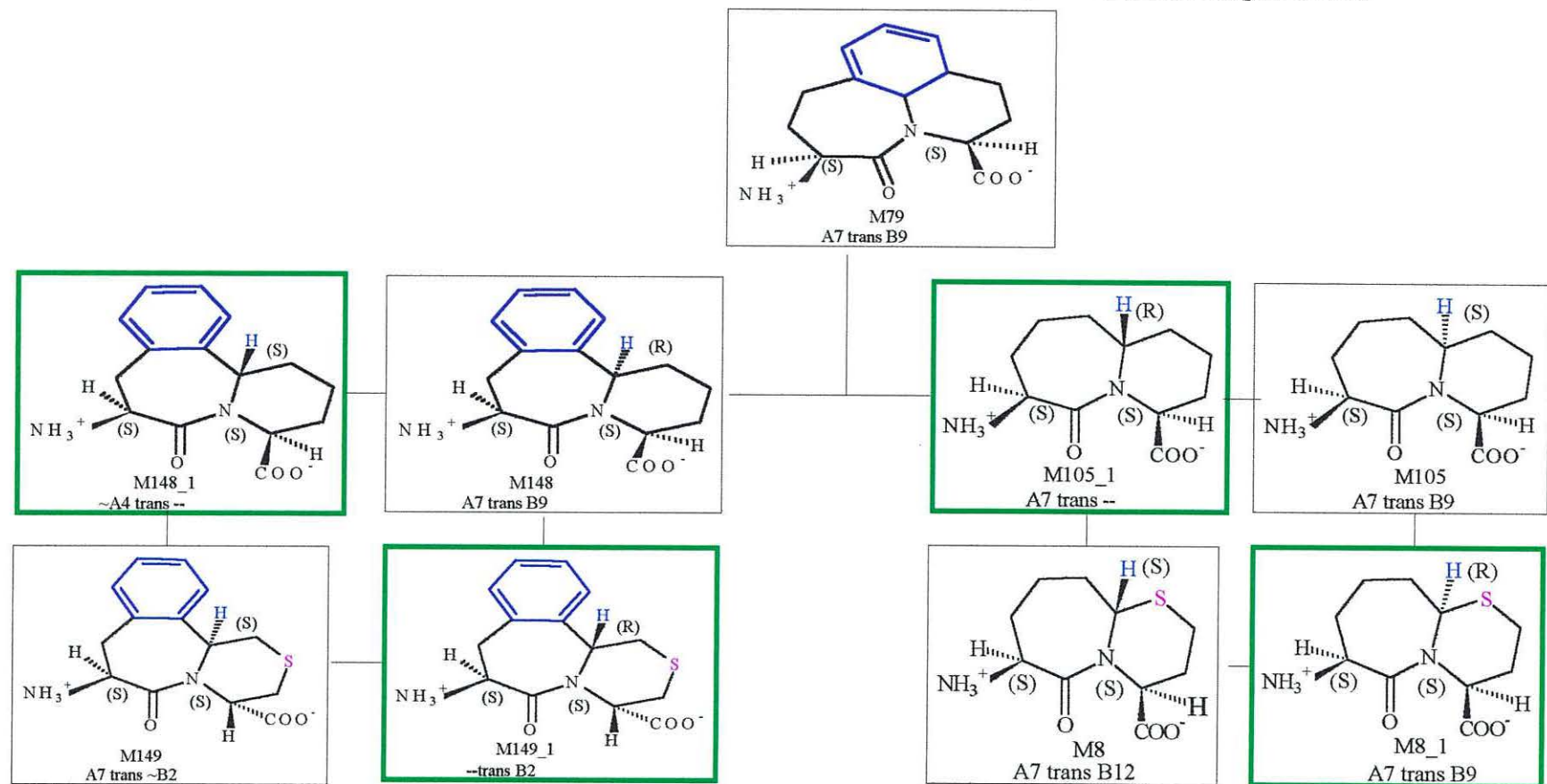


Figure 4-10: 3DPR Plots of Ψ vs Φ vs % Conformers for M105, M105_1, M8 and M8_1.

ψ (Tor2) angles were in or outside A7 or A4, with *trans* ω , and ϕ (Tor4) angles near B12, with a few in or near B9. Based on these results, M105 would be predicted to have higher Dpp activity than M105_1, as all its conformers are constrained within A7B9. M105_1 may show some Dpp and Tpp activity as it contains A7B12 and A4B9 conformers.

M8* (Hanessian *et al.*, 1997) is similar to M105, but has a sulphur atom in the second 6-membered ring. The bridging carbon had S chirality and ψ (Tor2) angles mainly in A7, with fewer in A4. ϕ (Tor4) angles were in B12 or outside B9. All the conformers had *trans* ω bonds. The conformations obtained with M8 were similar to those for M105_1. Changing the chirality of the bridging carbon to R in **M8_1**, produced exclusively A7 conformers with ϕ (Tor4) angles constrained in or near B9. The conformer range obtained for M8_1 was similar to that obtained for M105. Both M8 and M8_1 would be predicted to have transport activity for Dpp, as they contain A7B12 and A7B9 conformations respectively. Fig. 4-10 shows 3DPR plots for M105, M105_1, M8 and M8_1. Chart 6 shows structures and conformations for all 7-membered lactams fused with 6-membered ring mimetics modelled.


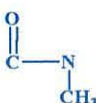



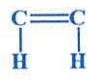
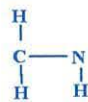
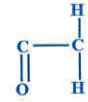
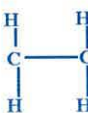
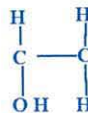
Chart 6: Structure and Conformations for 7-Membered Lactams fused with 6-Membered Ring Mimetics.



Green Frame = Modified Mimetics

4.2.5. Summary of Results for Conformational Analysis of Peptidomimetics

Table 4.10. Summary of Results for Peptide Bond Mimetics

| PBM | Name | Structure | Omega Conformation |
|-----|--------------------------|---|--------------------|
| AA | Amide |  | Trans |
| 1 | N-methylamide |  | Trans and Cis |
| 2 | Retro-Amide |  | Trans |
| 3 | Trans C=C Isostere |  | Trans and Cis |
| 4 | Thioamide |  | Trans |
| 5 | Cis-olefinic Double Bond |  | Trans |
| 6 | Methyleneamino |  | Variable |
| 7 | Keto-methylene |  | Variable |
| 8 | Ethylene |  | Variable |
| 9 | Hydroxyethylene |  | Variable |

PBM denotes Peptide Bond Mimetic

Table 4.11. Summary of Results for Lactam-Constrained Mimetics

| Structural Feature | Omega | A7 | A4 | A10 | B9 | B12 | B2 | E.g. |
|--|-------|----|----|-----|----|-----|----|------------|
| 4-MR | trans | x | x | x | ✓ | ✓ | ✓ | M65 |
| 5-MR | trans | x | ✓ | x | x | x | x | M55 |
| 6-MR | trans | x | x | x | ✓ | ✓ | ✓ | M56 |
| 7-MR | trans | ✓ | x | x | ✓ | x | x | M69_1 |
| 8-MR | trans | ✓ | x | x | ✓ | x | ✓ | M80_1 |
| 6-MR + S atom | trans | ✓ | x | x | ✓ | x | ✓ | M68 |
| 6-MR + S atom + 2CH ₃ gps at C6 and Cα' S | trans | ✓ | x | x | ✓ | x | ✓ | M68_3 |
| 6-MR + S atom + 2CH ₃ gps at C6 and Cα' R | trans | x | x | x | ✓ | x | ✓ | M68_2 |
| 7-MR + S atom and Cα' S | trans | x | x | x | ✓ | x | ✓ | M57-3 |
| 7-MR + S atom and Cα' R | trans | ✓ | x | x | ✓ | x | ✓ | M57_2 |
| 7-MR + BR at C6 & C7 and 8-MR +BR at C7 & C8 | trans | ✓ | x | x | ✓ | x | ✓ | M80 M58 |
| 7-MR + BR at C5 & C6 | trans | ✓ | x | x | ✓ | x | x | M75 |
| Phenyl Group at Cα'' | trans | - | - | - | - | ✓ | ✓ | M55 |
| CH ₃ Group at Cα'' | trans | - | - | - | - | ✓ | ✓ | M69 |

✓ = can only be x = cannot be - = depending on C or N-terminus moiety MR=Membered Ring
 BR=Benzene Ring Cα'=Cα near N-terminus
 Cα''= Cα near C-terminus S,R = Stereochemistry

Summary Chart of Structures and Conformations for 4-, 5-, 6-, 7- and 8-Lactam Ring Mimetics.

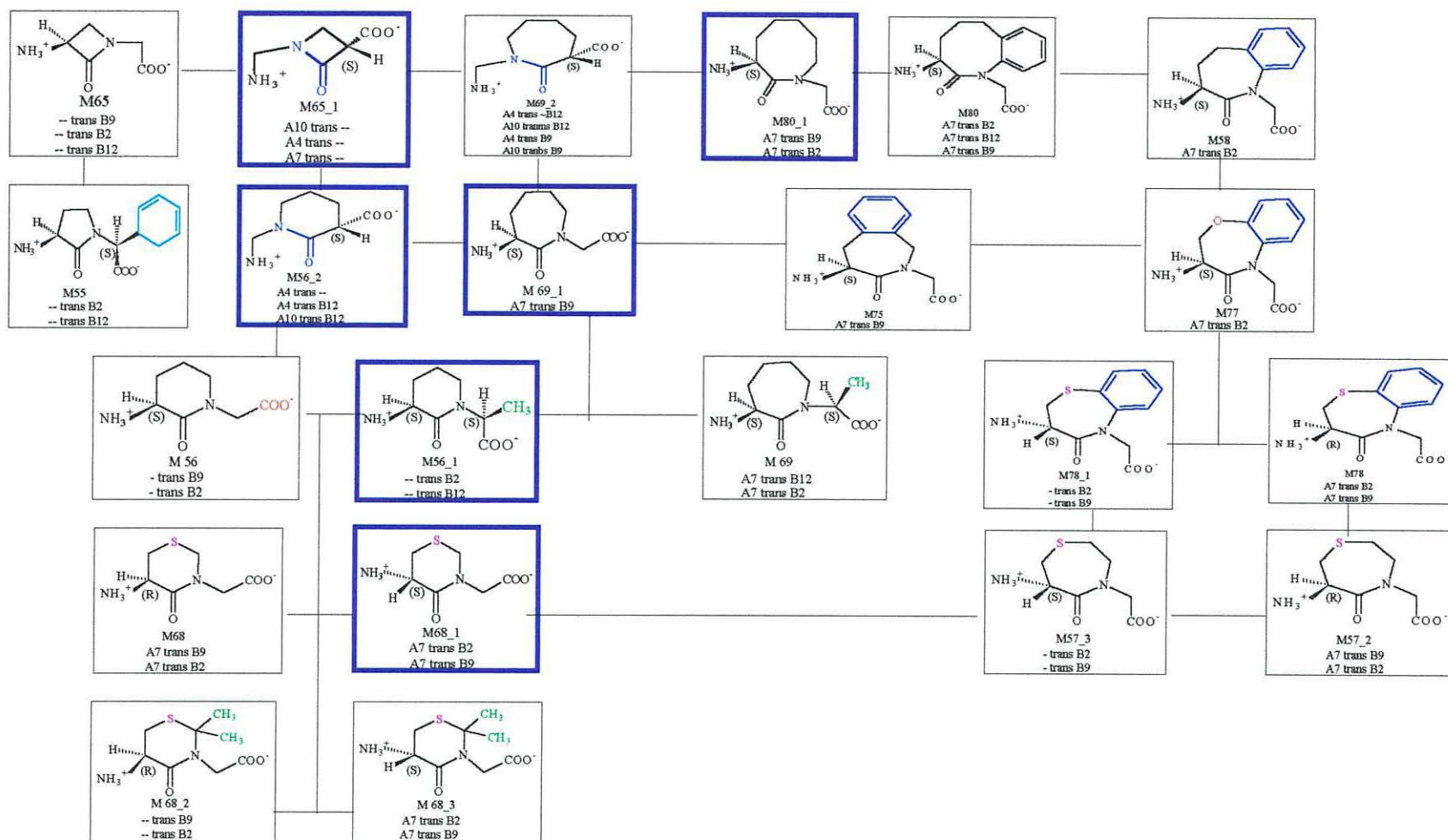


Table 4.12. Summary of Results for Torsionally-Constrained Mimetics

| Ring 1 | bC | Ring 2 | A7 | A4 | A10 | B9 | B12 | B2 | E.g. |
|-----------------------------------|-------------|--|----|----|-----|----|-----|----|---------|
| X | R/S | 5-MR | x | x | x | ✓ | x | x | |
| 7-MR | S | 5-MR | ✓ | x | x | ✓ | x | x | M127 |
| 7-MR | R | 5-MR | x | ✓ | x | ✓ | x | x | M127_1 |
| 6-MR | R/S | 5-MR | x | x | x | ✓ | x | x | M113/_3 |
| 6-MR + O atom | R/S | 5-MR | x | x | x | ✓ | x | x | M111/2 |
| 6-MR + S atom and Cα' R | R | 5-MR | ✓ | x | x | ✓ | x | x | M113_1 |
| 6-MR + S atom and Cα' R | S | 5-MR | ✓ | x | ✓ | ✓ | x | x | M113_2 |
| 7-MR | S | 6-MR | ✓ | x | x | ✓ | x | x | M105 |
| 7-MR | R | 6-MR | ✓ | x | x | x | ✓ | x | M105_1 |
| 7-MR + BR at C5 and C6 | R | 6-MR | ✓ | x | x | ✓ | x | x | M148 |
| 7-MR + BR at C5 and C6 | S | 6-MR | x | ✓ | x | x | x | x | M148_1 |
| 7-MR | + BR | 6-MR | ✓ | x | x | ✓ | x | x | M79 |
| 7-MR | + BR | 5-MR | ✓ | x | x | ✓ | x | x | M138 |
| 7-MR | S | 5-MR + S atom | x | ✓ | x | x | x | ✓ | M4* |
| 7-MR | R | 5-MR + S atom | ✓ | x | x | x | x | ✓ | M5* |
| 7-MR | R/S | 5-MR + S atom and Cα'' R | ✓ | ✓ | x | ✓ | x | x | |
| 7-MR + S atom | - | - | x | - | - | - | - | - | |

✓ = can only be x = cannot be - = depending on C or N-terminus moiety MR=Membered Ring
 BR=Benzene Ring bC= bridging carbon Cα'=Cα near N-terminus
 Cα''= Cα near C-terminus X= 7 or 6 MR
S,R = Stereochemistry

Summary Chart of Structures and Conformations for Torsionally-Constrained Mimetics.

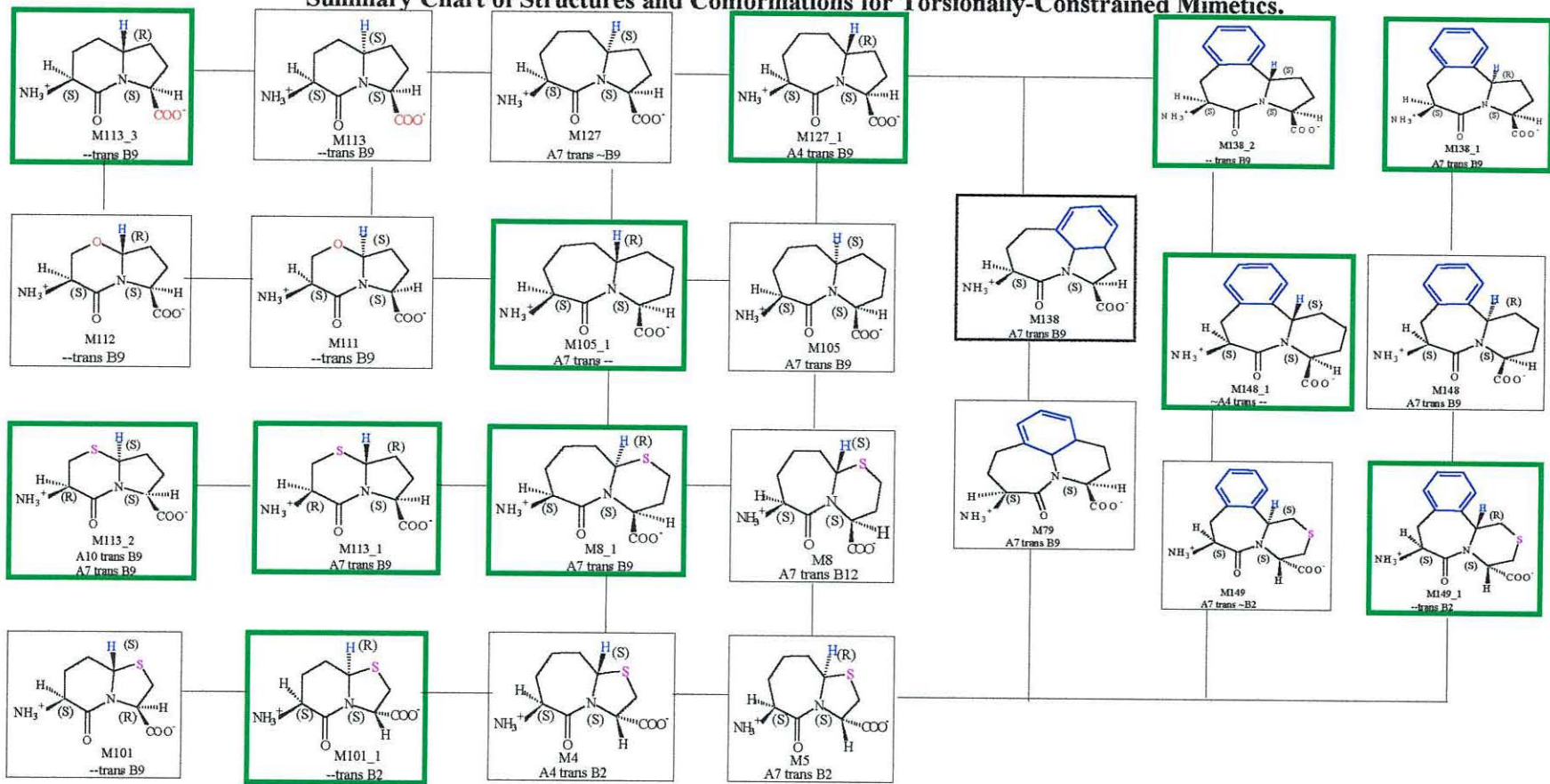


Table 4.13. Putative Dpp and Tpp Substrates Based on Acceptable Backbone Torsion Angles.

| Mimetic | Dpp | Tpp |
|---------|-----|-----|
| M46 | ✓ | × |
| M47 | ✓ | × |
| M48 | ✓ | × |
| PBM1 | ✓ | × |
| PBM4 | ✓ | ✓ |
| M56_2 | × | ✓ |
| M68 | ✓ | × |
| M69 | ✓ | × |
| M69_1 | ✓ | × |
| M69_2 | × | ✓ |
| M75 | ✓ | × |
| M58 | ✓ | × |
| M77 | ✓ | × |
| M78 | ✓ | × |
| M57_1 | ✓ | × |
| M80 | ✓ | × |
| M80_1 | ✓ | × |
| M127 | ✓ | × |
| M127_1 | × | ✓ |
| M138_1 | ✓ | × |
| M148 | ✓ | × |
| M79 | ✓ | × |
| M105 | ✓ | × |
| M8* | ✓ | × |
| M8_1 | ✓ | × |
| M113_1 | ✓ | × |
| M113_2 | ✓ | ✓ |

✓ = Can be a substrate × = Can not be a substrate M_ = Modified Mimetic

4.3. DISCUSSION

4.3.1. Conformational Analysis of Dipeptide Isosteres

These compounds have an isosteric replacement of the peptide backbone in order to determine the functional role of a particular amide bond, or to increase the strength of binding to an enzyme using a transition state mimic, or to enhance bioavailability and metabolic stability (Gillespie *et al.*, 1997). Dipeptide isosteres generally have a flexible peptide backbone, and this was reflected in their conformational analysis where a large number of unique conformers were obtained for these structures. Most of these compounds would be predicted to have poor transport activity as they have backbone torsion angles outside the MRTs, and do not have the *trans* ω peptide bond that is required for transport by Dpp and Tpp. The *cis* olefins and tetrazoles have been used as mimics of *cis* amide bonds, and the aromatic **M5** has been designed to mimic the proposed *cis* amide bond bioactive conformation of a potent cyclic hexapeptide analogue of somatostatin (Gillespie *et al.*, 1997), however, it would be predicted to have poor bioavailability based on its conformational analysis for transport in this study. The dipeptide isosteres **M46**, **M47** and **M48** would be predicted to show some Dpp activity compared with all the isosteres analysed, as they have backbone torsion angles that match the Dpp MRT (Table 4.13), but the chi-space of their side chains would also need to be considered for their activity *in vivo*.

4.3.2. Conformational Analysis of Peptide Bond Mimetics

A range of peptide bond mimetics was investigated to see whether they had a high percentage of conformers with *trans* ω bonds, as occurs for natural peptides. **PBM1-5** all had high percentage of conformers with *trans* ω peptide bonds. Based on their conformational analysis, the *N*-methylethylamide (**PBM1**) would be predicted to have Dpp activity, and the thioamide (**PBM4**) would be predicted to have both Dpp and Tpp activity (Table 4.13). These amide bond modifications would increase stability against proteolytic enzymes, and also retain the *trans* ω conformations required for transport. PBM1 and PBM4 could be synthesised and their activity tested using Dpp and Tpp *E.coli* mutants.

The trans C=C isostere and cis-olefinic double bond compounds would have poor transport activity as their ψ and ϕ torsion angles are not in the MRTs for the peptide transporters, even though they have *trans* ω conformations. **PBM6-9** had variable ω torsion angles that were near *trans*, or neither *cis* nor *trans*. Although **PBM6-9** may be incorporated into larger compounds such as enzyme inhibitors, these isosteric replacements of the peptide bond would result in these compounds having poor intestinal transport activity. The methylenethio isostere [CH_2S], has been used as an amide replacement in enkephalin analogues. Renin inhibitors have both the methyleneamino [CH_2NH] and hydroxyethylene [CHOHCH_2] isosteres at the scissile Leu-Val amide bond of the 6-13 octapeptide derived from angiotensinogen. Ketomethylene isosteres [COCH] have formed part of potent angiotensin-converting enzyme (ACE) inhibitors, which have shown good properties *in vitro*, but poor *in vivo* (Gillespie *et al.*, 1997).

4.3.3. Conformational Analysis of Lactam-Constrained Mimetics

Conformational constraints have been used in peptide mimetics to probe conformations of secondary structural elements such as β - and γ -turns, or to determine bioactive conformations, or to enhance binding of enzymes or receptors by pre-organising the ligand and reducing the entropic cost of the binding process. Freidinger *et al.* (1980) have used lactams to constrain peptides in turn-like conformations and enforce *trans* amide conformations and this was reflected in their conformational analysis, as all of the mimetics in this group had peptide bonds constrained in the *trans* ω conformation. **M57**, **58**, **69-80** have been incorporated into many potent metallo-protease inhibitors, as conformationally constrained analogues of Phe-Pro or Ala-Pro (Hanessian *et al.*, 1997). **M57**, **58**, **69-80** had their ψ (Tor2) angles constrained in A7 due to the 7-membered ring, with ϕ (Tor4) angles in B2, B9 and B12, therefore these compounds would be predicted to have better bioavailability, compared with 4,5, or 6-membered lactam ring mimetics (Table 4.11).

Structural modifications of lactam-mimetics produced Tpp substrates such as **M56_2**, **M69_2** and **M64_1** and Dpp substrates such as **M68**, **M69**, **M69_1**, **M69_2**, **M75**, **M58**, **M77**, **M71**, **M78**, **M57_2**, **M73**, **M80** and **M80_1** that warrant synthesis and testing for transport activity using Tpp and Dpp *E.coli* mutants (Table 4.13).

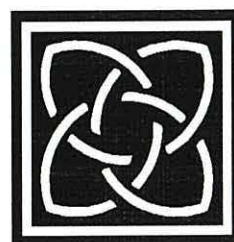
4.3.4. Conformational Analysis of Torsionally-Constrained Mimetics

The torsionally-constrained mimetics only had a few unique conformers in solution, with the minimum energy conformers forming a large percentage of the conformer distribution range. Nearly all torsionally-constrained mimetics were constrained into the B9 region due to the 5-membered ring (Table 4.12). 6-membered lactams fused with 5-membered rings did not restrict ψ angles in A7, A4/A10 MRTs and would be predicted to have poor bioavailability. The bicycle turn dipeptide (BTD) **M101** was prepared to enforce a β -turn, and has been incorporated into various peptides hypothesised to contain β -turns in the bioactive conformation (Gillespie *et al.*, 1997). Molecular modelling of **M101** has shown it would be predicted to have poor Dpp and Tpp activity as it does not have A7 or A4/A10 conformers. **M111** and **M112** contain O atoms in their 6-membered lactam rings, and have been incorporated into Leu-enkephalin analogues. Conformational analysis of **M111** and **M112** showed they had the B9 template but they did not have A7 or A4/A10 templates, therefore these mimetics would be predicted to have poor bioavailability. Conformational analysis of torsionally-constrained mimetics has highlighted the importance of *stereochemistry* of the bridging carbon, which can be used to produce substrates exclusively for Dpp or Tpp systems (Table 4.12). For example, **M113** and **M113_3** would be poor substrates for transport as they do not have A7 or A4/A10 conformers. However, insertion of a S atom in their 6-membered lactam rings produced A7 and A10 conformers, depending on the stereochemistry of the bridging carbon. Molecular modelling of **M127** and **M127_1** also illustrates how the stereochemistry of the bridging carbon can produce either all A4B9 conformers or all A7B9 conformers. Both **M127** and **M127_1** would be predicted to have good bioavailability as they can have both Dpp and Tpp activity (Table 4.13). These *rationally* designed mimetics would need synthesis and testing for uptake activity using *E.coli* Dpp and Tpp mutants.

4.3.5. Design of Peptidomimetics with Oral Bioavailability

The design of peptidomimetic ligands with biological activities *in vitro* and *in vivo* has been challenging. A systematic stepwise strategy has been developed to produce compounds with biological potency, high stability and pharmacological efficacy *in vitro* and *in vivo*. These include determining the primary amino acid side chain residues required for molecular recognition, and determination of preferred backbone conformation which can serve as a template for the bioactive conformation (an alpha-helix, beta-turn or beta-sheet). In some cases, the preferred side chain conformations in chi space are also examined in order to constrain side chains at the highly preferred gauche (-), or gauche (+), or trans conformations. These methodologies have commonly been used to provide insight into the topographical requirements for ligand receptor interactions (Hruby, *et al.*, 1997).

This study has shown how conformational analysis, using molecular modelling, can be used to assess the *bioavailability* of peptidomimetics as part of a rational design cycle at the initial drug discovery stages, by applying the MRTs established in Chapter 3. Peptidomimetic ligands can now be designed that have the key side chain residues placed in the correct template in 3-D space to produce biological potency as well as oral activity. The use of molecular modelling for the *rational* design peptidomimetics has also been illustrated. Structural modifications of a wide range of peptide mimetics has identified chemical motifs that can be applied to the design of substrates that match the MRT backbone torsion angles for recognition by peptide transporters. Structural modifications such as stereochemistry and insertion of sulphur atoms can be applied to produce theoretical compounds that not only have the bioactive conformation required for binding to intracellular target sites, but also have features that enable good oral delivery across intestinal membranes. This provides interesting prospects for computer-directed combinatorial chemistry. Multiple structure-activity models can now be investigated in parallel, thus overcoming the one-at-a-time throughput limitations of the conventional process of analogue synthesis, testing and redesign that characterise both structure-based design and conventional analogue chemistry approaches to drug discovery.



CHAPTER 5

MOLECULAR MODELLING OF

ANGIOTENSIN-CONVERTING ENZYME

(ACE) INHIBITORS

5.1. INTRODUCTION



The rational design of ACE inhibitors, such as captopril and enalapril, was initiated by the discovery that certain snake-venom peptides were effective inhibitors of ACE *in vitro*. The enzyme ACE has not been crystallised and comparison of the C-terminal sequence TrpAlaPro of the snake-venom peptides provided a model for the side chain interactions required to bind to ACE. Since 1977, various orally active ACE inhibitors have been designed and synthesised according to a biochemical model of the ACE active site based on the X-ray crystal structure of a related enzyme, carboxypeptidase A (Cleland, 1993). Currently, there are 3 main chemical classes of ACE inhibitors used for the treatment of hypertension and these include carboxyl group-containing drugs, a newer class of ACE inhibitors have a phosphoryl group, and captopril and related compounds are sulphhydryl-containing drugs. The majority of the ACE inhibitors are administered as prodrugs, because of the poor bioavailability of the active compound that binds to the enzyme. As ACE inhibitors are peptide-based therapeutics they can potentially act as substrates for the intestinal peptide transporters for their oral delivery. Conformational analysis of a variety of natural peptide substrates has allowed the definition of molecular recognition templates (MRTs) of substrates that can be recognised by peptide transporters (Chapter 3) (Payne *et al.*, 2000). In this study, molecular modelling of a variety of ACE inhibitors will be done in order to determine whether their *backbone torsion angles* are in defined MRTs required for transport. Predictions of activity gained by modelling studies will be experimentally explored by the use of radioligand competition filter binding assays. The charge and chi-space of these drugs will then also be considered when correlating their activity to modelling studies. If a correlation between the molecular modelling data and activity data is found, there will be good justification for use of computer models to direct the *rational* design of peptide-based therapeutics with structural features needed for improved oral absorption. An improvement in oral delivery has a number of advantages, including the use of low drug dosage and decreased unit costs per patient.

5.2. RESULTS

5.2.1 Conformational Analysis of ACE Inhibitors

ACE inhibitors were modelled (section 2.7.2.3.) and conformational and data analysis was carried out as described (section 2.7.3.3.). Table 5.1. shows the results for conformational analysis of Ala-Pro and related ACE inhibitors. Most of the ACE inhibitors had a large percentage of their conformers with ψ (Tor2) angles outside A7, A4 and A10. The peptide bond angles were either *cis* or *trans* ω , but often outside the defined *cis* and *trans* MRT. Nearly all of the ACE inhibitors had their ϕ (Tor4) angles constrained in or near B9 due to the conformational constraint of the proline ring at the C-terminus.

Table 5.1. Minimum Energy Conformers for Ala-Pro and ACE Inhibitors Showing their ψ (Tor2), ω (Omega), ϕ (Tor4) Torsion Angles, N-C Distance and their Total Percentage of Conformer Distribution Range.

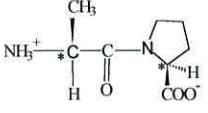
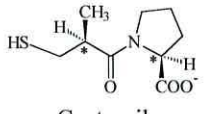
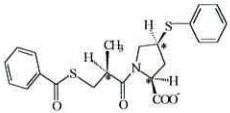
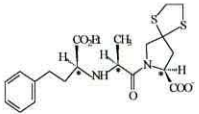
| Structure | Energy kcal/mol | % | ψ ° (Tor2) | ω ° Omega | ϕ ° (Tor4) | NC Å | %Total Range |
|--|--------------------|-------|--------------------|---------------------|--------------------|---------|---------------------|
|  Ala Pro (S,S) | 9.48 | 30.04 | 147.4 | -1.2 | -77.7 | 4.38 | 43% A7 <i>t</i> B9 |
| | 9.47 | 28.1 | 148.0 | 179.3 | -75.9 | 5.48 | 34% A7 <i>c</i> B9 |
| | 10.16 | 9.12 | 148.6 | 179.2 | -75.2 | 5.46 | 13% -- <i>c</i> B9 |
|  Captopril (S,S) | 8.95 | 28.78 | 145.7 | -1.3 | -77.2 | 4.40 | 40% A7 <i>c</i> B9 |
| | 9.24 | 18.03 | 148.4 | 179.3 | -76.1 | 5.57 | 32% A7 <i>t</i> B9 |
| | 9.99 | 5.28 | 147.6 | -1.9 | -77.7 | 4.44 | 13% -- <i>t</i> B9 |
|  Zofenopril (S,S,S) | 5.02 | 38.96 | 153.4 | 173.5 | -46.4 | 5.30 | 39% A7 <i>t</i> ~B9 |
| | 5.60 | 15.22 | 107.6 | 176.3 | -49.1 | 5.45 | 19% -- <i>t</i> ~B9 |
| | 6.19 | 5.79 | 151.1 | 178.6 | -69.9 | 5.51 | 19% A7 <i>t</i> B9 |
|  Spirapril (S,S,S) | 6.99 | 17.15 | 58.0 | 179.2 | -50.5 | 5.35 | 50% A10 <i>t</i> B9 |
| | 7.11 | 14.24 | 58.5 | 179.3 | -50.1 | 5.34 | 16% A7 <i>c</i> B9 |
| | 7.65 | 5.87 | 68.8 | -178.8 | -55.5 | 5.38 | 14% A7 <i>t</i> B9 |

Table 5.1. Continued.

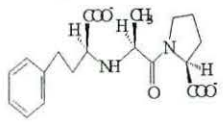
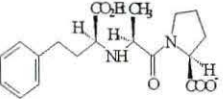
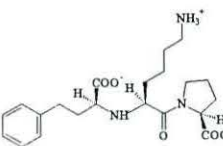
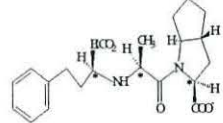
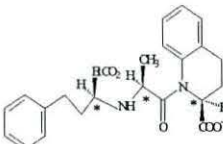
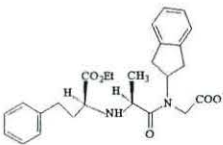
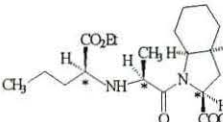
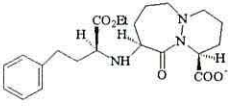
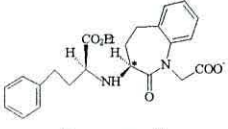

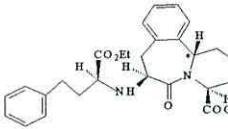
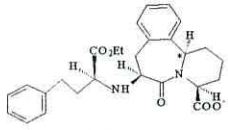
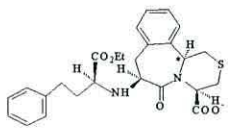
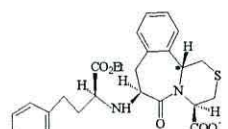
| Structure | Energy kcal/mol | % | ψ° (Tor2) | ω° Omega | ϕ° (Tor4) | NC Å | % Total Range |
|---|--------------------|-------|------------------------|-------------------------|------------------------|---------|----------------------|
|  Enalaprilat (S,S,S) | 7.91 | 13.37 | 52.9 | -177.9 | -76 | 5.33 | 35% A10 <i>t</i> B9 |
| | 8.08 | 10.24 | 145.3 | -0.7 | -76.7 | 4.33 | 23% A7 <i>c</i> B9 |
| | 8.30 | 7.11 | 53.2 | -178.1 | -75.7 | 5.33 | 12% A7 <i>t</i> B9 |
|  Enalapril (S,S,S) | 7.3 | 15.55 | 146.0 | -0.6 | -76.8 | 4.34 | 33% A7 <i>c</i> B9 |
| | 7.68 | 8.4 | 60.2 | 178.9 | -48.5 | 5.35 | 16% A7 <i>t</i> B9 |
| | 7.69 | 8.16 | 52.7 | -179.5 | -75.3 | 5.33 | 14% A10 <i>t</i> B9 |
|  Lisinopril (S,S,S) | 7.8 | 38.9 | 149.0 | 178.8 | -76.2 | 5.48 | 56% A7 <i>t</i> B9 |
| | 8.32 | 16.78 | 145.4 | -1.7 | -76.5 | 4.34 | 25% A7 <i>c</i> B9 |
| | 8.91 | 6.41 | 146.2 | 2.1 | -76.5 | 4.35 | 4% -- <i>t</i> B9 |
|  Ramipril (S,S,S) | 25.05 | 32.21 | 55.6 | -174.3 | -69.1 | 5.30 | 48% A10 <i>t</i> B9 |
| | 25.74 | 10.50 | 144.4 | 0.9 | -70.6 | 4.28 | 29% A7 <i>c</i> B9 |
| | 25.76 | 10.01 | 141.8 | -0.4 | -70.3 | 4.22 | 11% -- <i>t</i> B9 |
|  Quinapril (S,S,S) | 6.76 | 18.18 | 129.7 | 7.6 | -75.7 | 4.07 | 38% -- <i>t</i> B9 |
| | 7.29 | 7.63 | 98.2 | -164.1 | -74.8 | 5.42 | 32% -- <i>c</i> B9 |
| | 7.30 | 7.47 | 115.1 | -164 | -75.5 | 5.42 | 12% A7 <i>c</i> B9 |
|  Delapril (S,S,S) | 10.93 | 11.18 | 66.7 | -1.8 | 86.8 | 3.99 | 23% A7 <i>c</i> B9 |
| | 11.14 | 7.86 | 66.4 | 2.6 | 79.5 | 3.90 | 19% A10 <i>c</i> B2 |
| | 11.48 | 4.57 | 147.5 | 0.3 | -81.1 | 4.40 | 11% A10 <i>c</i> ~B2 |
|  Perindopril (S,S,S) | 10.63 | 42.09 | 82.7 | -1.0 | -58.2 | 2.80 | 47% A10 <i>c</i> B9 |
| | 11.24 | 15.35 | 123.5 | -179.7 | -55.1 | 5.34 | 15% -- <i>t</i> B9 |
| | 11.33 | 13.41 | 67.8 | -175.8 | -65.3 | 5.33 | 13% A10 <i>t</i> B9 |

Table 5.1. Continued.

| Structure | Energy kcal/mol | % | ψ° (Tor2) | ω° Omega | ϕ° (Tor4) | NC Å | % Total Range |
|--|--------------------|-------|------------------------|-------------------------|------------------------|---------|---------------|
|  Cilazapril (S,S,S) | 6.77 | 41.36 | 160.4 | -174.9 | -102.1 | 5.78 | 83% A7 t -- |
| | 7.42 | 14.27 | 154.8 | -172.8 | -103.0 | 5.80 | 8% A7 t B9 |
| | 7.44 | 13.91 | 158.0 | -173.8 | -107.4 | 5.84 | |
|  Benazepril (S) | 5.26 | 19.15 | 157.8 | -174.8 | 73.6 | 5.17 | 34% A7 t B2 |
| | 5.57 | 11.57 | -57.1 | 178.6 | -65.7 | 4.78 | 23% A7 t B9 |
| | 5.86 | 7.15 | 159.3 | -176.8 | -151.9 | 6.14 | 17% A4 t B9 |
|  Benazepril (R) | 4.31 | 17.6 | 46.5 | -177.8 | -54.5 | 5.19 | 25%~A10 t B12 |
| | 4.40 | 15.25 | -158.7 | 175.7 | 150.9 | 6.10 | 23% -- t B12 |
| | 4.58 | 11.24 | 47.6 | -176.2 | -153.1 | 5.25 | 21% ~A10 t B9 |
|  MDLa (S) | 14.82 | 34.16 | -57.4 | 173 | -85.8 | 4.52 | 57% A4 t -- |
| | 14.91 | 29.16 | -66 | 179.6 | -106.8 | 4.82 | 36% A4 t B9 |
| | 15.23 | 17.57 | -80 | -175.5 | -110.6 | 5.08 | |
|  MDLa (R) | 15.98 | 19.95 | 168 | 172.7 | -88 | 5.47 | 52% A7 t B9 |
| | 16.26 | 12.66 | 170 | 171.3 | -113.6 | 5.76 | 26% A7 t -- |
| | 16.30 | 11.9 | 170.8 | 171.3 | -88.9 | 5.47 | 8% -- t -- |
|  MDLb (S) | 11.66 | 54.18 | 175.3 | 171.2 | -91.3 | 5.45 | 67% A7 t B9 |
| | 12.83 | 8.08 | 168.5 | 174.6 | -90.1 | 5.49 | 14% -- t -- |
| | 13.01 | 6.05 | -120.3 | 179.7 | -113.6 | 5.24 | 9% A7 t -- |
|  MDLb (R) | 12.79 | 37.83 | -71.7 | 178.3 | -122.5 | 4.98 | 45% A4 t -- |
| | 13.14 | 21.42 | -65.3 | -168.2 | -89.7 | 5.05 | 31% A4 t B9 |
| | 13.97 | 5.56 | -80.9 | -178.5 | -123 | 5.16 | 5% -- t B9 |

-- denotes outside the MRT regions of A7, A4, A10 and B9, B2 and B12 t denotes trans omega c denotes cis omega

5.2.1.1. Ala-Pro

The C-terminus sequence Ala-Pro was originally used in the design of ACE inhibitors. Molecular modelling of Ala-Pro showed that most of its conformers had ψ (Tor2) angles in A7 with a few conformers in or near A10, and ϕ (Tor4) angles constrained in B9. All the conformers had *cis* or *trans* ω , but the *cis* ω was outside the defined regions of $\pm 0.0^\circ$ to $\pm 5.0^\circ$. Ala-Pro would be expected to have better Dpp activity than Tpp activity, as it has more A7 *trans* B9 than A10 *trans* B9 conformers. However, the large percentage of *cis* conformers, would make Ala-Pro a poor substrate for transport.

5.2.1.2. Captopril

Captopril is an analogue of Ala-Pro and had a similar conformer distribution profile to Ala-Pro. The majority of its conformers were in A7, with fewer conformers in or near A10, and ϕ (Tor4) angles were constrained in B9. Like Ala-Pro, captopril also had *cis* and *trans* conformers, with *cis* ω being outside the defined *cis* ω range (Table 5.1.). Captopril would be predicted to act as a Dpp substrate, based on its backbone torsion angles but the presence of a large percentage of *cis* conformers, may result in captopril having poor Dpp activity.

5.2.1.3. Zofenopril

Zofenopril also had a similar conformer distribution range as Ala-Pro, with most of its conformers having *trans* ω conformations. ψ (Tor2) angles were mainly in A7, with some conformers in or near A10, and ϕ (Tor4) angles were constrained in or near B9 (Table 5.1.). Zofenopril would be predicted to act as a substrate for both Dpp and Tpp based on its backbone torsion angles.

5.2.1.4. Spirapril

Spirapril is an ester prodrug with the N-terminus having a phenylester side chain. The majority of its conformers were in A10 with fewer conformers in A7, and ϕ (Tor4) angles were constrained in B9. All the conformers had *cis* or *trans* ω (Table 5.1.). Spirapril would be predicted to have better Tpp activity than Dpp activity, as it has a higher percentage of Tpp conformers than Dpp conformers. Fig. 5-1 shows 3DPR plots for Ala-Pro, Captopril, Zofenopril and Spirapril showing their percentage conformer distribution ranges.

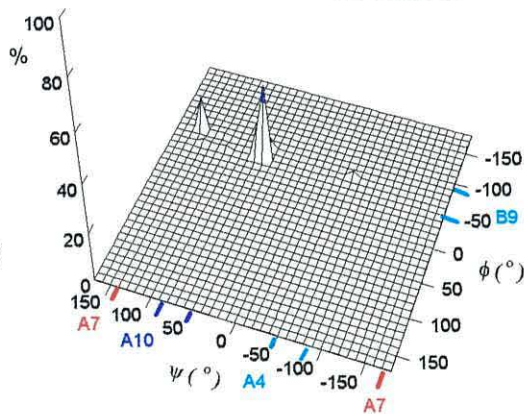
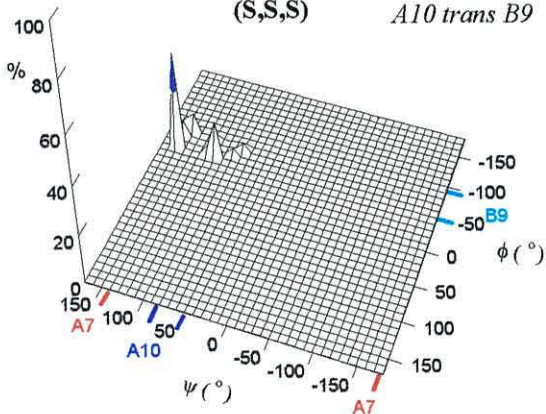
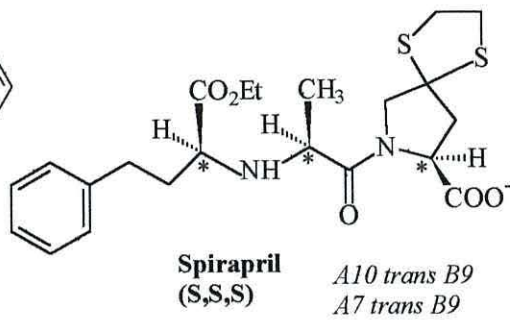
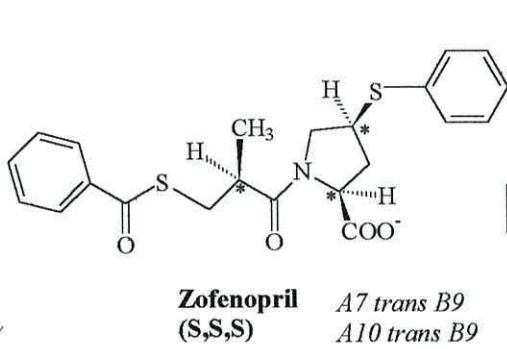
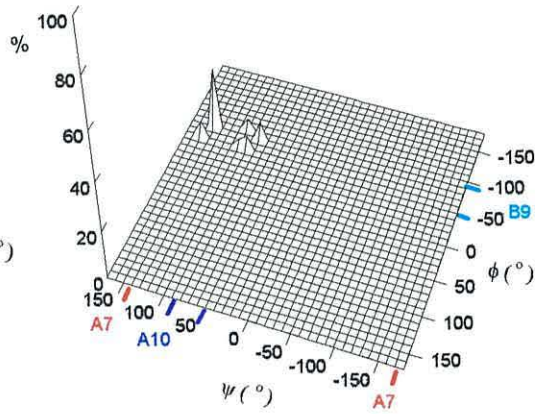
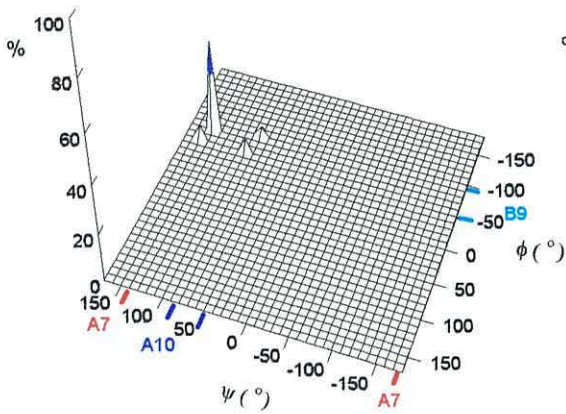
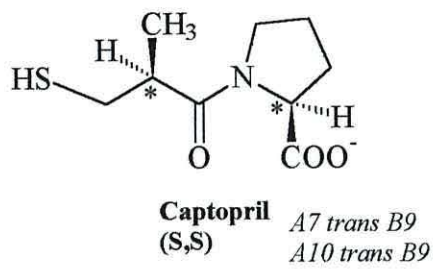
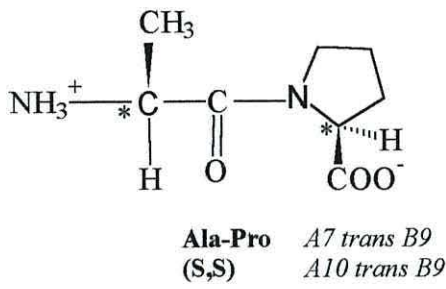


Figure 5-1: 3DPR Plots of ψ vs ϕ vs % Conformers for AlaPro, Captopril, Zofenopril and Spirapril.

5.2.1.5. Enalaprilat

Enalaprilat is the diacid of the prodrug enalapril, and had *cis* and *trans* ω conformations, with *cis* ω outside the defined MRT (Table 5.1.). Enalaprilat had most of its conformers in A10 and some in A7, with ϕ (Tor4) angles constrained in B9. Based on these backbone torsion angles, enalaprilat would be expected to have better Tpp activity than Dpp activity. However, as seen with *N*-terminal Asp and Glu peptides in Chapter 3, the negatively charged carboxylic group attached near the pseudo-*N*-terminus of enalaprilat would interfere with it binding to DppA, and this may result in it having poor Dpp activity.

5.2.1.6. Enalapril

Enalapril is the ester prodrug of enalaprilat and had most of its conformers with *cis* ω and fewer *trans* ω conformations. ψ (Tor2) and ϕ (Tor4) angles were in A7B9 and A10B9 (Table 5.1.). Based on its backbone torsion angles, enalapril would be predicted to have both Dpp and Tpp activity, as it has both Dpp and Tpp conformers, but may show poor transport because of the large percentage of *cis* conformers.

5.2.1.7. Lisinopril

Lisinopril contains a Lys-Pro dipeptide backbone and a carboxylic group near the pseudo-*N*-terminus like enalaprilat. This had most of its conformers in A7B9, with only a few conformers outside A7 and A10. All the conformers had *cis* and *trans* ω , with the *trans* ω bond angle being in the defined MRT (Table 5.1.). Even though lisinopril has backbone torsion angles in A7B9, with *trans* ω s, the negatively charged carboxylic group near the *N*-terminus, and the positively charged lysine side chain may result in lisinopril having poor Dpp activity. In addition, lisinopril contains a large percentage of *cis* conformers which would also make it a poor substrate for transport.

5.2.1.8. Ramipril

Ramipril also had *cis* and *trans* conformations with ψ (Tor2) angles mainly in A10, and a few conformers outside A7 or in A4, with ϕ (Tor4) angles constrained in B9 (Table 5.1.). As ramipril has most of its conformers in A10 *trans* B9 MRT, it would be expected to have better Tpp activity than Dpp activity.

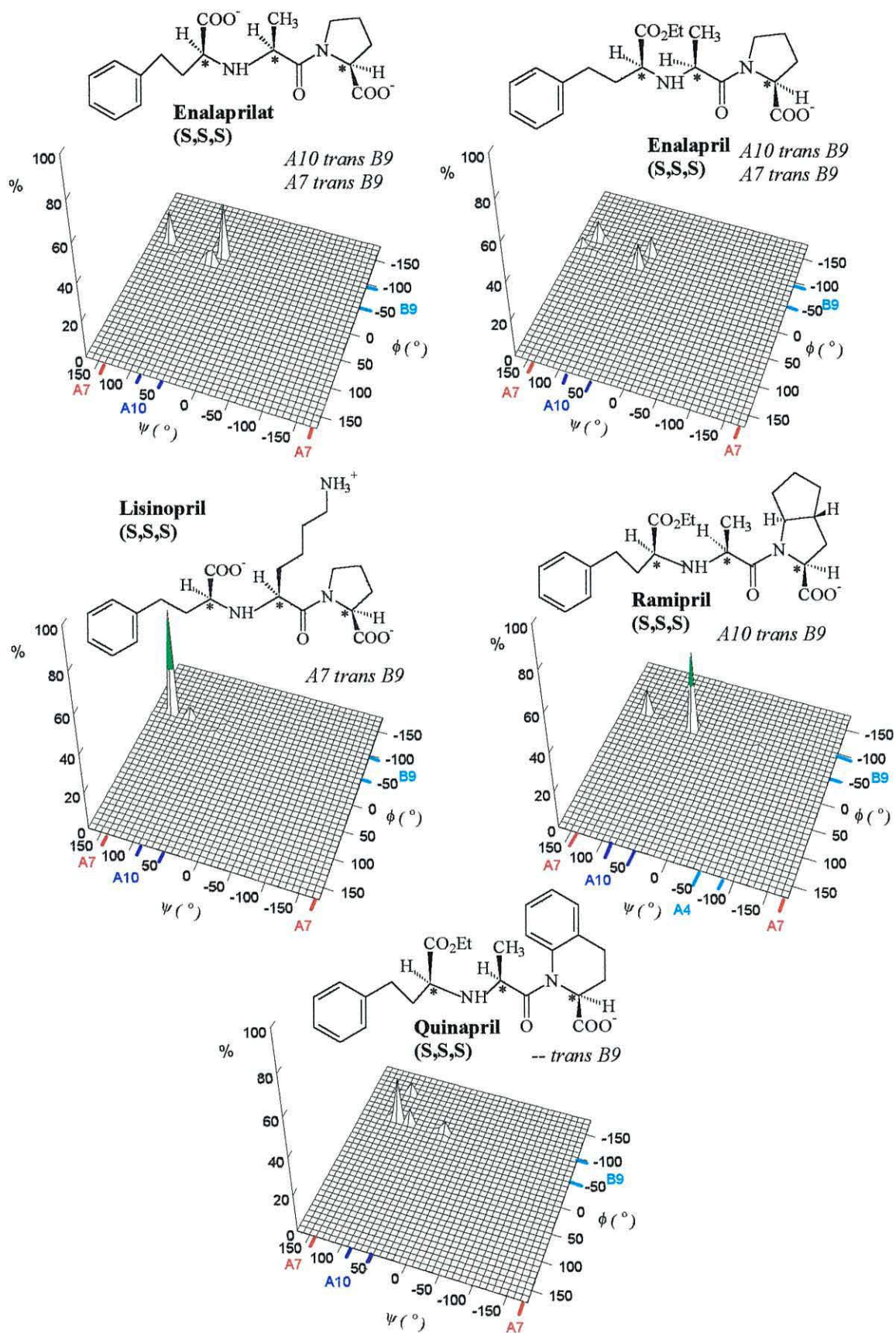


Figure 5-2: 3DPR Plots of ψ vs ϕ vs % Conformers for Enalaprilat, Enalapril, Lisinopril, Ramipril and Quinapril.

5.2.1.9. Quinapril

Quinapril had its *trans* ω conformations outside the +180° to +175° and -180° to -175° range, and as a result, these conformers had ψ (Tor2) angles outside A7 and A10. ϕ (Tor4) angles were mainly in B9 with fewer conformers in B12 (Table 5.1.). These results indicated that quinapril would be a poor Dpp and Tpp substrate as most of its conformers are outside A7 and A10. Fig. 5-2 shows 3DPR plots for Enalaprilat, Enalapril, Lisinopril, Ramipril and Quinapril, illustrating their percentage conformer distribution ranges.

5.2.1.10. Delapril

Delapril had the majority of its conformers with *cis* ω , with ψ (Tor2) angles in A7 and A10, and ϕ (Tor4) angles in B9 or near B2. Delapril would be expected to have poor transport activity as it does not have *trans* ω conformations, and has B2 conformers that are poor substrates for transport (Table 5.1.).

5.2.1.11. Perindopril

This prodrug has a propyl instead of phenethyl side chain attached to the pseudo *N*-terminus, and had *cis* and *trans* ω conformations. The *trans* conformers had ψ (Tor2) angles mainly in A10 with a fewer conformers outside A7, and ϕ (Tor4) angles constrained in B9 (Table 5.1.). As perindopril contains most of its conformers in A10 *trans* B9 MRT, it would be expected to have better Tpp activity than Dpp activity. However, the high percentage of *cis* conformers would make perindopril a poor substrate for transport.

5.2.1.12. Cilazapril

Cilazapril has its dipeptide backbone conformationally constrained by a 7-membered lactam ring fused with a 6-membered ring. All the conformers had ψ (Tor2) angles constrained in A7, with *trans* ω that was outside the defined *trans* MRT. The majority of conformers had ϕ (Tor4) angles outside B9 (Table 5.1.), with a few percentage of conformers in A7 *trans* B9. This may result in cilazapril having some Dpp activity, but it would not be expected to show any Tpp activity as it does not contain any A10B9/A4B9 conformers.

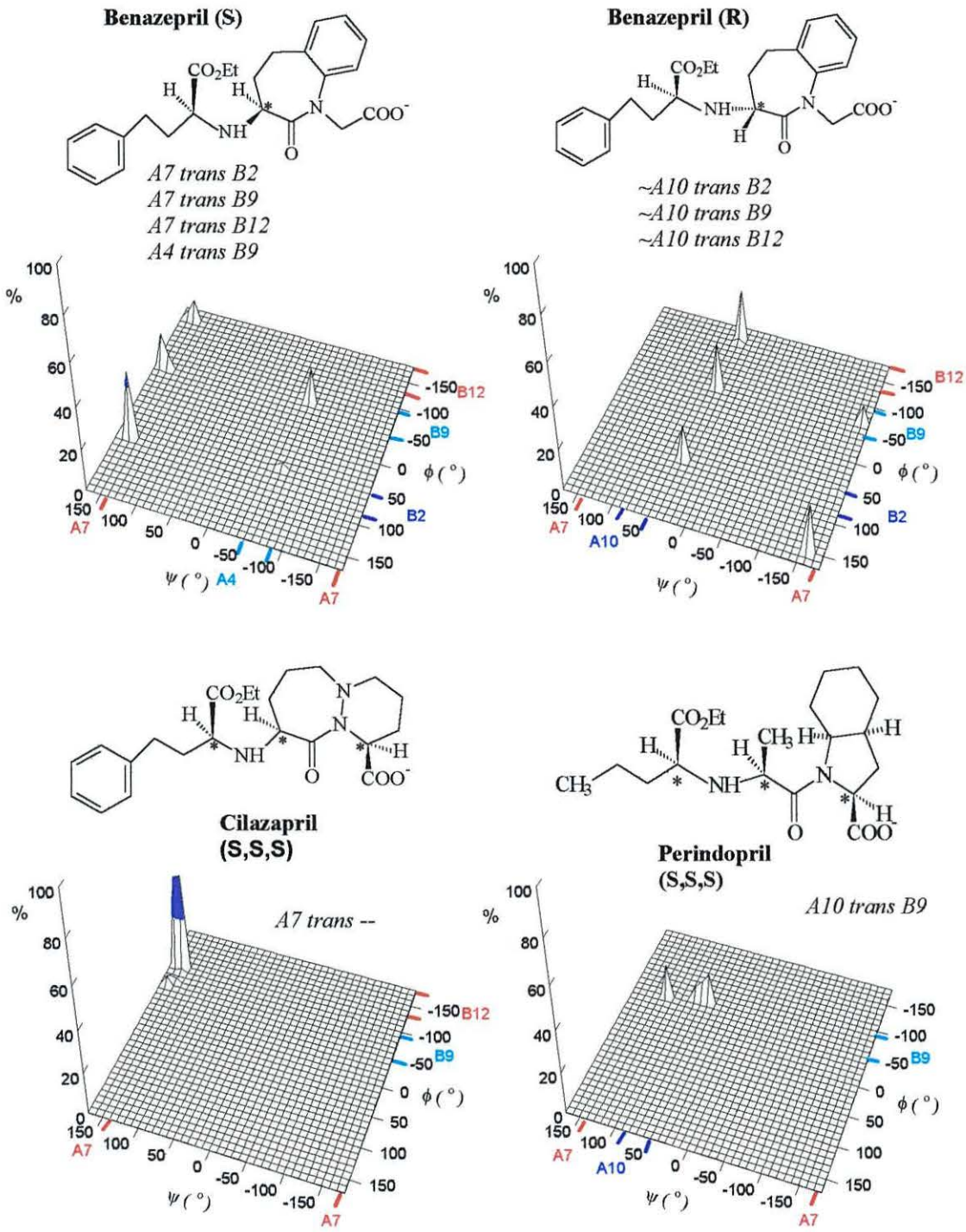


Figure 5-3: 3DPR Plots of ψ vs ϕ vs % Conformers for Benazepril (S), Benazepril (R), Cilazapril and Perindopril.

5.2.1.13. Benazepril (S)

Benazepril has its peptide bond cyclized by a 7-membered lactam ring, with a benzene ring fused at C6 and C7. The pseudo-*N*-terminus was modelled as having S (L) chirality, and this produced conformers in A7, with some in A4, with peptide bonds constrained in or near the *trans* ω conformation (Table 5.1.). In contrast to the other ACE inhibitors modelled, ϕ (Tor4) angles were in B2, B9 and B12. These results show that cyclization of the peptide bond, and the absence of a proline ring, increases the amount of *trans* conformers with their ψ (Tor2) and ϕ (Tor4) angles in the MRT regions. Benazepril (S) would be predicted to be both a Dpp and Tpp substrate, as it has A7 *trans* B9/B12 and A4 *trans* B9 conformers, but the presence of B2 conformers may result in it having poor activity.

5.2.1.14. Benazepril (R)

The chirality of the pseudo-*N*-terminus was altered from S to R, and this caused a significant change in the conformer distribution range. The majority of conformers had ψ (Tor2) angles near A10 or outside the edge of A7, with *trans* ω bonds, and ϕ (Tor4) angles in B9 and B12, like benazepril (S). A decrease in B2 conformers was obtained (Table 5.1.). These results indicate that benazepril (R) would have poor Dpp activity, than benazepril (S) as it does not contain any A7B9/B12 conformers. Benazepril (R) may also have poor Tpp activity as most of its conformers are outside A10B9/B12, in contrast to benazepril (S) which had some A4B9 conformers. Fig. 5-3 shows 3DPR plots for Benazepril (S), Benazepril (R), Cilazapril and Perindopril, illustrating their percentage conformer distribution ranges.

5.2.1.15. MDLa (S)

MDLa has its backbone conformationally constrained by a 7-membered lactam ring fused with a 6-membered ring, with an additional benzene ring fused at position C5 and C6. MDLa with the bridging carbon at S chirality had conformers constrained in or near A4, with *trans* ω , and ϕ (Tor4) angles constrained in or near B9 (Table 5.1.). Based on A4 *trans* B9 backbone torsion angles, MDLa (S) would be expected to have Tpp activity, but not Dpp activity as it does not have any A7B9/B12 conformers.

5.2.1.16. MDLa (R)

Changing the bridging carbon's chirality to R, produced a significant shift in the conformer distribution range. The majority of conformers were in A7, in contrast to MDLa (S) that had mostly A4 conformers, and ϕ (Tor4) angles were in or near B9. All the conformers had *trans* ω outside the $+180^\circ$ to $+175^\circ$ *trans* ω range (Table 5.1.). These results indicate that MDLa with the bridging carbon at R chirality would have some Dpp activity as it has some A7 *trans* B9 conformers, in contrast to MDLa (S), which had mostly A4 *trans* B9 conformers.

5.2.1.17. MDLb (S)

MDLb has a similar structure to MDLa, but the second 6-membered ring contains a sulphur atom at C9. MDLb with the bridging carbon at S chirality had conformers constrained in A7, with a few conformers outside A4, and ϕ (Tor4) angles in B9 or near B12. All the conformers had *trans* ω in or near the defined *trans* ω range. The conformer distribution range for MDLb (S) was similar to MDLa (R), with a small increase in the percentage of A7B9 conformers (Table 5.1.). Like MDLa (R), MDLb (S) would be predicted to have Dpp activity as it has A7B9 conformers, but have poor Tpp activity as it does not contain any Tpp conformers.

5.2.1.18. MDLb (R)

Changing the bridging carbon's chirality to R produced conformers with a similar distribution profile to MDLa (S). The majority of conformers were in A4, in contrast to MDLb (S), with ϕ (Tor4) angles in B9 or near B12. All the conformers had *trans* ω in or outside the defined regions of -180° to -175° (Table 5.1.). MDLb (R) like MDLa (S), would be predicted to show some Tpp activity, but no Dpp activity as it contains mostly A4B9 conformers. Fig. 5-4 shows 3DPR plots for MDLa (S), MDLa (R), MDLb (S), MDLb (R), illustrating the differences in their conformer distribution range based on the chirality of the bridging carbon.

Molecular modelling of MDLa and MDLb compounds has shown how the conformers distribution range can be altered depending on the *stereochemistry* of the bridging carbon similar to the results obtained for conformational analysis of torsionally-constrained dipeptide mimetics in Chapter 4.

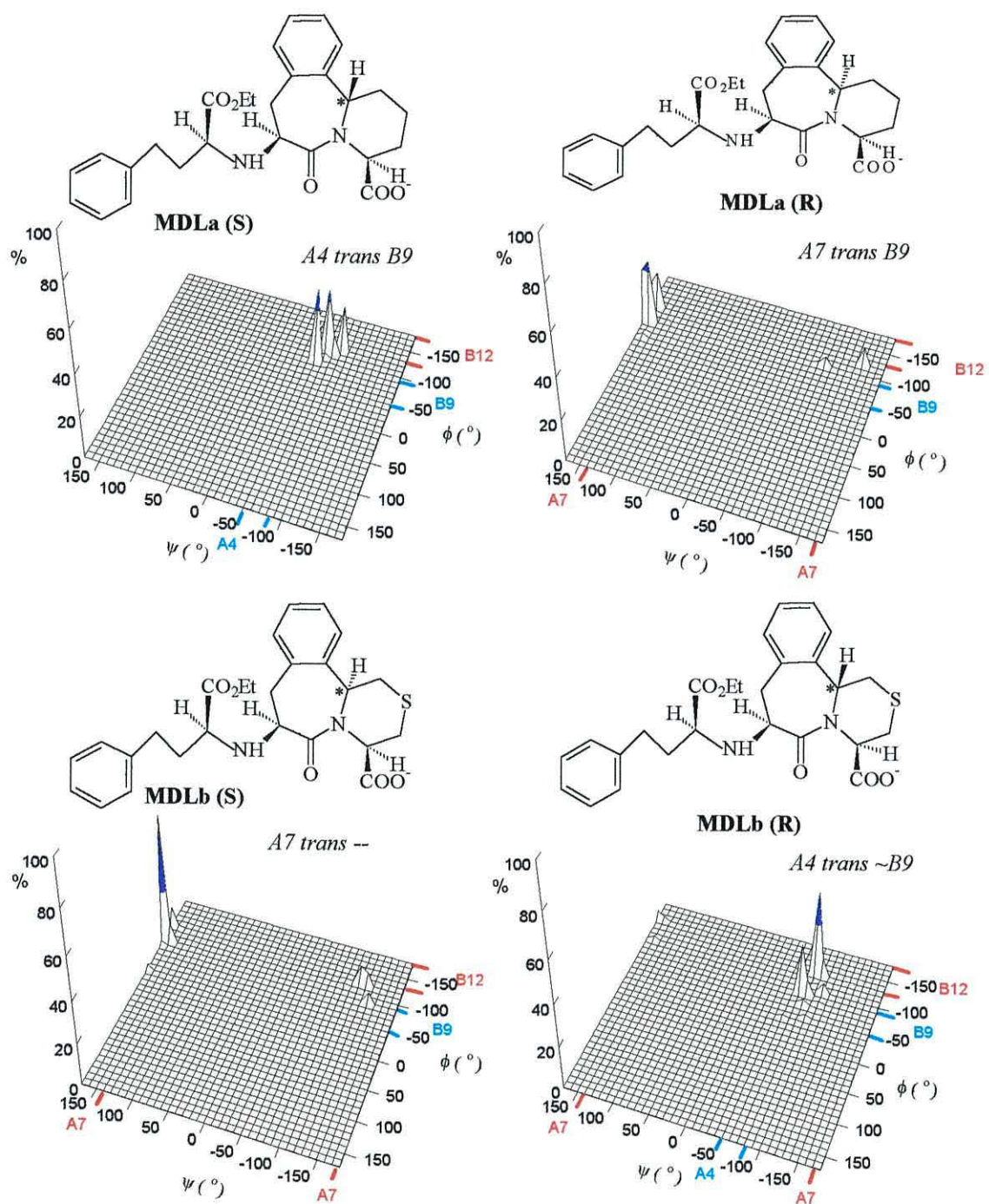


Figure 5-4: 3DPR Plots of ψ vs ϕ vs % Conformers for MDLa (S), MDLa (R), MDLb (S) and MDLb(R).

The results from conformational analysis were used for the initial ranking of ACE inhibitors for their predicted bioavailability, based on their percentage distribution of conformers in A7B9/B12, A4B9/B12 and A10B9/B12 MRTs.

Table 5.2. Ranking of ACE Inhibitors for Their Predicted Bioavailability Based on their Percentage Distribution of Conformers with Acceptable Backbone Torsion Angles.

| ACE Inhibitor | % Dpp Conformers A7B9/B12 | % Tpp Conformers A4B9/B12 & A10B9B12 | Total % of Dpp and Tpp Conformers | Predicted Ranking for Transport |
|----------------|---------------------------|--------------------------------------|-----------------------------------|---------------------------------|
| Captopril | 32 | 5 | 37 | 7 |
| Zofenopril | 19 | 5 | 24 | 11 |
| Spirapril | 14 | 50 | 64 | 2 |
| Enalapril | 16 | 14 | 30 | 10 |
| Ramipril | 0 | 48 | 48 | 5 |
| Quinapril | 0 | 0 | 0 | 15 |
| Delapril | 0 | 7 | 7 | 14 |
| Lisinopril | 56 | 0 | 56 | 3 |
| Perindopril | 0 | 13 | 13 | 12 |
| Cilazapril | 8 | 0 | 8 | 13 |
| Benazepril (S) | 23 | 17 | 40 | 6 |
| Benazepril (R) | 0 | 0 | 0 | 15 |
| MDLa (S) | 0 | 36 | 36 | 8 |
| MDLa (R) | 52 | 0 | 52 | 4 |
| MDLb (S) | 67 | 0 | 67 | 1 |
| MDLb (R) | 0 | 31 | 31 | 9 |

Table 5.2. show that the ACE inhibitors modelled have a very low percentage of conformers with *backbone torsion angles* in the MRTs. This is mainly due to these compound having a high percentage of *cis* ω conformations. In addition, the distortion of the *trans* ω bond from the defined *trans* ω MRT torsion angles of $+180^\circ$ to $+175^\circ$ and -180° to -175° range, has also resulted in some of these ACE inhibitors having their conformers with ψ (Tor2) angles in MRTs of A7, A4 and A10, but ϕ (Tor4) angles outside B9 and B12 templates, and vice versa.

5.2.2. Correlation of Molecular Modelling Data with Activity Data

The results obtained from section 5.2.1. were used to rank a number of ACE inhibitors that were available for experimental work with their predicted ability to bind to DppA based on their percentage distribution of conformers with backbone torsion angles in A7 *trans* B9. It is important to emphasize that this initial prediction screen is using only *backbone torsions*, whilst it is appreciated that additional structural features such as charge and chi-space may be of importance with particular compounds.

Table 5.3. Ranking of ACE Inhibitors for Dpp Activity based on their Percentage Distribution of Conformers in A7B9 MRT.

| ACE Inhibitor | % Dpp Conformers A7B9/B12 | Predicted Ranking for Dpp Activity |
|---------------|---------------------------|------------------------------------|
| Lisinopril | 56 | 1 |
| Captopril | 32 | 2 |
| Enalapril | 16 | 3 |
| Cilazapril | 8 | 4 |
| Quinapril | 0 | 5 |
| Perindopril | 0 | 6 |

The ACE inhibitors in Table 5.3. were tested for their Dpp activity by doing IEF competition assays and radiolabelled, ligand-binding assays, to establish whether a correlation exists between their percentage Dpp conformers and their affinity for binding to DppA.

5.2.2.1. IEF Competition Assay of DppA Binding to ACE Inhibitors

Initial results with IEF of DppA binding to ACE inhibitors did not show a shift in the band position of unliganded DppA to DppA bound with ligand. Therefore, the IEF assay was modified to a competition assay as described (sections 2.4.2. and 3.2.2.). Fig. 5-5 shows an IEF gel of δ -Aminolevulinic acid, Gly-Sar and lisinopril competing with Ala-Phe for binding to DppA. A single band was seen corresponding to the pI of DppA bound to Ala-Phe. No change in band positions were seen with Ala-Phe and δ -aminolevulinic acid at 1:1000 protein:competitor ratio, indicating poor competitor for binding to DppA.

Only a single band corresponding to DppA bound with Ala-Phe was also obtained with Gly-Sar and lisinopril at 1:500 and 1:1071 protein: competitor ratio, respectively, indicating no competition and binding to DppA. Fig. 5-6 shows an IEF gel of δ -Aminolevulinic acid and captopril competing with Ala-Ala for binding to DppA. A single band was seen corresponding to the pI of DppA bound to Ala-Ala, 2 bands were obtained at increasing molar protein: competitor ratios of δ -aminolevulinic acid and captopril competing with Ala-Ala. The top band corresponded to the pI of DppA bound to Ala-Ala, and the second band corresponded to the competitor binding to DppA, but having the same pI as unliganded DppA. At 1:2000 protein:competitor ratio, DppA was approximately 50% bound to the competitor and Ala-Ala. These results showed that δ -Aminolevulinic acid and captopril can act as substrates for DppA but have poor binding affinity.

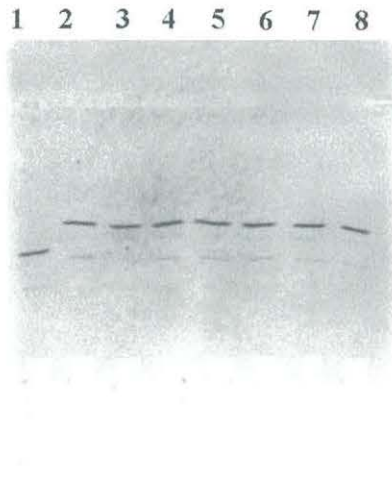


Figure 5-5 : IEF gel of δ -Aminolevulinic Acid, Gly-Sar and Lisinopril Competing with Ala-Phe for Binding to DppA.

Lane 1; RPC-purified DppA; Lane 2; DppA bound to Ala-Phe at 1:1 protein:peptide ratio, pI 5.9; Lane 3; DppA, Ala-Phe and δ -Aminolevulinic Acid at 1:1000 protein:competitor ratio; Lanes 4-5: DppA, Ala-Phe and Gly-Sar at 1:50 and 1:5000 protein:competitor ratio, respectively. Lanes 6-8; DppA, Ala-Phe and Lisinopril at 1:100, 1:500 and 1:1071 protein:competitor ratio, respectively. At the highest molar ratios of protein: competitor, only a single band corresponding to DppA bound to Ala-Phe was obtained, indicating poor competition for binding to DppA.

1 2 3 4 5 6 7 8



Figure 5-6 : IEF gel of δ -Aminolevulinic Acid and Captopril Competing with Ala-Ala for Binding to DppA.

Lane 1; RPC-purified DppA; Lane 2; DppA bound to Ala-Ala at 1:1 protein:peptide ratio; Lane 3-5; DppA, Ala-Ala and δ -Aminolevulinic Acid at 1:500, 1:1000 and 1:2000 protein:competitor ratio, respectively. Lanes 6-8; DppA, Ala-Ala and Captopril at 1:100, 1:500 and 1:2000 protein:competitor ratio, respectively. At the highest molar ratios of 1:2000 protein: competitor, two bands are obtained. The top band corresponds to DppA bound to Ala-Ala, and the second band corresponds to DppA bound to competitor having the same pI value as unliganded-DppA.

5.2.2.2. Competition Filter-Binding Assays of DppA Binding to ACE Inhibitors

Competition filter-binding assays using radiolabelled [14 C]Gly-Sar and [14 C]Gly-Leu were carried out as described (section 2.5.), and importantly these compounds all showed affinity for DppA. This finding endorses the relationship between intestinal, bacterial and other transporters in recognising similar substrates. Furthermore it indicates the potential of using these model bacterial transport proteins to assess the specificity of drugs for oral transport.

Fig. 5-7 and Fig. 5-8 show inhibition binding curves of [14 C]Gly-Sar and [14 C]Gly-Leu dipeptide substrates to purified DppA by a variety of ACE inhibitors, respectively. The values for 50% inhibition of binding by ACE inhibitors were determined by a curve fitting programme. Table 5.4. shows the concentrations of inhibitors required to produce 50% inhibition of binding of radiolabelled [14 C]Gly-Sar and [14 C]Gly-Leu to purified DppA.

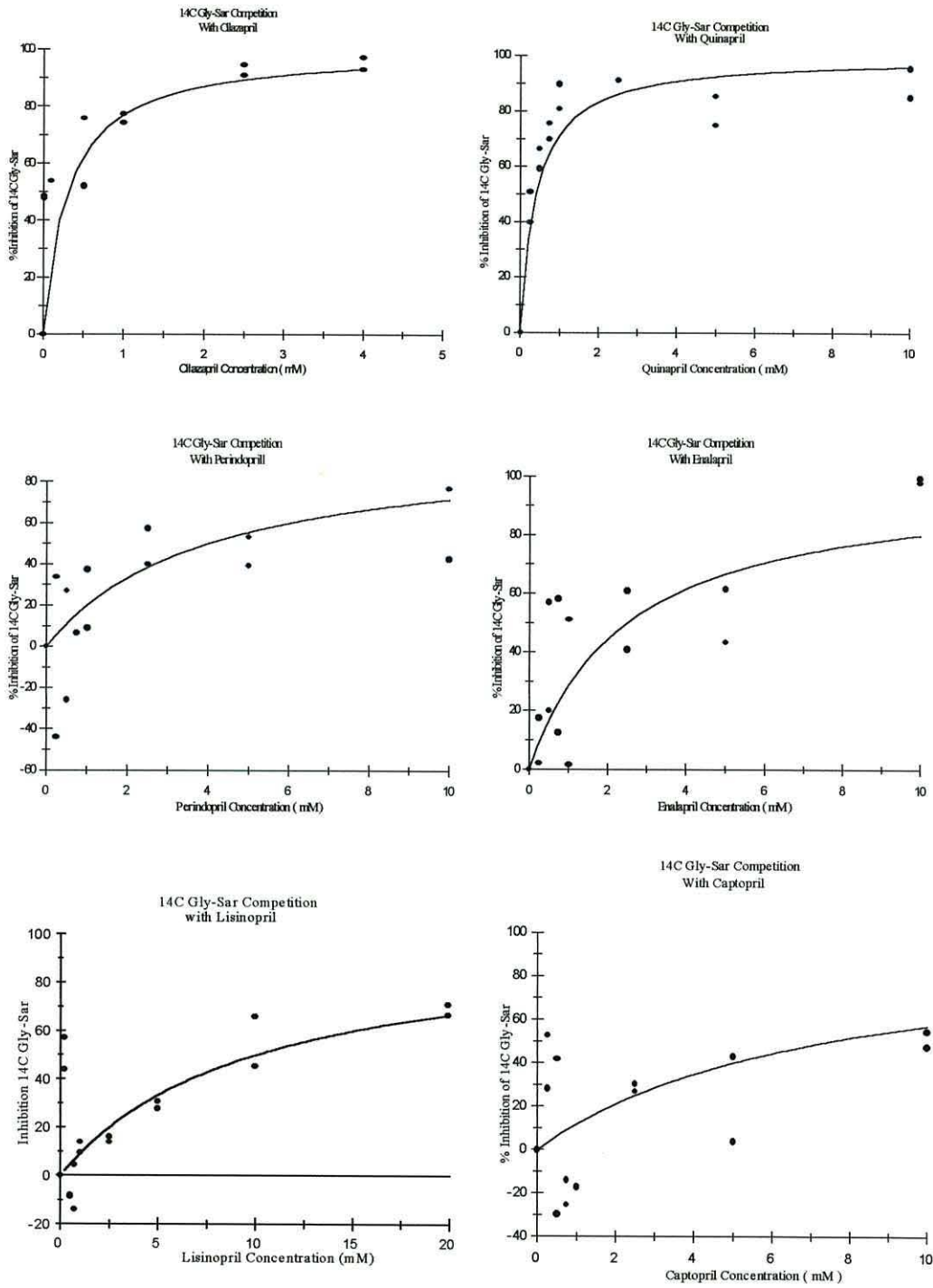


Figure 5-7 : Competition Graphs for the Inhibition of Binding of [14C]GlySar to DppA by ACE Inhibitors Cilazapril, Quinapril, Enalapril, Perindopril, Lisinopril and Captopril.

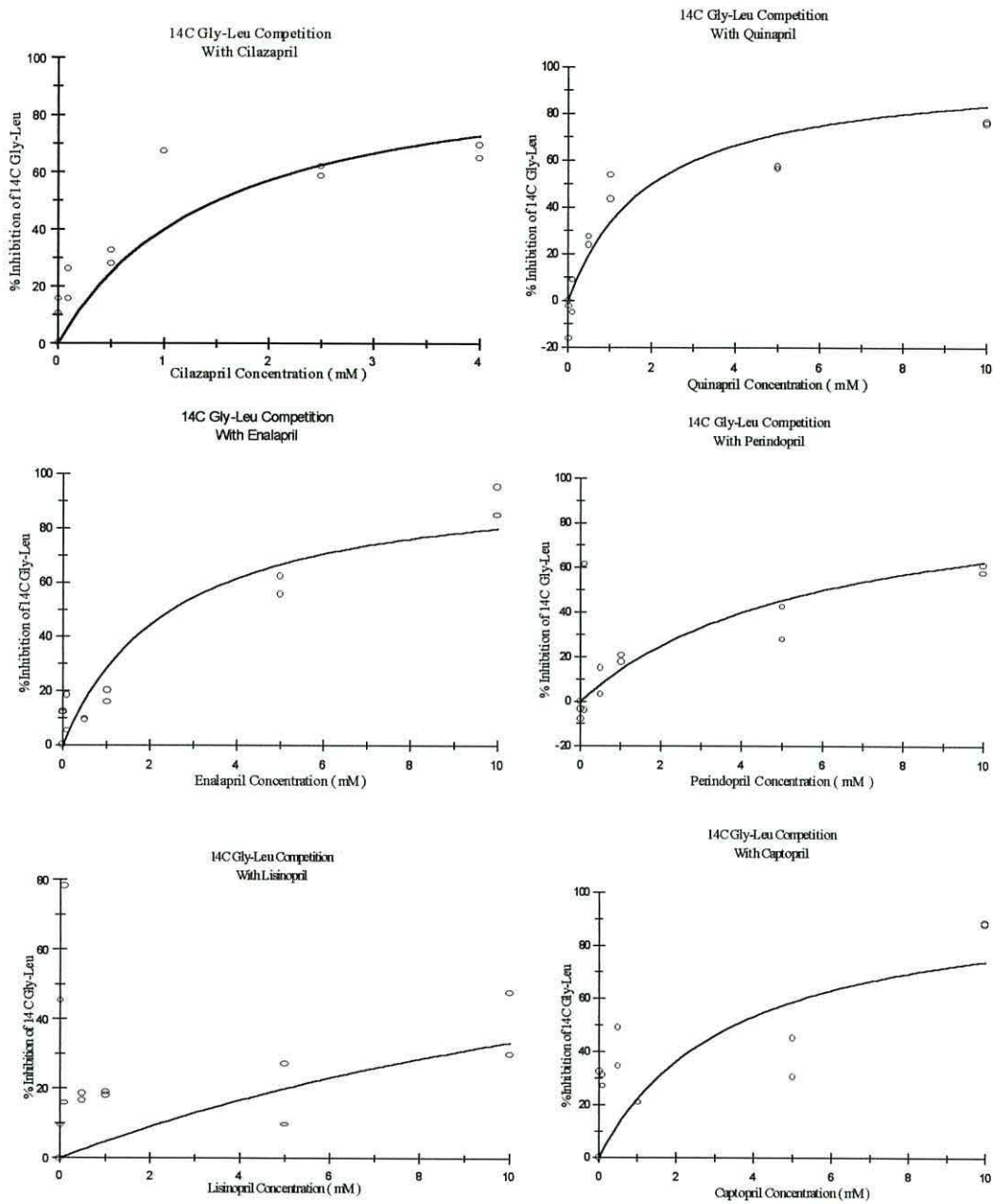


Figure 5-8 : Competition Graphs for the Inhibition of Binding of [14C]GlyLeu to DppA by ACE Inhibitors Cilazapril, Quinapril, Enalapril, Perindopril, Lisinopril and Captopril.

Table 5.4. Concentration of Dipeptide Substrates and Ace Inhibitors Required to Produce 50% Inhibition of Binding of [¹⁴C]Gly-Sar and [¹⁴C] Gly-Leu to Purified DppA.

| Inhibitor | Concentration Range Tested (mM) | 50% Inhibition Concentration [¹⁴ C]Gly-Sar (mM) | 50% Inhibition Concentration [¹⁴ C]Gly-Leu (mM) |
|-----------------------|---------------------------------|---|---|
| Ala-Ala | | | <0.006 |
| Gly-Sar | | | 0.9 |
| δ-Aminolevulinic acid | 0-10 | | 2.6 |
| Cilazapril | 0-5 | 0.3 | 1.5 |
| Quinapril | 0-10 | 0.4 | 2 |
| Enalapril | 0-10 | 2.5 | 2.5 |
| Perindopril | 0-10 | 4 | 6 |
| Captopril | 0-10 | 7.5 | 3.5 |
| Lisinopril | 0-20 | 10 | 20 |

The control substrates Gly-Sar and δ-Aminolevulinic acid, as expected, required a higher concentration to produce 50% inhibition of binding of [¹⁴C]Gly-Sar and [¹⁴C]Gly-Leu, compared with Ala-Ala which had a high affinity for DppA. The ranking of ACE inhibitors for their competitive ability to bind to DppA was similar using either [¹⁴C]Gly-Sar or [¹⁴C] Gly-Leu. Only perindopril and captopril had a different order of ranking, as perindopril was a better competitor than captopril for the inhibition of binding [¹⁴C]Gly-Sar; captopril had a lower 50% inhibition value than perindopril for competing with [¹⁴C] Gly-Leu for binding to DppA.

Cilazapril had best activity for DppA, followed by quinapril, which was not in accordance with the predictions made from backbone torsions derived from modelling studies that indicated these ACE inhibitors would have relatively poor affinity for DppA. Lisinopril was the poorest competitor for DppA compared with all the other ACE inhibitors, which is also against the predictions made from torsional angles that suggested lisinopril would be a good Dpp substrate. Enalapril was a better competitor than captopril, even though the ranking from modelling studies suggested it would have lower activity than captopril (Table 5.3.).

The ranking of ACE inhibitors according to their backbone torsional angles and the activity data obtained from filter binding assays are shown in Table 5.5. The ACE inhibitors showed poor correlation between DppA binding activity and their predicted ranking based on backbone torsion angles. Therefore, further examination of structural features of these compounds was required to seek an explanation for the observed activities.

Table 5.5. Ranking of ACE inhibitors According to Modelling Data and Activity Data.

| ACE Inhibitor | % Dpp Conformers A7B9/B12 | Predicted Ranking for Dpp Activity | Ranking based on Filter Binding Assays |
|---------------|---------------------------|------------------------------------|--|
| Lisinopril | 56 | 1 | 6 |
| Captopril | 32 | 2 | 5 (4) |
| Enalapril | 16 | 3 | 3 |
| Cilazapril | 8 | 4 | 1 |
| Quinapril | 0 | 5 | 2 |
| Perindopril | 0 | 6 | 4 (5) |

5.2.3. Superimposition of Ala-Ala with Minimum Energy Conformers of Cilazapril and Quinapril.

The aim of this study was to determine whether the minimum energy conformers of the ACE inhibitors cilazapril and quinapril would match with the dipeptide Ala-Ala in the A7 *trans* B9 MRT conformation required for binding to DppA. 3DPR plot in Fig. 5-3 showed that cilazapril had 83% conformers with ϕ (Tor4) angles just outside -50° to -95° B9 range, with all ψ (Tor2) angles constrained A7. This initially suggested that the B9 template may require some adjustment i.e. expansion from -95° to -110° , to allow for the high activity seen with the filter binding competition assay. All the conformers had *trans* conformations, however the ω torsion angle was just outside the *trans* range of -175 to -180 for a dipeptide (Table 5.1.). Although cilazapril does not have a true peptide bond and the C-terminus is just outside B9, superimposition with Ala-Ala with ψ (Tor2) of 170° (A7), ω of 180° (*trans*), and ϕ (Tor4) of -95° (far end of B9) gave a very good match with the minimum energy conformer of cilazapril.

3DPR plot of quinapril in Fig. 5-2 showed that it had 42% of its conformers with ψ (Tor2) angles outside A7 and A10, but with ϕ (Tor4) angles constrained in B9. All the conformers had *cis* or *trans* conformations, with an ω torsion angle of -164° , which is $\sim 25^\circ$ outside $+180^\circ$ to -180° *trans* ω MRT (see Table 5.1.). Superimposition with Ala-Ala with ψ (Tor2) of 140° (A7), ω of 180° (*trans*) and ψ (Tor4) of -95° (far end of B9) with the third minimum energy conformer of quinapril gave a good match. These results showed that even though the torsion values evaluated for ψ (Tor2) and ϕ (Tor4) for quinapril and cilazapril are outside the strict definition of A7 and B9, respectively, the backbone of these molecules still look like and match to the dipeptide MRT of A7 *trans* B9, with the *N*- and *C*-termini being in the right orientation to bind to the protein. It seems that even though the ω angle is distorted from a true *trans*, quinapril and cilazapril maintains their *N-C* distance by slight modification in their ψ (Tor2) and ϕ (Tor4) angles, respectively, allowing them to be recognised by DppA.

5.3. DISCUSSION

5.3.1. Molecular Modelling of ACE Inhibitors

Conformational analysis using Random search in SYBYL has been used to evaluate the MRTs required for recognition of substrates by peptide transporters (Grail & Payne, 2000). These have been defined by sets of torsion angles for psi (ψ), omega (ω) and phi (ϕ) corresponding to the backbone of peptide substrates (Chapter 3) (Payne *et al.*, 2000). As ACE inhibitors have a dipeptide-backbone, molecular modelling was used to determine the *backbone* torsion angles of a variety of ACE inhibitors. Results from this study have shown that the majority of the ACE inhibitors have a large percentage of conformers with ψ (Tor2) angles outside the (strictly) defined MRT of A7, A4 and A10, with ϕ (Tor4) angles in or near B9. Compounds that were analogues of Ala-Pro had a large percentage of *cis* ω bonds due to the proline ring at the C-terminus. Pharmacological disadvantages have been associated with captopril, enalapril and lisinopril due to their existence as mixtures of *cis* and *trans* isomers (Cleland, 1993). Structurally modified forms of ACE inhibitors incorporating conformational constraints, such as lactam rings and bicyclic units, have been prepared in order to obtain the biologically active *trans* isomers (Hassall *et al.*, 1982; Attwood *et al.*, 1984; Weller *et al.*, 1984; Thorsett *et al.*, 1986). Molecular modelling of these conformationally constrained ACE inhibitors, showed that the ω bond was constrained in a *trans* conformation. However, the distortion of the *trans* ω torsion angles from $+180^\circ$ to $+175^\circ$ and -180° to -175° MRT range resulted in most of these ACE inhibitors having their conformers with ψ (Tor2) or ϕ (Tor4) angles outside the MRT.

Swaan and Tukker (1997) have also used computer-aided conformational analysis to characterise a pharmacophore for an intestinal peptide carrier. In contrast to this study, they used Systematic search in SYBYL with a set of torsional angles corresponding to the *side-chains* of ACE inhibitors, with ψ fixed at 130° (Swann & Tukker, 1997). Therefore their results do not provide an adequate comparison of torsion angles obtained from molecular modelling of ACE inhibitors in this study.

5.3.2. Correlation of Molecular Modelling Data with Activity Data

Conformational analysis of lisinopril showed that it had the majority of its conformers in A7 *trans* B9 and fewer conformers in A10 *trans* B9. Based on these *backbone torsion* angles, lisinopril was predicted to have the highest activity for binding to DppA, but filter binding results showed that it had the poorest competitive ability compared with the ACE inhibitors tested. The poor binding of lisinopril to DppA may be explained by its negatively-charged, carboxylate group near the pseudo-*N*-terminus, which may interfere with the binding of the NH group to the negatively-charged Asp⁴⁰⁸ residue of DppA.

The structure of lisinopril is similar to enalaprilat, which also contains a carboxylate group that is thought to interfere with transport. Unlike enalaprilat, lisinopril does not require esterification for oral absorption and, therefore, it must be able to overcome the problem of a large negative charge near the pseudo-*N*-terminus. Theoretically, this may involve either the carboxyl group interacting with the NH group, with the epsilon amino group of the lysine side chain substituting for the *N*-terminus or, the epsilon amino group of the lysine interacting with the carboxylate neutralising the negative charge, and thereby enabling the NH group to interact with the protein. To explore these possibilities the relevant lisinopril conformers were studied.

All A7 *trans* B9 conformations were examined for the chi space distribution of the lysine side chain and this showed that the overwhelming majority of the conformers did not adopt an orientation in which the epsilon amino group neutralises the negative charge of the carboxylate. This finding provides an explanation for the low binding affinity seen with the competition assay. Initially, based on the fact that 56% of its conformers were A7 *trans* B9, lisinopril seemed like a good substrate for Dpp however, the presence of a charged carboxylic group and the requirement for the correct orientation of the lysine side chain, reduced its active conformers to 6%, which is compatible with its poor activity in the filter binding assay. Clinically lisinopril is reported to have good oral activity, which can be related to these few effective percentage of conformers. These active conformers would be expected to be substrates for Dpp, as for e.g. the chi, (*trans*) isomers of *N*-terminal Asp-X peptides (Chapter 3).

Swann *et al.* (1995) have also investigated the affinity of the structurally related ACE-inhibitors enalapril, enalaprilat and lisinopril for the intestinal peptide carrier system *in vitro*, using rat intestinal tissue. The affinity of these compounds was evaluated based on their ability to competitively inhibit the transport rate of cephalexin, which is absorbed by intestinal peptide carriers. They found the inhibition constants (K_i) of enalapril, enalaprilat and lisinopril to be 0.15, 0.28 and 0.39mM, respectively (Swann *et al.*, 1995). This would give the same ranking of activity of these ACE inhibitors as found in this study, with enalapril having a higher activity than lisinopril.

Captopril was predicted to have the second highest activity for DppA and its structure is similar to Ala-Pro but the *N*-terminus is replaced by a SH group. Molecular modelling studies showed that captopril had 32% conformers in A7B9, with *cis* and *trans* ω bond angles matching a dipeptide. Hu and Amidon (1988) have shown that the intestinal permeability of captopril is both pH and concentration-dependent and is decreased by co-perfusion with 2,4-dinitrophenol, cephadrine, or di- and tripeptides. This finding was the first demonstration that a peptide carrier may be involved in the transport of ACE inhibitors and supported the idea that the peptide carrier can transport a substrate without an *N*-terminal nitrogen atom (Hu & Amidon, 1988).

In this study captopril was shown to have poor activity for binding to DppA. Compared with certain other ACE inhibitors, captopril does not have problems with side chain carboxyl group or chi space, but it does lack a comparably-positively charged *N*-terminus that is required to bind to the negatively-charged Asp⁴⁰⁸ residue in the DppA. Given its lower pK, a much smaller proportion of the SH terminus will be protonated compared with an NH₂. This may explain its low activity seen in the filter binding assays, as the theoretical 32% A7 *trans* B9 conformers may only show an activity corresponding to ~10% of efficiently recognised conformers.

Enalapril was predicted to have a lower binding affinity than lisinopril and captopril, as it had less percentage of Dpp conformers than these ACE inhibitors.

However, in the filter binding assays it showed higher activity than captopril, which may be due to the fact it has a pseudo-*N*-terminus, unlike captopril, therefore it can bind more efficiently to the protein. In addition, enalapril does not contain the carboxylate group found in lisinopril, which results in it having greater activity than lisinopril, even though lisinopril has a larger number of A7 *trans* B9 conformers. The phenylethylester side chain attached to the *N*-terminus of enalapril has to be in a right chi space in order to bind to the protein, this may explain its overall low binding activity.

The higher activity of enalapril than lisinopril seen in the radioligand filter binding assays is also supported by Thwaites and co-workers study. They investigated the role of proton-linked solute transport in the absorption of captopril, enalapril and lisinopril in human intestinal epithelial (Caco-2) cell monolayers. The inhibitory effects of enalapril and captopril on pH-dependent [¹⁴C]Gly-Sar transport, suggested that these two ACE inhibitors share the H⁺-coupled mechanism involved in dipeptide transport (Thwaites *et al.*, 1995). The absence of pH-dependent [¹⁴C]lisinopril transport, the relatively small inhibitory effect on [¹⁴C]Gly-Sar transport and the absence of lisinopril-induced pH changes, all suggested that lisinopril is a poor substrate for the di/tripeptide carrier in Caco-2 cells. These observations were consistent with the greater oral availability and time-dependent absorption profile of enalapril and captopril, compared with lisinopril (Thwaites *et al.*, 1995).

Cilazapril had the best DppA activity compared with other ACE inhibitors for binding to DppA, followed by quinapril. The results from superimposition with Ala-Ala showed that even though the torsion values evaluated for ψ (Tor2) and ϕ (Tor4) for quinapril and cilazapril are outside the strict definition of A7 and B9, respectively, the backbone of these molecules still look like and match to the dipeptide MRT of A7 *trans* B9, with the *N*- and *C*-terminus being in the right orientation and distance to bind to the protein. It seems that even though the ω bond angle is distorted from a true *trans* ω , quinapril and cilazapril maintains their *N-C* distance by slight modification in their ψ (Tor2) and ϕ (Tor4) angles, respectively, in order to be recognised and transported by Dpp.

Cilazapril has a torsionally-constrained mimetic structure and nearly all of its conformers are constrained with ψ (Tor2) angles in A7 and ϕ (Tor4) angles in B9. In theory Cilazapril has ~100% Dpp conformers, but as it is not a true dipeptide due to cyclization around the peptide backbone it has lower binding affinity for DppA compared with natural dipeptide substrates such as Ala-Ala.

Perindopril was predicted to be a poor substrate for Dpp, since most of its conformer distribution was in A10 *trans* B9, but results from filter binding assays indicated it must have some conformers which can act as Dpp substrates. 3DPR plot showed that perindopril had some conformers 20° outside A7. Superimposition with Ala-Ala in A7 *trans* B9 conformation showed that the second minimum energy conformer may act like a Dpp substrate, even though it is outside A7. As with the other ACE inhibitors that are outside A7B9, it seems that they can act as Dpp substrates by maintaining the *N-C* distance required to bind to active site residues of the protein. However they have poor activity as they are outside the strict MRT regions, with distortion in their ω bond angles.

5.3.3. Prospects for Improving the Design of ACE Inhibitors

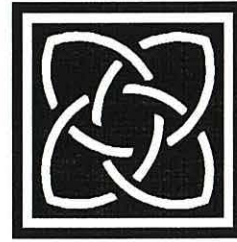
Studies in various *in vitro* and *in vivo* models to determine the uptake of peptidomimetic-type drugs such as ACE inhibitors, have used radiolabelled Gly-Sar as peptidase-resistant substrates for intestinal and renal peptide transporters. The uptake of other compounds is determined by their ability to compete with these substrates, however molecular modelling studies and transport assays in our laboratory have shown that Gly-Sar is a poor substrate for DppA and cannot be recognised by Tpp (unpublished results). Therefore, even poor peptidomimetic-type substrates designed for transport by intestinal transporters will show good activity based on their ability to compete with Gly-Sar. This can lead to anomalies than can occur between predicted oral uptake of certain compounds based on competition with Gly-Sar, and results of other direct measures of uptake (Yang *et al.*, 1999). In this study, filter binding assays were done to determine the DppA-binding activity of ACE inhibitors by using [¹⁴C]Gly-Sar and [¹⁴C]Gly-Leu. These dipeptides are poor substrates for DppA, making it easier to detect competition.

The results obtained in this study have provided further insight into additional features that are required for recognition and transport, including chi-space torsional angles of side chains of ACE inhibitors, particularly when they are charged, and the importance of a charged *N*-terminus. These features have further refined the MRTs for effective transport and delivery of peptide-based drugs.

It has always been stressed in considering MRTs, that although ψ , ω and ϕ angles allow a good primary screen, it is always necessary to consider a range of other structural and charged features, such as those above, before reaching a final conclusion on how well a putative substrate will match an MRT and be transported (Chapter 3) (Payne *et al.*, 2000). Molecular modelling of ACE inhibitors has shown that reducing the amount of *cis* conformers will increase the percentage of MRT conformers. Proline is usually placed in substrates to avoid hydrolysis of the peptide bond by intestinal peptidases, but studies in our laboratory have shown that *C*-terminal proline residues are poor substrates for transport by Dpp (Payne *et al.*, 2000). This correlation indicates comparable recognition processes for transporters and peptidases.

Most of the ACE inhibitors are analogues of Ala-Pro, replacement of the *C*-terminal proline residue by aliphatic or aromatic side chains, with modifications in their peptide bond, may improve the affinity of these substrates for binding to DppA. In addition, improving the conformation of the ω bond of conformationally-constrained ACE inhibitors, to more closely match the *trans* ω angles seen in natural dipeptide substrates will result in these ACE inhibitors having nearly all of their conformers in the MRT for effective transport.

Molecular modelling of ACE inhibitors has identified structural features required for improvement in their oral delivery. Preliminary studies with filter binding assays have shown that compounds with the best activity for binding to DppA are those that contain the majority of their conformers constrained in or near A7 *trans* B9 MRT (and that satisfy additional criteria, see above), and this validates the use of the MRT for prediction of activity.



CHAPTER 6
THE RATIONAL DESIGN OF
ANGIOTENSIN-CONVERTING ENZYME
(ACE) INHIBITORS

6.1. INTRODUCTION

ACE inhibitors are important therapeutic agents for the treatment of hypertension and cardiovascular diseases. Their rational design has led to the synthesis of a large number of specific and potent compounds that bind to the active site of the enzyme. The molecular model used in their design presumed that there are a relatively small number of specific drug-enzyme interactions important in determining specificity and binding affinity. These include chelation of a catalytic zinc ion, ionic binding to a cationic residue located in the protein and a terminal carboxyl group (Cleland, 1993).

Mercaptoalkanoyl amino acids inhibitors are not cleaved by peptidases and were thought to bind to the active site of ACE in a manner similar to the binding of the terminal dipeptide residue of a substrate, but with an additional strong interaction of the sulphhydryl group with the catalytic important zinc ion of the enzyme. The side chains (R_1 and R_2) of propanoyl and aminoacyl residues of mercaptopropanoyl amino acids were thought to interact with the enzyme in the same way as the side chains of the *N*-terminal and *C*-terminal amino acid residues of a dipeptide (Fig. 6-1) (Cushman *et al.*, 1977; Cheung *et al.*, 1980).

The first orally active ACE inhibitor captopril, was designed to have a sulphhydryl group capable of interacting with the zinc ion and a polar ketone moiety attached to a dipeptide backbone which terminates with a proline residue. The rigid proline ring structure was thought to be an important structural feature determining high affinity binding to ACE. Preclinical results for the use of captopril as an antihypertensive agent were encouraging despite some side-effects associated with the sulphhydryl moiety. Compounds alternative to captopril which possessed a sterically orientated carboxyl group in place of the sulphhydryl moiety, such as enalapril and lisinopril had already been produced by the time clinical studies with captopril were published (Patchett *et al.*, 1980; Cleland, 1993). Potential pharmacological disadvantages associated with captopril, enalapril, and lisinopril were identified in that they existed as mixtures of *cis* and *trans* isomers, of which only the *trans* isomers are thought to be biologically active.

Therefore, conformationally-constrained ACE inhibitors, such as benazepril and cilazapril, containing lactam rings and bicyclic units were synthesised that were incapable of isomerisation during preparation (Attwood *et al.*, 1984; Thorsett *et al.*, 1986; Attwood, 1989). These ACE inhibitors, which are di- and tripeptide mimetics have been designed to interact with the active site of ACE and are shown in Fig. 6-2. Most ACE inhibitors are administered as prodrug esters in order to improve their intestinal membrane solubility, and are dependent on hepatic de-esterification for their activation (Fig. 1-9). Research into new ACE inhibitors has been extensive and there is a clinical need for ACE inhibitors that not only have high affinity for binding to ACE, but also good oral bioavailability (Cleland, 1993).

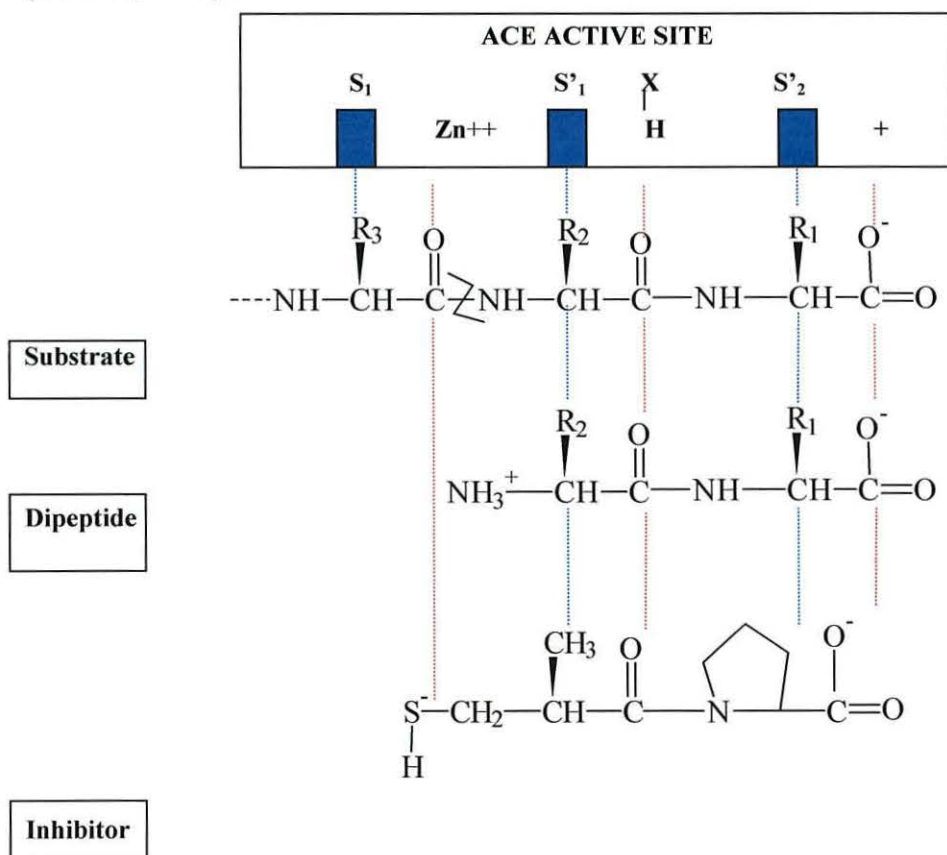


Figure 6-1: A hypothetical model for the proposed binding of substrates, dipeptide products and mercaptoalkanoyl amino acid inhibitors to the active site of angiotensin-converting enzyme.

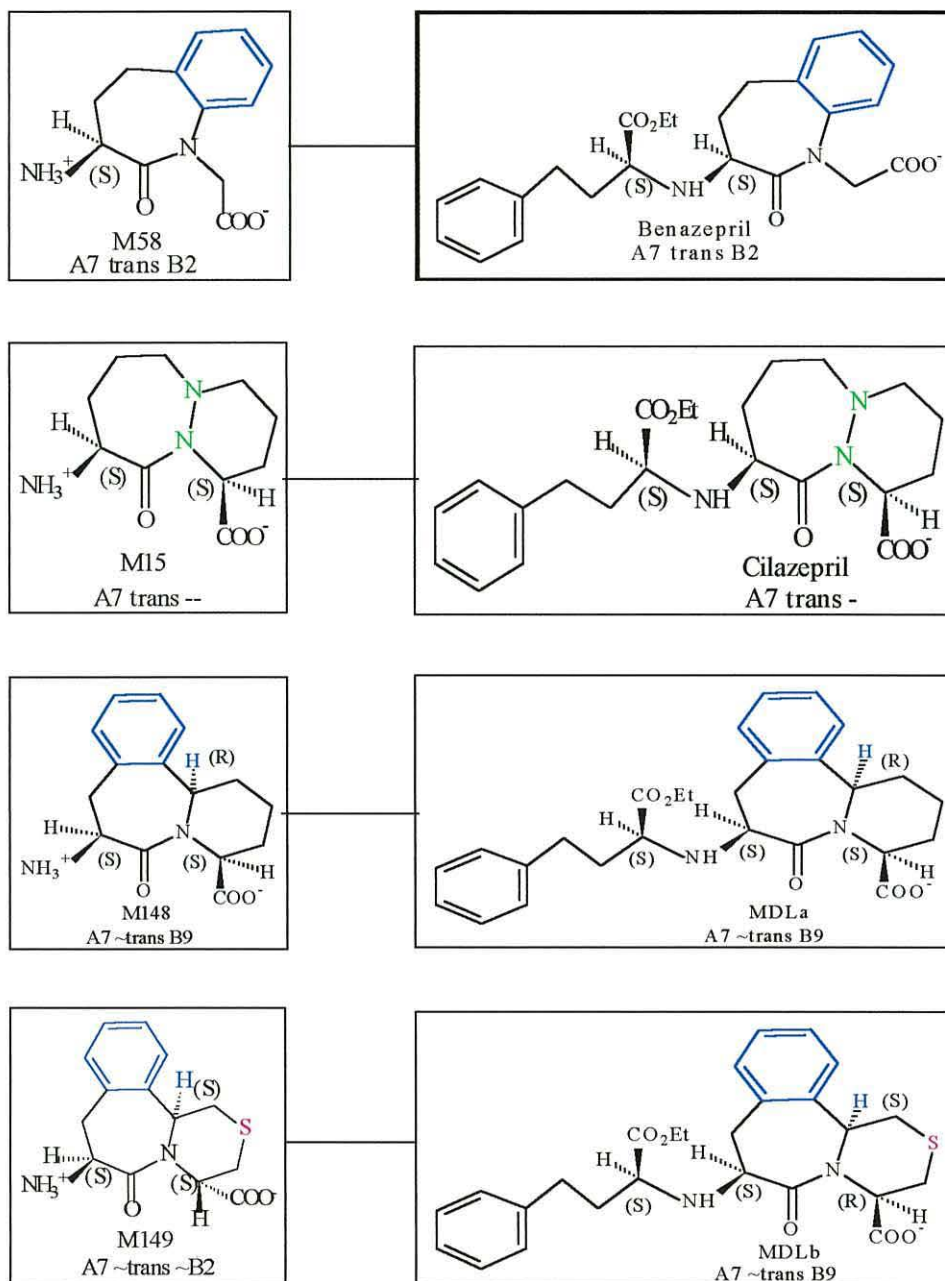


Figure 6-2: Dipeptide Mimetics Incorporated into ACE Inhibitors and their Conformations (Section 4.3. and Section 5.3.)

6.1.1. Aims of Study

Studies on ACE substrate specificity have revealed that the nature of the C-terminal amino acid is the most important determinant for the overall binding of dipeptides to the active site of the enzyme (Cheung *et al.*, 1980). The amino acid Trp was the most effective for enhancing binding to the enzyme, followed by Tyr, Pro and Phe. The dicarboxylic amino acids such as Asp or Glu had poor binding affinity. The most potent dipeptide inhibitor Val-Trp was 10,000 times more inhibitory than the weakest inhibitor Gly-Pro (Cheung *et al.*, 1980). The results from Cheung and co-workers' study correlate well with the substrate affinity for DppA obtained in Chapter 3, where N-terminus aliphatic side chains such as Val, and C-terminus aromatic side chains such as Phe, also showed high affinity for binding to DppA. Gly-Pro was also a poor substrate for DppA, as well as Asp and Glu-containing dipeptides (Payne *et al.*, 2000).

Molecular modelling of ACE inhibitors in Chapter 5 has identified structural features required for improvement in their oral delivery. These include reducing the amount of *cis* ω conformations and replacing the C-terminal Pro residue by aromatic side chains based on the results for substrate affinities of ACE (Cheung *et al.*, 1980). Introduction of peptide bond modifications to avoid proteolysis may produce structurally modified analogues that have a higher percentage of conformers with *backbone torsion angles* in the MRTs, but still retain the structural features required to bind to ACE. The chi-space of these structurally modified analogues with aromatic amino acid side chains will also be considered when assessing their ability to be transported. In Chapter 4, a variety of peptidomimetics were modified, either by introducing different size lactam ring structures or by changing the atom types and stereochemistry, in order to produce analogues that had a high percentage of conformers with *backbone torsion angles* of the MRTs. Knowledge gained from structural modifications of these peptidomimetics will be applied for the *rational* design of conformationally-constrained ACE inhibitors, in order to improve their conformer distribution range to better match the MRTs of peptide transporters. The results from this study will show how molecular modelling can be applied for the *rational* design of ACE inhibitors for improved delivery by intestinal peptide transporters.

6.2. RESULTS

A selection of ACE inhibitors were structurally modified and their conformational and data analysis was carried out as described (sections 2.7.2.3. and 2.7.3.3.).

6.2.1. Changes in the C-Terminus Amino Acid Residue

Table 6.1. shows the results for conformational analysis of ACE inhibitors and their modified analogues based on changes in their C-terminus amino acid residue.

6.2.1.1. Captopril Modifications

In order to decrease the percentage of *cis* conformers of captopril, the C-terminus Pro was changed to a Trp residue and the peptide bond modified to a thioamide (PBM4, Table 4.2.). This produced a greater percentage of *trans* ω conformers with 20% in A4 *trans* B12 MRT (Table 6.1.). Modified captopril would be predicted to have better Tpp activity than captopril as it has a higher percentage of Tpp conformers.

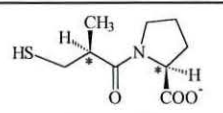

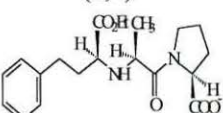
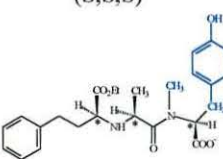
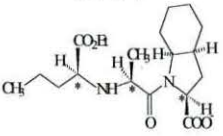
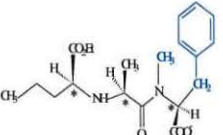
6.2.1.2. Enalapril Modifications

Enalapril also had a large amount of *cis* ω conformers, with a few A7/A10 *trans* B9 conformers. Changing the C-terminal Pro to a Tyr residue and modifying the peptide bond to an *N*-methyamide (PBM1, Table 4.2.), produced an increase in *trans* ω conformers. Nearly all the conformers were constrained in A7 with ϕ (Tor4) angles only 3° outside B12 (Table 6.2.). Modified enalapril would be an exclusively Dpp substrate as it has the majority of its conformers in A7 *trans*-B12 MRT, and would be predicted to have better Dpp activity than enalapril.

6.2.1.3. Perindopril Modifications

Perindopril also had *cis* and *trans* ω conformers, its C-terminus Pro was changed to a Phe residue with an *N*-methyamide peptide bond. This resulted in an increase in *trans* ω conformers with ψ (Tor2) angles in A7 and ϕ (Tor4) angles near B12, as seen with enalapril (Table 6.2.). Modified perindopril would also be predicted to be a good Dpp substrate and have better uptake activity than perindopril. Fig. 6-3 shows 3DPR plots of Captopril, Enalapril and Perindopril and their modified analogues, showing the increase in percentage of conformers in MRTs.

Table 6.1. Minimum Energy Conformers of ACE Inhibitors and their Rationally Designed Analogues Based on Changes in the C-Terminus Amino Acid Residue.

| Structure | Energy kcal/mol | % | ψ° (Tor2) | ω° Omega | ϕ° (Tor4) | NC Å | % Total Range |
|--|--------------------|-------|------------------------|-------------------------|------------------------|---------|----------------------|
|  Captopril (S,S) | 8.95 | 28.78 | 145.7 | -1.3 | -77.2 | 4.40 | 40% A7 <i>c</i> B9 |
| | 9.24 | 18.03 | 148.4 | 179.3 | -76.1 | 5.57 | 32% A7 <i>t</i> B9 |
| | 9.99 | 5.28 | 147.6 | -1.9 | -77.7 | 4.44 | 13% -- <i>t</i> B9 |
|  Modified Captopril (S,S) | 15.14 | 11.54 | -90.1 | 179.6 | -145.3 | 5.25 | 20% A4 <i>t</i> B12 |
| | 15.19 | 10.70 | -78.0 | -179.2 | -148.0 | 5.12 | 20% -- <i>t</i> B12 |
| | 15.52 | 6.21 | -81.6 | -178.9 | -147.7 | 5.14 | 9% A10 <i>t</i> B12 |
|  Enalapril (S,S,S) | 7.3 | 15.55 | 146.0 | -0.6 | -76.8 | 4.34 | 33% A7 <i>c</i> B9 |
| | 7.68 | 8.4 | 60.2 | 178.9 | -48.5 | 5.35 | 16% A7 <i>t</i> B9 |
| | 7.69 | 8.16 | 52.7 | -179.5 | -75.3 | 5.33 | 14% A10 <i>t</i> B9 |
|  Modified Enalapril (S,S,S) | 1.03 | 30.45 | 147.8 | -179.6 | -127.7 | 5.99 | 59% A7 <i>t</i> ~B12 |
| | 1.41 | 16.5 | 147.6 | 178.5 | -126.9 | 5.98 | 10% A7 <i>t</i> B2 |
| | 1.61 | 11.93 | 150.2 | 179.4 | -128.1 | 5.99 | |
|  Perindopril (S,S,S) | 10.63 | 42.09 | 82.7 | -1.0 | -58.2 | 2.80 | 47% A10 <i>c</i> B9 |
| | 11.24 | 15.35 | 123.5 | -179.7 | -55.1 | 5.34 | 15% -- <i>t</i> B9 |
| | 11.33 | 13.41 | 67.8 | -175.8 | -65.3 | 5.33 | 13% A10 <i>t</i> B9 |
|  Modified Perindopril (S,S,S) | 2.95 | 25.61 | 146.3 | 178.8 | -127.2 | 5.98 | 58% A7 <i>t</i> ~B12 |
| | 3.17 | 17.9 | 148.9 | 176.6 | -126.1 | 5.97 | 9% A7 <i>t</i> B2 |
| | 3.48 | 10.85 | 147.1 | 179.8 | -127.4 | 5.98 | 7% A7 <i>t</i> B12 |

-- denotes outside the MRT regions of A7, A4, A10 and B9, B2 and B12 *t* denotes trans omega *c* denotes cis omega
 Dpp substrate Tpp substrate

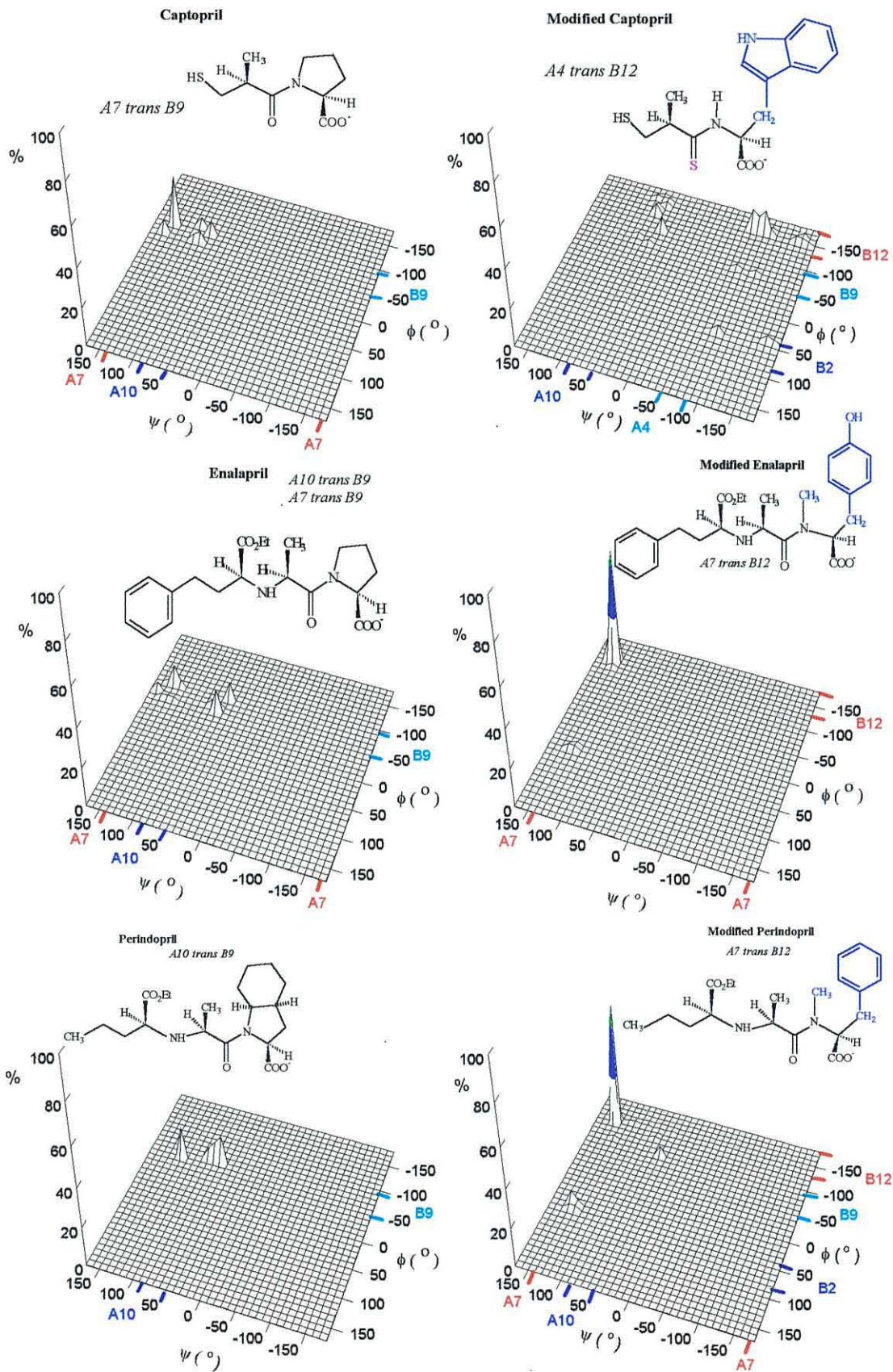


Figure 6-3: 3DPR Plots of ψ vs ϕ vs % Conformers for Captopril, Enalapril, Perindopril and Their Modified Analogues.

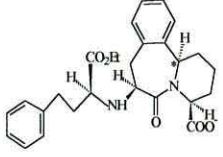
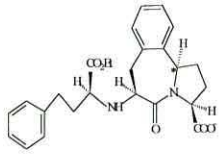
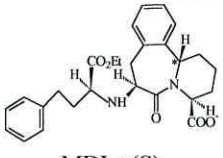
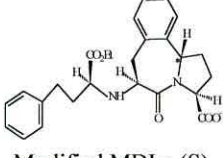

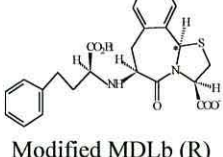
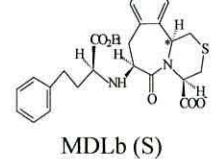
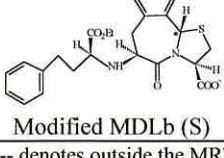
6.2.2. Changes in Mimetic Structure

Results for conformationally-constrained ACE inhibitors and their modified analogues based on changes in their mimetic structures are shown in Table 6.2.

Table 6.2. Minimum Energy Conformers of ACE Inhibitors and their Rationally Designed Analogues Based on Changes in their Dipeptide Mimetic Structure.

| Structure | Energy kcal/mol | % | ψ° (Tor2) | ω° Omega | ϕ° (Tor4) | NC Å | % Total Range |
|------------------------------------|--------------------|-------|------------------------|-------------------------|------------------------|---------|---------------------|
| Benazepril (S) | 5.26 | 19.15 | 157.8 | -174.8 | 73.6 | 5.17 | 34% A7 <i>t</i> B2 |
| | 5.57 | 11.57 | -57.1 | 178.6 | -65.7 | 4.78 | 23% A7 <i>t</i> B9 |
| | 5.86 | 7.15 | 159.3 | -176.8 | -151.9 | 6.14 | 17% A4 <i>t</i> B9 |
| Modified Benazepril (S,S,S) | 19.77 | 21.16 | -58.1 | 159.9 | -25.1 | 4.67 | 29% A7 <i>t</i> B9 |
| | 20.29 | 9.17 | -177.1 | -177.5 | -85.1 | 5.42 | 25% A4 <i>~t</i> -- |
| | 20.37 | 8.05 | -96.4 | -178.3 | -68.8 | 4.87 | 18% A4 <i>~t</i> B9 |
| Quinapril (S,S,S) | 6.76 | 18.18 | 129.7 | 7.6 | -75.7 | 4.07 | 38% -- <i>t</i> B9 |
| | 7.29 | 7.63 | 98.2 | -164.1 | -74.8 | 5.42 | 32% -- <i>c</i> B9 |
| | 7.30 | 7.47 | 115.1 | -164 | -75.5 | 5.42 | 12% A7 <i>c</i> B9 |
| Modified Quinapril (S,S,S) | 11.41 | 33.27 | 167.1 | -178.6 | -84.0 | 5.46 | 99% A7 <i>t</i> B9 |
| | 11.84 | 16.56 | 172.9 | 177.1 | -95.0 | 5.53 | |
| | 11.9 | 14.92 | 168.7 | 178.7 | -94.0 | 5.56 | |
| Cilazapril (S,S,S) | 6.77 | 41.36 | 160.4 | -174.9 | -102.1 | 5.78 | 83% A7 <i>t</i> -- |
| | 7.42 | 14.27 | 154.8 | -172.8 | -103.0 | 5.80 | 8% A7 <i>t</i> B9 |
| | 7.44 | 13.91 | 158.0 | -173.8 | -107.4 | 5.84 | |
| Modified Cilazapril (S) | 13.26 | 30.13 | -57.8 | -171.9 | -47.6 | 4.95 | 32% A4 <i>t</i> B9 |
| | 13.35 | 26.19 | -56.8 | 165 | -61.8 | 4.31 | 30% A4 <i>t</i> ~B9 |
| | 13.8 | 12.52 | -76.2 | -177.3 | -95.3 | 5.03 | 27% A4 <i>t</i> B9 |
| Modified Cilazapril (R) | 12.28 | 25.12 | 178.1 | 175.9 | -100 | 5.54 | 51% A7 <i>t</i> -- |
| | 12.42 | 19.8 | 175.2 | 166.7 | -77.3 | 5.26 | 27% A7 <i>t</i> B9 |
| | 12.94 | 8.54 | 173.8 | -179.2 | -102.3 | 5.65 | 17% A7 <i>t</i> B9 |

Table 6.2. Continued.

| Structure | Energy kcal/mol | % | ψ° (Tor2) | ω° Omega | ϕ° (Tor4) | NC Å | % Total Range |
|--|--------------------|-------|------------------------|-------------------------|------------------------|---------|----------------------|
|  MDLa (R) | 15.98 | 19.95 | 168 | 172.7 | -88 | 5.47 | 52% A7 <i>t</i> B9 |
| | 16.26 | 12.66 | 170 | 171.3 | -113.6 | 5.76 | 26% A7 <i>t</i> -- |
| | 16.30 | 11.9 | 170.8 | 171.3 | -88.9 | 5.47 | 8% -- <i>t</i> -- |
|  Modified MDLa (R) | 11.39 | 52.29 | 165.1 | 177.3 | -82.1 | 5.52 | 93% A7 <i>t</i> B9 |
| | 12.11 | 16.15 | 162.2 | 179.1 | -83.3 | 5.54 | |
| | 12.52 | 8.26 | 166.2 | 178.9 | -84.5 | 5.51 | |
|  MDLa (S) | 14.82 | 34.16 | -57.4 | 173 | -85.8 | 4.52 | 57% A4 <i>t</i> -- |
| | 14.91 | 29.16 | -66 | 179.6 | -106.8 | 4.82 | 36% A4 <i>t</i> B9 |
| | 15.23 | 17.57 | -80 | -175.5 | -110.6 | 5.08 | |
|  Modified MDLa (S) | 11.9 | 47.83 | -51.8 | 176.1 | -44.5 | 4.81 | 48% A4 <i>t</i> ~B9 |
| | 12.75 | 11.9 | -52.2 | 179.1 | -46.7 | 4.86 | 47% A4 <i>t</i> B9 |
| | 13.08 | 7.03 | -49.8 | -178.2 | -51.8 | 4.82 | |
|  MDLb (R) | 12.79 | 37.83 | -71.7 | 178.3 | -122.5 | 4.98 | 45% A4 <i>t</i> -- |
| | 13.14 | 21.42 | -65.3 | -168.2 | -89.7 | 5.05 | 31% A4 ~ <i>t</i> B9 |
| | 13.97 | 5.56 | -80.9 | -178.5 | -123 | 5.16 | 5% -- <i>t</i> B9 |
|  Modified MDLb (R) | 8.27 | 65.34 | 164.8 | 175.9 | -84.6 | 5.52 | 67% A7 <i>t</i> B9 |
| | 9.48 | 9.12 | 172.9 | 172.5 | -46.9 | 5.11 | 12% A7 <i>t</i> ~B9 |
| | 9.75 | 5.92 | 169.3 | 171.2 | -45.8 | 5.15 | 10% A7 <i>t</i> -- |
|  MDLb (S) | 11.66 | 54.18 | 175.3 | 171.2 | -91.3 | 5.45 | 67% A7 <i>t</i> B9 |
| | 12.83 | 8.08 | 168.5 | 174.6 | -90.1 | 5.49 | 14% -- <i>t</i> -- |
| | 13.01 | 6.05 | -120.3 | 179.7 | -113.6 | 5.24 | 9% A7 <i>t</i> -- |
|  Modified MDLb (S) | 9.54 | 18.99 | -50.9 | -177.3 | -49.4 | 4.83 | 42% A4 <i>t</i> ~B9 |
| | 9.57 | 18.32 | -57.3 | -174.7 | -81.9 | 4.83 | 33% A4 <i>t</i> B9 |
| | 9.88 | 11.06 | -50.2 | -178.5 | -47.9 | 4.81 | 13% A4 <i>t</i> -- |

-- denotes outside the MRT regions of A7, A4, A10 and B9, B2 and B12 *t* denotes trans omega *c* denotes cis omega

Dpp substrate Tpp substrate

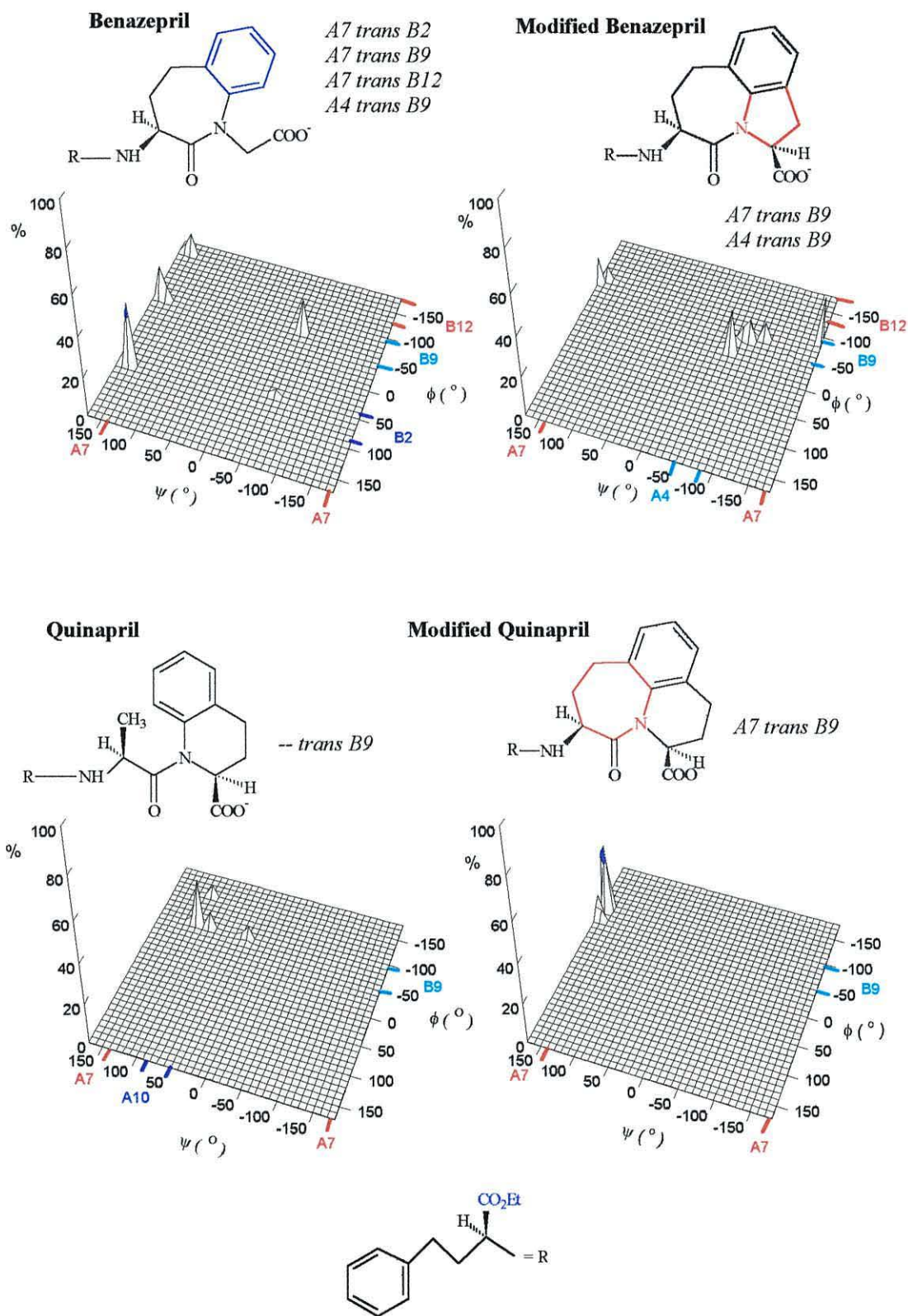


Figure 6-4: 3DPR Plots of ψ vs ϕ vs % Conformers for Benazepril, Quinapril and Their Modified Analogues.

6.2.2.1. Benazepril Modifications

Benazepril had majority of its conformers in A7B2/B9/B12, with *trans* ω bonds, and M58 (Fig. 6-2) as part of its structure. To reduce the amount of inactive B2 conformers, benazepril was modified by fusing the 7-membered lactam ring with a 5-membered ring, to form a torsionally-constrained structure similar to M138 that had all B9 conformers (Table 4.8.). Modified benazepril also had conformers constrained in B9 (Table 6.2.), and based on these results, it would be predicted to have better transport activity than benazepril as it does not have B2 conformers. In addition, it has a slightly higher percentage of A7/A4 *trans* B9 conformers.

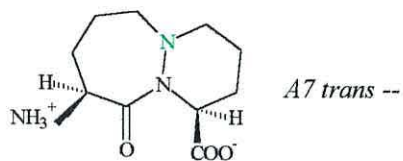
6.2.2.2. Quinapril Modifications

Results from Chapter 5 showed that quinapril had *cis* and *trans* ω peptide bond conformations, with *trans* ω outside the MRT range. The majority of its conformers were outside A7 and A10, with ϕ (Tor4) angles constrained in B9. Quinapril was modified by cyclization with a 7-membered lactam ring from the C α near the pseudo *N*-terminus to amide nitrogen of the peptide bond. This modification formed a torsionally-constrained structure similar to M79 that had all A7 conformers (Table 4.9.). Modified quinapril also had all its conformers constrained in A7B9, with *trans* ω that was in the defined MRT (Table 6.2.). Modified quinapril would be predicted to have better Dpp activity as it has an increase in percentage of Dpp conformers with *trans* ω bonds, compared with quinapril. Fig. 6-4 shows 3DPR plots for benazepril and quinapril and their modified structural analogues showing the differences in their percentage distribution of conformers in the MRT regions.

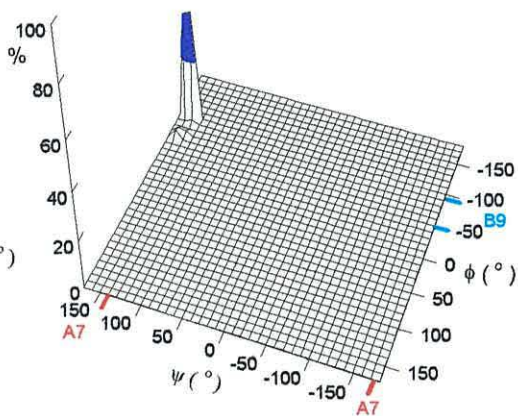
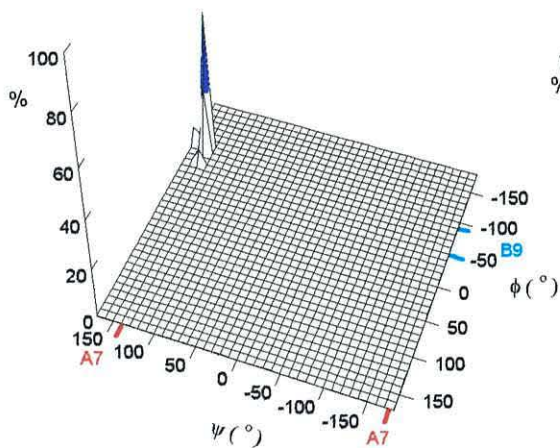
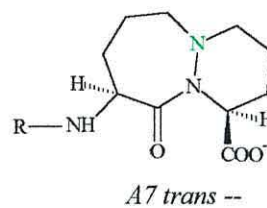
6.2.2.3. Cilazapril Modifications

Cilazapril has its dipeptide backbone conformationally-constrained by M15 (Fig. 6-2). Conformational analysis showed that cilazapril had conformers constrained in A7, with *trans* ω , but outside B9. To change its conformer distribution profile to more closely match the MRTs, the bridging N7 atom was changed to a C atom with S stereochemistry, making the mimetic structure similar to M105 (Table 4.9.). This modification produced conformers with ψ (Tor2) angles constrained in A4, in contrast to cilazapril, and ϕ (Tor4) angles in or near B9.

M15

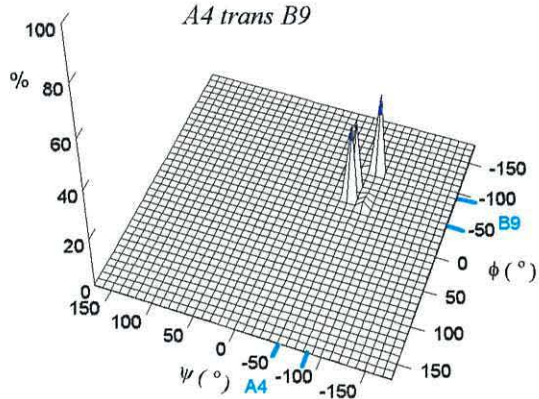


Cilazapril



Modified Cilazapril

(S) * = (S)



Modified Cilazapril

(R) * = (R)

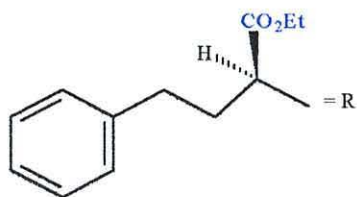
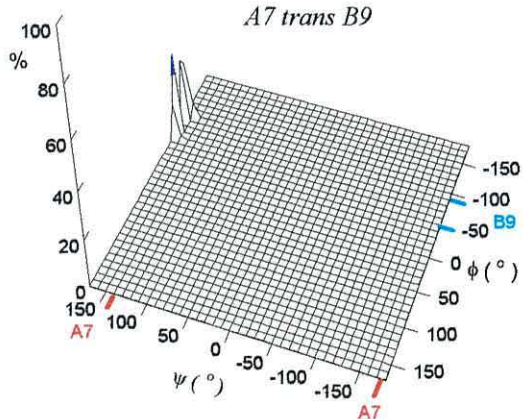
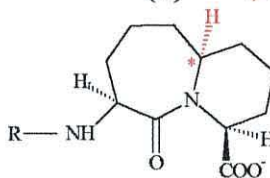


Figure 6-5: 3DPR Plots of ψ vs ϕ vs % Conformers for M15, Cilazapril and its Modified Analogues.

These results show that substitution of the N atom at position 7 of cilazapril with a C atom with S chirality, would make cilazapril an exclusively Tpp substrate as it has nearly all A4 *trans* B9 conformers. Changing the stereochemistry of C7 to R as in M105_1 (Table 4.9.), caused a significant change in the conformer distribution range. All the conformers were constrained in A7, as in cilazapril, with an increase in B9 conformers (Table 6.2.). Modified cilazapril with R chirality at C7, would be predicted to have better Dpp activity as it has a greater percentage of A7 *trans* B9 conformers compared with cilazapril. Fig. 6-5 shows 3DPR plots of M15, cilazapril and modified cilazapril, showing the change in percentage distribution of conformers in MRT regions.

6.2.2.4. MDLa (R) Modifications

MDLa (R) is conformationally-constrained by a 7-membered lactam ring fused to a 6-membered ring, with the bridging C7 at R chirality. It also has a benzene ring fused at C5 and C6 of the 7-membered lactam ring, similar to M148 (Fig. 6-2). MDLa (R) had a large percentage of A7 conformers that were in or outside B9, with *trans* ω bonds. In order to constrain all the conformers in a B9 template, the second 6-membered ring was changed to a 5-membered ring, with the bridging C7 at R chirality, as in M138_1 that had all A7B9 conformers (Table 4.8.). This modification of MDLa (R) also produced conformers that were all constrained in A7 *trans* B9 MRT (Table 6.2.). Modified MDLa (R) would have better Dpp activity as it has a higher percentage of Dpp conformers than MDLa (R).

6.2.2.5. MDLa (S) Modifications

MDLa (S) is like M148_1 (Table 4.9.) and has the bridging C7 at S chirality with the majority of conformers constrained in or near A4 *trans* B9 MRT. As with MDLa (R), the second 6-membered ring was changed to a 5-membered ring, with C7 at S chirality, like M138_2, that had A4B9 conformers (Table 4.8.). This modification in MDLa (S) also produced an increase in A4 *trans* B9 conformers (Table 6.2.). Modified MDLa (S) would be predicted to have better Tpp activity, compared with MDLa (S), as it has a greater percentage of A4 *trans* B9 conformers. Fig. 6-6 shows 3DPR plots for MDLa (S), MDLa (R) and their modified structural analogues, showing the increase in their percentage of conformers in Dpp and Tpp MRTs.

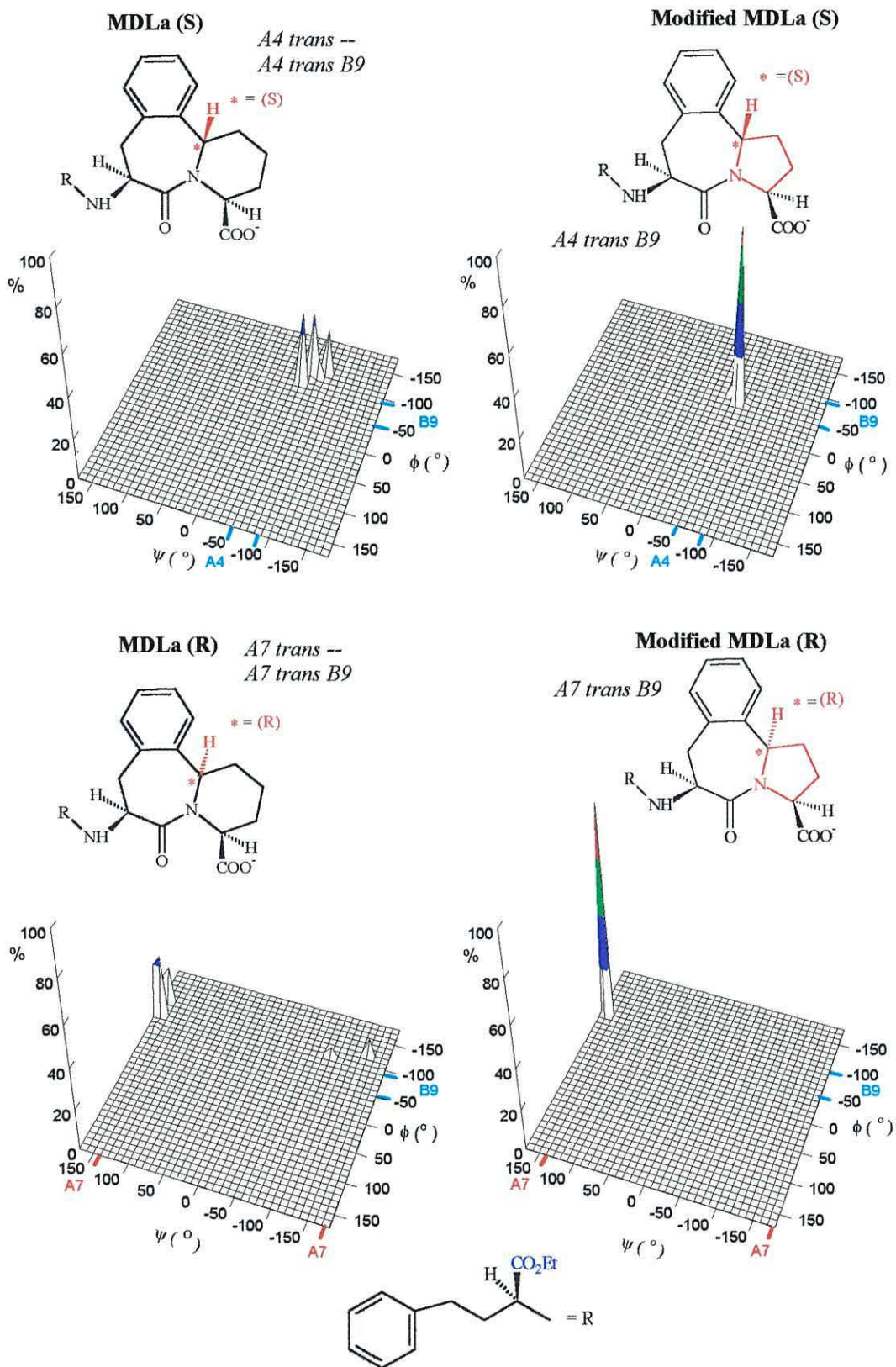


Figure 6-6: 3DPR Plots of ψ vs ϕ vs % Conformers for MDLa and its Modified Analogues.

6.2.2.6. MDLb (R) Modifications

MDLb has a similar structure to MDLa, but the second 6-membered ring contains a sulphur atom at position 9, the bridging C7 and C11 near the C-terminus have R chirality. This ACE inhibitor is similar to M149_1 with C7 at R chirality but C11 at S chirality (Table 4.9.). MDLb (R) had the majority of its conformers in or near A4 *trans* B9. As with MDLa, the second 6-membered ring was changed to a 5-membered ring with a sulphur atom at C8 and this shifted the conformers distribution range to A7 *trans* B9 MRT (Table 6.2.). These results indicate that modified MDLb (R) with a bicyclic unit of a 7-membered lactam ring fused to a sulphur-containing 5-membered ring, with the bridging carbon at R stereochemistry, has its conformer distribution profile changed from a Tpp substrate to a Dpp substrate.

6.2.2.7. MDLb (S) Modifications

MDLb (S) has a similar structure to M149 (Fig. 6-2). The bridging C7 of MDLb at S chirality produced conformer in A7 *trans* B9 or near A7 *trans* B12. As with MDLb (R), the second 6-membered ring was changed to a 5-membered ring with a sulphur atom at C8 and the bridging carbon at S chirality. This produced conformers constrained in A4 *trans* B9 MRT (Table 6.2.). Modified MDLb (S) would be predicted to have better Tpp activity than MDLb (R), as it contains a greater percentage of A4 *trans* B9 conformers.

Modified MDLb (R) would be predicted to have better Dpp activity than MDLb (S), as it has a greater percentage of Dpp conformers. The modifications in the sulphur containing MDLb compounds were based on the results from M4* and M5* that had nearly all A4 *trans* B2 and A7 *trans* B2 conformers (Table 4.8.). Fig. 6-7 shows 3DPR plots for MDLb (S), MDLb (R) and their modified structural analogues, showing the differences in their conformers distribution range in Dpp and Tpp MRT regions.

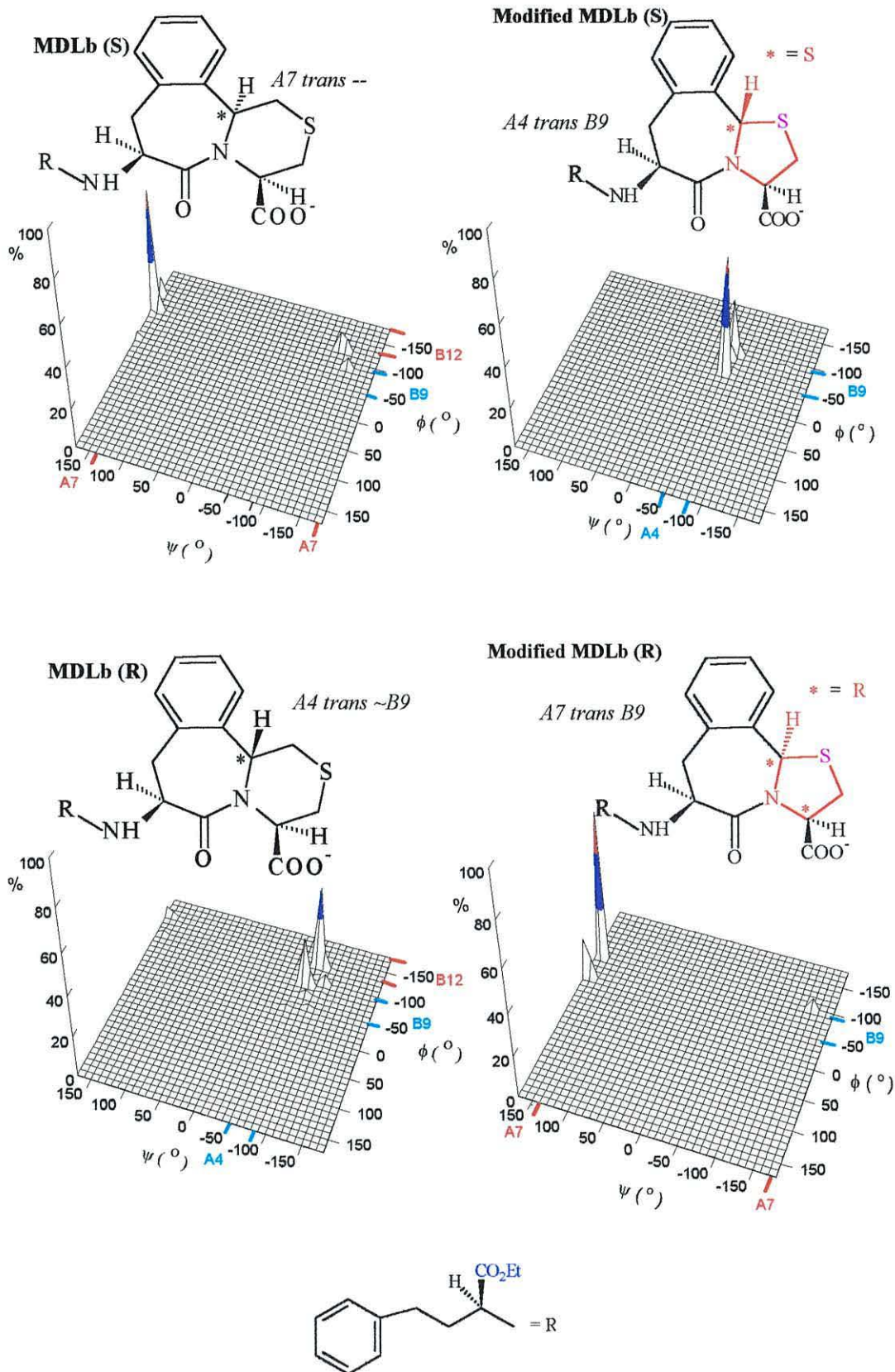


Figure 6-7: 3DPR Plots of ψ vs ϕ vs % Conformers for MDLb and its Modified Analogues.

6.3. DISCUSSION

6.3.1. *The Rational Design of ACE Inhibitors*

ACE inhibitors are important for the treatment of hypertension and cardiovascular diseases. As hypertensives usually have to be taken over extended periods of time, both oral availability and long duration of action are important parameters in the development of new compounds (Cleland, 1993). Captopril was the first orally active sulphhydryl Ala-Pro derivative approved for clinical use, however it has poor activity because of the presence of large amount of *cis* ω conformers caused by the C-terminal proline ring. In order to improve its activity both for oral delivery and for affinity for ACE, the C-terminal proline residue was replaced by a tryptophan side chain, based on Cheung and co-workers' study (Cheung *et al.*, 1980), and also a thioamide peptide bond to avoid proteolysis. This produced an increase in *trans* ω conformers which may result in modified captopril having better bioavailability. However, the chi-space of the bulky aromatic side chain will have to be examined to see if it has the right orientation to fit into the binding pocket of DppA and produce activity.

Patchett and colleagues synthesised over 200 *N*-carboxymethyl-L-alanyl-L-proline derivatives as transition-state inhibitors of ACE. They showed that dicarboxylates such as enalapril, could be effective ACE inhibitors comparable to captopril. This was providing an additional lipophilic group such as a phenalkyl was present to compensate for the difference in zinc complexation capacity of the thiol and carboxylate groups (Patchett *et al.*, 1980). Enalapril also has poor pharmacological activity as it has both *cis* and *trans* isomers, and very few conformers with backbone torsion angles in MRTs for intestinal transport. Enalapril was modified by changing the C-terminus proline to a tyrosine, and modifying the peptide bond to an *N*-methanamide to avoid enzyme hydrolysis. This produced an increase in percentage of conformers with *trans* ω peptide bonds, compared with enalapril, and *backbone torsion* angles of A7B12 of Dpp MRT. Therefore, modified enalapril would be predicted to have better oral activity than enalapril, as it has nearly *all* its conformers in Dpp MRT.

However, even though modified enalapril would be predicted to have nearly all “active” B12 conformers for transport and for binding to ACE, the orientation of the aromatic tyrosine side chain will need to be considered to see if all the conformers can produce activity.

Perindopril also had very few conformers for transport, with a large amount of *cis* conformers. Its C-terminus group was substituted for a phenylalanine side chain, and the peptide bond modified to a *N*-methyamide. As with enalapril, this caused a greater percentage of *trans* conformers of A7B12 required for Dpp activity. Modified perindopril is also designed as a Dpp substrate that will have better transport activity. As with modified enalapril, the orientation of the phenylalanine side chain will also have to be considered to see if all the “active” conformers can produce transport activity.

The activities of benazapril and its ring analogues have been investigated by Thorsett and co-workers (1986). In their study, the alanylproline portion of enalaprilat was replaced by a series of monocyclic lactams containing the required recognition and binding elements. They showed a correlation of the IC₅₀ of these compounds for inhibiting ACE and their psi angles. They defined psi angles from 130° to 170°, which seem to be acceptable to the ACE active site (Thorsett *et al.*, 1986). This is similar to the A7 MRT ψ torsion angles of +140° to -175° required to bind to DppA (Payne *et al.*, 2000). Conformational analysis of benazapril showed that the majority of its ψ (Tor2) angles were in A7 MRT but ϕ (Tor4) angles were in B2, B9 and B12. Benazapril was modified by fusing the 7-membered lactam ring with a 5-membered ring to form a torsionally-constrained structure that had all ϕ (Tor4) angles constrained only in the B9 template. Modified benazepril would be predicted to have better transport activity than benazepril as it does not contain any B2 conformers.

Molecular modelling of quinapril showed it had a large percentage of *cis* conformers, and backbone torsion angles outside the MRTs. Quinapril was modified to form a torsionally-constrained structure consisting of a 7-membered lactam ring fused with a 6-membered ring, with an additional benzene ring fused in the middle. This produced all conformers that matched the Dpp MRT of A7 *trans* B9.

Therefore modified quinapril would be predicted to have better activity as it has all *trans* conformers, and to have improved bioavailability, compared with quinapril. In a similar study to Thorsett *et al.* (1986), Attwood (1989) used bicyclic units that were modified to incorporate a 7-membered instead of a 6-membered ring to bring ψ into the range of accessible conformation of alanylproline. The corresponding IC_{50} results indicated that ψ was closer to that of the active conformations of enalaprilat and captopril, and removal of one of the carbonyls further improved the ACE inhibitory potency, and resulted in the ACE inhibitor cilazaprilat (Attwood, 1989). Conformational analysis of cilazapril, the ester prodrug of cilazaprilat, showed that it had all its conformers constrained in A7, with *trans* ω , and near B9. To change its conformer distribution profile to more closely match the MRTs, the bridging N atom at position 7 of cilazapril was changed to a C atom. C7 at R chirality produced all conformers constrained in A7B9, and therefore modified cilazapril would be predicted to have a higher affinity for ACE and be a better Dpp substrate than cilazapril. Modified cilazapril with C7 at S chirality would be an exclusively Tpp substrate as it has nearly all A4B9 conformers.

The different MRTs profiles obtained for cilazapril, based on the *stereochemistry* of the bridging carbon, are a useful structural feature for transport, since mixed isomers of modified cilazapril can be synthesised that have all their conformers constrained in MRTs for intestinal peptide transporters, and this may allow more effective drug delivery.

The conformationally-restricted MDL compounds were synthesised as a result of a molecular modelling study of the Phe-His-Leu moiety of angiotensin I, and showed picomolar potency as ACE inhibitors (Flynn *et al.*, 1987). Molecular modelling of MDLa (R) showed it had a large percentage of A7 conformers, that are in or outside B9, with *trans* ω . In order to constrain all the conformers in B9 template, the second 6-membered ring was changed to a 5-membered ring, with the bridging C7 at R chirality. This produced all Dpp conformers and therefore, modified MDLa (R) would be predicted to have better oral bioavailability than MDLa (R). MDLa (S) had all its conformers constrained in or near A4 *trans* B9.

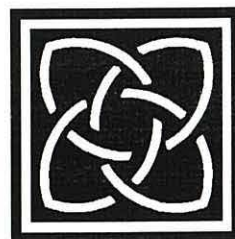
As with MDLa (R), changing the second 6-membered ring to a 5-membered ring, with C7 at S chirality, produced an increase in A4B9 conformers. Therefore modified MDLa (S) would be predicted to have better Tpp activity than MDLa (S). The MDLb compounds have a similar structure to MDLa compounds, but their second 6-membered ring contains a sulphur atom at position 9. MDLb (R) had conformers in or near A4B9 or outside A4B12. Modification in its second ring structure to a 5-membered ring with a sulphur atom produced a change in its conformer distribution profile from a Tpp substrate to a Dpp substrate. MDLb (S) had its conformer distribution profile changed from a Dpp substrate to a Tpp substrate. Therefore both these modified MDLb compounds would be predicted to have better bioavailability than the generic MDLb compounds.

6.3.2 Future Prospects

Systematic changes in chemical structure of a variety of dipeptide mimetics (Chapter 4) provided identification of structural motifs that could produce conformer profiles to match the MRTs' *backbone torsion angles* for substrate recognition and transport by intestinal peptide transporters. By applying the knowledge gained from molecular modelling of dipeptide mimetics, this study has shown how the *rational* design of some ACE inhibitors can be improved for effective oral delivery. Future studies would involve the chemical synthesis of these rationally designed structural analogues in order to determine their predicted activity.


This study has also shown that substrates that can be designed to bind to a transporter such as DppA, may also be predicted to show activity for a peptidase such as ACE. The computed backbone psi angles of 130° to 170° for conformationally-constrained compounds that seem to be acceptable to the ACE active site, are similar to the A7 MRT ψ torsion angles of +140° to -175° required to bind to DppA. Although the phi angles have not been computed for these inhibitors, it would be reasonable to assume that ACE may recognise the ϕ B9 template of DppA. This is based on the fact that proline has been shown to have high binding affinity for ACE and has its phi angle constrained in B9.

In addition, cilazapril had nearly all of its conformers near A7B9, and has been shown to have good binding affinity for DppA, compared with all the ACE inhibitors (Chapter 5). Studies by Cheung and colleagues (1980) on substrate affinity of ACE have also shown that C-terminal aromatic residues such as tryptophan tyrosine, proline and phenylalanine are the most effective for enhancing binding to the enzyme (Cheung *et al.*, 1980). Molecular modelling of dipeptides in Chapter 3 has shown that these C-terminal aromatic amino acids produce a high percentage of B12 conformers. Therefore, it may be reasonable to assume that as ACE has a high affinity for these C-terminal dipeptide inhibitors, it may also recognise the B12 conformation of DppA. This further provides evidence that the MRTs established for the peptide transporters may be applied for the design of substrates of peptidases for therapeutic use.



CHAPTER 7
CONFORMATIONAL ANALYSIS OF
NATURAL ANTIMICROBIAL
SMUGGLINS

7.1. INTRODUCTION



There is a growing demand on pharmaceutical industries to develop antibiotic agents that can not only overcome the problem of resistance, developed by infectious organisms, but also have improved pharmacokinetic properties. A range of natural dipeptide smugglins has been isolated and characterised (section 1.5.1.). These compounds generally consist of a transport moiety, which may be one or more L-amino acids at either the *N*-or *C*-terminus, and a warhead moiety, linked by a peptidase-labile bond (Fig. 1-3).

The aims of this study are to perform conformational analysis of representative antimicrobial compounds, and to investigate the extent to which their conformer distribution range is in the MRT regions identified for transport by the peptide permeases. The *backbone torsion angles* of these prodrugs will be determined, and the charge and chi-space of their amino acid side chains will also be considered when assessing their ability to be transported. As well as modelling the natural smugglin structures, the amino acid residues of these prodrugs will be changed, as well as the positions of the toxic warhead and the transport moiety at the *N*-and *C*-terminus, to obtain evidence for the optimisation of the design of the natural compound for effective transport via Dpp and Tpp.

The results gained from these studies should clarify why these natural prodrugs have specific amino acid side chains as the transport moiety, and allow an improved definition of structural and conformational features that can be used in the *rational* design of peptide carriers with specificity for particular peptide transport systems. By using molecular modelling and applying the MRTs for substrate recognition by peptide transporters, optimal peptide carriers can be then be proposed for diverse applications in prodrug development.

Table 7.1: Conformer Range for Natural Smugglins and their Modified Analogues.

| | A7 B9 | A7 B12 | Dpp | A4 B9 | A4 B12 | A10 B9 | A10 B12 | Tpp | A7 B2 | A4 B2 | A10 B2 | B2 Total | % Total |
|----------------------------------|-------|--------|-------|-------|--------|--------|---------|-------|-------|-------|--------|----------|---------|
| Bacilysin (Ala-X) | 8.26 | 22.38 | 30.64 | 3.51 | 8.01 | 3.25 | 10.49 | 25.26 | 19.34 | 5.44 | 6.23 | 31.01 | 86.91 |
| Modified Bacilysin (X-Ala) | 23.18 | 14.55 | 37.73 | 9.84 | 10.66 | 2.46 | 2.4 | 25.36 | 12.96 | 7.69 | 1.74 | 22.39 | 85.48 |
| Modified Bacilysin (Val-X) | 10.98 | 33.18 | 44.16 | 4.14 | 8.44 | 0.61 | 3.6 | 16.79 | 11.58 | 3.61 | 2.31 | 17.5 | 78.45 |
| Tabtoxin (X-Thr) | 19.45 | 9.75 | 29.2 | 13.08 | 21.36 | 3.34 | 4.06 | 41.84 | 10.01 | 4.98 | 1.48 | 16.47 | 87.51 |
| Tabtoxin (X-Ser) | 25.05 | 8.06 | 33.11 | 9.99 | 8.56 | 3.76 | 3.01 | 25.32 | 18.78 | 7.24 | 5.04 | 31.06 | 89.49 |
| Modified Tabtoxin (Thr-X) | 12 | 11.44 | 23.44 | 12 | 27.7 | 1.69 | 3.18 | 44.57 | 10.27 | 11.86 | 1.48 | 23.61 | 91.62 |
| Modified Tabtoxin (X-Ala) | 25.99 | 11.19 | 37.18 | 9.66 | 8.04 | 7.03 | 4.78 | 29.51 | 16.81 | 5.49 | 4.93 | 27.23 | 93.92 |
| Acm-Dipeptide | | | | | | | | | | | | | |
| Stravidin (MeIle-X) Acm | 7.29 | 17.77 | 25.06 | 2.24 | 24.27 | 0.47 | 1.82 | 28.8 | 19.34 | 2.19 | 0.88 | 22.41 | 76.27 |
| Dipeptide (Ile-X) Acm | 14.62 | 11.57 | 26.19 | 2.10 | 14.13 | 1.17 | 2.04 | 19.44 | 25.56 | 2.96 | 2.11 | 30.63 | 76.26 |
| Dipeptide (MeVal-X) Modified Acm | 10.46 | 24.27 | 34.73 | 3.13 | 19.07 | 0.65 | 2.62 | 25.47 | 12.92 | 3.42 | 1.69 | 18.03 | 78.23 |
| Dipeptide (Val-X) Modified Acm | 18.63 | 17.68 | 36.31 | 3.21 | 20.74 | 0.9 | 2.68 | 27.53 | 18.29 | 3.96 | 0.69 | 22.94 | 86.78 |
| Dipeptide (MeAla-X) Modified | 10.54 | 23.26 | 33.8 | 9.13 | 13.1 | 1.9 | 7.85 | 31.98 | 11.25 | 8.09 | 2.02 | 21.36 | 87.14 |
| Stravidin (MeX-Ile) | 3.82 | 5.76 | 9.58 | 17.03 | 30.61 | 0.37 | 1.7 | 49.71 | 10.17 | 4.03 | 0.39 | 14.59 | 73.88 |
| Lindenbein (X-Ala) Modified | 22.49 | 46.91 | 69.4 | 2.57 | 4.58 | 1.62 | 1.39 | 10.16 | 9.64 | 2.8 | 1.23 | 13.67 | 93.23 |
| Lindenbein (Ala-X) | 6.92 | 29.03 | 35.95 | 2.97 | 9.59 | 2 | 17.06 | 31.62 | 18.7 | 5.04 | 7.81 | 31.55 | 99.12 |

= Total % Conformers in A7B9/B12 Dpp Regions

= Total % Conformers in A4/A10 (B9+B12) Tpp Regions

= Total % Conformers in Inactive B2 Regions

7.2. RESULTS

A range of antimicrobial prodrugs and their modified analogues were modelled (section 2.7.2.4.), and analysis of results was carried out as described (section 2.7.3.4.). Random search of these compounds produced a large number of unique conformers because of their flexible structures. The minimum energy conformers only contributed a small percentage of the total conformer distribution range. For each compound, the percentage distribution of conformers in MRT regions, and the total percentage of conformers in Dpp and Tpp regions, was determined in order to assess which system is favoured for transport. Table 7.1. shows the results obtained after conformational analysis of natural dipeptide smugglins and their modified analogues.

7.2.1. *Bacilysin (Ala-X)*

Bacilysin has its Ala transport moiety attached to the C α near the *N*-terminus with its toxic anticapsin warhead near the *C*-terminus. Nearly all of its conformers distributed in the defined MRT regions. The majority of conformers had ψ (Tor2) and ϕ (Tor4) angles in A7B12 and A7B2, and the amount of B2 conformers was similar to the amount of Dpp conformers. As bacilysin has a higher percentage of Dpp conformers than Tpp conformers (Table 7.1.), it would be expected to be transported by both Dpp and Tpp, but may have better uptake activity by Dpp than by Tpp.

7.2.1.1. *Modified Bacilysin (X-Ala)*

Changing the toxic warhead to the C α near the *N*-terminus also produced conformers in the defined MRT regions, with a decrease in B2 conformers and an increase A4B9/B12 and A7B9 conformers. The total percentage of Tpp conformers was the same as bacilysin, but an increase in the total percentage of Dpp conformers was obtained (Table 7.1.). This bacilysin analogue (X-Ala) would also be a Dpp and Tpp substrate like bacilysin, but may have greater Dpp activity than bacilysin.

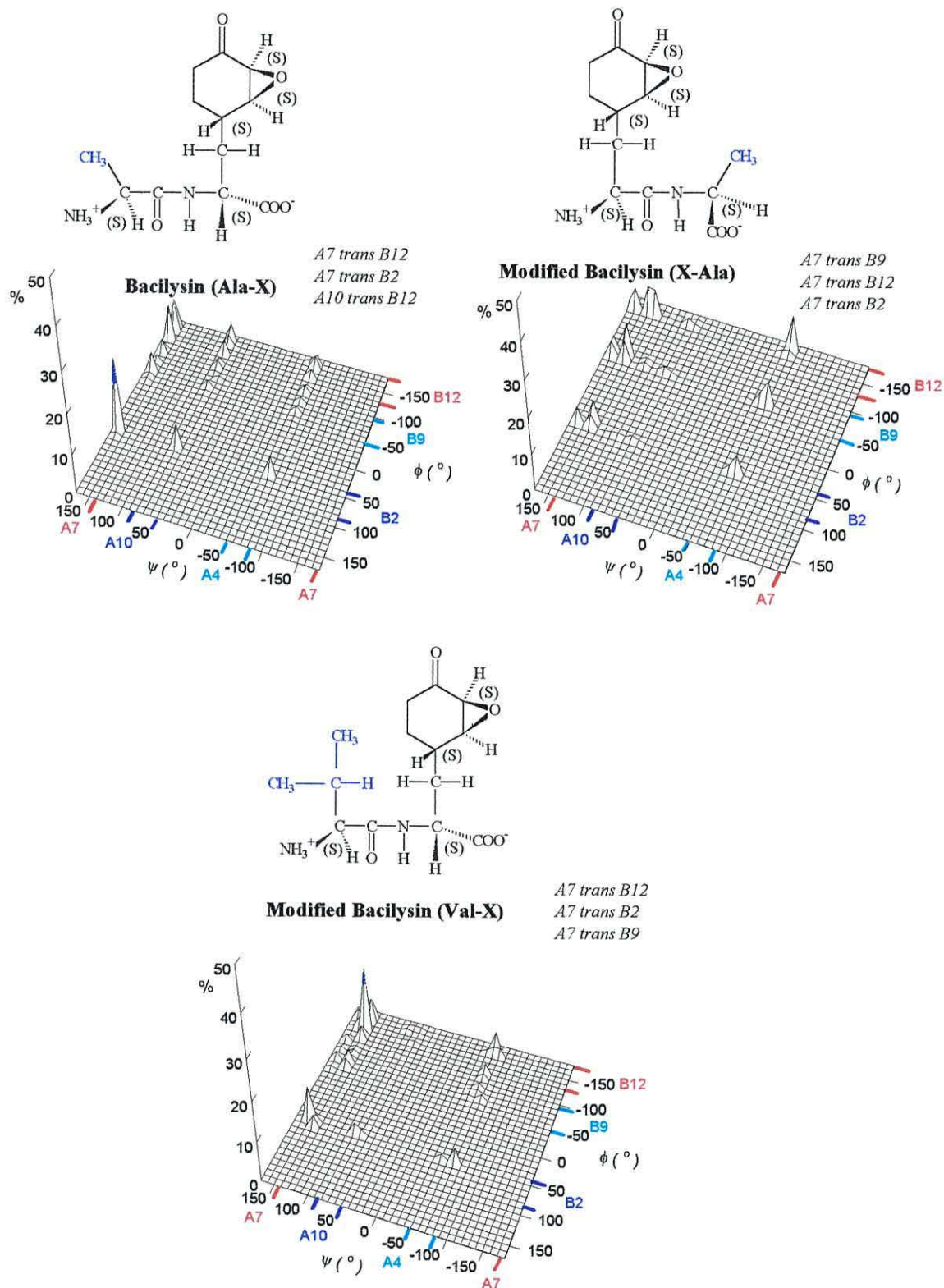


Figure 7-1: 3DPR Plots of ψ vs ϕ vs % Conformers for Bacilysin and its Modified Analogues.

7.2.1.2. Modified Bacilysin (Val-X)

Bacilysin was modified by changing the Ala side chain to Val, and this resulted in less conformers being present in the MRT regions than bacilysin and its modified analogue (X-Ala). Val-X analogue had less B2 conformers and more A7B9/B12 conformers compared with bacilysin. This resulted in an increase in the total percentage of Dpp conformers. A decrease in A10B9/B12 conformers was obtained which caused a reduction in the total percentage of Tpp conformers (Table 7.1.). Modified bacilysin (Val-X) would be predicted to have better Dpp activity and poorer Tpp activity than bacilysin. Fig. 7-1 shows 3DPR plots for bacilysin and its modified analogues.

7.2.2. Tabtoxin (X-Thr)

Tabtoxin contains an *N*-terminal β -lactam side chain and the *C*-terminal moiety is usually a Thr but can also be Ser. Tabtoxin (X-Thr) had the majority of its conformers in the defined MRT regions. A large percentage of conformers had ψ (Tor2) angles in A4 with ϕ (Tor4) angles in B12. Tabtoxin (X-Thr) had a higher percentage of Tpp conformers than Dpp conformers. The total percentage of B2 conformers was less than the total percentage of B9/B12 conformers (Table 7.1.). These results show that tabtoxin (X-Thr) can be transported by both Dpp and Tpp, but would be expected to have greater uptake by Tpp.

7.2.2.1 Tabtoxin (X-Ser)

Conformational analysis of the other form of tabtoxin (X-Ser) showed that it also had most of its conformers in the MRT regions. The majority of its conformers were in A7B9, in contrast to tabtoxin (X-Thr) which had most of its conformers in A4B12 (Table 7.1.). The total percentage of Dpp conformers was higher than the total percentage of Tpp conformers. Tabtoxin (X-Ser) had a greater percentage of B2 conformers compared with tabtoxin (X-Thr). These results show that tabtoxin (X-Ser) can be transported by both Dpp and Tpp like tabtoxin (X-Thr), but having a serine side chain allows for better uptake by the Dpp transport system. Thus, producing both forms of tabtoxin maximises uptake by both transporters.

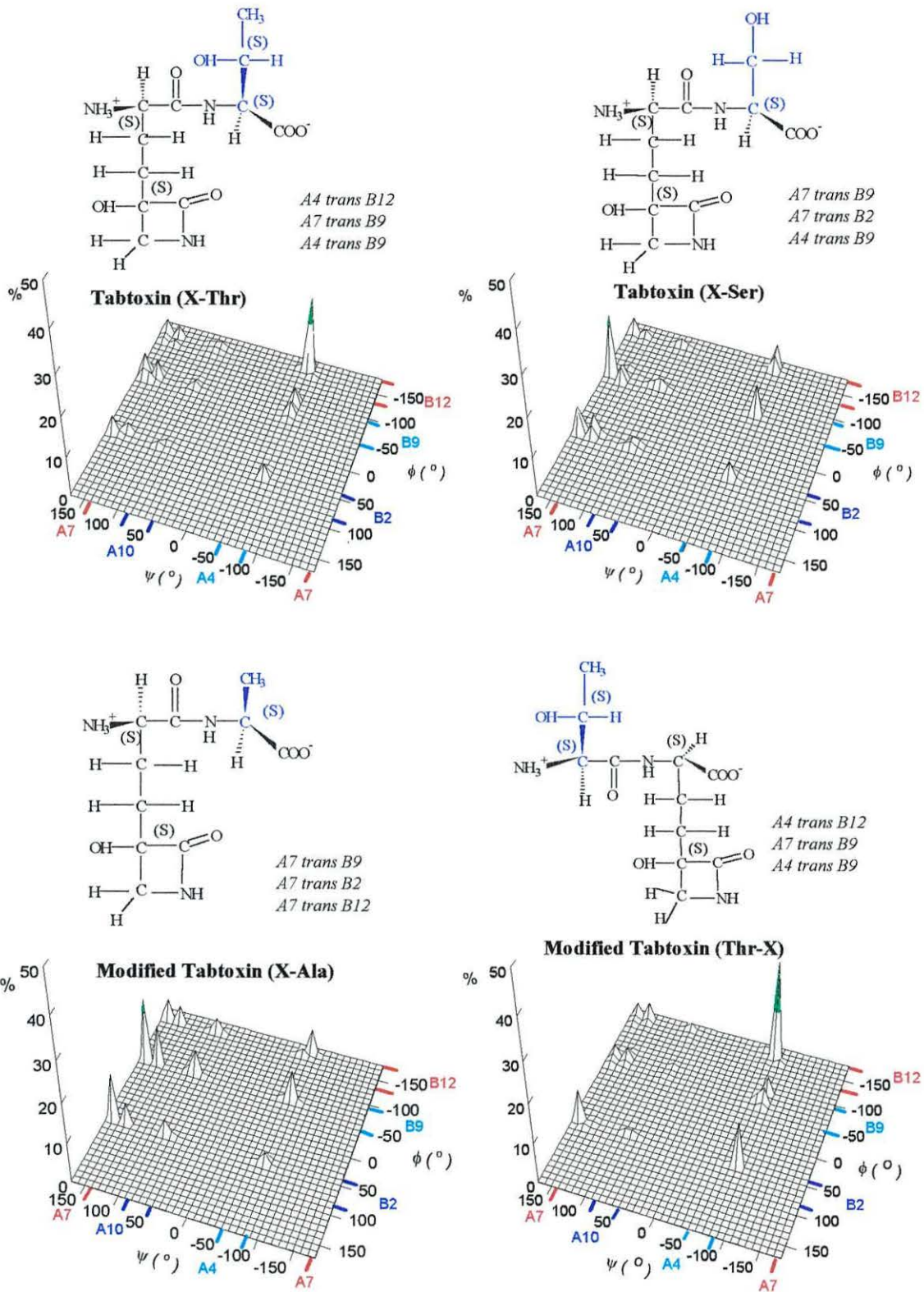


Figure 7-2: 3DPR Plots of ψ vs ϕ vs % Conformers for Tabtoxin and its Modified Analogues.

7.2.2.2. *Modified Tabtoxin (Thr-X)*

The C-terminal Thr was changed to the C α near the N-terminus and this also produced conformers that were nearly all in the MRT regions. Modified tabtoxin (Thr-X) showed no major change in the conformer distribution range compared with tabtoxin (X-Thr), although an increase in the total percentage of B2 conformers was seen (Table 7.1.). These results show that modified tabtoxin (Thr-X) would also be transported by both Dpp and Tpp, with higher uptake by Tpp, like tabtoxin (X-Thr), but overall would be less effective through having an increased amount of inactive B2 conformers.

7.2.2.3. *Modified Tabtoxin (X-Ala)*

The side chain of tabtoxin was changed to a Ala (as most natural smugglins are X-Ala), and this resulted in a greater percentage of conformers in the MRT regions, compared with the other forms of tabtoxin. However, an increase in B2 conformers was seen compared to tabtoxin (X-Thr), but less than tabtoxin (X-Ser). Modified tabtoxin (X-Ala) had a higher percentage of Dpp conformers than both forms of tabtoxin, with a similar amount of Tpp conformers as tabtoxin (X-Ser) (Table 7.1.). These molecular modelling results show that modified tabtoxin (X-Ala) could be a good substrate for both transport systems, but by having both forms of tabtoxin (X-Thr) and (X-Ser), both Dpp and Tpp transport systems can be optimally used. Fig. 7-2 shows 3DPR plots for tabtoxin and its modified analogues illustrating their conformer distribution range.

7.2.3. *Amiclenomycin-Peptides*

7.2.3.1. *Stravidin (Melle-X)*

Stravidin contains a N- methylated terminus and an Ile side chain as its transport moiety, with the C α near the C-terminus having an amiclenomycin toxic group. The majority of its conformers were distributed in the MRT regions, with most conformers being present in A4B12. The total percentage of Dpp conformers was similar to the total percentage of Tpp conformers. The total amount of B2 conformers was a little less than the total percentage of conformers in Dpp and Tpp regions (Table 7.1.). Stravidin (Melle-X) would be expected to be transported by both Dpp and Tpp systems.

7.2.3.2. *Acm-Dipeptide (Ile-X)*

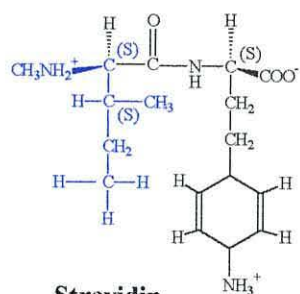
This dipeptide does not have a *N*-methylated terminus, but has an Ile side chain like stravidin, and had a similar total percentage of conformers in MRT regions as stravidin (Melle-X). Ile-X had a significant increase in A7B2 conformers, and a decrease in the total percentage of Tpp conformers, compared with Melle-X stravidin. Ile-X had a greater percentage of A7B9 conformers compared with Melle-X stravidin, but the total percentage of conformers required for Dpp activity was similar to Melle-X stravidin (Table 7.1.). Ile-X smugglin would also be predicted to be a Dpp and Tpp substrate, like Melle-X stravidin, but may have lower Tpp transport activity than Melle-X stravidin.

7.2.3.3. *Acm-Dipeptide (MeVal-X)*

This dipeptide also contains a *N*-methylated terminus and a Val side chain as its transport moiety. Most of its conformers were distributed in the MRT regions, with an increase in AB9/B12 conformers compared with Melle-X stravidin. This resulted in MeVal-X having a higher percentage of Dpp conformers than Melle-X and Ile-X smugglins. The amount of Tpp conformers was less than that for Melle-X, and greater than the amount for Ile-X peptide. The total percentage of B2 conformers was less than the total percentage of Dpp and Tpp conformers, and less than that for stravidin and Ile-X peptide (Table 7.1.). MeVal-X dipeptide would also be predicted to be transported by both Dpp and Tpp like stravidin (Melle-X), but may have greater uptake activity by Dpp than Tpp, compared with stravidin and Ile-X smugglins.

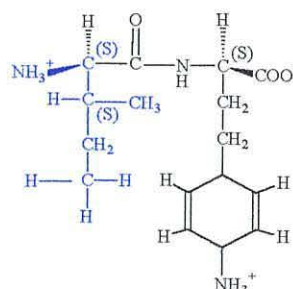
7.2.3.4. *Modified Acm-Dipeptide (Val-X)*

The natural dipeptide MeVal-X was modified by removing the methyl group from the *N*-terminus to give Val-X, and this produced an increase in the total percentage of conformers distributed in the MRT regions. An increase in A4B12 and A7B9 conformers was seen, compared with the natural MeVal-X, Ile-X and Melle-X smugglins. The total percentage of Dpp and Tpp conformers for Val-X was greater than for MeVal-X, and the total percentage of inactive B2 conformers was less than the total percentage of Dpp and Tpp conformers.



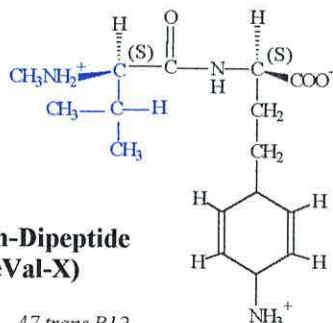
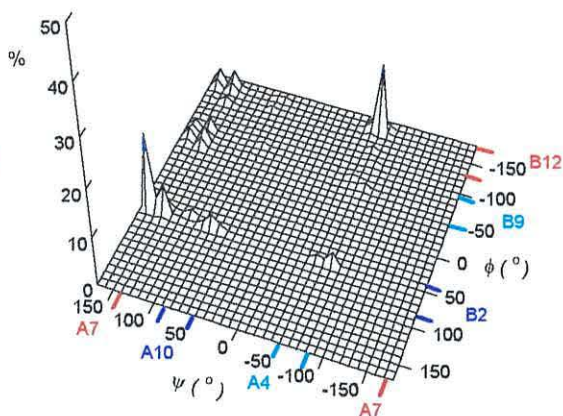
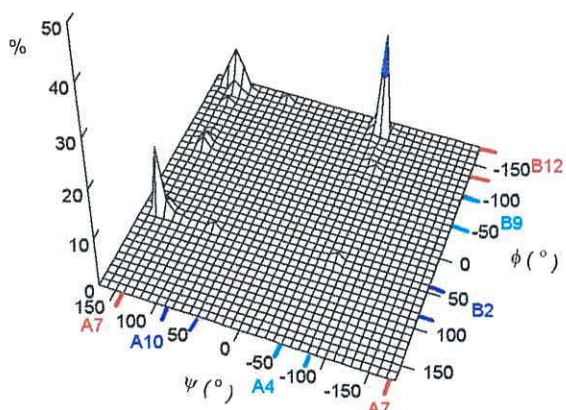
**Stravidin
(Melle-X)**

*A4 trans B12
A7 trans B2*



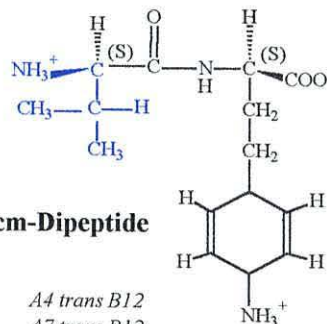
**Acm-Dipeptide
(Ile-X)**

*A7 trans B2
A4 trans B12*



**Acm-Dipeptide
(MeVal-X)**

*A7 trans B12
A4 trans B12*



**Modified Acm-Dipeptide
(Val-X)**

*A4 trans B12
A7 trans B12*

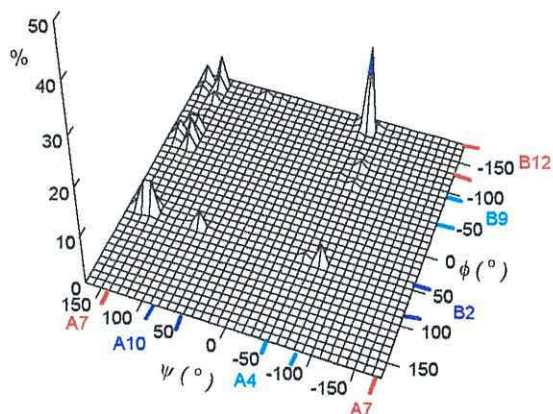
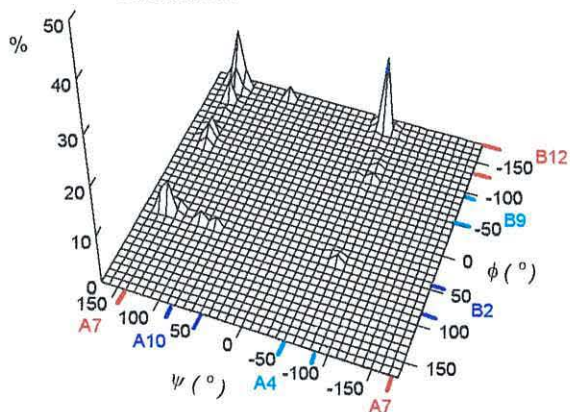


Figure 7-3: 3DPR Plots of ψ vs ϕ vs % Conformers for Acm-Dipeptides and their Modified Analogues.

As Val-X has more Dpp and Tpp conformers, it would be expected to have better Dpp activity than Tpp activity (Table 7.1.). Fig. 7-3 shows 3DPR plots for stravidin (MeIle-X) and other naturally-occurring amiclennomycin-peptides, and their modified analogues, showing their percentage conformer distribution range.

7.2.3.5. Modified Acm-Dipeptide (MeAla-X)

The Ile and Val side chains near the *N*-methylated terminus of natural amiclennomycin-peptides was replaced by an Ala residue. This produced an increase in the percentage of conformers in the MRT regions, compared with the natural amiclennomycin-peptides. The majority of conformers had ψ (Tor2) angles in A7 with ϕ (Tor4) angles in B12, B2 and B9. Modified stravidin (MeAla-X) had a similar percentage of Dpp and Tpp conformers, and this was greater than that obtained for MeIle-X stravidin (Table 7.1.). Modified stravidin (MeAla-X) could also be a good Dpp and Tpp substrate and may have better transport activity for both systems than stravidin (MeIle-X).

7.2.3.6. Modified Stravidin (MeX-Ile)

Stravidin (MeIle-X) was modified by placing the toxic warhead near the methylated *N*-terminus, and placing the Ile transport moiety near the *C*-terminus. This also produced conformers in the MRT regions, however, a significant decrease in A7B12 conformers was obtained. This may result in MeIle-X having poorer Dpp activity than stravidin. In contrast to stravidin, the modified analogue MeX-Ile had an increase in A4B9/B12 conformers, which resulted in an overall increase in the total percentage of Tpp conformers. The total percentage of B2 conformers was higher than the percentage of Dpp conformers, but MeX-Ile had the least amount of B2 conformers compared with the other amiclennomycin-peptides modelled (Table 7.1.). These results indicate that the modified stravidin (MeX-Ile) would have better Tpp activity than Dpp activity, compared with stravidin. MeX-Ile had the majority of its conformers in Tpp regions this is in contrast to the naturally occurring amiclennomycin-peptides such as MeIle-X, Ile-X and MeVal-X that have sufficient amount of conformers distributed in both regions to allow effective transport by both Dpp and Tpp. Fig.7-4 shows 3DPR plots for the modified analogues of amiclennomycin-peptides, illustrating the differences in their percentage conformer distribution range.

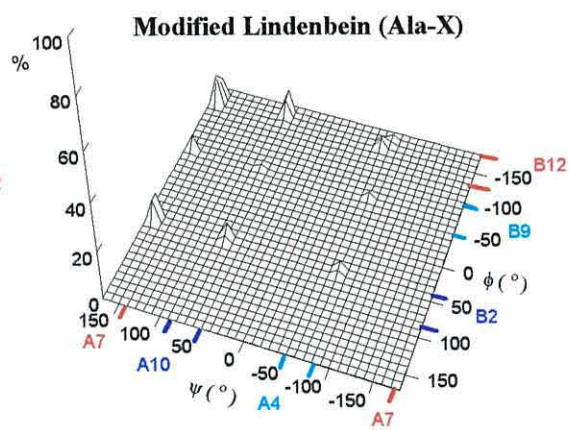
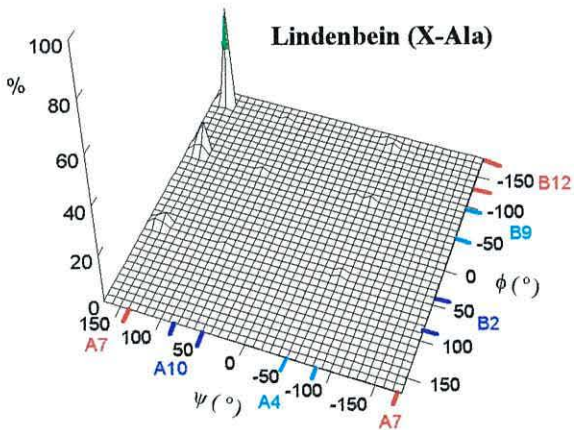
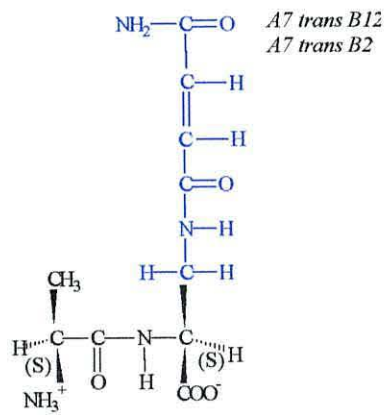
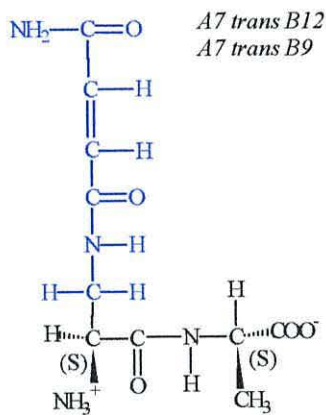
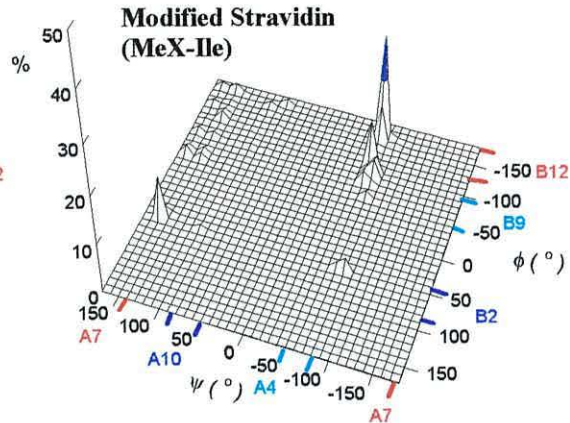
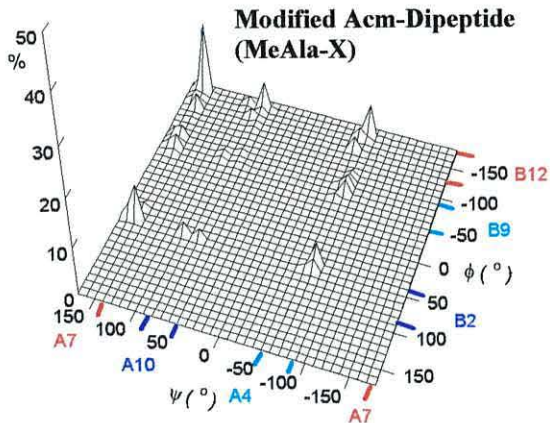
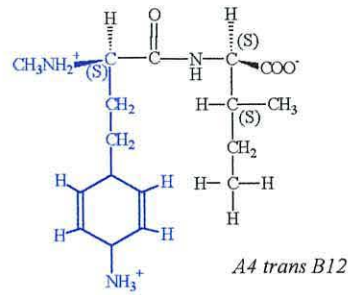
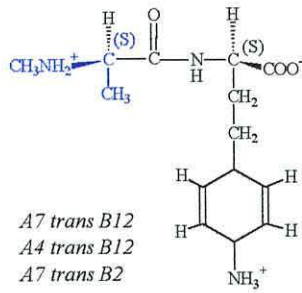


Figure 7-4: 3DPR Plots of ψ vs ϕ vs % Conformers for Acm-Dipeptides and their Modified Analogues, Lindenbein and Modified Lindenbein.

7.2.4. Lindenbein (FCDP-Ala) (X-Ala)

Lindenbein has its toxic warhead attached to the *N*-terminus, with Ala as its transport moiety attached at the *C*-terminus. Lindenbein had nearly all of its conformers present in the defined MRT regions, with the majority of conformers in A7B9 and A7B12, with some conformers in A7B2. Very few Tpp conformers were present and this indicates that lindenbein is designed as a Dpp substrate, as most of its conformers are for transport by Dpp.

7.2.4.1. Modified Lindenbein (Ala-FCDP) (Ala-X)

The Ala transport moiety was attached at the *N*-terminus (which is usually found in most smugglins) and the toxic side chain was placed at the *C*-terminus. This produced an increase in A7B2 conformers, and a decrease in A7B9 and A7B12 conformers, compared to FCDP-Ala. An increase in the total percentage of Tpp conformers was obtained, and similar amounts of Dpp and Tpp conformers and inactive B2 conformers were present for Ala-FCDP (Table 7.1.). These molecular modelling results show that lindenbein (FCDP-Ala) has most of its conformers in the MRTs required for efficient uptake by the Dpp, with minimum amount of B2 conformers. Modification in its structure to Ala-FCDP, produces conformers that are required for both Dpp and Tpp uptake but also causes a detrimental increase in the percentage of inactive B2 conformers. Fig. 7-4 shows 3DPR plots for lindenbein and modified lindenbein, illustrating the differences in their percentage conformer distribution range.

7.3. DISCUSSION

7.3.1 Molecular Modelling of Natural Smugglins

Antimicrobial smugglins generally consist of an amino acid transport moiety and a toxic warhead. One of the aims of this study was to investigate why these natural smugglins have specific amino acid side chains as transport moieties. In addition to conformational analysis, *the charge and chi-space* of the amino acid side chains of these smugglins was also considered when assessing their ability to be transported and to act as peptide carriers. The DppA binding pocket contains a negatively charged Asp⁴⁰⁸ residue and a positively charged Arg³⁵⁵ residue that interact with the positively and negatively charged *N*- and *C*-terminus of peptide substrates. None of the natural smugglins had the amino acid residues Lys, Asp, Arg or Glu as their transport moiety as these charged side chains may interfere with the binding of the *N*- and *C*-termini of these prodrugs to DppA. It has already been shown in Chapter 3 that dipeptides containing charged side chains, such as Asp-Ala and Glu-Lys, have poor Dpp and Tpp transport activity.

Molecular modelling has shown how these prodrugs have been rationally designed for efficient delivery via the peptide permeases, nearly all of the antimicrobial agents modelled could effectively be transported by both Dpp and Tpp. An exception was lindenbein which was predominantly a Dpp substrate. When its FCDP warhead was modelled at the *C*-terminus, this resulted in a greater proportion of Tpp conformers, but also greatly increased the amount of inactive B2 conformers. It seems that by placing its warhead at the *N*-terminus, Nature has optimised its transport to the efficient dipeptide transport system. Molecular modelling of bacilylsin showed it would be transported by Dpp and Tpp, and this is in accordance with studies with *E.coli* cells by Chmara *et al.* (1981). Conformational analysis of Acm-dipeptides has shown that they can act as Dpp substrates. Studies by Poetsch and co-workers have shown their uptake by mutants deficient in Opp, but no uptake was detected with mutants deficient in Opp and Dpp, which suggests that they are transported by Dpp (Poetsch *et al.*, 1985).

Although some Acm-peptides are unusual in that their terminal amino group is *N*-methylated, modelling shows this may be an advantage here in the distribution of conformers available to the mixed forms found naturally. Conformational analysis of modified analogues of these natural smugglins has also produced compounds that may be used as prodrugs for transport predominantly by Dpp and/or Tpp systems. Some of these antimicrobial agents may already exist in Nature and require identification. In addition, further transport studies are required using mutants for Dpp and Tpp to examine the uptake of these natural smugglins and their modified analogues.

7.3.2. Choice of Amino Acid As The Transport Moiety

The fact that L-alanine is a common transport moiety of many natural smugglins can be explained by the results gained from this study. Ala-X prodrugs have the majority of their conformers with backbone torsion angles distributed in MRT regions for transport by Dpp and Tpp. In addition, alanine has a small uncharged side chain that does not present problems of chi space for fitting into the binding pocket and therefore, has the general optimised features required for efficient recognition and transport by peptide transporters.

A number of natural smugglins also have aliphatic side chains such as Val, Ile, Thr, Ser and Leu. It seems that these smugglins make good prodrugs as they have optimised distribution of conformers for both Dpp and Tpp by linking the same toxic warhead to these different transport moieties, as seen with tabtoxin and Acm-dipeptides. Their short aliphatic side chains can be easily accommodated into the DppA binding pocket minimising problems with chi space and charge.

Natural antimicrobial smugglins are found not to have bulky aromatic amino acids such as Phe, Tyr or Trp as transport moieties. This feature was investigated (results not shown) by modelling valclavam (Fig. 1-4) and a range of analogues in which Val was replaced by Ala, Gly, Ile, Leu, Met, Phe, Ser, Thr, Trp and Tyr. Many of these analogues had large percentages of conformers with acceptable backbone conformers for Dpp and Tpp e.g. Ala (33%; 30%), Gly (24%; 42%), Ile (68%; 10%), Leu (14%; 19%), Met (33%; 30%), Phe (42%; 13%), Ser (26%; 37%), Thr (29%; 29%), Trp, (46%; 8%), Tyr (39%; 17%) and Val (40%; 18%) respectively.

However, with Phe, Trp and Tyr the minimum energy A7B9/B12 Dpp conformers accounted for a very high proportion of these percentages, and their aromatic side chains adopted unacceptable chi-space. Valclavam did not suffer from these problems. Val proved superior to Ala here in having significantly less inactive B2 conformers, 19% compared with 30%, respectively. Thus this extended study provided substantial support for the contention that valclavam has been designed for optimal transport, an important conclusion that impacts on considerations of biosynthetic pathways. In this laboratory, we have shown that valclavam is indeed transported effectively by Dpp and Tpp, and its binding to DppA results in a clean change in pI value (unpublished results).



CHAPTER 8
FINAL DISCUSSION

8. FINAL DISCUSSION

8.1. Introduction

Peptide transport systems in all species have evolved to transport a wide range of peptide substrates in a largely sequence independent manner. The substrate specificity of peptide transporters has been extensively studied (Matthews & Payne, 1980; Matthews, 1991; Payne & Smith, 1994; Becker & Naider, 1995; Steiner *et al.*, 1995; Daniel & Herget, 1997; Fei *et al.*, 1998; Smith *et al.*, 1999). Recently, a main aim of studies conducted in this laboratory has been to identify the individual molecular recognition templates (MRTs) of substrates recognised by peptide transporters (Payne *et al.*, 2000). In addition to their nutritional role, peptides are also important therapeutic agents that act as competitive or non-competitive inhibitors of enzymes or receptors. The pharmacological efficacy of peptide drugs depends not only on recognition and binding to intracellular targets, but also upon their oral delivery via peptide transporters (Yang *et al.*, 1999).

Bacterial peptide permeases have been used as convenient model systems for the study of SAR of peptide transport in this laboratory (Smith *et al.*, 1999). Using a range of biochemical and microbiological techniques, as well as computer modelling, the molecular recognition parameters involved in protein-ligand interactions of peptide transporters have been revealed (Payne *et al.*, 2000; Grail & Payne, 2000). The information gained from these studies has been used to aid the *rational* design of peptidomimetics and peptide drugs for effective oral delivery via the pharmacologically important PepT1 and PepT2 transporters in this study.

8.2. Molecular Recognition of Peptides by Peptide Permeases

Conformational analysis, using Random search in SYBYL, has been used to evaluate the bioactive conformations of peptides, and has identified the *structural* and *conformational* features involved in molecular recognition of peptide substrates. Chapter 3 described how the MRTs for peptide transporters were obtained by relating the activity of peptides to their conformers' distribution range in solution (Payne *et al.*, 2000).

Peptide conformers were identified by a set of *backbone torsion angles* for psi (ψ), omega (ω) and phi (ϕ) for recognition by Dpp and Tpp. The preferred ψ values were identified as -50 to -85° , $+140$ to -175° ; and $+50^\circ$ to $+85^\circ$, designated A4, A7 and A10, respectively; and for ϕ , $+40$ to $+85^\circ$; -95 to -50° ; and -130° to $+175^\circ$, designated B2, B9 and B12, respectively. Compounds with conformers in A7(B9,B12) sectors were recognised by Dpp, and conformers in A4(B9,B12) and A10(B9,B12) were recognised by Tpp. Most dipeptides have a majority of their conformers in both MRT recognition types, A7(B9+B12) and A4,A10(B9+B12), making them good substrates for both Dpp and Tpp. Conformers with B2 torsion angles are “inactive” and not recognised by peptide transporters. The B2 conformers have their side chains orientated so as to preclude interaction of the C-terminus to Arg³⁵⁵ in the binding pocket when the N-terminus is anchored to its cognate negatively-charged Asp⁴⁰⁸ residue (Grail & Payne, 2000).

Incorporation of these features has led to a definition of molecular recognition template(s) (MRTs) of peptide substrates which includes: i) charged N-terminal and C-terminal groups, allowing electrostatic and H-bond donor and acceptor interactions; ii) combinations of torsion angles (ψ , ϕ and ω) in the backbone; iii) stereochemistry at α -carbon chiral centres; iv) N-C distance between terminal amino N and carboxylate C atoms; v) chi (χ)-space torsion angles of the side chain; vi) H-bond acceptor and donor properties of peptide bond O and N atoms; and vii) charge fields around N-terminal α -amino and C-terminal α -carboxylate groups. Features that define the MRT can be considered as influencing the effectiveness of substrate recognition and binding in two ways. Firstly, each feature influences the conformer repertoire in solution upon which recognition depends, and secondly, each is required for consolidating interactions with the transporter that ensures specificity and affinity. For peptides, the binding/transport ability is mainly determined by the proportion of conformers that exist in the relevant MRT. This conclusion is essentially an alternative way of stating a central tenet of structure-based ligand design, that for a flexible ligand its binding affinity will be improved if its conformational motion can be restricted to that of the ligand-bound form (Payne *et al.*, 2000).

8.3. Rational Design of Peptidomimetics

Computer-modelling, NMR, and X-ray crystallography have generally been used to search for the bioactive conformation of a peptide required to bind to a receptor or enzyme. Molecular design and synthetic chemistry approaches have then been applied for the modification of peptides into peptidomimetics (Taylor & Amidon, 1995). However, these processes do not allow for the selection of peptidomimetic compounds with good oral bioavailability, in addition to biological potency and synthetic feasibility. The MRTs for peptide substrates (Chapter 3) were applied to assess the *bioavailability* of peptidomimetics based on their conformational analysis of backbone torsion angles. Molecular modelling was also used to design peptidomimetics with conformational features required for recognition and transport by peptide transporters. The results gained from this study show how conformational analysis, using molecular modelling, can be used as part of a design cycle for the discovery and development of peptide mimetics.

8.3.1. Synthesis of 'Ideal' Dpp and Tpp Substrates

Conformational analysis of a range of peptidomimetics has identified some ideal substrates with unique Dpp and/or Tpp specificity, based on their backbone torsion angles. These include the dipeptide isosteres M46, M47 and M48, the *N*-methylamide PBM and the thioamide PBM. These compounds are all predicted to have Dpp activity, as well as increased stability against proteolytic enzymes and retain the *trans* ω conformations required for transport. The 7-membered lactam-mimetics M57, M58, M69-M80 are predicted to have better bioavailability by PepT1, compared with the 4,5, or 6-membered lactams. Structural modifications of lactam-mimetics produced Dpp and Tpp substrates such as M56_2, M69_2, M64_1, M69_1, M69_2, M57_2, M80_1, M113_3, and M127_1. These *rationally* designed peptide mimetics warrant synthesis and testing for transport activity using Tpp and Dpp *E.coli* mutants. The availability of such compounds would be an invaluable tool for all researchers studying the delivery of putative drugs by the oral route.

8.4. Molecular Modelling of ACE Inhibitors

The development of ACE inhibitors was initiated by the discovery of natural snake-venom peptides that were effective inhibitors of ACE *in vitro*, but their peptidic nature prevented their clinical use (Amidon & Taylor, 1995). ACE inhibitors for therapeutic use were designed based on the C-terminal sequence Trp-Ala-Pro of a natural inhibitor (Cleland, 1993). Being peptidomimetic-drugs they can act as substrates for peptide transporters for their oral delivery. Molecular modelling of ACE inhibitors in Chapter 5 provided further insight into additional parameters that are required for recognition by peptide transporters. It has always been stressed in considering MRTs that although ψ , ω and ϕ angles allow a good primary screen, it is always necessary to consider a range of other structural and charged features, such as those above, before reaching a final conclusion on how well a putative substrate will match an MRT and be transported (Chapter 3) (Payne *et al.*, 2000). For ACE inhibitors, these included the chi-space torsional angles of side chains of these compounds, particularly when they are charged, and the importance of a charged N-terminus.

The activity data obtained in Chapter 5 also showed that substrates that are designed to bind to a peptidase such as ACE, may also be predicted to show activity for a transporter such as DppA. The majority of ACE inhibitors are analogues of Ala-Pro. Studies in our laboratory have shown that C-terminal proline residues are poor substrates for transport by Dpp (Payne *et al.*, 2000), and the majority of ACE inhibitors also showed poor binding affinity for DppA. This correlation with binding affinity indicates comparable recognition processes for transporters and peptidases.

Studies with filter binding assays showed that compounds with the best activity for binding to DppA are those that contain the majority of their conformers constrained in or near A7 *trans* B9 MRT (and that satisfy additional criteria, see above) and this validates the use of the MRT for prediction of activity. In addition, the ψ angles for conformationally-constrained compounds that seem to be acceptable to the ACE active site are similar to the ψ A7 MRT required to bind to DppA.

Although the ϕ angles have not been computed for these inhibitors, it would be reasonable to assume that ACE may also recognise the ϕ B9/B12 templates of DppA. This provides further evidence that the MRTs established for the peptide transporters may be applied for the design of substrates of peptidases for therapeutic use.

8.5. Rational Design of ACE Inhibitors

Molecular modelling of ACE inhibitors identified structural features required for improvement in their oral delivery. Systematic changes in chemical structures of dipeptide mimetics (Chapter 4) provided identification of structural motifs that could produce conformer profiles to match the MRTs' *backbone torsion angles* for substrate recognition and transport by intestinal peptide transporters. Knowledge gained from molecular modelling of dipeptides and dipeptide mimetics was applied to the *rational* design of ACE inhibitors. This produced a set of theoretical compounds with structural and conformational features for recognition by bacterial peptide permeases, that may show improved oral delivery by intestinal peptide transporters (Chapter 6). Future studies would involve the chemical synthesis of these rationally designed structural analogues in order to determine their predicted activity.

8.6. Rational Design of Antimicrobial Smugglins

The recent establishment of MRTs for substrates for peptide transporters (Payne *et al.*, 2000; Grail & Payne, 2000), and the results gained from molecular modelling of natural smugglins and their modified analogues (Chapter 7), has provided information on the structural features required for the rational design of peptide carriers for synthetic smugglins. Prodrugs may be designed containing aliphatic side chains such as Ala, Val, Ile, Thr, Ser and Leu as the transport moiety. These antimicrobial agents will not only have conformer with backbone torsion angles in the MRT regions for Dpp and Tpp, but their side chains can be easily accommodated into the peptide transporters' binding pocket minimising problems with charge and chi space. By using conformational analysis, structures can also be designed to produce minimum amounts of inactive B2 conformers.

Synthetic smugglins may also be designed to use more than one permease, and molecular modelling of several natural smugglins has illustrated this principle (Chapter 7). Alternatively, a smugglin mixture could be used, linking a single warhead with two or more carrier moieties that facilitates complementary transport through several permeases. This approach occurs in Nature where peptide antibiotics are produced as mixtures incorporating various amino acid residues that provide beneficial variation in the delivery routes and activation mechanisms, as well as varied resistance to enzyme inactivation (Payne, 1994). Additionally, the design of smugglins might be tailored to overcome the problem of resistance by having two or more different warheads, which have unrelated targets or are aimed at different enzymes within a common pathway (Ringrose, 1980). Using the information and principles already discussed, innovations in the design and application of novel synthetic smugglins are possible. However, the development of therapeutically useful agents will require additional factors such as the use of peptidomimetics (Chapter 4) for the rational design of prodrugs that retain the structural features required for transport and activity, but also have good oral absorption and resistance to hydrolysis by mammalian enzymes.

8.7. Rational Design of Peptide Drugs for Improved Oral Delivery

This study has illustrated how the identification of MRTs for substrates for peptide transporters can have a major impact on the drug discovery process by assessing the *bioavailability* of potential drug candidates. The design of new peptide therapeutics has largely been based upon a combinatorial chemistry and screening approach with reference to crystal structure data obtained from X-ray crystallography and NMR (Ooms, 2000). Although structure-based drug design is widely used, it is limited by its focus on the enhancement of pharmacological potency and specificity of drug candidates, and provides little direction for improving their *in vivo* properties such as bioavailability. The oral bioavailability of a compound often determines whether a drug candidate is ultimately developed and has been exceedingly difficult to predict quantitatively. Drug-designers have mainly used structural information, gained from medicinal chemistry, to introduce chemical groups which are known from experience to aid bioavailability in ways that will not adversely affect drug binding affinity (Salemme *et al.*, 1997).

8.7.1. *Virtual Combinatorial Chemistry*

Combinatorial chemistry approaches are based on the development of highly reliable reaction protocols that allow the synthesis of vast number of compounds through an exhaustive combination of all possible reactions. Although targeted-combinatorial schemes produce libraries of drug-like compounds with 10^6 or more members, current automated equipment is practically limited to the synthesis of 10^2 - 10^3 compounds for each multistep synthesis cycle. This practical limitation on synthetic throughput motivates the development of effective computer-search strategies that can iteratively define and refine the selection of sub-libraries that will best investigate the structure-property relationships for a given library-target combination.

The most effective way to implement the search of large combinatorial libraries is to precompute the structures and properties of all synthetically accessible compounds within the library, and then to apply computational screens to this 'virtual library', in order to select subsets of compounds for iterative rounds of synthesis and testing (Salemme *et al.*, 1997).

In principle, any known property or SAR relationship can be introduced as a selection criteria and can be used as a part of a multi-parameter optimisation scheme for a given combinatorial sub-library. A typical library-design optimisation might identify a set of 1000 compounds from a virtual library containing 500 000 compounds that fulfil the parameters of meeting geometrical and functional criteria for fitting a target receptor or enzyme, and maintaining desired pharmacokinetic properties (Salemme *et al.*, 1997).

Future studies in this laboratory involve the development of software aimed to allow the following operations to be carried out with minimal user intervention: i) a combinatorial modification operation that would effect systematic structural changes to drug molecules (ii) subject library of virtual analogues created above to conformational analysis by Random search iii) compute parameters of each analogue's conformers and analyse individual profiles (iv) compare profiles with MRTs for each peptide transporter and rank analogues with respect to recognition by peptide transporters. Best candidates could then be evaluated for synthetic feasibility to prioritise for drug development programme.

The approach applied in this study using SYBYL (Tripos) software is rather labour intensive in determining MRTs and predicting transport activities. This methodology could be adapted and developed to a structure-modification protocol, to form two modules integrated into a single software package to predict oral availability. The first module would generate a database of conformers for each lead compound and compare them with the MRTs. This module would automate the procedures for conducting Random search, computing parameters, e.g. % conformer distribution, backbone torsion angles, *N-C* distance.

Dedicated macros, written in SYBYL programming language would be further developed to calculate and enter these variables into the spreadsheet. Conformers would be ranked using SPL macros for their percentage match to the MRTs of peptide transporters and added to a database. In principle, any MRT could be used as a matching target. These databases would be useful in the design of peptidase and protease inhibitors.

The second module would create a combinatorial library of starting structures for input into the first module by systematic modification, e.g., fragment addition, cyclisation of the lead compound at user defined positions with options selected from menus defined using Spl scripts. These conformer databases would, in their own right, represent a useful resource and complement crystallographic databases of small molecules. This integration would allow compound synthesis and evaluation in parallel and also help assure that the compounds produced have properties consistent with good bioavailability.

8.7.1.1. *Application of Structural Modification Rules*

Structural modifications of a range of peptidomimetics in this study has produced some chemical features that can be applied to the design of substrates that match the MRT backbone torsion angles of peptide transporters. These include the addition of methyl and phenyl groups to the second C α near the *C*-terminus of lactam-constrained mimetics to increase the percentage of B9 and B12 conformers. Conformational analysis of torsionally-constrained mimetics has highlighted the importance of *stereochemistry* of the bridging carbon, which can be used to produce substrates exclusively for Dpp or Tpp systems.

The insertion of a sulphur atom can introduce flexibility into ring systems that can be used to force ψ angles of 6-membered lactam rings into A7 conformations. The insertion of sulphur atoms into the second 5-membered ring of torsionally-constrained mimetics produces B2 conformers as the orientation of the C α near the C-terminus changes from R to S. The production of B2 conformers can be diminished by changing the chirality of the C α near the C-terminus from S to R, and this shifts the conformer distribution profile from B2 to B9. The structural modification 'rules' described here can be developed for possible incorporation into the second module, and be applied to produce theoretical compounds that not only have the bioactive conformation required for binding to intracellular target sites, but also have features that enable good oral delivery. This can lead to the *rational* design of peptidomimetic-type drugs, such as ACE inhibitors, that have conformational and structural features optimised for effective oral bioavailability.

8.8. Conclusions and Future Prospects

An important conclusion drawn from investigations into the molecular recognition of substrates by peptide transporters is that peptide transporters in all organisms have evolved their MRTs similarly, each responding to recognise the products of protein hydrolysis. This clarifies why such similar substrate specificities are found for analogous peptide transporters in man and microbes.

The establishment of MRTs for substrates for peptide transporters are expected to have significant impacts in the rational design and delivery of peptide drugs. The integration of virtual combinatorial chemistry with structure-based drug design will play a key role in the development of new drugs whose molecular targets are being discovered as a result of the human genome sequencing project. The availability of information of protein-ligand interactions gained in this study, will enable the development of targeted combinatorial libraries based on the MRTs that are known to give good oral delivery. These libraries can be searched in order to produce new pharmaceuticals possessing good oral bioavailability as well as specificity for a receptor or enzyme subtype.



CHAPTER 9
REFERENCES

9. REFERENCES

- Abel, M.G., Zhang, Y.L., Lu, H.F., Naider, F. & Becker, J.M. (1998) Structure-function analysis of the *Saccharomyces cerevisiae* tridecapeptide pheromone using alanine-scanned analogues. *J. Pep. Res.* **52**, 95-106.
- Abouhamad, W.N. & Manson, M.D. (1994) The dipeptide permease of *Escherichia coli* closely resembles other bacterial transport systems and shows growth-phase dependent expression. *Mol. Microbiol.* **14**, 1077-1092.
- Abouhamad, W.N., Manson, M., Gibson, M.M. & Higgins, C.F. (1991) Peptide-transport and chemotaxis in *Escherichia coli* and *Salmonella-typhimurium*: characterisation of the dipeptide permease (Dpp) and the dipeptide-binding protein. *Mol. Microbiol.* **5**, 1035-1047.
- Adang, A. E. P., Hermkens, P. H. H., Linders, J. T. M., Ottenheijm, H. C. J. & Staveren, C. J. v. (1994) Case histories of peptidomimetics: progression from peptides to drugs. *Recl. Trav. Chim. Pays-Bas.* **113**, 63-78.
- Adibi, S.A. (1997) The oligopeptide transporter (Pept-1) in human intestine: biology and function. *Gastroenterology* **113**, 332-340.
- Allen, J.G., Atherton, F.R., Hall, M.J., Hassall, C.H., Holmes, S.W, Lambert, R.W., Nisbet, L. J., & Ringrose, P. S. (1979a) Phosphono-peptides as antibacterial agents: alaphosphin and related phosphono-peptides. *Antimicrob. Agents. Chemother.* **15**, 685-695.
- Allen, J.G., Havas, L., Leicht, E., Lenox-Smith, I. & Nisbet, L. J. (1979b) Phosphono-peptides as antibacterial agents: metabolism and pharmacokinetics of alafosfalin in animals and humans. *Antimicrob. Agents. Chemother.* **16**, 306-313.
- al-Obeidi, F., Hurby, V.J. & Swayer, T.K. (1998) Peptides and peptidomimetic libraries. Molecular diversity and drug design. *Mol. Biotechnol.* **9**, 205-223.
- Alves, R.A. & Payne, J.W. (1980) The number and nature of the peptide-transport systems of *Escherichia coli*: characterisation of specific transport mutants. *Biochem. Soc. Trans.* **8**, 704-705.
- Ames, B.N., Ames, G.F.L., Young, J.D., Isuchiya, D. & Lecocq, J. (1973) Illicit transport: the oligopeptide permease. *Proc. Natl. Acad. Sci. USA.* **70**, 456-458.
- Ames, G.F. & Lecar, H. (1992) ATP-dependent bacterial transporters and cystic fibrosis: analogy between channels and transporters. *FASEB J.* **6**, 2660-2666.

- Andrews, J.C. & Short, S.A. (1985) Genetic analysis of *Escherichia coli* oligopeptide transport mutants. *J. Bacteriol.* **161**, 484-492.
- Andruszkiewicz, R., Chmara, H., Milewski, S. & Borowski, E. (1987) Synthesis and biological properties of N³-(4-methoxyfumaryl)-L-2,3-diaminopropanoic acid dipeptides, a novel group of antimicrobial agents. *J. Med. Chem.* **30**, 1715-1719.
- Atherton, F.R., Hall, M.J., Hassall, C.H., Lambert, R.W., Lloyd, W.J., Lord, A.V., Ringrose, P.S. & Westmacott, D. (1983) Phosphonopeptides as substrates for peptide transport systems and peptidases of *Escherichia coli*. *Antimicrob. Agents. Chemother.* **24**, 522-528.
- Attwood, M. (1989) Chemical design of cilazapril. *Br. J. Clin. Pharmacol.* **27**, 133S-137S.
- Attwood, M., Francis, R. J., Hassall, C. H., Krohn, A., Lawton, G., Natoff, I. L., Nixon, J. S., Redshaw, S. & Thomas, W.A. (1984) New potent inhibitors of angiotensin converting enzyme. *FEBS Lett.* **165**, 201-206.
- Bai, J.P.F. & Amidon, G.L. (1992) Structural specificity of mucosal-cell transport and metabolism of peptide drugs: implication for oral peptide drug delivery. *Pharm. Res.* **9**, 969-978.
- Bailey, P.D., Boyd, C.A.R., Bronk, J.R., Collier, I.D., Meredith, D., Morgan, K.M. & Temple, C.S. (2000) How to make drugs more orally active: a substrate template for peptide transporter PepT1. *Angew. Chem. Int. Ed.* **39**, 506-508.
- Baldwin, J.E., Claridge, T.D.W., Goh, K.C., Keeping, J.W. & Schofield, C.J. (1993) Revised structures for Tu 1718B and valclavam. *Tetra. Letts.* **34**, 5645-5648.
- Balimane, P.V. & Sinko, P.J. (1999) Involvement of multiple transporters in the oral absorption of nucleoside analogues. *Adv. Drug Delivery Rev.* **39**, 183-209.
- Barak, Z. & Gilvarg, C. (1975) Specialized peptide transport systems in *Escherichia coli*. *J. Bacteriol.* **122**, 1200-1207.
- Becker, J.M. & Naider, F. (1995) Fungal peptide transport as a drug delivery system. In *Peptide-Based Drug Design: Controlling Transport and Metabolism*. Taylor, M.D. & Amidon, G.L. (eds). ACS: Washington, D.C. pps. 369-384.
- Bohm, J. (1996) Towards the automatic design of synthetically accessible protein ligands: peptides, amides and peptidomimetics. *J. Comput. Aided. Mol. Des.* **10**, 265-272.
- Borchardt, R.T. (1999) Optimizing oral absorption of peptides using prodrug strategies. *J. Control. Release.* **62**, 231-238.

- Borchardt, R.T., Aube, J., Siahaan, T.J., Gangwar, S. & Pauletti, G.M. (1997) Improvement of oral peptide bioavailability: peptidomimetics and prodrug strategies. *Adv. Drug. Del. Rev.* **15**, 235-256.
- Börner, V., Fei, Y.L., Hartrodt, B., Ganapathy, V., Leibach, F.H., Neubert, K. & Brandsch, M. (1998) Transport of amino acid aryl amides by the intestinal H⁺/peptide cotransport system, PEPT1. *Eur. J. Biochem.* **255**, 698-702.
- Brandsch, M., Brandsch, C., Ganapathy, M.E., Chew, C.S., Ganapathy, V. & Leibach, F.H. (1997) Influence of proton and essential histidyl residues on the transport kinetics of the H⁺/peptide cotransport systems in intestine (PEPT1) and kidney (PEPT2). *Biochim. Biophys. Acta* **1324**, 251-262.
- Brandsch, M., Knütter, I., Thunecke, F., Hartrodt, B., Born, I., Börner, V., Hirche, F., Fischer, G. & Neubert, K. (1999) Decisive structural determinants for the interaction of proline derivatives with the intestinal H⁺/peptide symporter. *Eur. J. Biochem.* **266**, 502-508.
- Brandsch, M., Thunecke, F., Küllertz, G., Schutkowski, M., Fischer, G. & Neubert, K. (1998) Evidence for the absolute conformational specificity of the intestinal H⁺/peptide symporter, PEPT1. *J. Biol. Chem.* **273**, 3861-3864.
- Cheung, H. & Cushman, D. (1973) Inhibition of homogeneous angiotensin-converting enzyme of rabbit lung by synthetic venom peptides of *Bothrops jararaca*. *Biochim Biophys Acta* **293**, 451-463.
- Cheung, H.-S., Wang, F.-L., Ondetti, M., Sabo, E. & Cushman, D. (1980) Binding of peptide substrates and inhibitors of angiotensin-converting enzyme: importance of the COOH-terminal dipeptide sequence. *J Biol Chem* **255**, 401-407.
- Chmara, H. & Zahner, H. (1984) The inactivation of glucosamine synthetase from bacteria by anticapsin, the C-terminal epoxyamino acid of the antibiotic tetracycline. *Biochim. Biophys. Acta.* **787**, 45-52.
- Chmara, H. (1985) Inhibition of glucosamine synthase by bacilysin and anticapsin. *J. Gen. Microbiol.* **131**, 265-271.
- Chmara, H., Milewski, S., Andruszkiewicz, R., Mignini, F. & Borowski, E. (1998) Antibacterial action of dipeptides containing an inhibitor of glucosamine-6-phosphate isomerase. *Microbiology* **144**, 1349-1358.
- Chmara, H., Andruszkiewicz, R. & Borowski, E. (1984) Inactivation of glucosamine-6-phosphate synthetase from *Salmonella typhimurium* LT 2 SL 1027 by N beta-fumaryl carboxyamido-L-2,3-diamino-propionic acid. *Biochem. Biophys. Res. Commun.* **120**, 865-872.

- Chmara, H., Woynarowska, B. & Borowski, E. (1981) Epoxy peptide antibiotic tetaine mimics peptide transport in bacteria. *J. Antibiot. (Tokyo)* **34**, 1608-1612.
- Cleland, J.G.F. (1993) *The Clinician's Guide to ACE Inhibition*. Churchill Livingstone. Longman Group UK Limited. pp 3-26.
- Cornell, W.D., Caldwell, J.W. & Kollman, P.A. (1997) Calculation of the ϕ - ϕ maps for alanyl and glycyl dipeptides with different additive and non-additive molecular mechanical models. *J. Chim. Phys.* **94**, 1417-1435.
- Cushman, D. W., Cheung, H. S., Sabo, E. F. & Ondetti, M. A. (1977) Design of potent competitive inhibitors of angiotensin converting enzyme. Carboxyalkanoyl and mercaptoalkanoyl amino acids. *Biochemistry* **16**, 5484-5491.
- Daniel, H. & Herget, M. (1997) Cellular and molecular mechanisms of renal peptide transport. *Amer. J. Physiol. Renal Physiol.* **42**, ppF1-F8.
- Daniel, H. (1996) Function and molecular structure of brush border membrane peptide/H⁺ symporters. *J. Membr. Biol.* **154**, 197-203.
- Daniel, H., Morse, E.L. & Adibi, S.A. (1992) Determinants of substrate affinity for the oligopeptide/ H⁺ symporter in the renal brush border membrane. *J. Biol. Chem.* **267**, 9565-9573.
- Davies, T.G., Hubbard, R.E. & Tame, J.R.H. (1999) Relating structure to thermodynamics: the crystal structures and binding affinity of eight OppA-peptide complexes. *Protein Sci.* **8**, 1432-1444.
- Davis, B.D. & Mingioli, E.S. (1950) Mutants of *Escherichia coli* requiring methionine or vitamin B12. *J. Bacteriol.* **60**, 17-28.
- Diddens, H., Zahner, H., Kraas, E., Gohring, W., & Jung, G. (1976) On the transport of tripeptide antibiotics in bacteria. *Eur. J. Biochem.* **66**, 11-23.
- Diddens, H., Dorgerloh, M. & Zahner, H. (1979) Metabolic products of microorganisms. 176. On the transport of small peptide antibiotics in bacteria. *J. Antibiot. (Tokyo)* **32**, 87-90.
- Döring, F., Walter, J., Will, J., Föcking, M., Boll, M., Amasheh, S., Clauss, W. & Daniel, H. (1998) Delta-aminolevulinic acid transport by intestinal and renal peptide transporters and its physiological and clinical implications. *J. Clin. Invest.* **101**, 2761-2767.
- Döring, F., Will, J., Amasheh, S., Clauss, W., Ahlbrecht, H. & Daniel, H. (1998) Minimal molecular determinants of substrates for recognition by the intestinal peptide transporter. *J. Biol. Chem.* **273**, 23211-23218.

- Dunten, P. & Mowbray, S.L. (1995) Crystal-structure of the dipeptide binding-protein from *Escherichia-coli* involved in active-transport and chemotaxis. *Protein Sci.* **4**, 2327-2334.
- Elliott, T. (1993) Transport of 5-aminolevulinic acid by the dipeptide permease in *Salmonella-typhimurium*. *J. Bacteriol.* **175**, 325-331.
- Fei, Y.J., Liu, J.C., Fujita, T., Liang, R., Ganapathy, V. & Leibach, F.H. (1998) Identification of a potential substrate binding domain in the mammalian peptide transporters PEPT1 and PEPT2 using PEPT1-PEPT2 and PEPT2-PEPT1 chimeras. *Biochem. Biophys. Res. Commun.* **246**, 39-44.
- Fei, Y.J., Liu, W., Prasad, P.D., Kekuda, R., Oblak, T.G., Ganapathy, V. & Leibach, F.H. (1997) Identification of the histidyl residues obligatory for the catalytic activity of the human H⁺/peptide cotransporters PEPT1 and PEPT2. *Biochem.* **36**, 452-460.
- Fei, Y.J., Ganapathy, V. & Leibach, F.H. (1998) Molecular and structural features of proton-coupled oligopeptide transporter superfamily. *Prog. Nucleic Acid. Res. Mol. Biol.* **58**, 239-261.
- Fickel, T.E. & Gilvarg, C. (1973) Transport of impermeant substances in *E. coli* by way of oligopeptide permease. *Nat. New Biol.* **241**, 161-163.
- Fletcher, M. D. & Campbell, M. M. (1998) Partially modified retro-inverso peptides: development synthesis and conformational behaviour. *Chem. Rev.* **98**, 763-795.
- Flynn, G., Giroux, E. & Dage, R. (1987) An acyl-iminium ion cyclization route to a novel conformationally restricted dipeptide mimic: applications to angiotensin-converting enzyme inhibition. *J. Am. Chem. Soc.* **109**, 7914-7915.
- Friedman, D. & Amidon, G. (1989a) Passive and carrier-mediated intestinal absorption components of two angiotensin converting enzyme (ACE) inhibitor prodrugs in rats: enalapril and fosinopril. *Pharm. Res.* **6**, 1043-1047.
- Friedman, D. & Amidon, G. (1989b) Intestinal absorption mechanism of dipeptide angiotensin converting enzyme inhibitors of the lysyl-proline type: lisinopril and SQ 29, 852. *J. Pharm. Sci.* **78**, 995-998.
- Furlong, C.E. (1987) Osmotic shock-sensitive transport systems. In *Escherichia coli and Salmonella typhimurium: Cellular and Molecular Biology*. Neidhardt, F.C. (ed.) pp.768-796. ASM, Washington DC.
- Ganapathy, M.E., Huang, W., Wang, H., Ganapathy, V. & Leibach, F.H. (1998) Valacyclovir: a substrate for the intestinal and renal peptide transporters PEPT1 and PEPT2. *Biochem. Biophys. Res. Commun.* **246**, 470-475.

- Ganapathy, V. & Leibach, F.H. (1996) Peptide transporters. *Curr. Opin. Nephrol. Hypertens.* **5**, 395-400.
- Giannis, A., & Kolter, T. (1993) Peptidomimetics for receptor ligands-discovery, development, and medical perspectives. *Angew. Chem. Int. Ed. Engl.* **32**, 1244-1267.
- Gibson, M.M., Price, M. & Higgins, C.F. (1984) Genetic characterization and molecular cloning of the tripeptide permease (tpp) genes of *Salmonella typhimurium*. *J. Bacteriol.* **160**, 122-130.
- Gillespie, P., Cicariello, J. & Olson, G. L. (1997) Conformational analysis of dipeptide mimetics. *Biopolymers* **43**, 191-217.
- Gochoco, C.H., Ryan, F.M., Miller, J., Smith, P.L. & Hidalgo, I.J. (1994) Uptake and transepithelial transport of the orally absorbed cephalosporin cephalexin, in the human intestinal cell line, Caco-2. *Int. J. Pharm.* **104**, 187-202.
- Grail, B.M. & Payne, J.W. (2000) Predominant torsional forms adopted by dipeptide conformers in solution: parameters for molecular recognition. *J. Peptide Sci.* **6**, 186-199.
- Guo, A., Hu, P., Balimane, P.V., Leibach, F.H. & Sinko, P.J. (1999) Interactions of a nonpeptidic drug, valacyclovir, with the human intestinal peptide transporter (hPEPT1) expressed in a mammalian cell line. *J. Pharmacol. Exp. Ther.* **289**, 448-454.
- Hagting, A., Velde, J.V.D., Poolman, B. & Konings, W.N. (1997) Membrane topology of the di- and tripeptide transport protein of *Lactococcus lactis*. *Biochemistry* **36**, 6777-6785.
- Han, H., de Vruet, R.L., Rhie, J. K., Covitz, K.M., Smith, P.L., Lee, C.P., Oh, D.M., Sadee, W. & Amidon, G.L. (1998) 5'-Amino acid esters of antiviral nucleosides, acyclovir, and AZT are absorbed by the intestinal PEPT1 peptide transporter. *Pharm. Res.* **15**, 1154-1159.
- Hanessian, S., McNaughton-Smith, G., Lombart, H-G. & Lubell WD (1997) Design and synthesis of conformationally constrained amino acids as versatile scaffolds and peptide mimetics. *Tetrahedron* **53**, 12789-12854.
- Hassall, C., Krohn, A., Moody, C., and Thomas, W. (1982) The design of a new group of angiotensin-converting enzyme inhibitors. *FEBS Letts* **147**, 175-179.
- Higgins, C.F. & Hardie, M.M. (1983) Periplasmic protein associated with the oligopeptide permease of *Salmonella typhimurium* and *Escherichia coli*. *J. Bacteriol.* **155**, 1434-1438.

- Hiles, I.D., Gallagher, M.P., Jamieson, D.J. & Higgins, C.F. (1987a) Molecular characterization of the oligopeptide permease of *Salmonella typhimurium*. *J. Mol. Biol.* **195**, 125-142.
- Hiles, I.D., Powell, L.M. & Higgins, C.F. (1987b) Peptide transport in *Salmonella typhimurium*: molecular cloning and characterization of the oligopeptide permease genes. *Mol. Gen. Genet.* **206**, 125-142.
- Hornak, V., Dvorsky, R. & Sturdik, E. (1999) Receptor-ligand interaction and molecular modelling. *Gen. Physiol. Biophys.* **18**, 231-248.
- Hruby, V.J., Li, G., Haskell-Luevano, C. & Shenderovich, M. (1997) Design of peptides, proteins and peptidomimetics in chi space. *Biopolymers* **43**, 219-266.
- Hu, M. & Amidon, G. (1988) Passive and carrier-mediated intestinal absorption components of captopril. *J. Pharm. Sci.* **77**, 1007-1011.
- Hung, L.W., Wang, I.X.Y., Nikaido, K., Liu, P.Q., Ames, G.F.L. & Kim, S.H. (1998) Crystal structure of the ATP-binding subunit of an ABC transporter. *Nature* **396**, 703-707.
- Kemp, D.S. (1990) Peptidomimetics and the template approach to nucleation of beta-sheets and alpha-helices in peptides. *Trends Biotechnol.* **8**, 249-255.
- Kenig, M. & Abraham, E.P. (1976) Antimicrobial activities and antagonists of bacilysin and anticapsin. *J. Gen. Microbiol.* **94**, 37-48.
- Kenig, M., Vandamme, E. & Abraham, E.P. (1976) The mode of action of bacilysin and anticapsin and biochemical properties of bacilysin-resistant mutants. *J. Gen. Microbiol.* **94**, 46-54.
- Kieber-Emmons, T., Murali, R. & Greene, M. I. (1997) Therapeutic peptides and peptidomimetics. *Curr. Opin. Biotechnol.* **8**, 435-441.
- Knapp-Mohammady, M., Jalkanen, K.J., Nardt, F., Wade, R.C. & Suhai, S. (1999) L-Alanyl-L-alanine in the zwitterionic state: structures determined in the presence of explicit water molecules and with continuum models using density functional theory. *Chem. Phys.* **240**, 63-77.
- Koehler, R.T. & Villar, H.O. (2000) Statistical relationships among docking scores for different protein binding sites. *J. Comp-Aided Mol. Design.* **14**, 23-37.
- Kramer, W., Girbig, F., Gutjahr, U., and Kowalewski, S. (1995) in Peptide-based drug design: controlling transport and metabolism. (Taylor, M., and Amidon, G., Eds.), pp. 148-179, American Chemical Society, Washington, DC.
- Kubo, S.H. & Cody, R.J. (1985) Clinical pharmacokinetics of the angiotensin converting enzyme inhibitors. A review. *Clin. Pharmacokinet.* **10**, 377-391.

- Laemmli, U.K. (1970) Cleavage of structural proteins during the assembly of the head of bacteriophage T4. *Nature* **227**, 680-685.
- Leibach, F.H. & Ganapathy, V. (1996) Peptide transporters in the intestine and the kidney. *Annu. Rev. Nutr.* **16**, 99-119.
- Li, J.B., Tamura, K., Lee, C.P., Smith, P.L., Borchardt, R.T. & Hidalgo, I.J. (1998) Structure-affinity relationships of Val-Val and Val-Val-Val stereoisomers with the apical oligopeptide transporter in human intestinal Caco-2 cells. *J. Drug. Targeting* **5**, 317-330.
- Linton, K.J. & Higgins, C.F. (1998) The *Escherichia-coli* ATP-binding cassette (ABC) proteins. *Mol. Micro.* **28**, 5-13.
- Liu, C.E., Liu, P.Q., Wolg, A., Lin, E. & Ames, G.F. (1999b) Both lobes of the soluble receptor of the periplasmic histidine permease, an ABC transporter (traffic ATPase), interact with the membrane-bound complex. Effect of different ligands and consequences for the mechanism of action. *J. Biol. Chem.* **274**, 739-747.
- Liu, C.F., Liu, P.Q. & Ames, G.F. (1997) Characterization of the adenosine triphosphatase activity of the periplasmic histidine permease, a traffic ATPase (ABC transporter). *J. Biol. Chem.* **272**, 21883-21891.
- Liu, P.Q. & Ames, G.F.L. (1998) In vitro disassembly and reassembly of an ABC transporter, the histidine permease. *Proc. Natl. Acad. Sci. USA* **95**, 3495-3500.
- Liu, P.Q., Liu, C.E. & Ames, G.F.L. (1999a) Modulation of ATPase activity by physical disengagement of the ATP-binding domains of an ABC transporter, the histidine permease. *J. Biol. Chem.* **274**, 18310-18318.
- Manson, M.D., Blank, V., Brade, G. & Higgins, C.F. (1986) Peptide chemotaxis in *E. coli* involves the Tap signal transducer and the dipeptide permease. *Nature* **321**, 253-256.
- Marshall, N. J. (1994) Antibacterial agents designed to exploit peptide transport systems. PhD Thesis. University of Wales, Bangor.
- Marshall, G.R., Beusen, D.D. & Nikiforovich, G.V. (1993) Peptide modelling: an overview. In Peptides: Chemistry, Structure and Biology. Proceedings of the 13th American Peptide Symposium. (Hodges, R.S. & Smith, J.A. (eds.)). ESCOM Science Publishers: Netherlands, pp 1105-1117.
- Matthews, D.M. & Payne, J.W. (1980) Transmembrane transport of small peptides. *Curr. Top. Memb. Transp.* **14**, 331-425.
- Matthews, D.M. (1991) *Protein Absorption: Development and Present State of the Subject*. Wiley-Liss: New York.

- Milewski, S., Andruszkiewicz, R., Kasprzak, I., Mazerski, J., Mignini, F. & Borowski, E. (1991) Mechanism of action of anticandidal dipeptides containing inhibitors of glucosamine-6-phosphate synthase. *Antimicrob. Agents. Chemother.* **35**, 36-43.
- Milewski, S., Chmara, H. & Borowski, E. (1986) Anticapsin: an active site directed inhibitor of glucosamine-6-phosphate synthetase from *Candida albicans*. *Drugs. Exp. Clin. Res.* **12**, 577-583.
- Miller, J.H. (1972) *Experiments in Molecular Genetics*. Cold Spring Harbor Laboratory, Cold Spring Harbor. New York.
- Miyamoto, Y., Ganapathy, V., Barlas, A., Neubert, K., Barth, A. & Leibach, F.H. (1987) Role of dipeptidyl peptidase IV in uptake of peptide nitrogen from β -casomorphin in rabbit renal BBMV. *Am. J. Physiol.* **252**, F670-F677.
- Molloy, B.B., Lively, D.H., Gale, R.M., Gorman, M. & Boeck, L.D. (1972) A new dipeptide antibiotic from *Streptomyces collinus*, Lindenbein. *J. Antibiot. (Tokyo)* **25**, 137-140.
- Moore, G.J. (1994) Designing of peptide mimetics. *Trends. Pharmacol. Sci.* **15**, 124-129.
- Morley, J.S., Hennessey, T.D. & Payne, J.W. (1983a) Backbone-modified analogues of small peptides: transport and antibacterial activity. *Biochem. Soc. Trans.* **11**, 798-800.
- Morley, J.S., Payne, J.W. & Hennessey, T.D. (1983b) Antibacterial activity and uptake into *Escherichia coli* of backbone-modified analogues of small peptides. *J. Gen. Microbiol.* **129**, 3701-3708.
- Morse, D.E. & Guertin, M. (1972) Amber *suA* mutations which relieve polarity. *J. Mol. Biol.* **63**, 605-608.
- Muller, G. & Giera, H. (1998) Protein secondary templates derived from bioactive natural products. Combinatorial chemistry meets structure-based drug design. *J. Comput. Aided. Mol. Des.* **12**, 1-6.
- Naider, F. & Becker, J.M. (1975) Multiplicity of oligopeptide transport systems in *Escherichia coli*. *J. Bacteriol.* **122**, 1208-1215.
- Naider, F. & Becker, J.M. (1988) Peptide transport in *Candida albicans*: implications for the development of antifungal agents. *Curr. Top. Med. Mycol.* **2**, 170-198.
- Naider, F.R. & Becker, J.M. (1997) Synthesis of prenylated peptides and peptide esters. *Biopolymers* **43**, 3-14.

- Neu, H.C. & Heppel, L.A. (1965) The release of enzymes from *Escherichia coli* by osmotic shock and during the formation of spheroplasts. *J. Biol. Chem.* **240**, 3685-3692.
- Nickitenko, A.V., Trakhanov, S., & Quioco, F.A. (1995) 2Å resolution structure of DppA, a periplasmic dipeptide transport/chemosensory receptor. *Biochemistry* **34**, 16585-16595.
- Nikaido, K. & Ames, G.F.L. (1999) One intact ATP-binding subunit is sufficient to support ATP hydrolysis and translocation in an ABC transporter, the histidine permease. *J. Biol. Chem.* **274**, 26727-26735.
- Nikiforovich, G.V. (1994) Computational molecular modelling in peptide drug design. *Int. J. Pep. Prot. Res.* **44**, 513-531.
- Nussberger, S., Steel, A. & Hediger, M. A. (1997) Structure and pharmacology of proton-linked peptide transporters. *J. Control. Release.* **46**, 31-38.
- Oakley, A.J. & Wilce, M.C.J. (2000) Macromolecular crystallography as a tool for investigating drug, enzyme and receptor interactions. *Clin. Expt. Pharm. Physiol.* **27**, 145-151.
- Oh, D.M., Han, H.K. & Amidon, G.L. (1999) Drug transport and targeting. Intestinal transport. *Pharm. Biotechnol.* **12**, 59-88.
- Olson, E.R., Duniak, D.S., Jurss, L.M. & Poorman, R.A (1991) Identification and characterization of dppA, an *Escherichia coli* gene encoding a periplasmic dipeptide transport protein. *J. Bacteriol.* **173**, 234-244.
- Ondetti, M. A., Rubin, B. & Cushman, D. W. (1977) Design of specific inhibitors of angiotensin-converting enzyme: New class of orally active antihypertensive agents. *Science* **196**, 441-444.
- Ooms, F (2000) Molecular modeling and computer aided drug design. Examples of their applications in medicinal chemistry. *Curr. Med. Chem.* **7**, 141-158.
- Patchett, A., Harris, E., Tristram, E., Wyvratt, M., Wu, M., Taub, D., Peterson, E., Ikeler, T., Broeke, J., Payne, L., Ondeyka, D., Thorsett, E., Greenlee, W., Lohr, N., Hoffsommer, R., Joshua, H., Ruyle, W., Rothrock, J., Aster, S., Maycock, A., Robinson, F., Hirschmann, R., Sweet, C., Ulm, E., Gross, D., Vassil, T. & Stone, C. (1980) A new class of angiotensin-converting enzyme inhibitors. *Nature* **288**, 280-283.
- Paulsen, I. T., Sliwinski, M. K., & Saier, M. H., Jr. (1998) Microbial genome analyses: global comparisons of transport capabilities based on phylogenies, bioenergetics and substrate specificities. *J. Mol. Biol.* **277**, 573-592.

- Payne, J.W. & Smith, M.W. (1994) Peptide transport by microorganisms. *Adv. Microbial. Physiol.* **36**, 1-80.
- Payne, J.W. (1968) Oligopeptide transport in *Escherichia coli*: specificity with respect to side chain and distinction from dipeptide transport. *J. Biol. Chem.* **243**, 3395-3403.
- Payne, J.W. (1976) Peptides and micro-organisms. *Adv. Microb. Physiol.* **13**, 55-113.
- Payne, J.W. (1980) Transport and utilisation of peptides by bacteria. In *Microorganisms and Nitrogen Sources*. Payne, J.W. (ed). New York: John Wiley and Sons, Inc., pp. 211-256.
- Payne, J.W. (1983) Peptide transport in bacteria: methods, mutants and energy coupling. *Biochem. Soc. Trans.* **11**, 794-798.
- Payne, J.W. (1995) Bacterial peptide permeases as a drug delivery target. In *Peptide-Based Drug Design: Controlling Transport and Metabolism*. Taylor, M.D. & Amidon, G.L. (eds). ACS: Washington, D.C. pps. 341-367.
- Payne, J.W., Grail, B.M. & Marshall, N.J. (2000) Molecular recognition templates of peptides: driving force for molecular evolution of peptide transporters. *Biochem. Biophys. Res. Commun.* **267**, 283-289.
- Payne, J.W., Morley, J.S., Armitage, P. & Payne, G.M. (1984) Transport and hydrolysis of antibacterial peptide analogues in *Escherichia coli*: backbone-modified aminoxy peptides. *J. Gen. Microbiol.* **130**, 2253-2265.
- Pellegrini, M. & Mierke, D.F. (1999) Structural characterisation of peptide hormone/receptor interactions by NMR spectroscopy. *Biopolymers* **51**, 208-220.
- Perry, D. & Gilvarg, C (1984) Spectrophotometric determination of affinities of peptides for their transport systems in *Escherichia coli*. *J. Bacteriol.* **160**, 943-948.
- Poetsch, M., Zahner, H., Werner, R.G., Kern, A. & Jung, G. (1985) Metabolic products from microorganisms²³⁰. Amiclenomycin-peptides, new antimetabolites of biotin-taxonomy, fermentation and biological properties. *J. Antibiotics.* **38**, 312-320.
- Quioco, F.A. & Ledvina, P.S. (1996) Atomic structure and specificity of bacterial periplasmic receptors for active transport and chemotaxis: variation of common themes. *Mol. Microbiol.* **20**, 17-25.

- Quioco, F.A. (1990) Atomic structures of periplasmic binding proteins and the high-affinity active transport systems in bacteria. *Philos. Trans. R. Soc. Lond. Ser. B.* **326**, 341-351.
- Quioco, F.A. (1992) Atomic structures and function of periplasmic receptors for active transport and chemotaxis. *Curr. Opin. Struct. Biol.* **1**, 922-933.
- Ringrose, P.S. (1980) Peptides as antimicrobial agents. In *Microorganisms and Nitrogen Sources*. Payne, J.W. (ed). New York: John Wiley and Sons, Inc., pp. 641-692.
- Rizo, J. & Gierasch, I. M. (1992) Constrained peptides: models of bioactive peptides and protein substructures. *Annu. Rev. Biochem.* **61**, 387-418.
- Rohl, F., Rabenhorst, J. & Zahner, H. (1987) Biological properties and mode of action of clavams. *Arch. Microbiol.* **147**, 315-320.
- Saier, M. H., Jr. (1998) Molecular phylogeny as a basis for the classification of transport proteins from bacteria, archaea and eukarya. In *Advances in Microbial Physiology*. Poole, R.K. (ed) pp. 81-136, Academic Press, San Diego, CA.
- Saier, M. H., Jr. (1999a) Classification of transmembrane transport proteins in living organisms. In *Biomembrane Transport*. VanWinkle, L. (ed) pp. 265-276, Academic Press, San Diego, CA.
- Saier, M. H., Jr. (1999b) Genome archeology leading to the characterization and classification of transport proteins. *Curr. Opin. Microbiol.* **2**, 555-561.
- Salemme, F. R., Spurlino, J. & Bone, R. (1997) Serendipity meets precision: the integration of structure-based drug design and combinatorial chemistry for efficient drug discovery. *Structure* **5**, 319-324.
- Schoenmakers, R.G, Stehouwer, M.C, & Tukker, J.J. (1999) Structure-transport relationship for the intestinal small-peptide carrier: is the carbonyl group of the peptide bond relevant for transport? *Pharm. Res.* **16**, 62-68.
- Sleigh, S.H., Seavers, P.R., Wilkinson, A.J., Ladbury, J.E. & Tame, J.R.H. (1999) Crystallographic and calorimetric analysis of peptide binding to OppA protein. *J. Mol. Biol.* **291**, 393-415.
- Sleigh, S.H., Tame, J.R.H., Dodson, E.J. & Wilkinson, A.J. (1997) Peptide binding in OppA, the crystal structures of the periplasmic oligopeptide binding protein in the unliganded form and in complex with lysyllysine. *Biochemistry* **36**, 9747-9758.
- Smith, M. W. (1992) Characterisation and exploitation of microbial transport systems. PhD Thesis. University of Wales, Bangor.

- Smith, M.W. & Payne, J.W. (1990) Simultaneous exploitation of different peptide permeases by combinations of synthetic peptide smugglins can lead to enhanced antibacterial activity. *FEMS Microbiol. Lett.* **70**, 311-316.
- Smith, M.W., Tyreman, D.R., Payne, G.M., Marshall, N.J. & Payne, J.W. (1999) Substrate specificity of the periplasmic dipeptide-binding protein from *Escherichia coli*: experimental basis for the design of peptide prodrugs. *Microbiology* **145**, 2891-2901.
- Smyth, M.S. & Martin, J.H.J. (2000) X-ray crystallography. *J. Clin. Path. Mol. Path.* **53**, 8-14.
- Steiner, H.Y., Naider, F. & Becker, J.M. (1995) The PTR family: a new group of peptide transporters. *Mol. Microbiol.* **16**, 825-834.
- Stewart, W.W. (1971) Isolation and proof of structure of wildfire toxin. *Nature* **229**, 174-178.
- Sutcliffe, I.C. & Russell, R.R. (1995) Lipoproteins of gram-positive bacteria. *J. Bacteriol.* **177**, 1123-1128.
- Swaan, P.W., Stehouwer, M.C. & Tukker, J.J. (1995) Molecular mechanism for the relative binding affinity to the intestinal peptide carrier. Comparison of three ACE-inhibitors: enalapril, enalaprilat and lisinopril. *Biochim. Biophys. Acta.* **1236**, 31-38.
- Swaan, P.W. & Tukker, J.J. (1997) Molecular determinants of recognition for the intestinal peptide carrier. *J. Pharm. Sci.* **86**, 596-602.
- Swaan, P.W., Koops, B.C., Moret, E.E. & Tukker, J.J. (1998) Mapping the binding site of the small intestinal peptide carrier (PepT1) using comparative molecular field analysis. *Receptors Channels* **6**, 189-203.
- SYBYL Theory Manual (1994) Tripos, Inc. St. Louis.
- Tame, J.R.H., Dodson, E.J., Murshudow, G.N., Higgins, C.F. & Wilkinson, A.J. (1995) The crystal structures of the oligopeptide binding protein OppA complexed with tri- and tetrapeptide ligands. *Structure* **3**, 1395-1406.
- Tame, J.R.H., Murshudow, G.N., Dodson, E.J., Neil, T.K., Dodson, G.G., Higgins, C.F. & Wilkinson, A.J. (1994) The structural basis of sequence-independent peptide binding by OppA protein. *Science* **264**, 1578-1581.
- Tame, J.R.H., Sleigh, S.H., Wilkinson, A.J. & Ladbury, J.E (1996) The role of water in sequence-independent ligand binding by an oligopeptide transporter protein. *Nat. Struct. Biol.* **3**, 998-1001.

- Taylor, M.D. & Amidon, G.L. (eds) (1995) *Peptide-based Drug Design: Controlling Transport and Metabolism*. Washington, DC: American Chemical Society.
- Temple, C.S., Stewart, A.K., Meredith, D., Lister, N.A., Morgan, K.M., Collier, I.D., Vaughan-Jones, R.D., Boyd, C.A.R., Bailey, P.D. & Bronk, J.R. (1998) Peptide mimics as substrates for the intestinal peptide transporter. *J. Biol. Chem.* **273**, 20-22.
- Terada, T., Saito, H., Aawada, K., Hashimoto, Y. & Inui, K. (2000) N-terminal halves of rat H⁺/peptide transporters are responsible for their substrate recognition. *Pharm. Res.* **17**, 15-20.
- Thorsett, E. D., Harris, E. E., Aster, S., Peterson, E. R., Taub, D., Patchett, A. A., Ulm, E. H. & Vassil, T. C. (1983) Dipeptide mimics. Conformationally restricted inhibitors of angiotensin converting enzyme. *Biochim. Biophys. Res. Commun.* **111**, 166-171.
- Thorsett, E., Harris, E., Aster, S., Peterson, E., Snyder, J., Springer, J., Hirshfield, J., Tristram, E., Patchett, A. & Ulm, E. H. et al. (1986) Conformationally restricted inhibitors of angiotensin converting enzyme: synthesis and computations. *J. Med. Chem.* **29**, 251-260.
- Thwaites, D.T., Cavet, M., Hirst, B.H. & Simmons, N.L. (1995) Angiotensin-converting enzyme (ACE) inhibitor transport in human intestinal epithelial (Caco-2) cells. *Br. J. Pharmacol.* **114**, 981-986.
- Thwaites, D.T., Hirst, B.H., & Simmons, N.L. (1994) Substrate specificity of the di/tripeptide transporter in human intestinal epithelia (Caco-2): identification of substrates that undergo H⁺-coupled absorption. *Br. J. Pharmacol.* **113**, 1050-1056.
- Tiruppathi, C., Ganapathy, V. & Leibach, F.H. (1990) Evidence for tripeptide-proton symport in renal brush border membrane vesicles. Studies in a novel rat strain with a genetic absence of dipeptidyl peptidase IV. *J. Biol. Chem.* **265**, 2048-2053.
- Tyreman, D. R. (1990) Peptide transport systems and antibiotic design. PhD Thesis. University of Wales, Bangor.
- Tyreman, D.R., Smith, M.W., Marshall, N.J., Payne, G.M., Schuster, C.M., Grail, B.M. & Payne, J.W. (1998) Peptides as prodrugs: the smugglin concept. In *Peptides in Mammalian Protein Metabolism: Tissue Utilization and Clinical Targeting*. Grimble, G.K. & Backwell, F.R.C. (eds). Portland Press: London pp 141-157.

- Tyreman, D.R., Smith, M.W., Payne, G.W. & Payne, J.W. (1991) Exploitation of peptide transport systems in the design of antimicrobial agents. In *Molecular Aspects of Chemotherapy* (Shugar, D., Rode, W. & Borowski, E., eds.), pp. 127-142. Springer-Verlag, Berlin.
- vanVeen, H.W. & Konings, W.N. (1997) Multidrug transporters from bacteria to man: similarities in structure and function. *Seminars in Canc. Biol.* **8**, 183-191.
- vanVeen, H.W. & Konings, W.N. (1998) The ABC family of multidrug transporters in microorganisms. *Biochim. et Biophys. Acta-Bioenerg.* **1365**, 31-36.
- Verkamp, E., Backman, V.M., Bjornsson, J.M., Soll, D. & Eggertsson, G. (1993) The periplasmic dipeptide permease system transports 5-aminolevulinic acid in *Escherichia coli*. *J. Bacteriol.* **175**, 1452-1456.
- Walter, E., Kissel, T. & Amidon, G.L. (1996) The intestinal peptide carrier: a potential transport system for small peptide derived drugs. *Adv. Drug Delivery Rev.* **20**, 33-58.
- Wang, W., Jiang, J., Ballard, C.E. & Wang, B. (1999) Prodrug approaches to the improved delivery of peptide drugs. *Curr. Pharm. Des.* **5**, 265-287.
- Weller, H. N., Gordon, E. M., Rom, M. B. & Pluscec, J. (1984) Design of conformationally constrained angiotensin-converting-enzyme inhibitors. *Biochim. Biophys. Res. Commun.* **125**, 82-89.
- Wilkinson, A.J. (1996) Accommodating structurally diverse peptides in proteins. *Chem. Biol.* **3**, 519-524.
- Yang, C.Y., Dantzig, A.H. & Pidgeon, C. (1999) Intestinal peptide transport systems and oral drug availability. *Pharm. Res.* **16**, 1331-1343.
- Zboinska, E., Lejczak, B. & Kafarski, P. (1993) Antibacterial activity of hosphonopeptides based on 4-amino-4-phosphonobutyric acid. *FEMS Microbiol. Lett.* **108**, 225-230.
- Zhang, Y.L., Marepalli, H.R., Lu, H.F., Becker, J.M. & Naider, F. (1998) Synthesis, biological activity, and conformational analysis of peptidomimetic analogues of the *Saccharomyces cerevisiae* alpha-factor tridecapeptide. *Biochemistry* **37**, 12465-12476.